

https://dspace.org/

The Design and Synthesis of Anti-Tubercular Lariatin a Peptidomimetics

Nyembe, Priscilla Lebohang

2023-07
University of the Witwatersrand, Johannesburg
https://hdl.handle.net/10539/41578
Nyembe, Priscilla Lebohang. (2023). The Design and Synthesis of Anti-Tubercular Lariatin a Peptidomimetics. [Master's dissertation, University of the Witwatersrand, Johannesburg]. https://hdl.handle.net/10539/41578

Downloaded from a DSpace repository. https://dspace.org/

THE DESIGN AND SYNTHESIS OF ANTI-TUBERCULAR LARIATIN A PEPTIDOMIMETICS

By

Priscilla Nyembe



UNIVERSITY OF THE
WITWATERSRAND,
JOHANNESBURG

A dissertation submitted to the Faculty of Science, University of the Witwatersrand, Johannesburg in fulfilment of the requirements for the Degree of Master of Science

Supervised by Dr. Maya Mellisa Makatini

2023

DECLARATION OF ORIGINALITY

I hereby state that the work recorded in this thesis was entirely conducted and written by myself under the supervision of Dr Maya Makatini. I have rightfully credited the sources were used in the thesis. This thesis has not been submitted before for any degree. It is submitted to the faculty of Science at the University of the Witwatersrand for the degree of Master of Science.



18-07-2023

Priscilla Nyembe Date

ACKNOWLEDGEMENTS

First and foremost, I would like to thank God for giving me the strength and knowledge to carry this project through.

My greatest gratitude goes to my supervisor, **Dr Maya Makatini** for giving me this exciting project and the opportunity to be her student and carry out this project. I am grateful for the guidance and support she has given me from the beginning to the end of my degree.

I also would like to express my gratitude the mass spec team. Thapelo Mbhele and Refilwe Moepya, thank you for your patience and kind assistance in training me to understand LC-MS. Thank you to Eric Morifi for the continuous access to mass spec lab.

Everyone from the peptide group has been supportive and encouraging during the progress of the project. To Lesotho Ntlama, Thandokuhle Ntombela, Ntomizanele Ngqinayo, Thabo Peme, Khanani Machumela, Refilwe Moepya, Thapelo Mbele, Mufaro, I would also like to thank them for always willing to lend a helping hand.

I am utterly thankful to my family for their continual support. To my parents, Matinkane and Mpatli Nyembe, I cannot thank God enough for giving me such loving and supportive parents. And to my siblings, thank you for the laughter's and light moments that served as a reminder that life can be fun in the midst of challenges.

I would like to thank the School of Chemistry support staff, glass blower; Mr Dzara, admin staff: Khwezi, Thuli, and the chemical store guys; David and Elias.

I also acknowledge the NRF bursary for providing me with financial support and the University of Witwatersrand for providing great research facilities to carrying out this project.

ABSTRACT

Tuberculosis (TB), caused by *Mycobacterium tuberculosis* (*Mtb*), is one of the major causes of death and morbidity worldwide. Approximately 10 million people worldwide are infected with *Mtb* annually, with an estimated 1.5 million deaths. However, potent anti-TB drugs with a new mechanism of action have not been developed in the last thirty years, and only 5 anti-TB drugs are still clinically used. Currently, available drugs and vaccines have failed to control its spread. Furthermore, the emergence of multidrug-resistant (MDR) and extensively drug-resistant (XDR) *Mtb* is a significant public health concern because most of the anti-TB drugs that have been in use for over 40 years are no longer effective for the treatment of these infections. Thus, there is an increased demand for novel anti-tubercular drugs with a different mode of action directed at new *Mtb* targets. Lariatin A, an anti-mycobacterial peptide, has received interest in the synthesis field due to its distinctive threaded structure which consist of a linear and cyclic portions and its unique bactericidal mechanism toward *Mtb*. This research focuses on designing and synthesizing derivatives of Lariatin A and investigating their binding properties to the mycobacterium caseinolytic protease (ClpP), a protein essential for the growth of *Mtb*. A simpler synthetic route for derivatizing Lariatin A peptides was achieved by incorporating two cysteine amino acid residues onto the sequence for cyclization of the peptide *via* the formation of a disulfide bond instead of a lactam bond. To further simplify the synthetic procedure, derivatives with shorter sequences as well as peptide-peptoids hybrids were also designed.

Eight mimetics of Lariatin A were synthesized [Pep_PNL1 (**1**), Pep_PNL2 (**2**), Pep_HA (**3**), Pep_TA (**4**), Pep_TAA (**5**), Pep_HAP (**6**), Pep_PTA (**7**), Pep_PHA (**8**)].

The proposed derivatives were synthesized using the solid phase peptide synthesis technique and a sub-monomeric approach was followed to synthesize the peptide-peptoid hybrids. Purification of the peptides was achieved by utilizing semi-preparative High-Pressure Liquid Chromatography and they were characterized by Liquid Chromatography-Mass Spectrometry. The peptides were obtained in low to moderate yields, and the linear tail portion derivative (**4**) showed 70% ClpP inhibition, while the linear tail derivative coupled to the adamantane moiety (**5**) showed a 49% inhibition factor. NMR (nuclear magnetic resonance spectroscopy) and CD

(circular dichroism) were utilized to determine the secondary structural features. The CD experiments indicated that peptide **1** adopts stable conformations while its separate tail (**4**) and cyclic (**3**) regions loss conformity. Pep_PTA (**7**) displayed the characteristics of both peptide and peptoid as seen from its formation of beta sheets. NMR and CD experiments confirmed that **4** exist in a helical conformation. Hence helical Lariatin A derivatives targeting the *Mycobacterium tuberculosis* caseinolytic protease can be synthesized using the solid phase peptide synthesis strategy.

LIST OF FIGURES

Figure 1: The scanning electron micrograph of Mtb.[3] 20
Figure 2: Pathogenicity of Mtb. [10] 21
Figure 3: Mechanism of action of current TB drugs.[17] 24
Figure 4: The biosynthesis of RiPPs. A) General overview of RiPP biosynthetic gene clusters. B) Procesess where the precursor peptide is turned into the mature RiPP.[23] 26
Figure 5: A) The production of a mature lasso peptide from the precursor peptide. B) The four different classes of lasso peptides.[23] 27
Figure 6: The secondary structures of lasso peptides with a molecular target that is known.[23] 28
Figure 7: The structures of A) lariatin A and B) lassomycin.[26] 29
Figure 8: A and B) the structure of lariatin A and B.[27] C) Simplified version of Lariatin A. 30
Figure 9: **A**) The model representing a compressed state of the Clp protease and **B**) structure of the caseinolytic protease with the serine catalytic site. [30] 32
Figure 10: The proteolysis of protein resulting from the interaction of ClpC1 and the caseinolytic protease.[30] 32
Figure 11: Mode of action of lassomycin where it decouples the ClpC1 from the ClpP inhibiting proteolysis.[30]. 33
Figure 12: a) The AMPs membrane disruptive and non-membrane disruptive mechanism for killing bacteria.[8] and b) the first electrostatic interaction with negatively charged cell envelope.[9] 43
Figure 13: Structure of peptoids vs peptides 44
Figure 14: Peptoids appear to act by disrupting the microbial membranes just as AMPs. Shown above are the Cryo-EM results from the studies conducted by Brice et al. and Diamond et al. for AMP and peptoids, respectively a) Shows the disruption of Kaposi's Sarcoma Herpes Virus (KSHV) envelope by the AMP called LL-37.[18] Similarly, **b**) when SARS-CoV-2 was treated with two active peptoids (MXB-4 and MXB-9) several slightly disrupted membranes (middle) were observed and what appear to be nucleocapsids without envelopes. These structures were not observed in the control samples, proposing that the peptoids act via the same membrane-disruptive mechanism on MXB-4 and MXB-9 virus types.[19] 45
Figure 15: The structure magainin-2 amide25 and b) the structure of alpha/beta peptoid chimeras.[24] ... 46
Figure 16: The structure of a) Lysine-type monomer and b) Arginine type monomer 50
Figure 17: The structures of cationic monomers used in the study. 50
Figure 18: The structures of a) Peptoid 1, b) Peptoid 1-$C13_{4mer}$ and c) 1_{mer}. 52
Figure 19: Structures of hydrophobic monomer. 54
Figure 20: The structures of peptoid monomers and their corresponding abbreviations and full names. Reprinted with permission from [11], published by AAC, 2015. 55
Figure 21: The chemical structures of peptoid 3, peptoid 9, peptoid 7 and peptoid 14. 57
Figure 22: The structures of Peptoid 4, peptoid 15 and peptoid 1 59
Figure 23: The Space-filling model of parent peptide V13KL. The region coloured in white represents the backbone of the peptide. The amino acids in green colour are hydrophobic the the ones in blue color are hydrophilic. The Lys substitution on the 13th positions ($V13K_L$) on the nonpolar face of the helix is highlighted in red.[51] 60
Figure 24: The proposed structural modifications in the outer outlet of the phospholipid membrane of the bacteria **a**) after inserting a linear **b**) and cyclic **c**) peptoids. Cyclization enables antimicrobial molecules to intercalate more effectively with lipid film characterization by molecular tilt.[11] 61

Figure 25: A plot of the six pairs of cyclic (C3, C4, C7, C8, C14, CGS) and linear (L3, L4, L7, L8, L14, LGS) peptoids against the MIC which illustrates that the macrocyclized peptoids enhanced the antimicrobial activity against E.coli.[7] 62
Figure 26: Comparison of the structure of N-alkyl glycine monomers and the N-Aryl monomers peptoid structures. 63
Figure 27: The structures of peptoids TM1 to TM10.[16] 66
Figure 28: The structure of Lariatin A with a (top) lactone bond and (bottom) with a disulfide bond. 76
Figure 29: The structure of Lariatin A highligng the (red) linear tail region and (blue) cyclic region. 77
Figure 30: Structures of (left) 1-Adamantanecarboxylic acid and (right) palmitic acid. 78
Figure 31: The general SPPS method.[12] 81
Figure 32: polystyrene (PS) cross-linked with 1% divinylbenzene (DVB).[7] 82
Figure 33: Wang resin results in Peptide Acids when cleaved, 2-Chlorotrityl resins results in Protected Peptide Acids under mildly acidic conditions, Rink Amides results in a Peptide Amides when cleaved, HMBA Resins (TFA stable) results in Peptide amides, hydrazide.[17] 83
Figure 34: The Orthogonal protection system using Fmoc/t-Bu chemistry.[17] 84
Figure 35: Cleavage of permanent and temporary protecting groups on peptide.[18] 85
Figure 36: The chromatogram of the full peptide showing the desired molecular peaks 1249.6009 $[M + 2H]^{2+}$ and 833.4028 $[M+3H]^{3+}$ 92
Figure 37: The chromatogram obtained after the cyclization of the peptide. 92
Figure 38: The coupling difficulty prediction spreadsheet. 93
Figure 39: top; The chromatogram of the full lariatin A peptide, (middle) the spectrum showing the mass of the peptide, and (bottom) the spectrum showing the impurity that elutes closely to the peaks of interest. 96
Figure 40: The chromatogram of the full lariatin A peptide after cyclization. 97
Figure 41: The spectra of Pep_PNL1 showing the co-eluting impurity peak. 98
Figure 42: The spectra for lariatin A peptidomimetic after cyclization. 100
Figure 43: The spectra of pure Pep_PNL1 101
Figure 44: The chromatogram of Pep_TA from prep-HPLC showing the two peaks with similar mass. 102
Figure 45: The LCMS spectrum of the pure Pep_TA peptide. 103
Figure 46: The LCMS spectrum of Pep_HA after purification. 104
Figure 47: The LCMS spectrum of the pure Pep_TAA peptide. 105
Figure 48: The LCMS spectrum of the pure Pep_HAP peptide. 107
Figure 49: The LCMS spectrum of the pure Pep_PNL2 peptide. 109
Figure 50: General methods for solid-phase peptoid synthesis. a) is the monomer approach and b) is the sub-monomeric approach. 115
Figure 51: The structure of Pep_PTA 118
Figure 52: The Mass spectrum of Pep_PTA after purification. 119
Figure 53: The structure of Pep_PHA. 119
Figure 54: The chromatogram for the Cys-BAA-Beta-alanine reaction. 121
Figure 55: The Mass Spectrum of the Cys-BAA-Beta-alanine-Arg-fmoc reaction. 122
Figure 56: The design of Pep_PHA 123
Figure 57: The chromatogram of Cys-Gln-Arg-Fmoc reaction. 123
Figure 58: The mass spectrum of Pep_PHA before purification. 124
Figure 59: The structures of (top) Pep_TA and (bottom) Pep_TAA peptides. 126

Figure 60: The procedure followed for the biological testing of Pep_TA and Pep_TAA against the ClpP. 127
Figure 61: The ClpP essay of Pep_TA and Pep_TAA. 127
Figure 62: Secondary structural components of protein structure. Most proteins contain the right-handed alpha helix and the beta-pleated sheet, which are frequent structural motifs. The amine and the carbonyl oxygen in the backbone of the amino acid form a hydrogen bond, which holds them together.[4] 130
Figure 63: Right-handed α-Helix Structure. A) Ball and Stick Model Side View. A total of 3.6 amino acids are required to form one turn of an α-helix. Hydrogen bonding between the carbonyl oxygen and the nitrogen of the 4th amino acid stabilizes the helical structure.[4] **B**) The Carbonyl of residue I in α-helices is hydrogen-bonded to the NH of residue i+4.[5] 131
Figure 64: Structure of pleated sheets. The parallel or antiparallel orientation of the -pleated sheet is depicted in (A) above, with the pleated sheet being represented by the red ribbon arrows. The direction of the arrow indicates the protein's orientation, which is pointing from N to C. The parallel and antiparallel pleated sheet structures (B right and B left, respectively) are both stabilized by hydrogen bonding between the backbone carbonyl and the backbone amine functional groups.[4] 131
Figure 65: "Pure" secondary structure circular dichroism spectra. From Brahms & Brahms, 1980, redrawn.[12] 134
Figure 66: The structure of Pep_TA. 137
Figure 67: The usual positions of the protons in a 1D spectrum.[16] 138
Figure 68: The fingerprint region for different amino acids. HA = alpha protons, HB = beta protons, HG = gamma protons, HD = delta protons, HE = epsilon protons.[17] 139
Figure 69: The TOCSY and COSY spectrums showing the fingerprint region. 140
Figure 70: Ultra-High-Performance Liquid Chromatography (Thermo Scientific Ultimate 3000, RS diodearray detectors) with a Diode Array (190, 195, 215, 254, and 300 nm) coupled to a Bruker Compact QTOF high-resolution mass spectrometer. 150
Figure 71: Structure of Pep_PNL1 156
Figure 72: Structure of Pep_HAP. 156
Figure 73: : Structure of Pep_TA 157
Figure 74: The structure of Pep_HA. 157
Figure 75: The structure of Pep_TAA 158
Figure 76: The structure of Pep_PNL2 159
Figure 77: Plot and secondary structure data of Pep_PNL1 CD data using BeStSel software 160
Figure 78: Plot and secondary structure data of Pep_TA CD data using BeStSel software. 161
Figure 79: Plot and secondary structure data of Pep_HA CD data using BeStSel software. 162
Figure 80: : Plot and secondary structure data of Pep_PNL2 CD data using BeStSel software. 163
Figure 81: Plot and secondary structure data of Pep_PTA CD data using BeStSel software. 164
Figure 82: ^{1}H NMR of Pep_TA. 165
Figure 83: ^{13}C NMR of Pep_TA. 165
Figure 84: DEPT NMR of Pep_TA 166
Figure 85: The HSQC of Pep_TA. 167
Figure 86: The ROESY of Pep_TA. 168
Figure 87: The HMBC of Pep_TA. 169

LIST OF TABLES

Table 1: The retention times of the peptoids as well as their corresponding in vitro antibacterial activities, haemolytic activities, and cytotoxicity. Reprinted with permission from [11], published by AAC, 2015. 48
Table 2: The linear and cyclic peptoids with their corresponding antimicrobial and hemolytic activities.[7] 54
Table 3: The designed lariatin A derivatives and their corresponding amino acid sequences. 79
Table 4: The purity and yield obtained for the synthesized Lariati A peptidomimetics. 109
Table 5: The sequence of peptide-peptoid hybrids. 114
Table 6: The percentage composition of presence of Helices, beta Sheets and Coils in Pep_PNL1, Pep_PNL2, Pep_HA, Pep_TA and Pep_PTA. 136
Table 7: NMR chemical shifts (ppm) of identified spin and assignment for Pep_TA using TOCSY and ROESY spectrum (Appendix II, Figure 86). 142
Table 8: The long-range correlations observed on ROESY NMR. 143
Table 9: The mass and average absorbances of samples from the resin after attaching the first amino acid. 153

LIST OF SCHEMES

Scheme 1: The activation mechanism of 2-chlorotrityl resin. 87
Scheme 2: The reaction of 2-chlorotrityl with fmoc-Pro-OH. 88
Scheme 3: (top) removal of fmoc protective group with piperidine and (bottom) activation of amino acid in presence of DIPEA and HBTU. 89
Scheme 4: Cleavage of the desired peptide from the 2-chlorotrityl resin. 90
Scheme 5: Amino acid insertion/addition mechanism. 99
Scheme 6: The general SPPS method used to synthesize Lariatin A peptidomimetics. 101
Scheme 7: The deprotection of the Fmoc group. 108
Scheme 8: The acylation step of the sub-monomeric synthetic procedure. 116
Scheme 9: The amine substitution step of the sub-monomeric synthetic procedure. 116
Scheme 10: The general synthetic procedure for the synthesis of peptide-peptoid derivatives. 117

LIST OF ABBREVIATIONS

δ	chemical shift
Arg (R)	arginine
Boc	Tert-Butyl-Oxycarbonyl
CD	circular dichroism
COSY	correlation spectroscopy
Cys (C)	cysteine
d	doublet
dd	doublet of doublets
DCM	dichloromethane
DIPEA	N,N-diisopropylethylamine
DMF	N,N-dimethylformamide
DMSO	dimethyl sulfoxide
EDT	1,2-Ethanedithiol
Et_2O	diethyl ether
Fmoc	9-Fluorenylmethoxycarbonyl
Glu (E)	glutamic acid
Gly (G)	glycine
HATU	1-[Bis(dimethylamino)methylene]-1H-1,2,3-triazolo[4,5-b]pyridinium 3-oxide hexaflourophosphate
HBTU	(2-(1H-benzotrial-1-yl-1,1,3,3-tetramethyluronium hexafluorophosphate

HMBC	heteronuclear multiple quantum coherence
HPLC	high performance liquid chromatography
HRMS	high resolution mass spectrometry
hrs	hours
HSQC	heteronuclear single quantum coherence
IPA	isopropyl alcohol
LC-MS	liquid chromatography-mass spectrometry
Lys	(K) lysine
J	coupling constant
m	multiplet
MBHA	rink Amide 4-methylbenzhydrylamine
MeCN	acetonitrile
MeOH	methanol
mg	milligram
mL	milliliter
min	minute
mM	millimolar
Mol	molar
MS	mass spectrometry
m/z	mass-to-charge ratio
NMR	nuclear magnetic resonance
NOE	nuclear Overhauser effect

NOESY	nuclear Overhauser effect spectroscopy
nm	nanometer
pep	peptide
s	singlet
SPPS	Solid phase peptide synthesis
Ser (S)	serine
t	triplet
TFA	trifluoroacetic acid
TIS	Triisopropyl silane
TOCSY	total correlation spectroscopy
RT	room temperature
ROESY	rotating frame Overhauser effect spectroscopy
Tyr (Y)	tyrosine
q	quartet

Table of Contents

DECLARATION OF ORIGINALITY II
ACKNOWLEDGEMENTS III
ABSTRACT IV
LIST OF FIGURES VI
LIST OF TABLES IX
LIST OF SCHEMES IX
LIST OF ABBREVIATIONS X
CHAPTER 1 19
Introduction 19
1.1 History and origin of tuberculosis 19
1.2 Tuberculosis global trend 20
1.3 Pathogenesis of TB 21
1.3.1 Primary TB infection or exposure: 22
1.3.2 Latent TB infection (LTBI) 22
1.3.3 Active TB disease: 22
1.4 Diagnosis and vaccination 23
1.5 Current anti-TB drugs approved by the FDA 23
1.6 Antimicrobial Resistance or acquired resistance 24
1.7 Antimicrobial peptides (AMPs). 25
1.8 Ribosomally synthesized and Post translationally modified peptides (RiPPs) 26
1.9 Lasso peptides 26
1.10 Lariatin A 29
1.11 Activity and Biological target of lariatin A 30
1.12 Biological role of ClpC 31
1.12.1 Mode of action 33
1.13 AMP limitations 33
2. Aim and objectives 34
2.1 Aim: 34
2.2 Objectives 34
3. Hypothesis and Questions 34
3.1 Hypothesis 34
3.2 Research question 35

4. Novelty of the study 35
5. Overview of the thesis 35
Chapter 1 35
Chapter 2 35
Chapter 3 35
Chapter 4 35
Chapter 5 35
Chapter 6 36
Chapter 7 36
References 37
CHAPTER 1.1: Literature review 41
Review: Structure-activity relationship of antimicrobial peptoids 41
1.1.1 Introduction 41
1.1.2 Main chain length 47
1.1.2.1 The effects of main chain length on antimicrobial activity 47
1.1.3 Cationic peptoids 49
1.1.3.1 Lysine or Arginine type side chains 49
1.1.3.2 The effect of cationic side chains on antimicrobial activity 50
1.1.4 Hydrophobicity 52
1.1.4.1 Influence of Hydrophobicity on the secondary structure of peptides 52
1.1.4.2 Effect of hydrophobic surface area (SA) on antimicrobial activity 53
1.1.5 Amphiphilicity 58
1.1.5.1 Effects of amphiphilicity by sequence rearrangement 58
1.1.6 Cyclization 60
1.1.6.1 Effect of cyclization on antimicrobial activity 62
1.1.7 Aromatic side chains 63
1.1.7.1 N-aryl groups within peptoid oligomers 63
1.1.8 Alkylated peptoids 64
1.1.8.1 Alkylated peptoids on antimicrobial activity 64
1.1.8.2 Influence of Alkyl tail for the formation of micellar structures 67
1.1.9 Halogen-substituted peptoids 67
1.1.10 Conclusions 68
References 68

CHAPTER 2: The design and synthesis of Lariatin A derivatives 75
2.1 Introduction 75
2.2 Design of Lariatin A derivatives 75
2.2.1 Structure activity relationship (SAR) of Lariatin A 75
2.2.2 Replacing lactone bond with disulfide bond 76
2.2.3 Short derivatives 77
2.2.4 Incorporation of lipid moiety onto a peptide 77
2.2.5 Lassomycine-Lariatin A hybrid 79
2.3 Peptide synthesis 79
2.3.1 Principles of the SPPS method 80
2.3.1.1 Solid supports (Resin and linkers) 81
2.3.1.1.1 Linkers 82
2.3.1.2 Protecting groups 83
2.3.1.3 Peptide cleavage 84
2.3.1.4 Peptide purification 85
2.4 Synthetic method 86
Method 1 86
2.4.1 Activation and swelling of 2-chlorotrityl resin 86
2.4.2 Activation of the first amino acid and its attachment to the resin 87
2.4.3 Determination of the loading capacity 88
2.4.4 Peptide elongation 88
2.4.5 Cleaving the peptide 90
2.4.6 Cyclization using iodine 90
2.4.7 Peptide purification and characterization 90
2.5 Results and discussion 91
2.5.1 Synthesis of Pep_PNL1 (lariatin A) 91
2.5.2 Problem identification for Method 1 93
Method 2 94
2.5.3 Problem Identification 99
Method 3 100
2.5.4 Purification of Pep_PNL1 100
2.5.5 Synthesis of shorter Lariatin A peptidomimetics 101
2.5.6 Purification of Pep_TA 102

2.5.7 Purification of Pep_HA 103
2.5.8 Incorporate a lipid moiety onto a peptide 104
2.5.8.1 Synthesis of Pep_TAA 104
2.5.8.2 Purification of Pep_TAA 105
2.5.8.3 Synthesis of Pep_HAP 106
2.5.9 Synthesis of Pep_PNL2 108
2.5.10 Swelling of rink amide resin and Fmoc removal 108
2.5.11 Purification of Pep_PNL2 108
Concluding remarks 110
References 110
CHAPTER 3: Design and synthesis of Lariatin A peptoids 113
3.1 Introduction 113
3.2 Design of lariatin A peptoid derivatives 113
3.3 Synthesis of peptoids 114
3.3 1 The Acylation Step 115
3.3.2 The Amine Substitution Step 116
3.3.3 Cleavage and deprotection 116
3.4 Synthetic method 116
3.5 Results and discussion 117
3.5.1 Synthesis of Tail alone peptoid synthesis (Pep_PTA) 117
3.5.2 Purification of Pep_PTA 118
3.5.3 Synthesis of Head alone peptoid synthesis (Pep_PHA) 119
Method 1 119
Method 2 122
2.6 Concluding remarks 125
References 125
Chapter 4: Biological testing 126
Concluding remarks 128
References 128
CHAPTER 5: Structural Elucidation of peptides 129
5.1 Introduction 129
5.2 Secondary structures 129
5.2.1 Alpha helix 130

5.2.2 Beta sheet 131
5.3 Solution-state NMR studies 132
5.3.1 How does it work? 132
5.3.2 NMR for peptides 132
5.4 CD measurements 133
5.5 Results and discussion 135
5.5.1 Determination of the secondary structure using CD 135
5.5.2 NMR structure elucidation of Pep_TA 137
5.5.2.1 Spin system and Sequential spin specific assignment of amino acid residues for Pep_TA 138
5.5.2.2 Determination of the secondary structural elements of Pep_TA 142
5.6 Concluding remarks 143
References 143
CHAPTER 6: Conclusion and recommendations 146
6.1 Summary and Conclusion 146
6.1.1 Summary 146
6.1.2 Conclusion 147
6.2 Future scope of research 148
CHAPTER 7: Experimental 149
7.1 Materials and reagents 149
7.2 Instrumentation used for peptides and amino acids and general techniques 149
7.2.1 Ultra High Pressure Liquid Chromatography (UHPLC) 149
7.2.2 Semi-Preparative High Pressure Liquid Chromatography (semi-PREP-HPLC) 150
7.2.3 Ultraviolet–visible spectroscopy 150
7.2.4 Mass spectroscopic analysis 151
7.2.5 Nuclear magnetic resonance spectroscopy (NMR) 151
7.2.6 CD 151
7.3 General procedure for the solid phase synthesis of the peptides 152
7.3.1 General procedure for the swelling, activation and coupling of the first amino acid to 2-chlorotitryl resin 152
7.3.2 General procedure for the swelling, activation and coupling of the first amino acid to rink amide resin 152
7.3.3 General procedure for analysing the substitution of the first amino acid on resin 152
7.3.4 General procedure for the synthesis of peptides 154

7.4 General procedure for the synthesis of the peptoids. 154
Appendices 155
Appendix I- Supplementary information for Chapter 2 156
Appendix II – Supplementary information for Chapter 5 160

CHAPTER 1

Introduction

The work presented herein is on the design and synthesis of a particular class of lasso peptides called Lariatin A as potential *Mycobacterium tuberculosis* (*Mtb)* caseinolytic protease inhibitors. This introductory chapter provides a general review of tuberculosis (TB) disease, the threat posed by antimicrobial resistance, and the possible role that antimicrobial peptides (AMPs) and their derivatives may play in solving the issue. A special focus is given to the structure-activity relationship of antimicrobial peptoids, which are structurally and mechanistically similar to naturally occurring AMPs, and their usage as novel antimicrobial agents to counteract the growth of antimicrobial resistance.

1.1 History and origin of tuberculosis

TB once referred to as "consumption" or phthisis, is mostly caused by *Mtb* (Figure 1) and *Mycobacterium africanum*, both members belong to a group of related species that are adapted to humans and animals and are called the *Mtb* complex (MTBC).[1, 2] Before the late eighteenth century, receiving a TB diagnosis was regarded as essentially a death sentence. Better treatment for this disease began after Dr. Robert Koch discovered *Mtb* as the causative agent in 1882.[2] TB became curable later when antibiotics were discovered, bringing a real revolution in TB chemotherapy. The 1940s-1960s are considered the golden age of antibiotics and a lot of TB treatment drugs were developed during this time, including streptomycin and p-aminosalicylic acid (PAS) in 1945.[2] TB cases began to decline sharply and continuously globally especially when rifampicin, ethambutol, pyrazinamide, and isoniazid were introduced. TB was no longer thought of as public health concern in the 1960s with hopes that it will soon be eliminated. Nevertheless, in the 1980s, the disease unexpectedly re-emerged in connection with the surging epidemic of acquired immuno deficiency syndrome (AIDS) and the emergence of drug-resistant TB strains.[2]

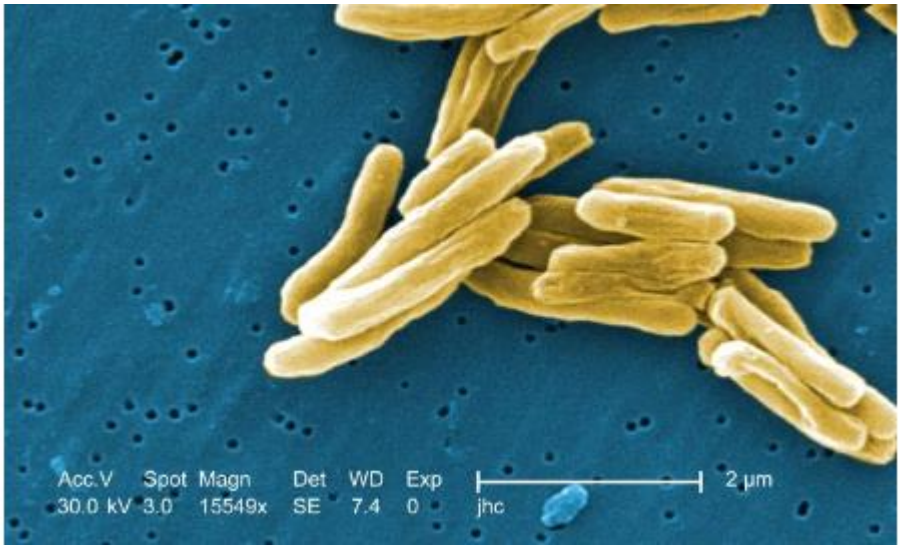


Figure 1: The scanning electron micrograph of Mtb.[3]

1.2 Tuberculosis global trend

Over 136 years since *Mtb* was discovered,[4] TB is still one of the world's life-threatening transmittable diseases. Before the COVID-19 epidemic in 2019, TB was among the primary causes of mortality by an infectious disease, surpassing human immunodeficiency virus (HIV) /AIDS. TB is the second-most common infectious killer in the world, behind COVID-19, and the thirteenth-leading cause of death.[5,6] TB is deemed a global pulmonary health crisis that can infect people of all age groups, largely affecting adults.[6] The World Health Organization (WHO) estimates that there are roughly 10.4 million new cases of TB each year and about 1.8 million people die from TB yearly.[6] Roughly 3 million (one-third) of the new TB cases are still unknown to the health system, and numerous people that are infected are not given the correct treatment. The majority of TB cases in developing nations were found in South-East Asia (29%), followed by Africa (27%) and the Western Pacific (19%). More than 95% of reported deaths took place in developing nations, and India alone is responsible for 26% of all TB cases.[7]

The fight against TB is greatly affected by restrained poverty and the effectiveness of regional health care systems and is further complicated by the fast increasing prevalence of antibiotic-resistant *Mtb* strains.[5] With a treatment success rate of just around 50% for multidrug-resistant (MDR) and 23% for extensively drug-resistant (XDR)-TB, the rise of MDR and XDR strains to the current medicines is a global public health concern.[8,9] Factors such as an unhealthy lifestyle, malnutrition, alcohol misuse, and poverty have drastically increased the

number of multi-drug resistance *Mtb* strains cases in recent years.[5] Regimens that will be effective against MDR-TB and XDR-TB isolates need to be developed.

1.3 Pathogenesis of TB

Mtb is an airborne transmittable particle of 1-5 microns in diameter, called droplet nuclei. People with pulmonary TB can disseminate the infectious droplet when they sneeze, shout, or cough. Once a person inhales the droplet nuclei containing *Mtb* (Figure 2 (**1)**), they travel to the alveoli in the lungs, where they are engulfed by the alveolar macrophages (Figure 2 (**2)**). Most of these tubercle bacteria are destroyed or inhibited while a few may multiply inside the cell and become released just after the macrophages die.[10] If the bacilli persist, they may travel through the bloodstream or lymphatic systems to other organs where TB disease may manifest, including the kidneys, bones, apex of the lung, brain, and local lymph nodes. The immune system is commanded to have a systemic response to this spreading process.[10]

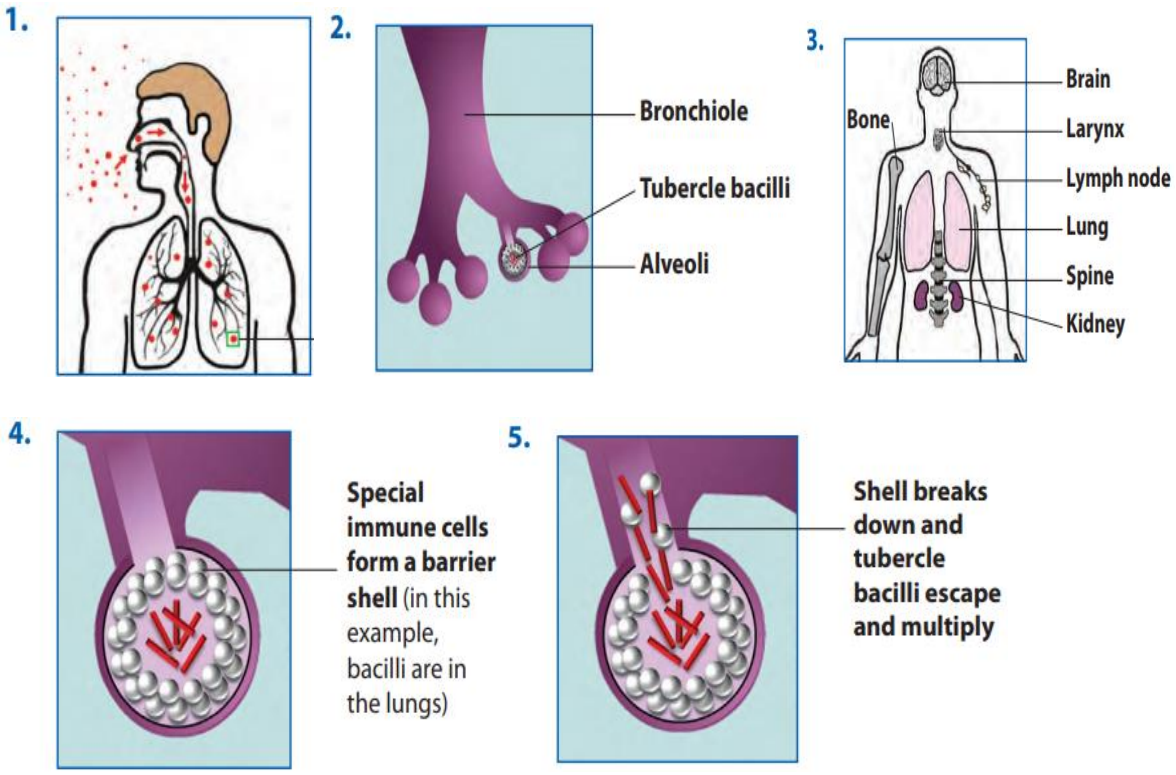


Figure 2: Pathogenicity of *Mtb*. [10]

The outcome of being exposed to TB depends on how the immune system responds and environmental variables. Furthermore, bacterial factors are involved as suggested by the global genomic diversity in the MTBC.[11] TB is better acknowledged as a spectrum instead of

one clinical entity. It normally does not cause symptoms instantly, instead it usually goes through three stages:

1.3.1 Primary TB infection or exposure:

Infection with *Mtb* begins when a person breathes in airborne bacteria. There are no TB symptoms at the early stages of infection, and the person will have an ordinary chest X-ray. For most people, the immune system immediately kills any inhaled bacteria, while TB bacteria are surrounded by macrophages and enter an inactive state for others.[10,12]

1.3.2 Latent TB infection (LTBI)

When TB bacteria are present in the body, but a person exhibits no symptoms and cannot infect others, they are said to have a latent TB infection. Latent TB infection (LTBI) starts when the macrophages ingest the extracellular bacilli and present it to other white blood cells. The immune system is triggered to respond in which most bacilli are killed by white blood cells or encapsulated, resulting in granuloma formation. At this stage, the bacteria enter an inactive state and can remain in this state for years or even a lifetime. The body's immune system can react to tuberculin 2 to 8 weeks after the initial TB infection. The infection can be identified with a tuberculin skin test (TST) or an interferon-gamma release assay (IGRA). The tuberculin is normally stopped from multiplying within a few weeks after infection to stop it from progressing. However, symptoms of active TB may start within weeks of primary infection in specific individuals, including infants, the elderly, and people with compromised immune systems.[12] About 10% of *Mtb* infected people develop TB disease in a lifetime and the probability is approximately 8% per annum for immunocompromised persons.[11]

1.3.3 Active TB disease:

For some persons, the tubercle bacilli can overpower the immune system and proliferate, progressing from dormant TB to TB illness. The bacteria multiplies in the body, causing noticeable symptoms including; shortness of breath, chest pain, coughing, sometimes with phlegm, fatigue, fever, weakness, slimming, and wheezing. This is the time when the disease can spread to other individuals. The transition from LTBI to TB illness can occur at any moment, from right away to years later. [10]

1.4 Diagnosis and vaccination

An acid-fast bacilli (AFB) smear and culture using bodily fluid or tissue from the illness site can be used to diagnose tuberculosis (TB). Microscopic analysis of sputum smears is mostly utilized in low- and middle-income countries (LMICs) to diagnose suspicious patients. The disadvantage of this examination is that it can detect at most 50 to 60% of all cases (smear-positive). Recently, there have been advancements in detection methods that are more sensitive and capable of identifying drug-resistant TB strains, but they are also more expensive. The illness has a greater likelihood of spreading if longer time passes between the time of the illness' commencement and the point at which a diagnosis is obtained and treatment is started.[10,13]

TB vaccination is a way of preventing infection in individuals who have not been infected with the *Mycobacterium tuberculosis*. Bacillus Calmette-Guérin(BCG) is a popular TB vaccine created using attenuated *M. Bovis* bacilli administered through injection. The BCG vaccine is still the most extensively used in the world, however, its efficiency varies greatly depending on the region and is only partially effective. Modeling indicates that more potent vaccines would be needed to eradicate TB.[14]

1.5 Current anti-TB drugs approved by the FDA

Small organic molecules are typically used as medicines to treat TB. Drugs such as isoniazid, pyrazinamide, rifampicin and ethambutol are used as a first-line treatment option. By using the recommended dosage of these anti-TB medications, TB that is treatable by these medications can be cured in six months. In cases where resistance to these first-line anti-TB medications is noticed, known as MDR-TB, then the second-line anti-TB drugs are administered, which include aminoglycosides, D-cycloserine, protionamide, capreomycin, ethionamide, aminosalicylic acid and fluoroquinolones.[15] The resistance of *Mtb* to first-line drugs, mainly isoniazid and rifampicin, has made TB the leading burden globally for the past two decades. The surge in MDR-TB cases has resulted in the usage of second-line medications, which are extremely expensive, toxic, and require long-term treatment, which results in low patient compliance.[7] The currently available anti-TB drugs can also cause other health complications, such as kidney failure liver, or heart disorder, hearing or visual impairment and psychosis. The adverse effects of frequently administered anti-TB medications may be minor or even fatal.[5]

The fight against antimicrobial resistance has a negative economic and social impact and threatens global health since it increases the cost of medical care, lengthens hospital stays, and restricted availability of effective treatments, particularly in economically deprived places. Due to the high expense of medication, the increasing prevalence of MDR-TB, and the negative side effects of the treatments that are now available, research on the treatment of TB has gained popularity once more. The first- and second-line anti-TB medications work similarly in that they inhibit *Mtb* from synthesizing DNA, RNA, proteins, and components of cellular membranes (Figure 3).[16] To treat the drug-resistant forms of TB, creating new anti-TB medications with a distinct mode of action is crucial.

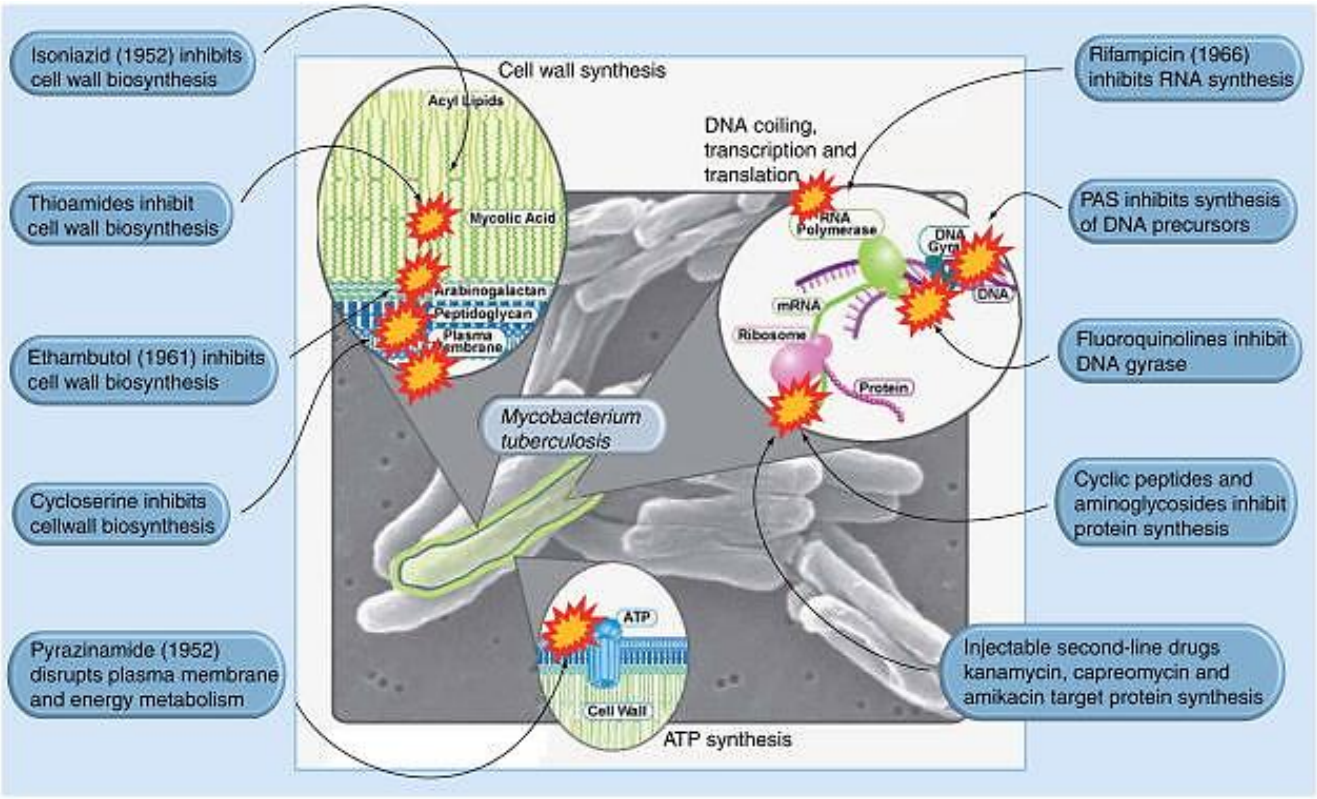


Figure 3: Mechanism of action of current TB drugs.[17]

1.6 Antimicrobial Resistance or acquired resistance

Drug resistance develops naturally and randomly as a result of genetic mutation or horizontal gene transfer carried out by phages, plasmids, or transposon elements.[18] The abuse of antibodies as well as widespread overuse of antibiotics and other antimicrobial compounds can also cause drug resistance. In some cases, this resistance can occur to the point that multi-drug-resistant microbes lead to infections that cannot be treated. Chromosome alterations

under the selective pressure of antibiotic usage are the primary cause of resistance in *Mtb*. Because antibiotic resistance helps mutants survive under selective pressure, it becomes a fundamental property of populations of *Mtb*, which is a strong example of Darwin's theory of evolution.[2]

The prodrugs ethionamide and isoniazid must be activated by redox enzymes in the cytoplasm of *Mtb* in order to become cytotoxic. The prodrug is activated during this process, generating reactive oxygen and radicals with mycobactericidal activity. Yet, since these reactive oxygen and radicals do not destroy the *Mtb* cell, they will promote cellular mutagenesis and the establishment of drug-resistance mutations.[2]

The known mechanism that microbes use to develop drug resistance includes changing the site that the drug targets, inactivating the drug with enzymes, changing the metabolic pathway and adjustments of the cell membrane, which lowers the permeability of the drug molecule.[19] Because of how diverse and specific the modes of resistance are, the hunt for novel antimicrobials usually focuses on discovering new compounds with non-specific killing mechanisms.[20] Antimicrobial peptides are in the group of molecules that have presently attracted attention in research because of their broad-spectrum antimicrobial activity at low concentrations.

1.7 Antimicrobial peptides (AMPs).

Antimicrobial peptides are peptides that are naturally occurring and their derivatives form a class of essential biopharmaceuticals and are currently gaining the interest of researchers. The market for antimicrobials currently contains more than 60% natural compounds or their derivatives.[21] AMPs act as the first line of innate immune response in numerous multicellular organisms and can starve off viral, fungal, and bacterial infections.[22]

Anti-TB peptides and peptidomimetics have emerged as crucial and growing classes of chemotherapeutic agents. Within the many promising anti-mycobacterial agents examined in the last few decades, it has been proven that anti-TB peptides have a current success rate of roughly twice that of small molecule drugs. These peptides have various advantages, including selective affinity to the negatively charged cell wall of the bacteria, different mechanisms of action, and fewer off-target side reactions and hence fewer side effects.[5]

1.8 Ribosomally synthesized and Post translationally modified peptides (RiPPs)

A class of natural compounds known as peptide antibiotics can be derived from ribosomes or other sources. The family of RiPPs is structurally diverse and how they function. During their biosynthetic pathway, the precursor peptide, which is genomically encoded to comprise of an N-terminal leader sequence and a C-terminal core sequence, is converted into the final natural product using one or more enzymes (Figure 4**A**). The enzymes that are in charge of the posttranslational changes in the C-terminal core recognizes the RiPP precursor by its leader sequence. The precursor peptide is then transformed into the natural product, and the N-terminal leader peptide, becomes cleaved off during the biosynthesis of RiPP resulting in the mature RiPP (Figure 4**B**).[23] In several RiPP gene clusters, specific transport and regulatory genes are encoded. RiPPs natural products acquire significant chemical and functional diversity by employing this tactic.[23]

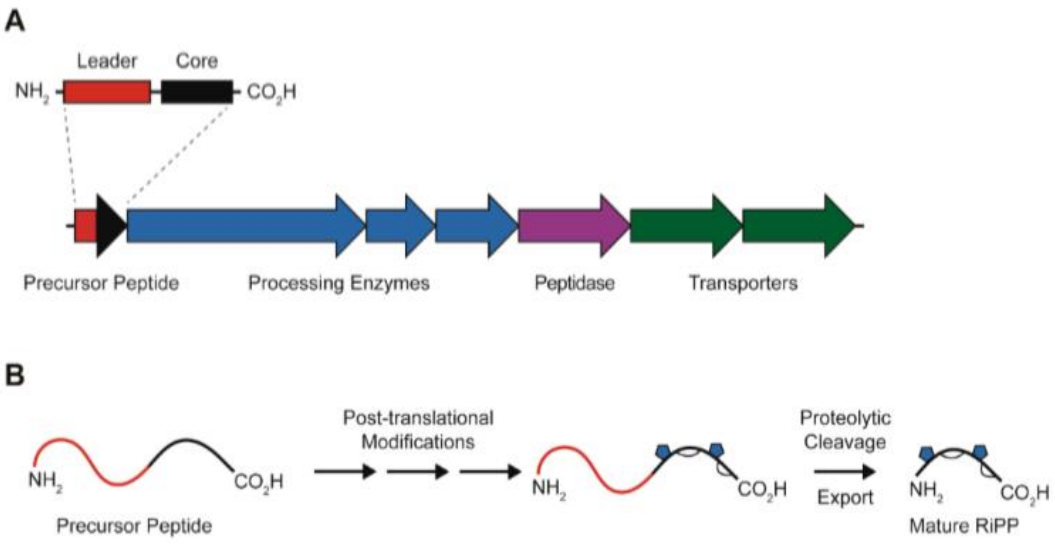


Figure 4: The biosynthesis of RiPPs. A) General overview of RiPP biosynthetic gene clusters. B) Procesess where the precursor peptide is turned into the mature RiPP.[23]

Although several RiPP sub-families have been studied, the lasso peptides, one of the most recent sub-families, will be the focus of this study.

1.9 Lasso peptides

Lasso peptides are obtained from a gene-encoded precursor protein like all RiPPs and require two enzymatic activities in their biosynthesis, the first to cleave the leader peptide from the precursor. The free core peptide N-terminus formed from this process is turned into the

isopeptide bond that is characteristic of lasso peptide fold by the other enzyme. In contrast to other popular peptide antibiotics, the lasso peptides are structurally and functionally unique due to the post-transitional modifications which tie the linear peptide in a knot. The length of these peptides varies with the longest peptide made of 24 amino acids and the shortest consisting of 14 amino acid residues. An N-terminal macrocycle is produced when the N-terminal amine is linked to a carboxyl group on a glutamate or aspartate residue in the 7th, 8th, or 9th position by the characteristic isopeptide bond. (Figure 5**A**).[23]

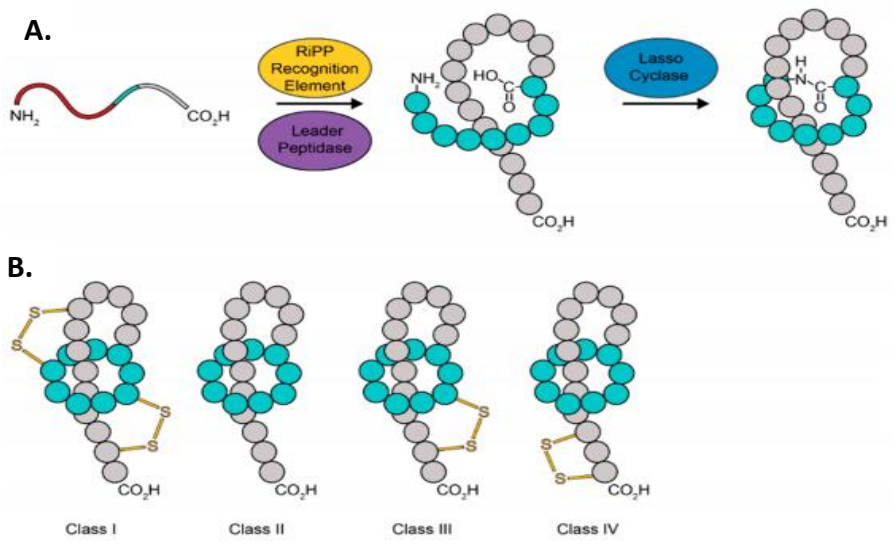


Figure 5: A) The production of a mature lasso peptide from the precursor peptide. B) The four different classes of lasso peptides.[23]

The number and placement of the intramolecular disulphide bridges in the lasso peptides separates them into four further subclasses. The macrocyclic ring and the threaded tail are connected by two disulphide bridges in class I peptides. The lasso peptides belonging to class II lack disulphide bridges while those in class III and IV each have a single disulphide bridge. For class III peptides, the disulphide occurs between the N-terminal ring and the carboxyl-terminus tail; for class IV peptides, it connects the carboxyl-terminus tail to itself (Figure 5**B**).[23,24]

The known lasso peptides show various types of bioactivity and majority of them are medically applicable. Most importantly, it has been discovered that at least 14 lasso peptides exhibit antimicrobial activity against both Gram-positive and Gram-negative bacteria.

Particularly, some lasso peptides, like lassomycin and lariatin A/B, show biological activity against *Mycobacterium* sp., while other lasso peptides, including siamycin-I and LP2006, exhibit bioactivity against Gram-positive pathogens.[23] Approximately 8 antibacterial lasso peptides (Figure 6) have been linked to a cellular or molecular target among all lasso peptides that have been described; and for most cases, the action mechanisms are still unknown.

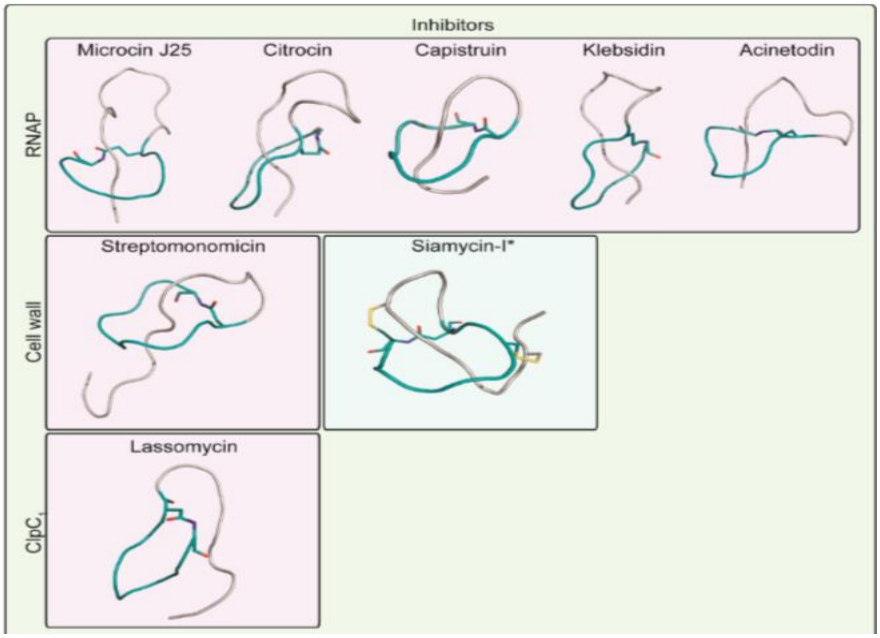


Figure 6: The secondary structures of lasso peptides with a molecular target that is known.[23]

Lassomycin, Ecumicin and CyclomarinA (CymA) are cyclic lasso peptides that contain a macro-lactam ring and are usually threaded; they target the acidic region of the *Mycobacterium* caseinolytic protease.[25]

Out of all the lasso peptides that are reported, lassomycin and lariatins uniquely display significant anti-TB activity. Lariatins and lassomycin (Figure 7) have become particularly popular in the field of total synthesis as well as in a number of other fields like biosynthesis, bioengineering, and structure-activity studies due to their characteristic threaded structure and the unusual bactericidal behavior toward *Mtb*. [23]

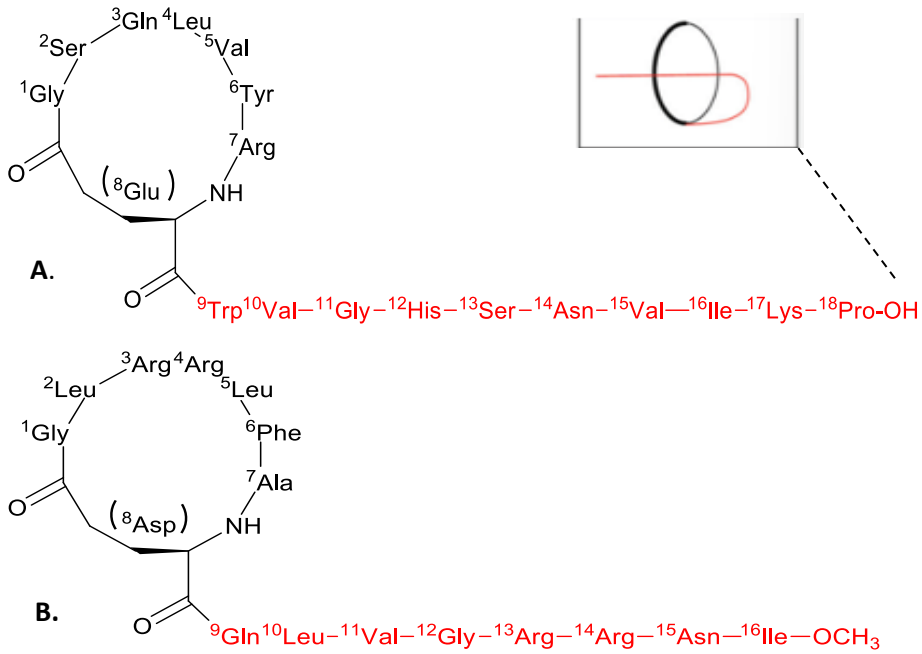


Figure 7: The structures of A) lariatin A and B) lassomycin.[26]

1.10 Lariatin A

Lariatins (Figure 8) were discovered in the year 2005 during the screening of antibiotics that particularly targeted *Mycobacterium smegmatis*. Lariatin A and Lariatin B were successfully extracted from Rhodococcus sp. K01-B0171 culture broth. They were identified as distinct cyclic peptides by spectral analysis and sophisticated protein chemistry techniques. These antimycobacterial compounds consist of 18 and 20 L-amino acid residues, respectively with an internal connection between the γ-carboxyl group of glutamic acid and the R-amino group of Glycine. The lariatin's three-dimensional structure, according to information gathered from nuclear magnetic resonance data, has a link between Gly1 and Glu8—through which the C-terminal tail (Trp-Pro) passes. This allows the lariatins to form a macrolactone ring. The thick His12 and Asn14 encircle the threaded tail within the ring.[27]

The hydrophobic regions and the polar residues were found to be distributed uniquely on the lariatin molecule. On the surface, there are three major hydrophobic regions: the side chains of Leu4 and His12, Val5, Tyr6, and Ile16, and Trp9 and Val10. Additionally, there are three residues with polar side chains: Ser2, Gln3, and Asn14, as well as the side chain of Arg7 with a positive charge on the opposite side. The lasso structure of lariatins A and B, along with their resistance to proteases, may account for their biological actions and protease resistance.[27]

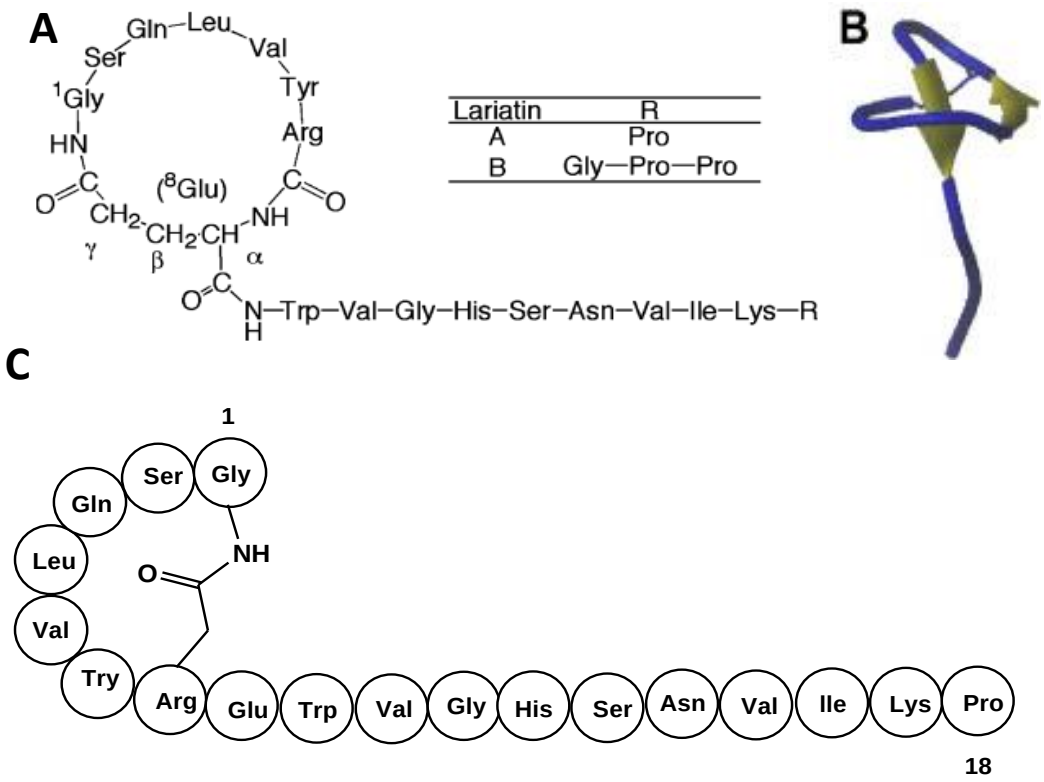


Figure 8: A and B) the structure of lariatin A and B.[27] C) Simplified version of Lariatin A.

1.11 Activity and Biological target of lariatin A

The Lariatins A and B inhibitory activity against the growth of *Mycobacterium smegmatis* was tested using the agar dilution method, and their minimum inhibitory concentrations (MICs) were 3.13 and 6.25 g/ml, respectively. Also, using the liquid microdilution method, lariatin A suppressed the growth of *Mycobacterium tuberculosis* with a MIC value of 0.39 g/ml.[27] The study showed that the lariatins' target molecule may persist inside the biosynthetic processes of the mycobacteria's distinctive cell wall (CW) structure. *Mycobacterium's* distinctive CW structural components are synthesized by several different enzymes. First-line anti-TB medications are isoniazid and ethambutol, which impede CW biosynthesis. Isoniazid target and block the function of Type II fatty acid synthase, which is responsible for mycolic acid synthesis. In contrast, ethambutol acts on arabinosyl transferase to prevent the development of arabinogalactan mycolate. It is interesting to note that these two medications specifically decrease mycobacterial growth. Lariatins share biological properties, hence it is conceivable that mycobacteria's cell wall is their target.[27]

Although the target site for Lariatin A has been hypothesized to be within the cell wall of *Mtb*, we believe that due to the structural similarities between Lariatin A and Lassomycin (Figure 7), they might have the same target. Lassomycin is a cyclic peptide from actinomycetes that has shown potent anti-TB activity against MDR and XDR *Mtb* and drug-susceptible *Mtb in vitro*. The target site of this antibiotic is the caseinolytic protease (ClpC), a protein essential for *Mtb* growth.[28]

1.12 Biological role of ClpC

Recently, there has been increased interest in the mycobacterial caseinolytic protease as a genetically and pharmacologically confirmed therapeutic target for TB. The mycobacterial caseinolytic protease (ClpP) is a degradative protease machine with a role in proteome housekeeping, comparable to the human proteasome.[29] A member of the AAA+ group of proteases, ClpP is a multi-subunit barrel-shaped complex, and related AAA+ ATPases strictly control its activity.[30] The Clp protease complex is made up of a degradative chamber consisting of two different serine protease subunits, ClpP1 and ClpP2, encoded by the clpP1P2 operon, which engages with unfoldases to recognize and transport proteins into the degradation chamber.[31] The catalytic sites are made up of a triad of serine (Ser), histidine (His) and aspartic acid (Asp) residues which are accessed via the axial openings (Figure 9**A**). On the catalytic side, the Ser residue cleaves the substrates, and the Asp residue stabilizes the complex. The complex is compressed when the Ser and His residues are further apart, resulting in no substrate degradation. An adenosine triphosphate enzyme (ATPase) binds to the ClpP to form a proteolytic complex (Clp) with an extended conformation to activate proteolysis. ATPase stores and provides the energy needed for substrate degradation. The caseinolytic enzyme (ClpC1) is an ATPase that belongs to the AAA+ superfamily of chaperons in *Mtb*. ClpC1 binds to the N-terminal region of the ClpP through hydrophobic pockets. The Ser and His residues in the extended state are closer and activated for substrate degradation (Figure 9**B**).[30]

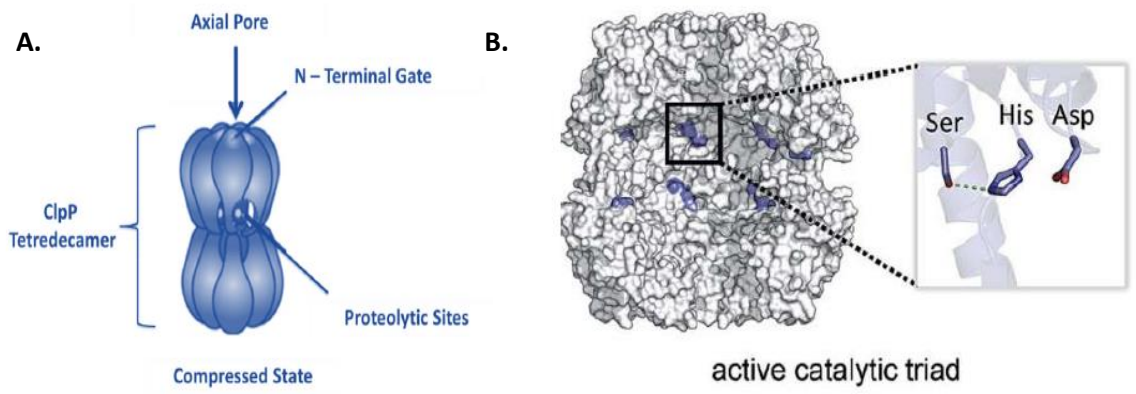


Figure 9: **A**) The model representing a compressed state of the Clp protease and **B**) structure of the caseinolytic protease with the serine catalytic site. [30]

The removal of translation products that were co-translationally tagged with the 11-amino-acid SsrA recognition sequence is one of the tasks performed by Clp.[31] The ClpC1 unfolds the folded, damaged and misfolded protein substrates tagged with a degradation signal. Furthermore, the ClpC1 translocates the unfolded substrates to the ClpP catalytic sites for degradation in an ATPase dependent-fashion where they are cleaved into smaller peptides (Figure 10). ClpP that is not bound to ClpC1 is unable to degrade protein substrates, however it can degrade peptides[30,32]

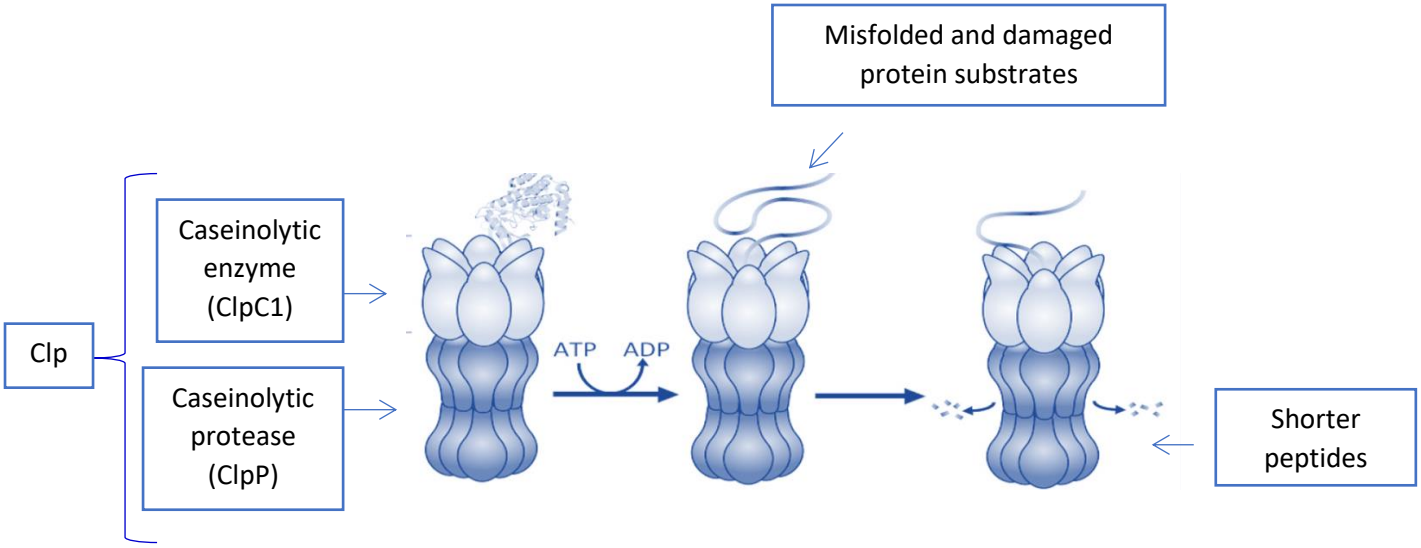


Figure 10: The proteolysis of protein resulting from the interaction of ClpC1 and the caseinolytic protease.[30]

1.12.1 Mode of action

Lassomycin has been used to conduct more thorough research on the inhibition of ClpP. Lassomycin binds to the very acidic area of ClpC1 with the extremely basic arginine (Arg) residues, according to X-ray studies. The docking studies revealed that the glutamine residue at position 17 (Gln17) in the ClpC1 forms a hydrogen bond with the lassomycin. As the ClpC1 can unfold the substrates in the presence of lassomycin, both the lassomycin and protein substrates bind to the ClpC1 at distinct locations (Figure 11).[28] The precise reason for *Mtb* cell death is unknown. Some studies have reported that cell death may be caused by toxicity from protein substrate accumulation when lassomycin binds to and decouples the ClpC1 from ClpP, making the protease inactive (Figure 11), or by the uncontrolled and non-selective unfolding of proteins as a result of the 10-fold increase in unfolding activity.

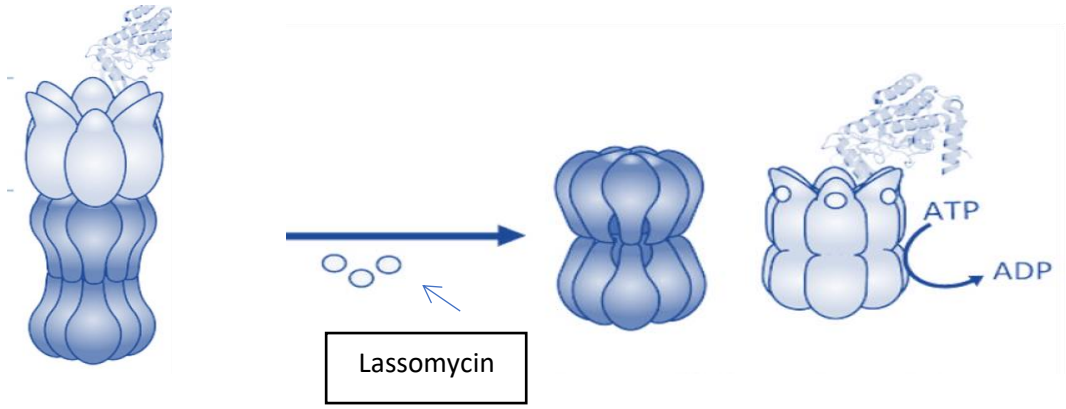


Figure 11: Mode of action of lassomycin where it decouples the ClpC1 from the ClpP inhibiting proteolysis.[30].

1.13 AMP limitations

AMPs like Lariatins are an important and efficient part of the innate immune response system. Additionally, they have been efficient in *in-vitro* tests against a variety of pathogens. Only a few AMP-based therapeutic agents have been authorized to be used in clinical settings. Three factors make AMPs unsatisfactory for therapeutic applications: cytotoxicity, stability, and cost. More on these will be covered in the literature study that follows. Peptidomimetics, like peptoids, have become a more plausible prospect for medicinal development due to AMPs drawbacks.

2. Aim and objectives

2.1 Aim:

The aim of this project was to design and synthesize Lariatin A derivatives and investigate their binding affinity to the *Mycobacterium tuberculosis* caseinolytic protease.

2.2 Objectives

The following outlined objectives were applied to achieve the aim of the project:

- To develop synthetic procedures for the synthesis of lariatin A peptidomimetics using the solid phase peptide synthesis technique as well as designing derivatives with a shorter synthetic route.
- To incorporate two cysteine residues onto the sequence to allow for cyclization of the peptide via a disulfide bond.
- To incorporate adamantane and palmitic acid moieties onto the shorter sequences to increase the hydrophobicity of the peptide and enhance their membrane permeability.
- To synthesize peptoid derivatives with improved protease stability.
- To evaluate the biological activity of the peptides against the *Mycobacterium tuberculosis* caseinolytic protease.

3. Hypothesis and Questions

3.1 Hypothesis

To date, lariatins are presumed to target the cell wall of the *Mycobacterium tuberculosis* although their mechanism of action has not been proven. However due to their structural similarities to the cyclic lasso peptides which act by inhibiting the *Mycobacterium tuberculosis* caseinolytic protease we hypothesize that lariatin A derivatives conjugated to lipophilic molecules can penetrate the bacterial cell wall and inhibit the caseinolytic protease by binding to the same site as lasso peptides such as lassomycin.

3.2 Research question

Our main research question is, can naturally occurring lariatin A and its derivatives be synthesized using the solid phase peptide synthesis strategy and can they bind to the *mycobacterium tuberculosis* caseinolytic protease?

4. Novelty of the study

Lariatin A has been reported to show biological activity against *Mtb*. However, to date, no work has been reported on synthesizing its peptidomimetics. The derivatives reported herein are the first lariatin A derivatives.

5. Overview of the thesis

Chapter 1

This introductory chapter provides a brief summary of tuberculosis disease, the threat posed by antibiotic resistance and the potential for Antimicrobial peptides (AMPs) and their derivatives to aid in combating this issue. The structural activity of antimicrobial peptoids and their usage as novel antibacterial agents to counteract the growth of antimicrobial resistance are given special consideration.

Chapter 2

The second part of this thesis details the design and synthesis of Lariatin A peptidomimetics and the synthetic method. A total of six peptidomimetics were designed and synthesized following the solid phase peptide synthetic procedure.

Chapter 3

This chapter formally describes the design and synthesis of novel Lariatin A peptoids. A total of two peptoids were designed and synthesized using the submonomeric method.

Chapter 4

The fourth chapter details the biological screening of the Lariatin A peptidomimetics from chapter 2.

Chapter 5

The structural elucidation and characterization of selected peptidomimetics are discussed using NMR (nuclear magnetic resonance) and CD (circular dichroism) to determine possible folding patterns and secondary structural features.

Chapter 6

This chapter summarizes the results obtained in the presented work in this dissertation, the conclusion, and recommendations for future work.

Chapter 7

This chapter provides a list of reagents and a description of the major equipment and instrumentation used to conduct this research.

References

(1) Cheng, Y.-L.; Lee, C.-Y.; Huang, Y.-L.; Buckner, C. A.; Lafrenie, R. M.; Dénommée, J. A.; Caswell, J. M.; Want, D. A.; Gan, G. G.; Leong, Y. C.; Bee, P. C.; Chin, E.; Teh, A. K. H.; Picco, S.; Villegas, L.; Tonelli, F.; Merlo, M.; Rigau, J.; Diaz, D.; Masuelli, M.; Korrapati, S.; Kurra, P.; Puttugunta, S.; Picco, S.; Villegas, L.; Tonelli, F.; Merlo, M.; Rigau, J.; Diaz, D.; Masuelli, M.; Tascilar, M.; de Jong, F. A.; Verweij, J.; Mathijssen, R. H. J. Virulence Factors and Pathogenicity of Mycobacterium. *Intech* **2016**, *11* (tourism), 13.

(2) Nguyen, L. Antibiotic Resistance Mechanisms in M. Tuberculosis: An Update. *Arch Toxicol 90* **2016**, *90*, 1585–1604.

(3) Todar, K. Mycobacterium Tuberculosis and Tuberculosis (Page 1). *Todar's Online Textb. Bacteriol.* **2020**, 1.

(4) Vilchèze, C.; Jr, W. R. J. The Isoniazid Paradigm of Killing, Resistance, and Persistence in Mycobacterium Tuberculosis. **2019**, *431* (18), 3450–3461. https://doi.org/10.1016/j.jmb.2019.02.016.

(5) Kolbe, K.; Veleti, S. K.; Reiling, N.; Lindhorst, T. K. Lectins of Mycobacterium Tuberculosis –Rarely Studied Proteins. *Beilstein J. Org. Chem.* **2019**, *15*, 1–15. https://doi.org/10.3762/bjoc.15.1.

(6) *Global Tuberculosis Report 2022*; 2022; Vol. 13.

(7) Khusro, A.; Aarti, C.; Agastian, P. Anti-Tubercular Peptides: A Quest of Future Therapeutic Weapon to Combat Tuberculosis. *Asian Pac. J. Trop. Med.* **2016**, *9* (11), 1023–1034. https://doi.org/10.1016/j.apjtm.2016.09.005.

(8) Catalão, M. J.; Filipe, S. R.; Pimentel, M. Revisiting Anti-Tuberculosis Therapeutic Strategies That Target the Peptidoglycan Structure and Synthesis. *Front. Microbiol.* **2019**, *10* (FEB), 1–11. https://doi.org/10.3389/fmicb.2019.00190.

(9) Casper, C.; Crane, H.; Menon, M.; Money, D. HIV/AIDS Comorbidities: Impact on Cancer, Noncommunicable Diseases, and Reproductive Health. *Dis. Control Priorities, Third Ed. (Volume 6) Major Infect. Dis.* **2017**, 45–66. https://doi.org/10.1596/978-1-4648-0524-0_ch3.

(10) Chapter 2 Transmission and Pathogenesis of Tuberculosis; pp 19–44.

(11) Coscolla, M.; Gagneux, S. Does M. Tuberculosis Genomic Diversity Explain Disease Diversity? *Drug Discov. Today Dis. Mech.* **2010**, *7* (1), 1–26. https://doi.org/10.1016/j.ddmec.2010.09.004.

(12) Drain, P. K.; Bajema, K. L.; Dowdy, D.; Dheda, K.; Naidoo, K.; Schumacher, S. G. Crossm Incipient and Subclinical Tuberculosis : A Clinical Review of Early Stages and Progression of Infection The Spectrum of Tuberculosis Infection to Disease. *Clin. Microbiol. Rev.* **2018**, 1–24.

(13) Chakravorty, S.; Sen, M. K.; Tyagi, J. S. Diagnosis of Extrapulmonary Tuberculosis by Smear, Culture, and PCR Using Universal Sample Processing Technology. *J. Clin. Microbiol.* **2005**, *43* (9), 4357–4362. https://doi.org/10.1128/JCM.43.9.4357-4362.2005.

(14) O'Shea, M. K.; McShane, H. A Review of Clinical Models for the Evaluation of Human TB Vaccines. *Hum. Vaccines Immunother.* **2016**, *12* (5), 1177–1187. https://doi.org/10.1080/21645515.2015.1134407.

(15) Cegielski, J. P.; Chan, P. C.; Lan, Z.; Udwadia, Z. F.; Viiklepp, P.; Yim, J. J.; Menzies, D. Aminoglycosides and Capreomycin in the Treatment of Multidrug-Resistant Tuberculosis: Individual Patient Data Meta-Analysis of 12 030 Patients from 25 Countries, 2009-2016. *Clin. Infect. Dis.* **2021**, *73* (11), E3929–E3936. https://doi.org/10.1093/cid/ciaa621.

(16) Reddy, D. S.; Sinha, A.; Kumar, A.; Saini, V. K. Drug Re-Engineering and Repurposing: A Significant and Rapid Approach to Tuberculosis Drug Discovery. *Arch. Pharm. (Weinheim).* **2022**, *355* (11). https://doi.org/10.1002/ardp.202200214.

(17) Kumar, K.; Awasthi, D.; Berger, W. T.; Tonge, P. J.; Slayden, R. A.; Ojima, I. Discovery of Anti-TB Agents That Target the Cell-Division Protein FtsZ. *Future Med. Chem.* **2010**, *2* (8), 1305–1323. https://doi.org/10.4155/fmc.10.220.

(18) Von Wintersdorff, C. J. H.; Penders, J.; Van Niekerk, J. M.; Mills, N. D.; Majumder, S.; Van Alphen, L. B.; Savelkoul, P. H. M.; Wolffs, P. F. G. Dissemination of Antimicrobial Resistance in Microbial Ecosystems through Horizontal Gene Transfer. *Front. Microbiol.*

2016, *7* (FEB), 1–10. https://doi.org/10.3389/fmicb.2016.00173.

(19) Zhang, F.; Cheng, W. The Mechanism of Bacterial Resistance and Potential Bacteriostatic Strategies. *Antibiotics* **2022**, *11* (9). https://doi.org/10.3390/antibiotics11091215.

(20) Hancock, R. E. W.; Falla, T. J. Antimicrobial Peptides: Broad-Spectrum Antibiotics from Nature. *Clin. Microbiol. Infect.* **1996**, *1* (4), 226–229. https://doi.org/10.1016/s1198-743x(15)60279-8.

(21) Choudhary, A.; Naughton, L. M.; Montánchez, I.; Dobson, A. D. W.; Rai, D. K. Current Status and Future Prospects of Marine Natural Products (MNPs) as Antimicrobials. *Mar. Drugs* **2017**, *15* (9). https://doi.org/10.3390/md15090272.

(22) Diamond, G.; Beckloff, N.; Weinberg, A.; Kisich, K. O. The Roles of Antimicrobial Peptides in Innate Host Defense. *Curr. Pharm. Des.* **2009**, *15* (21), 2377–2392. https://doi.org/10.2174/138161209788682325.

(23) Tan, S.; Moore, G.; Nodwell, J. Put a Bow on It: Knotted Antibiotics Take Center Stage. *Antibiotics* **2019**, *8* (3). https://doi.org/10.3390/antibiotics8030117.

(24) Tietz, J. I., Schwalen, C. J., Patel, P. S., Maxson, T., Blair, P. M., Tai, H. C., Zakai, U. I., & Mitchell, D. A. A new genome-mining tool redefines the lasso peptide biosynthetic landscape. *Nature Chemical Biology*. **2017**, *13* (5), 470–478. https://doi.org/10.1038/nchembio.2319.

(25) Gao, W.; Kim, J. Y.; Anderson, J. R.; Akopian, T.; Hong, S.; Jin, Y. Y.; Kandror, O.; Kim, J. W.; Lee, I. A.; Lee, S. Y.; McAlpine, J. B.; Mulugeta, S.; Sunoqrot, S.; Wang, Y.; Yang, S. H.; Yoon, T. M.; Goldberg, A. L.; Pauli, G. F.; Suh, J. W.; Franzblau, S. G.; Cho, S. The Cyclic Peptide Ecumicin Targeting CLpC1 Is Active against Mycobacterium Tuberculosis in Vivo. *Antimicrob. Agents Chemother.* **2015**, *59* (2), 880–889. https://doi.org/10.1128/AAC.04054-14.

(26) De Leon Rodriguez, L. M.; Kaur, H.; Brimble, M. A. Synthesis and Bioactivity of Antitubercular Peptides and Peptidomimetics: An Update. *Org. Biomol. Chem.* **2016**, *14* (4), 1177–1187. https://doi.org/10.1039/c5ob02298c.

(27) Iwatsuki, M.; Tomoda, H.; Uchida, R.; Gouda, H.; Hirono, S.; Omura, S. Lariatins, Antimycobacterial Peptides Produced by Rhodococcus Sp. K01-B0171, Have a Lasso Structure. *J. Am. Chem. Soc.* **2006**, *128* (23), 7486–7491. https://doi.org/10.1021/ja056780z.

(28) Gavrish, E., Sit, C. S., Cao, S., Kandror, O., Spoering, A., Peoples, A., Ling, L., Fetterman, A., Hughes, D., Bissell, A., Torrey, H., Akopian, T., Mueller, A., Epstein, S., Goldberg, A., Clardy, J., & Lewis, K. (2014). Lassomycin, a ribosomally synthesized cyclic peptide, kills mycobacterium tuberculosis by targeting the ATP-dependent protease ClpC1P1P2. *Chemistry and Biology*. **2014**, *21*(4), 509–518. https://doi.org/10.1016/j.chembiol.2014.01.014

(29) Raju, R. M.; Unnikrishnan, M.; Rubin, D. H. F.; Krishnamoorthy, V.; Kandror, O.; Akopian, T. N.; Goldberg, A. L.; Rubin, E. J. Mycobacterium Tuberculosis ClpP1 and ClpP2 Function Together in Protein Degradation and Are Required for Viability in Vitro and during Infection. *PLoS Pathog.* **2012**, *8* (2). https://doi.org/10.1371/journal.ppat.1002511.

(30) Culp, E.; Wright, G. D. Bacterial Proteases, Untapped Antimicrobial Drug Targets. *J. Antibiot. (Tokyo).* **2017**, *70* (4), 366–377. https://doi.org/10.1038/ja.2016.138.

(31) Yoshiyuki Yamada, T. D. Mycobacterial Caseinolytic Protease Gene Regulator ClgR Is a Substrate of Caseinolytic Protease. *Am. Soc. Microbiol.* **2017**, *2* (2), 1–7.

(32) Lupoli, T. J.; Vaubourgeix, J.; Burns-Huang, K.; Gold, B. Targeting the Proteostasis Network for Mycobacterial Drug Discovery. *ACS Infect. Dis.* **2018**, *4* (4), 478–498. https://doi.org/10.1021/acsinfecdis.7b00231.

.

CHAPTER 1.1: Literature review

Review: Structure-activity relationship of antimicrobial peptoids

(Under review in the journal of Pharmaceutics)

Abstract: Due to their broad-spectrum activity against Gram-negative and Gram-positive bacteria, natural antimicrobial peptides (AMPs) and their synthetic analogues have emerged as prospective therapies for treating illnesses brought on by multi-drug resistant pathogens. To overcome the limitations of AMPs, such as protease degradation, oligo-N-substituted glycines (peptoids) are a promising alternative. Despite having the same backbone atom sequence as natural peptides, peptoid structures are more stable because, unlike AMP, their functional side chains are attached to the backbone nitrogen (N)-atom rather than the alpha carbon atom. As a result, peptoid structures are less susceptible to proteolysis and enzymatic degradation. The advantages of AMPs, such as hydrophobicity, cationic character, and amphipathicity, are mimicked by peptoids. Furthermore, structure-activity relationship studies (SAR) have shown that tuning the structure of peptoids is a crucial step in developing effective antimicrobials.

Keywords: Antimicrobial peptides, Antimicrobial peptoids, chain length, cationic, hydrophobicity, cyclization, amphiphilicity

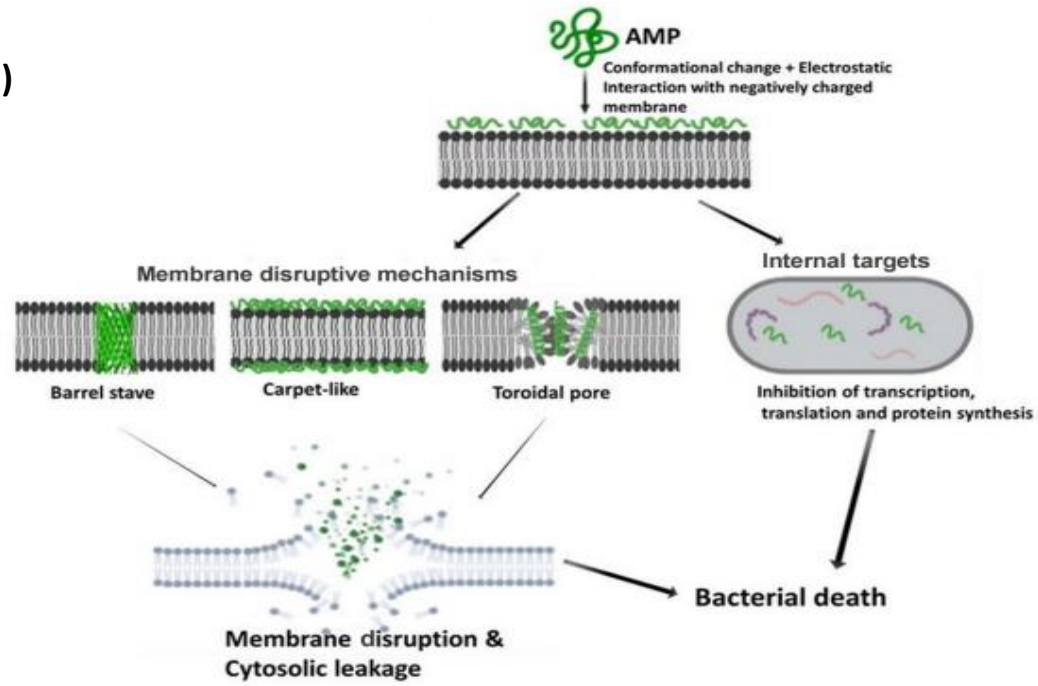
1.1.1 Introduction

The rising concern of antibiotic-resistant microorganisms has prompted a renewed interest in antimicrobial peptides (AMPs), which have good application potential in agriculture, medicine, aquaculture, and food. AMPs are defined as a group of antimicrobial agents capable of fighting infectious diseases in living organisms by killing or inhibiting pathogens.[1,2,3] They exhibit a wide range of activity against diverse microorganisms. Because of their unknown mechanism of action, the majority of bacteria rarely develop resistance against them.[4] According to the antimicrobial peptide database (APD31) revised on 24 August 2020, 3,240 AMPs have been recorded.[5] The common features observed in different types of AMPs are as follows: they are short, with an average of 33.26 amino acids, are amphipathic (having both

hydrophobic and hydrophilic regions), and just about every AMP is cationic (+2 to +9 net charge; average 3.32). Several anionic AMPs contain acidic amino acids, such as aspartic and glutamic acids. [5,6]

Together with hydrophobic interactions with the non-polar lipid acyl chains, the AMPs' amphiphilic structure aids the peptide's initial electrostatic connection with the anionic bacterial membrane lipids.[7] The cationic character of AMPs makes them more selective towards the negatively charged cytomembrane of the bacteria over the zwitterionic membrane of eukaryotes. The broad-spectrum success of AMPs can be attributed to the comprehensive membrane interactions they employ to eliminate foreign bodies in the host. AMPs mainly act by breaking down or disrupting the bacterial cell membrane, while some act via the non-membrane disruptive mechanism (Figure 12**a**). The AMPs class lethal to the cell is through the membrane disruptive mechanism, mostly by permeating the cytomembrane, which releases intracellular material. For the three proposed membrane disruptive mechanisms, namely the Barrel stave, toroidal pore, and carpet-like model, the AMP molecules accumulate and organize parallel to the cytomembrane surface. This is followed by the electrostatic attraction between the bacterial cell envelope that is slightly negative and the partly positive amino acid side-chains in the AMP (Figure 12**b**).[8]

a)



b)

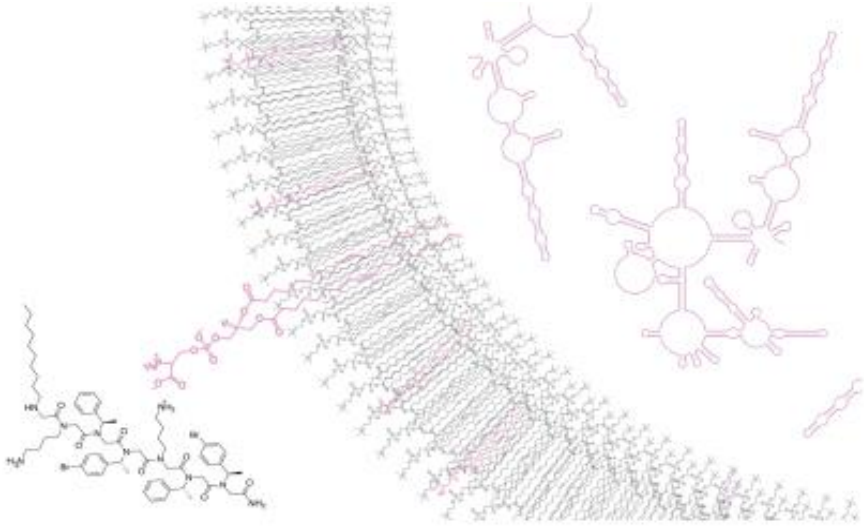


Figure 12: a) The AMPs membrane disruptive and non-membrane disruptive mechanism for killing bacteria.[8] and b) the first electrostatic interaction with negatively charged cell envelope.[9]

The folded peptide will position itself such that the charge centres are situated at the front of the membrane, then weak hydrophobic interactions are established. The non-membrane disruptive AMPs can exert intracellular effects like obstructing the synthesis of the cell wall, protein, and nucleic acid by passing through the cell membrane lipid bilayer without permeabilization.

Host-defense AMPs mainly targeting the bacterial membrane have been previously studied as new antibiotic agents. Despite their effectiveness, AMPs have various drawbacks. They are easily hydrolysed by the protease (*in vivo* protease degradation), which lowers their bioavailability, and their high synthesis costs limit their production. Also, they are unstable at certain pHs and have possible immunogenicity and/or systemic toxicity.[7,10,11,12,13]

These limitations pose a challenge for converting AMPs from the bench to the market as therapeutic agents for infections that have developed resistance to their respective drugs. Ideally, AMP should possess the following qualities: (1) high potency against microbial; (2) low toxicity towards mammalian membranes; (3) stability against protease degradation and the environment; (4) accessible and affordable cost of manufacturing.[6] The design of AMPs that exhibit the desired effect has attracted much attention in research. Much effort has been made to exploit and amplify the features present in naturally occurring AMPs. Therefore,

several non-natural mimics of AMPs with better bioavailability and biostability have been invented and synthesized, thus likely enhancing pharmaceutical suitability.

Oligo-N-substituted glycines (peptoids) are a favourable substitute for AMP. Peptoids have similar backbone atom sequences as AMPs, however, they are less vulnerable to enzymatic and protease breakdown, hence they have a higher potential to be utilized as pharmaceuticals and in biomaterials. Unlike AMP, peptoid functional side chains are anchored to the nitrogen (N)-atom rather than the alpha-carbon (Figure 13).[14] This structure makes peptoids more stable because no investigated protease can recognize and degrade them. Furthermore, there are more options for primary amines with different side chains, which can be included in the peptoid chain through the submonomer synthetic strategy.[15] Due to the peptides' prospective toxicity being a great barrier that limits their clinical use, peptoids' low cytotoxicity respective to the AMP pexiganan further strengthens their therapeutic potential.[16]

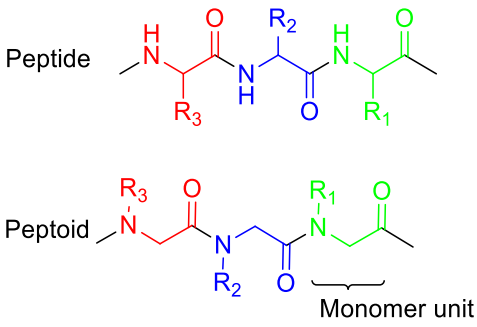


Figure 13: Structure of peptoids vs peptides

The bacterial membrane is more permeable to peptoids than peptides and similar to AMPs, peptoids act by either disrupting the membrane of the bacteria (Figure 14) or by targeting intracellular targets like bacterial DNA. Recent studies have shown the antimicrobial properties of peptoids, such as a cationic and amphipathic dodecamer peptoid 1[17], which displayed biological activity against a wide range of bacteria and fungi. Other studies have suggested that antimicrobial peptoids act through the same mechanism as AMPs due to the retained antimicrobial activity when peptides are translated to peptoids. Knowledge gained in the field of AMPs can be applied in the development of peptoid antibiotics because they mimic AMPs both structurally and functionally.

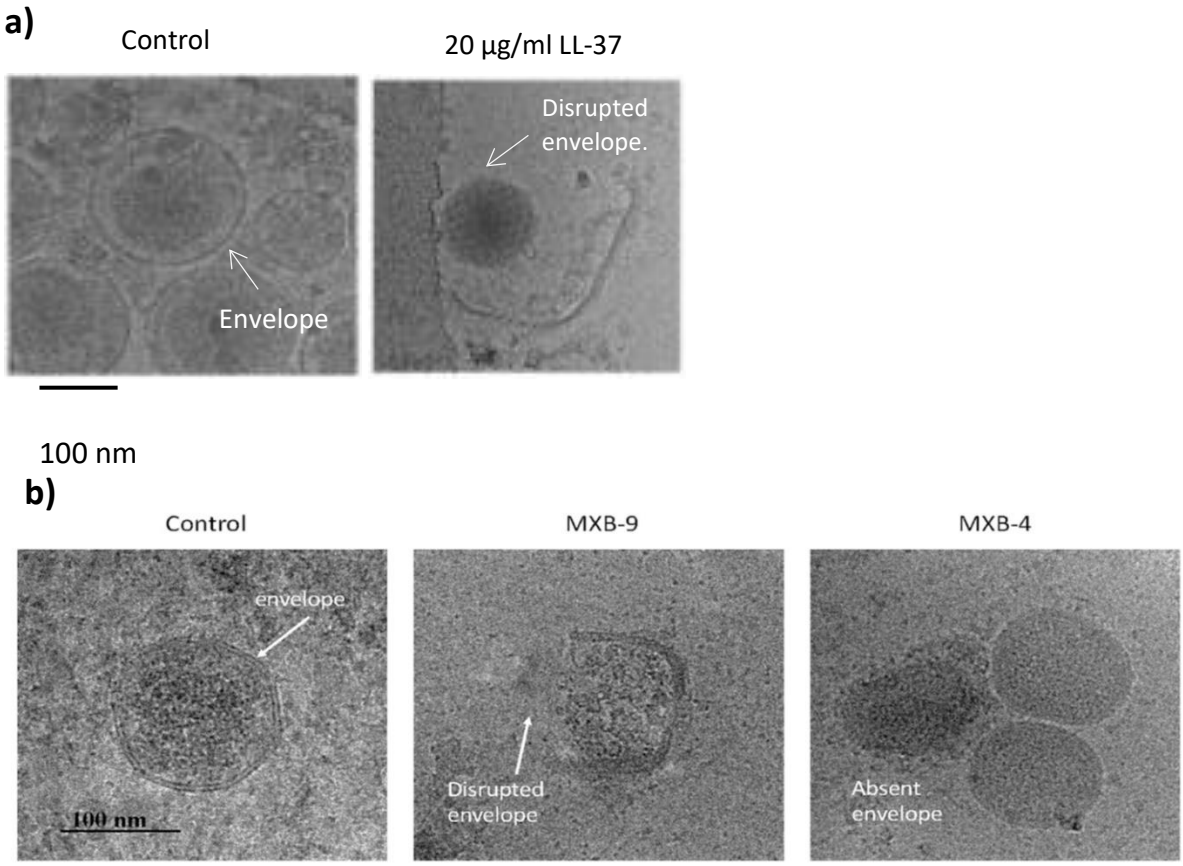
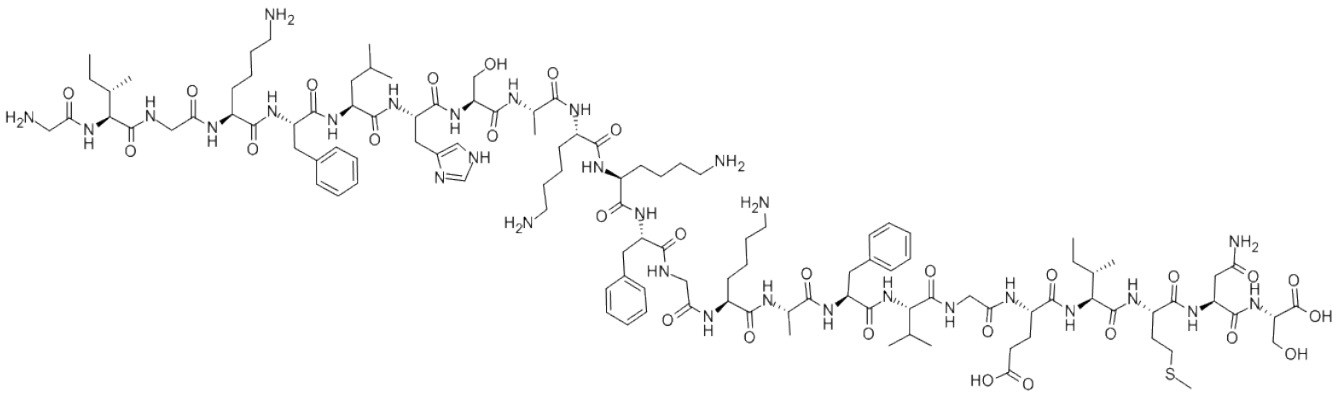


Figure 14: Peptoids appear to act by disrupting the microbial membranes just as AMPs. Shown above are the Cryo-EM results from the studies conducted by Brice *et al*. and Diamond *et al*. for AMP and peptoids, respectively a) Shows the disruption of Kaposi's Sarcoma Herpes Virus (KSHV) envelope by the AMP called LL-37.[18] Similarly, **b**) when SARS-CoV-2 was treated with two active peptoids (MXB-4 and MXB-9) several slightly disrupted membranes (middle) were observed and what appear to be nucleocapsids without envelopes. These structures were not observed in the control samples, proposing that the peptoids act via the same membrane-disruptive mechanism on MXB-4 and MXB-9 virus types.[19]

Barron *et al*., were the first group to demonstrate that peptoid mimicking the structure of AMP called magainin-2 amide (Figure 15**a**) displayed antibacterial effects with poor hemolytic activities.[20] This group recently assembled antimicrobial peptoid oligomers that mimic the structure of the AMP called pexiganan. These peptoids showed broad-spectrum activity (MIC 0.88-7.4 mg/L) and low mammalian cytotoxicity.[21,22,23] Jaroszewski *et al*. synthesized alpha-peptide/beta-peptoid chimeras (Figure 15**b**) that were selectively toxic towards bacterial cells

and displayed protease stability. These chimeras showed good antibacterial activity against *Bacillus subtils* and *Escherichia coli* (MICs7.5-13.5 mg/L).[21,24]

a)



b)

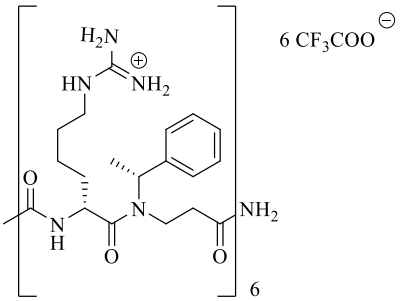


Figure 15: The structure magainin-2 amide25 and b) the structure of alpha/beta peptoid chimeras.[24]

Studies on the structural-activity relationship (SAR) have shown how important it is to modify the structure of peptoids when creating effective antimicrobials. Chongsiriwatana *et al.* studied helical peptoids that showed activity against a wide range of microorganisms and they demonstrated that the overall charge and average hydrophobicity are key for the antimicrobial activities displayed by the peptoids, while high hydrophobicity and amphipathicity resulted in hemolysis. Moreover, Mojsoka *et al*. (2005) looked at how hydrophobicity affects the activity of peptoids by designing a collection of short, linear, hydrophobic, and cationic peptoids whilst keeping the charge constant. They concluded that high hydrophobicity led to better potency against *Staphylococcus aureus* in vitro.[14]

A lot of studies have frequently mentioned five aspects which must be considered during the logical design of antimicrobial peptoids and these include; the length of the chain, hydrophobicity, secondary structure, net charge, and amphiphilicity. In this review, we

highlight how different structural properties of the peptoids influenced their biological activity against antimicrobials.

1.1.2 Main chain length

Recently, linear AMP have been designed to be ever-short for synthetic and pharmacological reasons.[26,27,28,29,30,31] Synthetic oligomers, particularly those that target the membrane of the bacteria, have notable potential for clinical development.[32] A lot of natural antimicrobial oligomers that are membrane-active are made up of over 10 monomeric residues, and their molecular weights are bigger than 1000 Daltons.[32,21] The downside of such compounds is that they may face inherent disadvantages with respect to pharmacological development and are usually restricted to being applied topically in the clinic. Chain length also influence the cost of production and hence the market price. With the intention of circumventing the issue of high cost of synthesizing AMP, Svendsen and colleagues worked on developing short AMP consisting of only three amino acid residues. These short cationic AMPs showed a wide-ranging antimicrobial activity against Gram-positive (MICs of 2.5 mg/L, including methicillin-resistant *S. aureus* (MRSA)) and Gram-negative bacteria (MIC of 5.0 mg/L, including *P. aeruginosa*).[10] Furthermore, these peptides were selective against bacterial cells as compared to mammalian cells.[10,21]It is crucial to investigate how the length influences the biological activity of the peptoids.

1.1.2.1 The effects of main chain length on antimicrobial activity

Mia Lace Huang and co-workers studied the influence that molecular size had on antimicrobial activity by analyzing oligomers made up of six, eight and ten subunits.[7] They noticed a correlation between the antibacterial activity of linear and cyclic oligomers and the length of the chains. For the six and eight subunits a decline in MIC value was observed indicating that in general, longer chain lengths improve the antimicrobial activity for both the cyclic and linear series. Their linear decamer, which was the largest out of the linear sequences showed the highest potency regarding antimicrobial activity (MIC of E. coli = 31.3 $\mu g.mL^{-1}$). Comparably for the cyclic series, their decamer with the largest macrocycle showed the highest antimicrobial activity potency (MIC of E. coli = 7.8 $\mu g.mL^{-1}$).[7]

Mojsoska *et al.* studied the implication of main chain length on the potency displayed by their peptoids by truncating two of their maternal peptoids that had simillar structural composition

(besides the residue on position 9) from the C-terminal end. They claim that the shortened peptoids have better antibacterial activity against *Staphylococcus aureus* and reduced retention time. They also deleted the 9th residue from peptoid 3 (Table 1) and observed no change in their results. These findings demonstrate that reducing the peptoid chain by one monomer can increase antimicrobial activity. Deleting the first monomer at the C-terminal can also result in higher toxicity as observed on their peptoid 3.[11] Comparably, an increase in antimicrobial activity and a decline in haemolytic property was seen when Leucine residue was deleted from the C-terminus of the peptide Ac-LKLLKKLL-KKLKKLLKKL-NH_2.[33] It can therefore be concluded that deleting one small hydrophobic residue from the carboxyl end decreased the hydrophobic character of the peptoid and increased the effectiveness of peptoids 7 and 3 as antibacterial agents against *E. coli* and *S. aureus* (Table 1).[33]

The effect of length on peptoids antimicrobial activity and selectivity can mainly be accredited to the varying hydrophobicity (higher RP-HPLC retention time), which increases correlatively with chain length. However, the antimicrobial activity is maximized at a specific ideal hydrophobicity and adding more hydrophobicity will only increase hemolytic activity.

Table 1: The retention times of the peptoids as well as their corresponding in vitro antibacterial activities, haemolytic activities, and cytotoxicity. Reprinted with permission from [11], published by AAC, 2015.

Peptoid no.	Peptoid nomenclature	Sequence[f] (N-C)	R_t (min)[a]	MIC (µ g/ml) for strain[b]:						Haemolytic Concn (µ g/ml)[c]	SR[d]	Cytotoxicity (µ g/ml)[e]
				S. aureus		*E. coli*		*P. aeruginosa*				
				ATCC 21213	C623 MRSA	ATCC 25922	63103 ESBL	PAO 1	H1027 MDR			
1	GN-2	H-*N*lys-*N*trp-*N*lys-*N*lys-*N*trp-*N*trp-*N*lys-*N*trp-*N*ile-NH2	10.54	64	32	32	32	32	4	>128	>2-32	168
3	GN-2-$Nlys_{1-4}Ntrp_{5-8}$	H-*N*lys-*N*lys-*N*lys-*N*lys-*N*trp-*N*trp-*N*trp-*N*trp-*N*ile-NH2	11.48	8	8	32	8	32	4	128	4-32	110
7	GN-4	H-*N*lys-*N*trp-*N*lys-*N*lys-*N*trp-*N*trp-*N*lys-Ntrp-*N*leu-NH2	10.51	32	ND	64	ND	64	ND	>128	>2-4	166
9	GN-4-$Nai_{2,5,6,8}$	H-*N*lys-*N*ai-*N*lys-*N*lys-*N*ai-*N*ai-*N*lys-*N*ai-Nleu-NH2	12.31	4	4	16-32	32	16-32	4	32	1-8	172
21	$Nlys_{1-4}Ntrp_{5-8}$	H-*N*lys-*N*lys-*N*lys-*N*lys-*N*trp-*N*trp-*N*trp-*N*trp-NH2	11.06	4	ND	16	ND	ND	ND	64	4-16	ND

[a] The estimated analytical retention durations (Rt) were performed using a reverse-phase C18 Kinetex 100 by 2.1 mm 100-column at 60 °C for 20 min with a gradient of 15 to 65% acetonitrile. [b] Median MICs, which represent 3 to 5 replicates, are reported in g/mL. [c] The results of three separate trials employing several blood donors were used to calculate hemolysis. [d] Selectivity ratio (SR) is the ratio of the bacterial strains' lowest and highest MIC values to 10% hemolysis. [e] Cytotoxicity is presented as the IC50, which refers to the concentration that inhibits 50% of the metabolic activity of HeLa WT cells utilizing the colorimetric tetrazolium salt-based MTS assay. *, IC50 for peptides as determined by an MTT experiment on HeLa WT cells. Antimicrobial peptides are taken as reference antimicrobial compounds. [f] Submonomeric solid-phase peptoid synthesis was used to make peptoids.[11]

1.1.3 Cationic peptoids

The side chains that are positively charged within the peptoid sequence provide some selectivity role between the zwitterionic plasma membrane of mammals and the more anionic plasmalemma of prokaryotes.[34]

1.1.3.1 Lysine or Arginine type side chains

The positively charged side chains in peptoids originate from lysine- or arginine-type monomers (Figure 16). Some groups have researched the distinction between the incorporation of arginine- and lysine-type side chains for cellular absorption and demonstrated that there is faster cellular uptake for peptoids that consisted of guanidine compared to their amino analogues.[34] Moreover, arginine-type monomers have been reported to possibly improve biological activity when incorporated into the sequence, although this may also increase toxicity toward mammalian cells.[34,35] This indicates the need for more research focusing on peptoids that consist of both the arginine- or lysine-type monomers to establish a balance between activity and toxicity. The majority of studied peptoids only contain all guanidino-functionalized (arginine-type) monomers or amino-functionalized (Lysine-type) monomers. This was due to the absence of a synthetic strategy to prepare mixed cationic peptoids. [34] H.L Bolt and S.L Cobb presented an efficient synthetic route to synthesize linear and cyclic novel cationic peptoids of lysine and arginine-type monomers within the same sequence.[34]

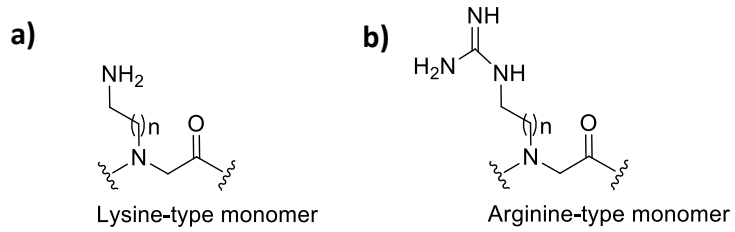


Figure 16: The structure of a) Lysine-type monomer and b) Arginine type monomer

It is worth noting that, in the study by Biljana Mojsoska's group[13], a decrease in antimicrobial activity was observed when arginine monomers within the structure of the peptide were completely replaced with lysine. This substitution might be the reason behind the peptoid mimics in their study exerting lower antibacterial activity. Previous studies have proven that for peptides in which lysine residues were replaced by arginine residues, a decrease in antimicrobial activity and the probable cause for this was the lower affinity to the membrane.[16,17] Furthermore, Amirkhanov *et al.* showed that replacing arginine residues with lysine or histidine residues in their synthetic antimicrobial peptides (SAMPs) fundamentally reduced their antibacterial properties in the succession: **P1**-Arg > **P2**-Lys ≫≫ **P3**-His.[36]

1.1.3.2 The effect of cationic side chains on antimicrobial activity

Studies from analysing peptoids that contain cationic residues with varying alkylamino and guanidino functional groups demonstrated that N-acetylated linear hexamers that consist of Nab or Nah (Figure 17) within their sequence were not active (MIC>500 μg.mL^{-1}) against all bacteria that were tested, whilst moderate antimicrobial activity was observed on Nap- and Ngb-containing hexamers (MIC: 125–250 μg.mL^{-1}). Among various cationic molecules tested in the same study, no consistent connection was observed between different chain lengths of the amino alkyl side chain or the nature of guanidino vs amino functionality and the antimicrobial activity.[7]

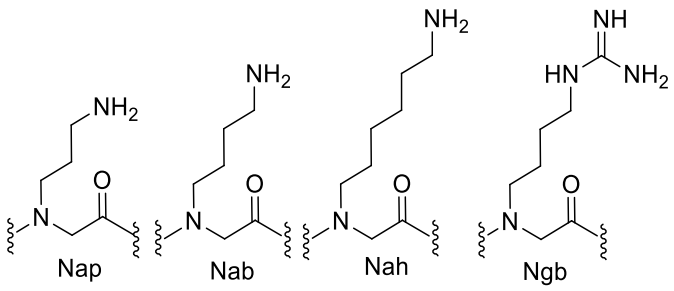
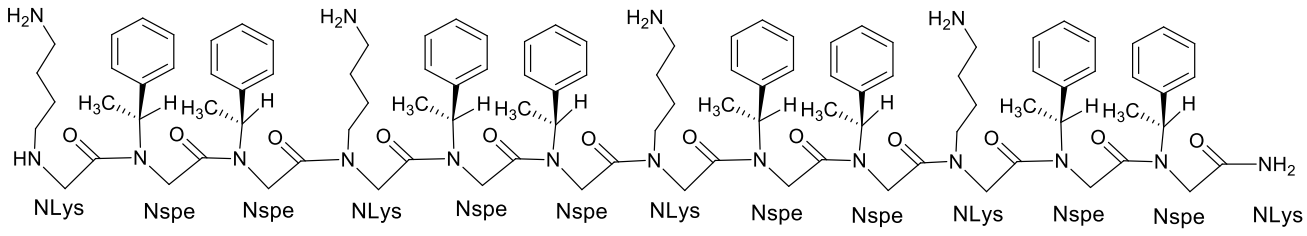


Figure 17: The structures of cationic monomers used in the study.

A study on anti-tubercular peptoids used a cationic, four residues long peptoid 1-$C13_{4mer}$ (Figure 18) to demonstrate the potency of cationic, biomimetic peptoids against a group of infectious bacteria that cause tuberculosis disease. The hydrophobic tail of peptoid 1-$C13_{4mer}$, which is a 13-carbon aliphatic tail attached to the N terminus, imparts it with a considerable surfactant character—as a monomer. This tail is ideal because it is more likely to have a stronger and disruptive interaction, with the hydrophobic, phospholipid bilayer of *Mtb*, thus allowing the peptoid to penetrate the membrane of the bacteria more efficiently when compared to the unalkylated peptoid 1_{4mer}. Cationic surfactants are generally toxic to the cells of mammals and bacteria, however in the case of peptoit-$C13_{4mer}$, its strong self-association enforced by the hydrophobic C13 tail should protect the outer membranes of the anionic (or hydrophobic, in the case of *Mtb*) microphages that are not significantly anionic in contrast with bacterial membrane.[37] *Mtb* has a cell membrane that is different to the normal Gram-positive and Gram-negative bacteria. Its cell membrane is made up of hydrophobic layers of mycolic acid, and this acyclic, hydrophobic barrier lowers the penetrable capability of anti-TB drugs towards *Mtb*, which is in part, the explanation behind the high resistance of *Mtb* to available antibiotics.

When NLys monomers were substituted with glutamate-like NGlu (Chongsiriwatana group), the resulting zwitterionic peptoid had considerably lower activity against *B.subtilis* and was not active against *E.coli*. This could be caused by the lack of favourable electrostatic interactions with the anionic bacterial cell membranes; but this Zwitterionic peptoid was moderately hemolytic. On the other hand, the fully anionic variant did not show both antibacterial and hemolytic activity. In conclusion, antimicrobial peptoids are selectively active given they are cationic and adequately but not extremely hydrophobic, compatible with what has been reported on selective AMPs.[38]

a)



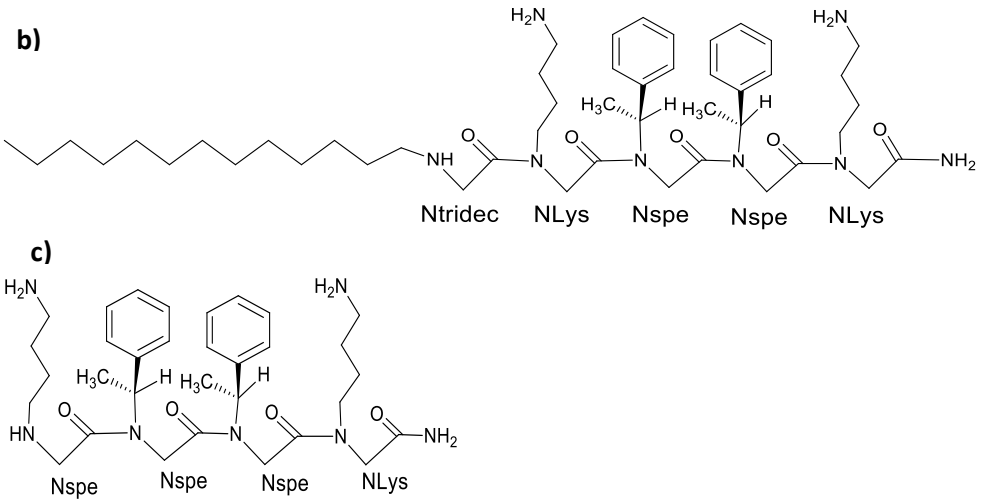


Figure 18: The structures of a) Peptoid 1, b) Peptoid 1-C13$_{4mer}$ and c) 1$_{mer}$.

1.1.4 Hydrophobicity

Antimicrobial molecules are driven by hydrophobic interactions to migrate from the aqueous environment and into the cell membrane.[39] Natural peptides that are extremely hydrophobic display higher cytotoxicity. It is therefore crucial to balance the hydrophobic and polar content of the peptide in order to regulate the selectivity of AMPs and non-peptidic therapeutic agents.[39,40,41]

1.1.4.1 Influence of Hydrophobicity on the secondary structure of peptides

According to research on linear cationic AMPs in model membrane bilayers using circular dichroism (CD) and ATR-FTIR, non-polar environments cause peptides with more hydrophobic surfaces to undergo conformational modifications, thus changing their secondary structure from random coil to alpha-helical and from alpha-helix to beta-sheet.[39,42] They also have a higher chance of forming aggregates as compared to their less hydrophobic analogues in such environments. This can be attributed to a charge compensatory effect. The binding of peptides to the anionic phospholipids on the membrane of the bacteria leads to the creation of a dehydrated environment that favours the formation of beta-strand aggregates.[43,44] Moreover, this behaviour is perceived in the viral fusion peptides from HIV-1 gp41 modulated by the cholesterol level in the targeted membrane.[45,46]

1.1.4.2 Effect of hydrophobic surface area (SA) on antimicrobial activity

SAR studies on AMPs have proposed a strong connection between net hydrophobicity and antimicrobial activity. This is slightly due to the powerful hydrophobic interconnections between peptides and the target plasmalemma, which is much stronger in cases such as mammalian membranes, where the membrane comprises zwitterionic lipids. Borron *et al.* also reported a similar study in which the hemolytic properties and antibacterial activity increased when the hydrophobic character of the peptoids that mimic AMPs was increased.[13,28] Mojsoska *et al.* (2015) studied how hydrophobicity affected the activity and cytotoxicity of peptoids by designing a library of peptoids that are short, cationic, hydrophobic and linear with modifications whilst keeping the charge constant. When tested *in vitro* against *Staphylococcus aureus*, peptoids with higher hydrophobicity showed improved potency, but not when tested against *Escherichia coli* or *Pseudomonas aeruginosa*. [11]

1.1.4.2.1 Phenyl monomers

Mia Lace Huang *et al.* studied how the hydrophobic surface area affected antimicrobial activity by using three sets of oligomers consisting of different phenyl residues of different levels of hydrophobic SA (Figure 19). The first set (L6 and C6) had the lowest hydrophobic SA in the group. The hydrophobic functional groups for this first set were three phenyl groups for each molecule. The second pair (L4 and C4) had the greatest hydrophobic SA than the first pair, consisting of three naphthyl groups on each molecule as the hydrophobic functional groups. The last pair (L3 and C3) had the highest hydrophobic SA in the group, and six phenyl groups were incorporated as the hydrophobic functional groups per molecule. The antimicrobial data compiled from this study showed that incorporating Ndp residues into sequences had greater antimicrobial activity than those made up of Npm or Nnm residues. This observation proposed a compelling connection between antimicrobial activity and hydrophobic surface area. Furthermore, greater improvement of antimicrobial activity with increasing hydrophobic SA was much more noticeable in cyclic peptoids than those that were linear (Table 2).[7]

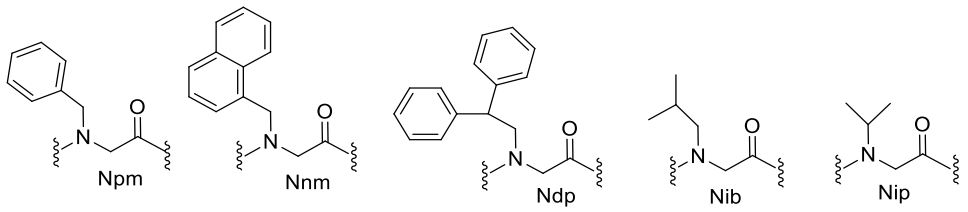


Figure 19: Structures of hydrophobic monomer.

Table 2: The linear and cyclic peptoids with their corresponding antimicrobial and hemolytic activities.[7]

	Sequence[a]	MIC [μgmL^{-1}][b]			HC [μgmL^{-1}][c]		SR[d]
		B. sub.	*E. coli*	*S. aur.*	HC_{50}	HC_{10}	
L3	Ac(NapNdp)$_3$	1	15.6	15.6	>250	>62.5	>4
L4	Ac(NapNnm)$_3$	2	62.5	125	>250	>250	>4
L6	Ac(NapNpm)$_3$	125	125	250	>250	>250	>2
C3	C(NapNnm)$_3$	1	15.6	7.8	>250	31.3	>2
C4	C(NapNnm)$_3$	0.5	31.3	31.3	>250	>250	>8
C6	C(NapNpm)$_3$	500	>500	500	>250	>250	NA

[a] The prefixes Ac and C, respectively, are utilized to refer to N-acetylated linear sequences. [b]Minimum inhibitory concentrations (MICs) against *Bacillus subtilis, Escherichia coli*, and *Staphylococcus aureus*. [c]Hemolytic concentrations: HC_{50}, concentration at which 50% hemolysis is observed; HC_{10}, concentration at which 10% hemolysis is observed. [d]Selectivity ratio: SR = HC_{10}/MIC *E. coli*; the abbreviation NA stands for not applicable because there was insufficient antibacterial activity; three independent trials were done in three replicates.[7]

1.1.4.2.2 Effects of increasing hydrophobicity by Nlys substitution.

New peptidomimetics with enhanced antibacterial and hemolytic activities have been previously synthesized using lysine length variants.[47,48] The Nlys residues (structure shown on Figure 20) contributed charge to the peptoids and are considered to be adequate for the first electrostatic interaction with bacteria, giving them superior affinity and thus anti-mycobacterial activity unlike their respective hydrophilic analogues.

A study was carried out to explore the implication that the length of a charged residue will have on the activity of the peptoid.[11] In this study a shorter monomer, Nae, was replaced with Nlys and this substitution led to minimal alteration to the retention time of the resulting peptoid. Similar observations were made for the substitution of Nae with Nlys, in which the little influence on the shorter lysine version could be noticed in the low dose needed to lyse 10% of human red blood cells. Additionally, when this amount was decreased to 50% within the same sequence, the peptoid was optimized and showed better antibacterial activity and a decreased in toxicity.[11]

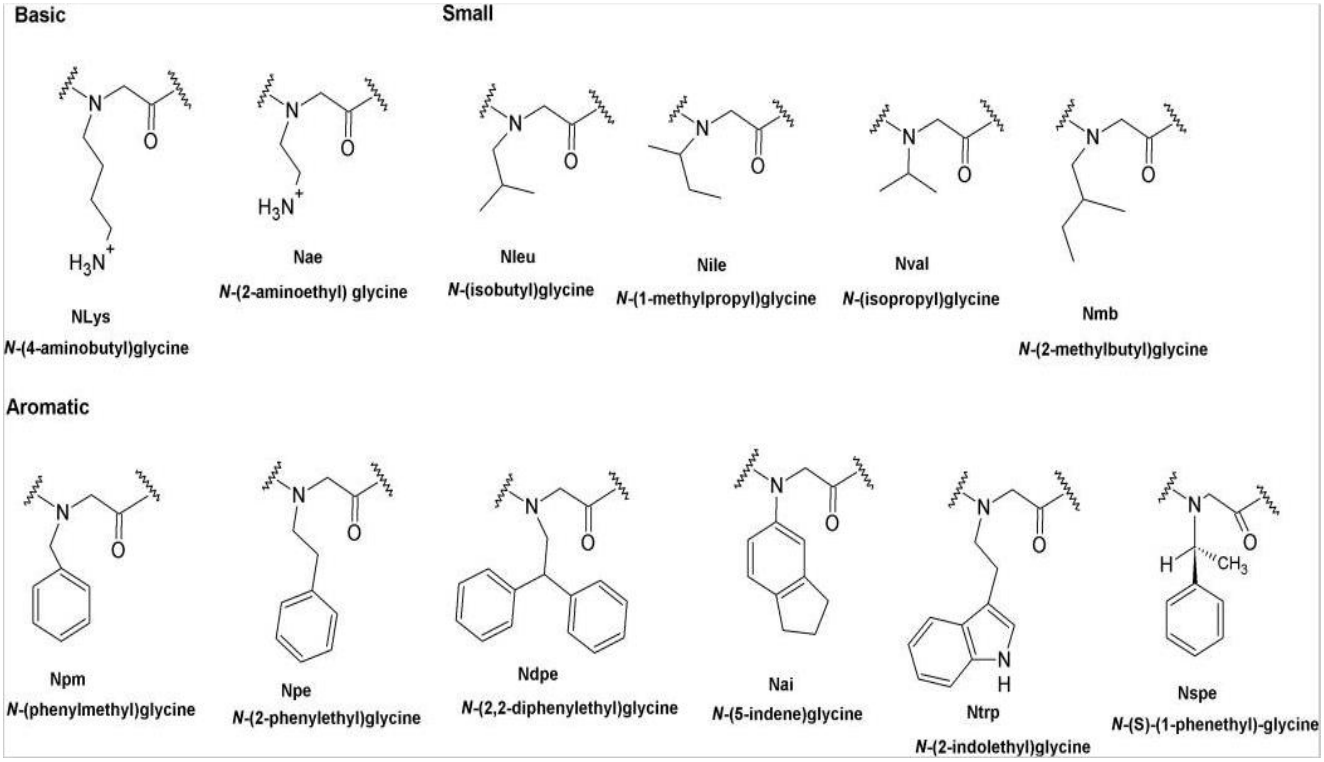


Figure 20: The structures of peptoid monomers and their corresponding abbreviations and full names. Reprinted with permission from [11], published by AAC, 2015.

1.1.4.2.3 Effects of increasing hydrophobicity by Ntrp substitution.

Replacing Ntrp with monomers within the sequence can significantly impact the overall hydrophobicity profiles of the peptoids. In the study conducted by Mojsoska and coworkers, exchanging Ntrp with Nspe showed an increase in retention time on the resulting peptoid; however, a decline in antimicrobial activity by 4-fold was observed for this peptoid against *S. aureus*. The antimicrobial activity did not improve when Ndpe was exchanged for Ntrp.[11] From

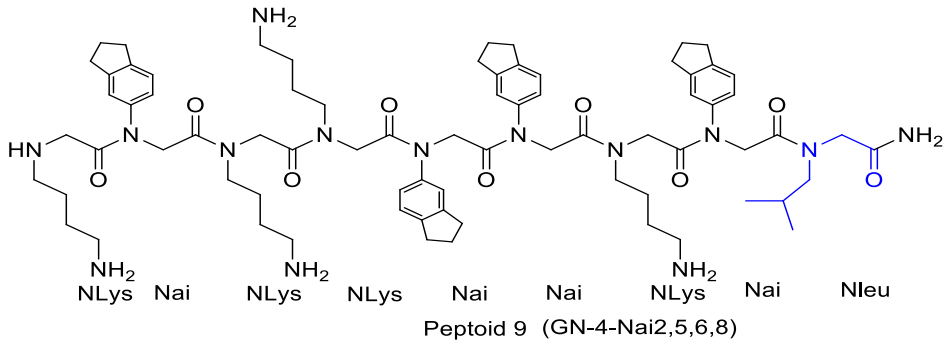
their results, they concluded that where the monomers are positioned within the backbone of the peptoid influenced the observed behaviour of the peptoid analogues in their study. They also suggested that extreme hydrophobicity may justify the observed decrease in antimicrobial activity for one of their peptoids (peptoid 16)[11], in which a strong peptoid-self association will hinder the peptoid from permeating across the bacterial cell wall. This has been proposed as a possible explanation for the substantial decline in the peptides antibacterial activity upon the increase in hydrophobicity.[49]

1.1.4.2.4 The effect of increasing hydrophobicity by single-monomer substitution.

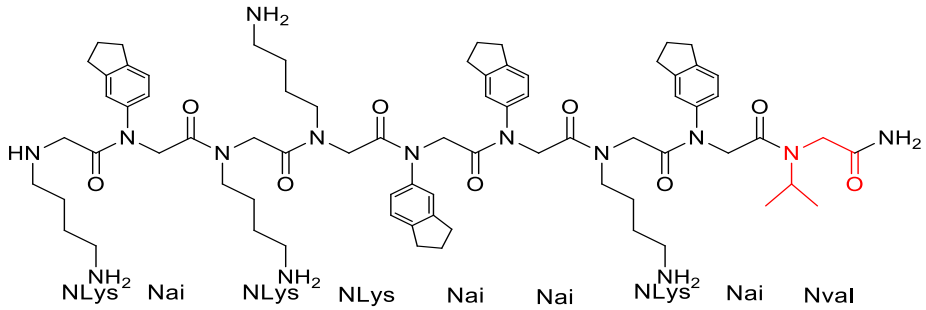
Hydrophobic amino acids that are small, like valine, isoleucine, and leucine, are frequently found in AMP structures in animals and bacteria.[50] The single-monomer change of leucine and isoleucine in the study by Mojsoska *et al.* resulted in no compelling change in antibacterial activity, and low toxicity was maintained when these peptoids were tested at the highest concentration. Opposite effect was observed when one Ntrp residue was substituted with an aromatic monomer that is bulkier, Ndpe. This exchange increased the hydrophobicity which significantly enhanced the potency of the peptoid against *S. aureus*, human red blood cells, and HeLa cells.[11] To further compare monomers with the same physiochemical traits but different in a single monomer, they synthesized peptoids that contain bulkier residue, Ndpe, instead of Ntrp. When tested against *S. aureus*, *P. aeruginosa*, and *E. coli* strains, each of the resulting peptoids demonstrated similar antimicrobial activities with high hemolytic activity, resulting in 10% hemolysis at lower concentrations.[11]

In the investigation of two peptoids (peptoids 9 and 14) (Figure 21) whose Nval and Nleu monomer compositions varied by Nai residue across the backbone rather than Ntrp, the much hydrophobic peptoid 9 showed improved antibacterial activity against the MRSA and the *E. coli* clinical isolate demonstrating extended spectrum-lactamases (ESBL) by 2-fold.[11] Despite a direct correlation between hydrophobicity and potency observed against *S. aureus*, this group determined that high hydrophobicity in peptoids does not consistently seem as highly powerful against *E. coli* and *P. aeruginosa*. Comparatively, increasing the antibacterial activity of the resultant peptide and decreasing its hemolytic property was achieved by deleting the leucine residue from the carboxylic end of the peptide with the sequence Ac-LKLLKKLL-KKLKKLLKKL-NH_2.

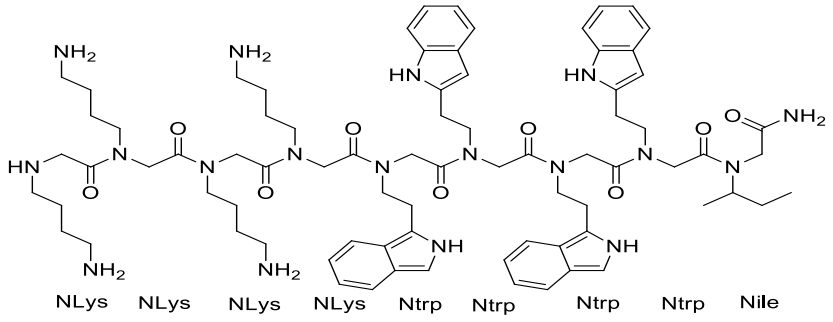
Therefore, deleting one small hydrophobic residue from the carboxylic end decreased the peptoids' hydrophobic character resulting in enhanced antimicrobial activity observed for peptoids 7 and 3 (Table 1, Figure 21) against *S. aureus* and *E. coli*.[11]



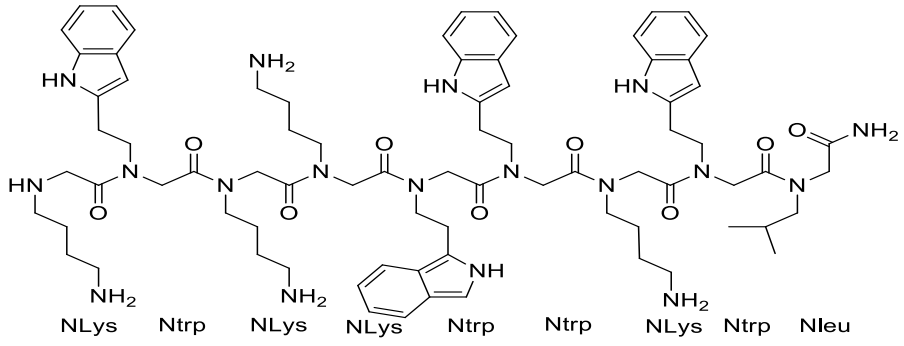
Peptoid 9 (GN-4-Nai2,5,6,8)



Peptoid 14GN-4-Nai2,4,6,8Nval9



Peptoid 3 GN-2-NLys1-4Ntpr5-8



Peptoid 7 GN-4

Figure 21: The chemical structures of peptoid 3, peptoid 9, peptoid 7 and peptoid 14.

1.1.5 Amphiphilicity

Peptidomimetics containing hydrophobic and charged groups in their sequence segregate into amphiphilic structures vital for interacting with the bacterial membrane. Antimicrobial peptoids are usually created to be amphipathic with a combination of hydrophobic and positively charged residues. As the introduction stated, this structural feature facilitates the first electrostatic interaction between the bacterial phospholipid head groups and the AMPs and the hydrophobic interactions with the non-polar lipid acyl chains. It also makes the peptoid selective for bacterial cells, lowering toxicity to the cells of mammals and enhancing their activity as molecular transporters.

1.1.5.1 Effects of amphiphilicity by sequence rearrangement

Several structural analogues where monomers in the peptoid were rearranged to give altered amphiphilicity and charge distribution were used to investigate this rearrangement's influence on the peptoid's potency. Mojsoska et al. (2015) group found that disarranging the charge cluster at the amine-terminus of peptoid resulted in a more prominent hydrophobic character, and no considerable improvement in the activity against *S. aureus* was observed. However, activity increased four times against Gram-negative strains of *P. aeruginosa* and *E. coli*. Hemolytic activity was not considerably affected by this shift. In contrast to peptoid 15, peptoid 4 (Figure 22) appeared more harmful to HeLa cells. Wimley proposed a model which stated that peptides with the imperfect arrangement of hydrophobic and charged residues showed an increase in potency for disrupting bacterial membranes. The enhancement in potency against Gram-negative bacteria due to the rearrangement in amphiphilicity for peptoid 4 agrees with this model. Furthermore, disrupting the hydrophobic region in melittin improved the capability to form pores.[11]

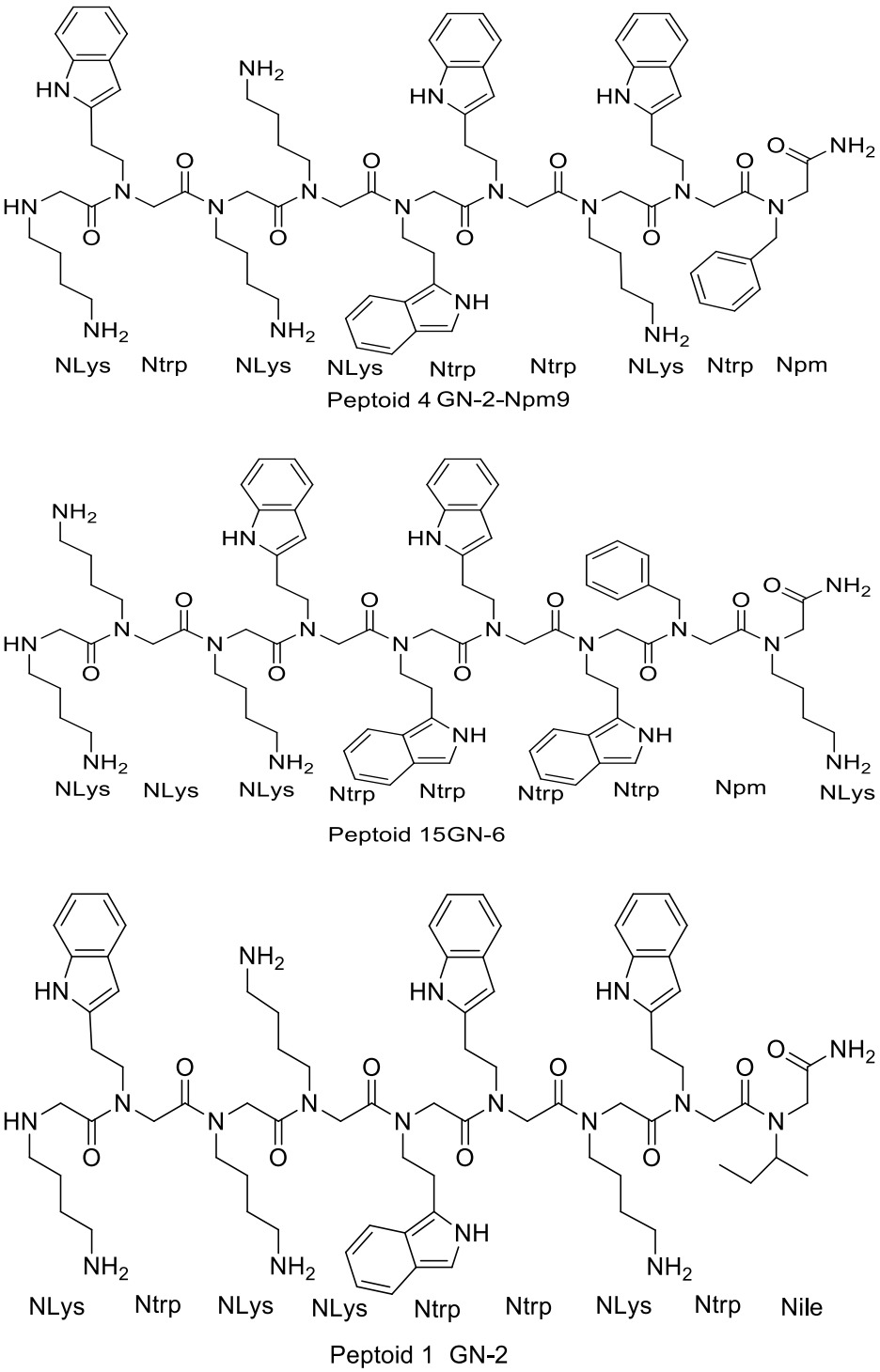


Figure 22: The structures of Peptoid 4, peptoid 15 and peptoid 1.

Disrupting the dimerization of the peptide V13K_L, an amphipathic 26 amino acid long peptide with a hydrophilic lysine residue in the middle of the non-polar face, (Figure 23) by incorporating a charged amino acid (Lys) in aqueous solution resulted in a decrease in toxicity. The plausible explanation for this is that the dimerization allowed for easier access of the peptide to the interface site of the plasma membranes of mammals while avoiding

permeating the membrane. In conclusion, sequence rearrangement can yield peptoids with optimal hydrophobicity that display the greatest selectivity.[11]

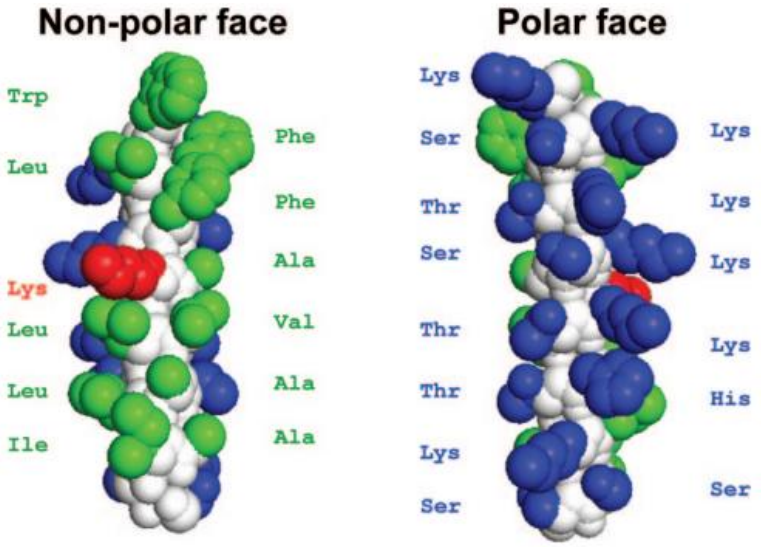


Figure 23: The Space-filling model of parent peptide V13KL. The region coloured in white represents the backbone of the peptide. The amino acids in green colour are hydrophobic the the ones in blue color are hydrophilic. The Lys substitution on the 13th positions ($V13K_L$) on the nonpolar face of the helix is highlighted in red.[51]

1.1.6 Cyclization

The charge, hydrophobicity, amphipathicity, and size are important when designing small membrane-active antimicrobial molecules. The conformational rigidity of these molecules has been recently suggested as an additional vital parameter to consider. Cyclization makes a molecule more rigid without extensive modifications in other physiochemical properties. Cyclic antimicrobial compounds' reduced structural flexibility may facilitate their ability to penetrate membranes, possibly increasing membrane-disruptive behaviour.[52] Unlike flexible linear molecules, cyclic analogues should experience lower entropy loss when incorporated into a lipid membrane (Figure 24). Packing disruptions in the lipid matrix frequently result when introducing a molecule into a lipid membrane. The maximization of hydrophobic and electrostatic interconnections between the antimicrobial molecules and the lipids results in the system gaining energy. The molecules membrane activity is defined by the accumulative change in energy.[52] Some reports have stated that macrocyclizing antimicrobial peptoids

enhanced their membrane activity. Their conformational stability and probable bioavailability makes them more attractive as drug candidates.

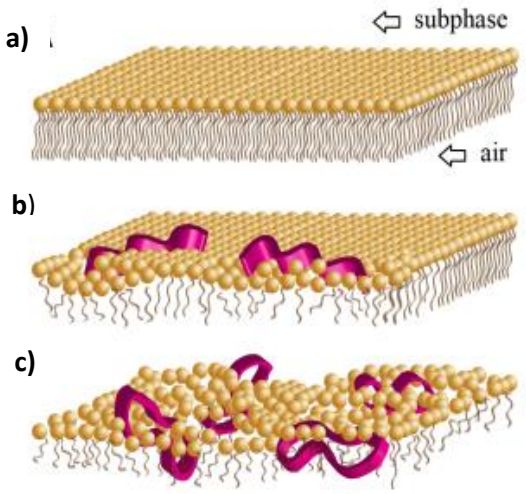


Figure 24: The proposed structural modifications in the outer outlet of the phospholipid membrane of the bacteria **a**) after inserting a linear **b**) and cyclic **c**) peptoids. Cyclization enables antimicrobial molecules to intercalate more effectively with lipid film characterization by molecular tilt.[11]

The most difficult task in designing stable peptoids with secondary structures is the fundamental conformational heterogeneity mainly found in the form of cis–trans amide bond isomerization. Scientists have come up with several methods to achieve defined conformations in peptoids. Incorporating bulky achiral side chains yielded peptoids that took on the structure of polyproline type I helix and peptoid sequences with such structures exhibiting powerful antimicrobial activity. Introducing covalent constraints by head-to-tail macrocyclization is another approach to impose rigidity in peptoid structures. A macrocyclized peptoid has its side chains arranged on opposite faces of the planar ring, implying that an amphiphilic peptoid structure could be achieved by properly placing the cationic and hydrophobic side chain groups in the cyclic peptoid sequences. This well-defined amphiphilic structure could produce powerful AMP mimetics that effectively fight bacterial pathogens.[52] Studies have previously proven this principle through cyclic peptoid oligomers exhibiting modest antimicrobial effects against bacteria and fungi. When tested against clinically relevant isolates of *S. aureus*, amphiphilic cyclic peptoid oligomers showed strong

antibacterial activity. A significant antimicrobial selectivity was observed for these compounds, even though they act on the surface of the bacteria. Furthermore, their non-hemolytic activity and powerful antimicrobial activity are analogous to those recorded for other peptidomimetic oligomers that are presently in clinical development.[52]

1.1.6.1 Effect of cyclization on antimicrobial activity

Several studies demonstrated a compelling connection between the stability of secondary structure brought about through macrocyclization and the potency to inhibit bacterial cell growth. The study conducted by Mia Lace Huang *et al.* focused on gram-negative (*E-coli*) bacteria to contrast the antimicrobial activity of the linear and cyclic peptoid analogues. They observed a decline in MIC values for the cyclic peptoid (figure 25) analogues correlative to the linear derivatives. This observation led to the conclusion that cyclization generally enhances antimicrobial activity. Among the six pairings of cyclic and linear sequences involved in this study, the cyclic peptoids C7 and C14 showed activity approximately 8-fold more active relative to their linear equivalents (L7 and L14). This improvement in the activity of macrocylised peptoids relative to linear peptoids agreed with the same result acquired by imposing a secondary structure in helical peptoid antimicrobial oligomers.[7]

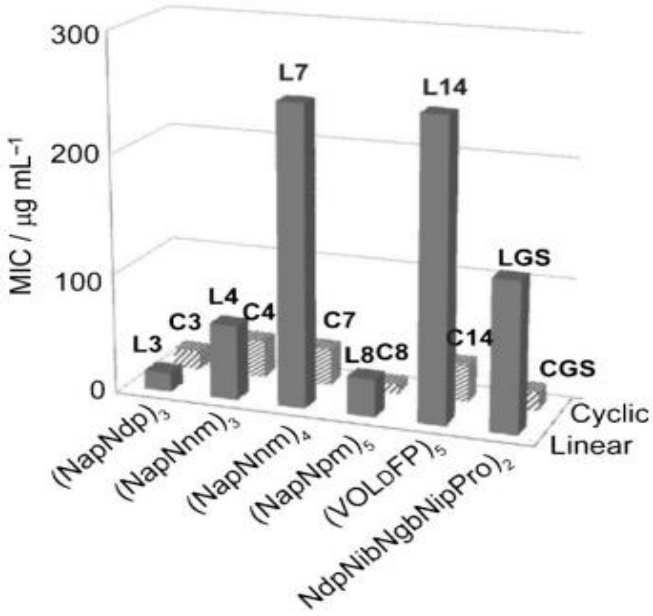


Figure 25: A plot of the six pairs of cyclic (C3, C4, C7, C8, C14, CGS) and linear (L3, L4, L7, L8, L14, LGS) peptoids against the MIC which illustrates that the macrocyclized peptoids enhanced the antimicrobial activity against *E.coli*.[7]

1.1.7 Aromatic side chains

1.1.7.1 N-aryl groups within peptoid oligomers

Using N-aryl glycine monomer units (Figure 26) together with other methods might eventually enable the creation of predictable structure-function relationships of peptidomimetic foldamers.[53]

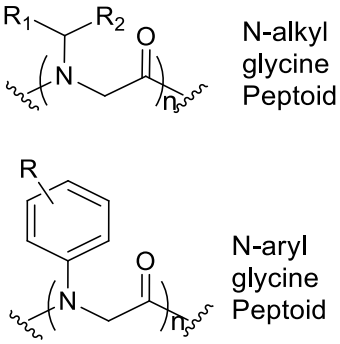


Figure 26: Comparison of the structure of N-alkyl glycine monomers and the N-Aryl monomers peptoid structures.

Previously, N-alkyl glycine monomer units that are relatively flexible were used in structural investigations of peptoids. Bradley *et al.* initially proposed that including N-aryl side chain groups can lower the conformational heterogeneity, but no additional investigations were made for this phenomenon. The N-aryl glycine monomers can be incorporated to give novel peptoid secondary structures conformationally defined in solution. This novel group of peptoid structures might simplify the *de novo* creation of biomimetic architectures that are chemically diverse.[53] The confined conformations of N-aryl glycine oligomers are distinct and encourage backbone conformational stability.

Including N-aryl groups within peptoid oligomers gives them a higher energetic inclination for trans-amide bond geometries. X-ray crystallography and solution NMR spectroscopy studies of N-aryl peptoid oligomer structures confirmed that these compounds favour trans-amide bonds across the backbone and they showed the predicted side chain rotamers. The capability to govern the presence of the trans-amide bonds anywhere within the sequence of the peptoid will improve the ability to foretell the final backbone structure, as indicated in the successful design of N-alkyl/N-aryl hybrid cyclic hexamers.[53]

Regarding the activity of peptoids with N-aryl side chains, one study demonstrated that introducing aromatic residues can lead to the loss of selectivity between the plasmalemma of mammals and bacteria. Besides this, while fine-tuning the hydrophobicity of peptoids, Mojsoska *et al.* found that to balance the structural requites that selectively kill the bacteria, Ntrp and Nai could preferably be utilized as the aromatic monomers.[11]

1.1.8 Alkylated peptoids

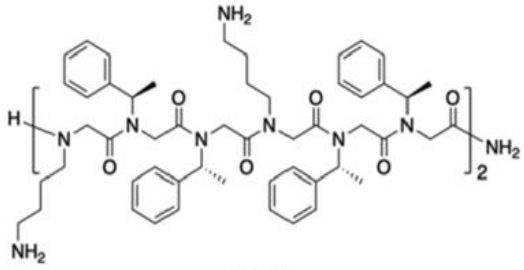
Alkylated peptides and peptoids can form micelle at the lowest inhibitory concentration,[54, 55] which may increase their local concentration upon their contact with the negatively charged bacterial plasmalemma. Presumably, cationic micelles naturally disassemble, succeeding in the adsorption to the surface of the membrane. Furthermore, it has been proven that including bulky, branched N-alkyl substituents can create nearby steric interactions capable of directing conformational preferences.

1.1.8.1 Alkylated peptoids on antimicrobial activity

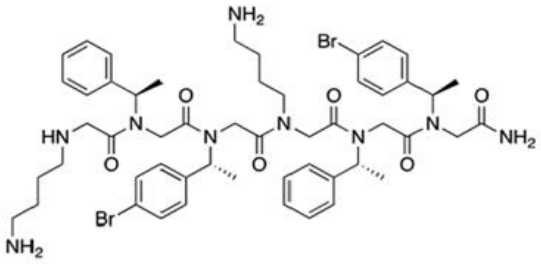
Fatty acid tails have previously been anchored to linear AMP that is rarely acylated,[56,57] sometimes making cationic peptides that are not active to show antimicrobial activity. The synthesis of peptoids allows alkylamines to be incorporated within the peptoid as an amine-terminus alkyl tail with ease. Nathaniel P. Chongsiriwatana and coworkers used this method to study alkylated peptoids as mimics of antimicrobial lipopeptides.[5] Following the submonomer strategy, this group created a series of peptoids using suitable alkylamine to incorporate alkyl tails that were 5, 10, or 13 carbons long as side chain groups. They discovered that, in some cases, alkylation remarkably enhanced the selectivity of the peptoids while maintaining antimicrobial potency. Noticeable enhancement in potency was observed for the alkylated peptoids with chain lengths of 9, 6, and 4 residues against bacteria and fungi, when contrasted to the peptoid that are not alkylated.[5]

It has been demonstrated in the previous studies that peptoid 1 is active against Gram-positive and Gram-negative bacteria, and the analogues with longer tail lengths and hence more hydrophobic either retain their antibacterial activity or start losing it. However, their antifungal potency increased.[26]

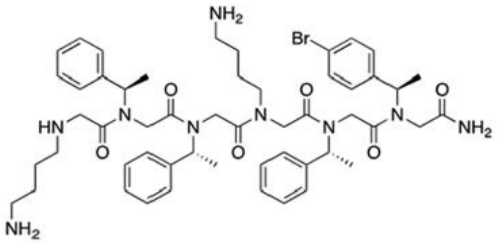
Nielsen *et al.* focused on two well-researched compounds called TM1 and TM5 and eight other variants and molecular hybrids (figure 27). This group of peptoids differed in their overall positive charge, hydrophobicity, and main chain length (6_{mer}-12_{mer}) due to including various Nspe monomers, halogens, and alkyl chains.



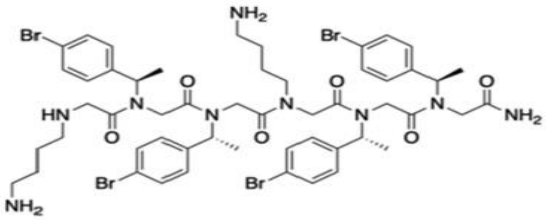
TM1
H-(*N*Lys-*N*spe-*N*spe)$_4$-NH$_2$
MW = 1819. 36



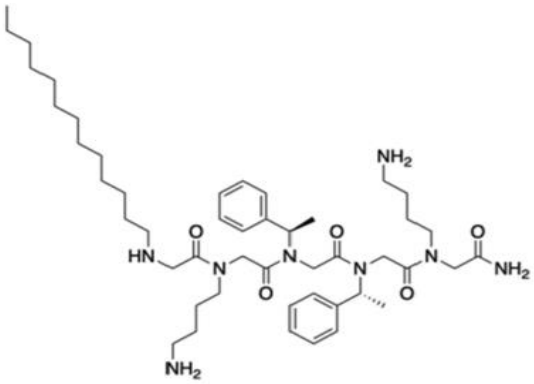
TM2
H-(*N*Lys-*N*spe-*N*spe(p-Br))$_2$-NH$_2$
MW = 1075.99



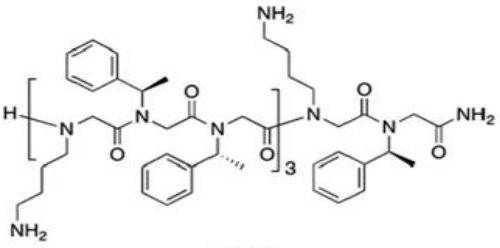
TM3
H-*N*Lys-*N*spe-*N*spe-*N*Lys-*N*spe-*N*spe(p-Br) -NH$_2$
MW = 997.09



TM4
H-(*N*Lys-*N*spe(p-Br)-*N*spe(p-Br))$_2$-NH$_2$
MW = 1233.78



TM5
H-*N*tridec-*N*Lys-*N*spe-*N*spe-*N*Lys-NH$_2$
MW = 835.19



TM6
H-(*N*Lys-*N*spe-*N*spe)$_3$-*N*Lys-*N*spe-NH$_2$
MW = 1658.16

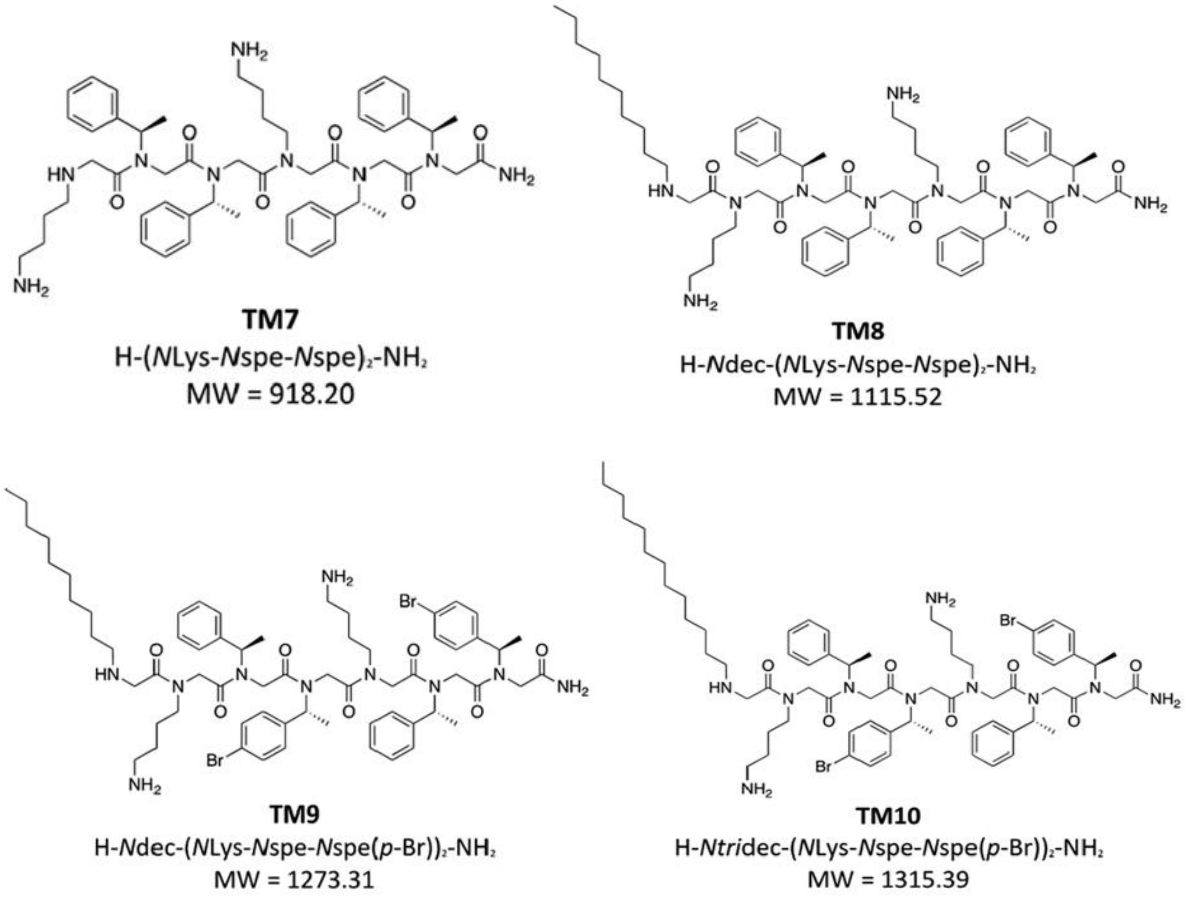


Figure 27: The structures of peptoids TM1 to TM10.[16]

The analogues TM9 and TM10 are structurally similar and only differ in their alkyl chain length (TM9 has 10 carbons while TM10 has 13 carbons). It was found that TM10 formed a significant percentage of worm-like micelles. This worm-like morphology was hypothesized to have the ability to inhibit antibacterial and antiviral activity, thus accounting for the reduced activity of TM10 relative to the analogues TM5, TM8, and TM9, which showed antimicrobial activity that is within 2-4 fold of TM1. It can be concluded from these results that micellar aggregation number, as well as hydrophobicity, affected the peptoids' biological function.

In agreement with this, a loss in activity was observed for the peptides YGAAKKAAKAAKKAAKAA (AKK) that were conjugated to varying lengths of fatty acids when the minimum active concentration was raised above the critical micelles concentration (CMC). Although this conjugation to fatty acid tails improves their attraction for the negatively charged phospholipid membranes, the self-assembled structure (acquired at concentrations exceeding the CMC) can hinder the effective interaction of the peptide to the plasma membrane of the bacteria.[16]

In conclusion, regarding alkylated AMPs, a balance between self-assembly and hydrophobicity may be required for optimal activity, dissimilar to several biological activities. However, further studies need to be carried out to investigate this hypothesis. In specifically, research examining the relationship between the morphology and stability of self-assembled structures and bioactivity, notably concerning the antibacterial activity of ellipsoidal micellar structures vs. longer, worm-like structures.[16]

1.1.8.2 Influence of Alkyl tail for the formation of micellar structures

The study by Nielsen *et al.* it has shown that adding a terminal alkyl tail to peptoids allowed for the structures of core-shell micellar to be formed. These structures had a higher aggregation number when compared to the helical bundles that assembled for peptoids TM1 and TM6. The formation of ellipsoidal micellar assemblies was observed for peptoids TM5, TM8 and TM9, with average aggregation numbers of about 98, 103, and 117 peptoids, respectively. These remarkable numbers of aggregates propose the existence of intermolecular interactions that exceed hydrophobic forces. These intermolecular interactions could be hydrogen bonding between *N*Lys residues and pi-stacking between *N*spe residues. The large aggregation numbers also showed that the physical stability of these ellipsoids were considerable. This may be favourable for the successful drugability of these peptoids, particularly because these supramolecular peptoid assemblies can operate as a vehicle-free self-controlled delivery system. This delivery system further eliminates the need for any physical encapsulation.[16]

1.1.9 Halogen-substituted peptoids

According to theoretical modeling, the peptoids TM2 and TM4 from Nielsen *et al.* work that were substituted with halogens generated bigger helical bundles, possibly due to an efficient "hydrophobic" contact between the heavy bromine para-benzyl substituent atoms. TM2, which consists of two Nspe residues that were substituted with bromine atoms, had a 0.005% percentage of bigger aggregates (dimensions of 120 Å × 280 Å × > 1000 Å), while for TM4, no larger aggregates were observed. At doses comparable to those of TM1 (1.56 and 12.5 g/mL, respectively), TM2 was able to inhibit the activity of *E. faecium* and *P. aeruginosa*; however, higher concentrations were necessary to prevent the development of the other bacterial species. Likewise, TM4 required lower concentrations (0.78 and 6.25 µg/mL) than TM1 to

inhibit *E. faecium* and *P. aeruginosa*, respectfully. However, equal or higher concentrations were essential for the inhibition of other species of bacteria.[16]

1.1.10 Conclusions

This review outlines recent work on the SAR of antimicrobial peptoids that mimic naturally occurring antimicrobial peptides. While evaluating how different structural features like chain length, hydrophobicity, cyclization, net charge, and amphiphilicity influenced antimicrobial activity, it is important to note that the design of peptoids with better antimicrobial, haemolytic, and cytotoxic activity may require a balance between these features. An excellent illustration is the finding that the antibacterial properties of helical peptoids, which are effective against a wide range of microbes, depending on both their total charge and average hydrophobicity and amphipathicity resulted in hemolysis. Peptoids also showed selective antibacterial action due to their net positive charge and sufficient but moderate hydrophobicity. There is hope that peptoid agents may represent a new and underrepresented class of new antibiotics.

References

1. Mojsoska, B.; Carretero, G.; Larsen, S.; Mateiu, R. V.; Jenssen, H. Peptoids Successfully Inhibit the Growth of Gram Negative E. Coli Causing Substantial Membrane Damage. *Nat. Publ. Gr.* **2017**. https://doi.org/10.1038/srep42332.
2. Jenssen, H.; Hamill, P.; Hancock, R. E. W. Peptide Antimicrobial Agents. *Clin. Microbiol. Rev.* **2006**, *19* (3), 491–511. https://doi.org/10.1128/CMR.00056-05/FORMAT/EPUB.
3. Mojsoska, B.; Jenssen, H. Peptides and Peptidomimetics for Antimicrobial Drug Design. *Pharm. 2015, Vol. 8, Pages 366-415* **2015**, *8* (3), 366–415. https://doi.org/10.3390/PH8030366.
4. Andreev, K.; Martynowycz, M. W.; Huang, M. L.; Kuzmenko, I.; Bu, W.; Kirshenbaum, K.; Gidalevitz, D. Hydrophobic Interactions Modulate Antimicrobial Peptoid Selectivity towards Anionic Lipid Membranes. *Biochim. Biophys. Acta - Biomembr.* **2018**, *1860* (6), 1414–1423. https://doi.org/10.1016/J.BBAMEM.2018.03.021.

5. Huan, Y.; Kong, Q.; Mou, H.; Yi, H. Antimicrobial Peptides: Classification, Design, Application and Research Progress in Multiple Fields. *Front. Microbiol.* **2020**, *11*. https://doi.org/10.3389/FMICB.2020.582779.

6. Malkoski, M.; Dashper, S. G.; O'Brien-Simpson, N. M.; Talbo, G. H.; Macris, M.; Cross, K. J.; Reynolds, E. C. Kappacin, a Novel Antibacterial Peptide from Bovine Milk. *Antimicrob. Agents Chemother.* **2001**, *45* (8), 2309–2315. https://doi.org/10.1128/AAC.45.8.2309-2315.2001.

7. Huang, M. L.; Shin, S. B. Y.; Benson, M. A.; Torres, V. J.; Kirshenbaum, K. A Comparison of Linear and Cyclic Peptoid Oligomers as Potent Antimicrobial Agents. *ChemMedChem* **2012**, *7* (1), 114–122. https://doi.org/10.1002/cmdc.201100358.

8. Mwangi, J.; Hao, X.; Lai, R.; Zhang, Z. Y. Antimicrobial Peptides: New Hope in the War against Multidrug Resistance. *Zool. Res.* **2019**, *40* (6), 488–505. https://doi.org/10.24272/j.issn.2095-8137.2019.062.

9. Diamond, G.; Figgins, E.; Gao, D.; Barron, A.; Kirschenbaum, K. Broad Spectrum Activity of Antimicrobial Peptoids Peptoids versus Peptides.

10. Haug, B. E.; Stensen, W.; Kalaaji, M.; Rekdal, Ø.; Svendsen, J. S. Synthetic Antimicrobial Peptidomimetics with Therapeutic Potential. *J. Med. Chem.* **2008**, *51* (14), 4306–4314. https://doi.org/10.1021/jm701600a.

11. Mojsoska, B.; Zuckermann, R. N.; Jenssen, H. Structure-Activity Relationship Study of Novel Peptoids That Mimic the Structure of Antimicrobial Peptides. *Antimicrob. Agents Chemother.* **2015**, *59* (7), 4112–4120. https://doi.org/10.1128/AAC.00237-15.

12. Turkett, J. A. Design and Screening of Antimicrobial Peptoid Libraries. **2017**, August.

13. Sun, J.; Chen, M.; Fu, Z.; Yang, J.; Zhou, S.; Yu, G.; Zhou, W.; Ma, Z. A Comparative Study on Low and High Salinity Tolerance of Two Strains of Pinctada Fucata. *Front. Mar. Sci.* **2021**, *8* (July). https://doi.org/10.3389/fmars.2021.704907.

14. Khara, J. S.; Mojsoska, B.; Mukherjee, D.; Langford, P. R.; Robertson, B. D.; Jenssen, H.; Ee, P. L. R.; Newton, S. M. Ultra-Short Antimicrobial Peptoids Show Propensity for Membrane Activity Against Multi-Drug Resistant Mycobacterium Tuberculosis. *Front. Microbiol.* **2020**, *11* (March), 1–11. https://doi.org/10.3389/fmicb.2020.00417.

15. Yoo, Barney. "N-substituted glycine oligomers: A versatile molecular scaffold" , Proquest, 20111004

16. Nielsen, J. E.; Alford, M. A.; Yung, D. B. Y.; Molchanova, N.; Fortkort, J. A.; Lin, J. S.; Diamond, G.; Hancock, R. E. W.; Jenssen, H.; Pletzer, D.; Lund, R.; Barron, A. E. Self-Assembly of Antimicrobial Peptoids Impacts Their Biological Effects on ESKAPE Bacterial Pathogens. *ACS Infect. Dis.* **2022**, *8* (3), 533–545. https://doi.org/10.1021/acsinfecdis.1c00536.
17. Kapoor, R.; Eimerman, P. R.; Hardy, J. W.; Cirillo, J. D.; Contag, C. H.; Barron, A. E. Efficacy of Antimicrobial Peptoids against Mycobacterium Tuberculosis. *Antimicrob. Agents Chemother.* **2011**, *55* (6), 3058–3062. https://doi.org/10.1128/AAC.01667-10.
18. Brice, D.C.; Toth, Z.; Diamond, G. LL-37 disrupts the Kaposi's sarcoma-associated herpesvirus envelope and inhibits infection in oral epithelial cells. *Antivir. Res.* **2018**, *158*, 25–33.
19. Diamond, G.; Molchanova, N.; Herlan, C.; Fortkort, J. A.; Lin, J. S.; Figgins, E.; Bopp, N.; Ryan, L. K.; Chung, D.; Adcock, R. S.; Sherman, M.; Barron, A. E. Potent Antiviral Activity against HSV-1 and SARS-CoV-2 by Antimicrobial Peptoids. *Pharmaceuticals* **2021**, *14* (4). https://doi.org/10.3390/ph14040304.
20. Patch, J. A.; Barron, A. E. Helical Peptoid Mimics of Magainin-2 Amide. *J. Am. Chem. Soc.* **2003**, *125* (40), 12092–12093. https://doi.org/10.1021/ja037320d.
21. Vooturi, S. K.; Firestine, S. M. Synthetic Membrane-Targeted Antibiotics. *Curr. Med. Chem.* **2010**, *17* (21), 2292–2300. https://doi.org/10.2174/092986710791331059.
22. Chongsiriwatana, N. P.; Patch, J. A.; Czyzewski, A. M.; Dohm, M. T.; Ivankin, A.; Gidalevitz, D.; Zuckermann, R. N.; Barron, A. E. Peptoids That Mimic the Structure, Function, and Mechanism of Helical Antimicrobial Peptides. *Proc. Natl. Acad. Sci. U. S. A.* **2008**, *105* (8), 2794–2799. https://doi.org/10.1073/pnas.0708254105.
23. Ryge, T.S.; Frimodt-Moller, N.; Hansen, P.R. Antimicrobial activities of twenty lysine-peptoid hybrids against clinically relevant bacteria and fungi. *Chemotherapy,* **2008**, 54, 152-6. https://doi.org/10.1159/000119707
24. Olsen, C. A.; Bonke, G.; Vedel, L.; Adsersen, A.; Witt, M.; Franzyk, H.; Jaroszewski, J. W. α-Peptide/β-Peptoid Chimeras. *Org. Lett.* **2007**, *9* (8), 1549–1552. https://doi.org/10.1021/ol070316c
25. Patch, J. A.; Barron, A. E. Helical Peptoid Mimics of Magainin-2 Amide. *J. Am. Chem. Soc.* **2003**, *125* (40), 12092–12093. https://doi.org/10.1021/ja037320d.

26. Chongsiriwatana, N. P.; Miller, T. M.; Wetzler, M.; Vakulenko, S.; Karlsson, A. J.; Palecek, S. P.; Mobashery, S.; Barron, A. E. Short Alkylated Peptoid Mimics of Antimicrobial Lipopeptides. *Antimicrob. Agents Chemother.* **2011**, *55* (1), 417–420. https://doi.org/10.1128/AAC.01080-10.
27. Kamysz, W.; Silvestri, C.; Cirioni, O.; Giacometti, A.; Licci, A.; Della Vittoria, A.; Okroj, M.; Scalise, G. In Vitro Activities of the Lipopeptides Palmitoyl (Pal)-Lys-Lys-NH 2 and Pal-Lys-Lys Alone and in Combination with Antimicrobial Agents against Multiresistant Gram-Positive Cocci. *Antimicrob. Agents Chemother.* **2007**, *51* (1), 354–358. https://doi.org/10.1128/AAC.00344-06.
28. Laverty, G.; McLaughlin, M.; Shaw, C.; Gorman, S. P.; Gilmore, B. F. Antimicrobial Activity of Short, Synthetic Cationic Lipopeptides. *Chem. Biol. Drug Des.* **2010**, *75* (6), 563–569. https://doi.org/10.1111/J.1747-0285.2010.00973.X.
29. Lipinski, C. A.; Lombardo, F.; Dominy, B. W.; Feeney, P. J. Experimental and Computational Approaches to Estimate Solubility and Permeability in Drug Discovery and Development Settings. *Adv. Drug Deliv. Rev.* **2001**, *46* (1–3), 3–26. https://doi.org/10.1016/S0169-409X(00)00129-0.
30. Makovitzki, A.; Avrahami, D.; Shai, Y. Ultrashort Antibacterial and Antifungal Lipopeptides. *Proc. Natl. Acad. Sci. U. S. A.* **2006**, *103* (43), 15997. https://doi.org/10.1073/PNAS.0606129103.
31. Makovitzki, A.; Baram, J.; Shai, Y. Antimicrobial Lipopolypeptides Composed of Palmitoyl Di- and Tricationic Peptides: In Vitro and in Vivo Activities, Self-Assembly to Nanostructures, and a Plausible Mode of Action. *Biochemistry* **2008**, *47* (40), 10630–10636. https://doi.org/10.1021/bi8011675
32. Huang, M. L.; Benson, M. A.; Shin, S. B. Y.; Torres, V. J.; Kirshenbaum, K. Amphiphilic Cyclic Peptoids That Exhibit Antimicrobial Activity by Disrupting Staphylococcus Aureus Membranes. *European J. Org. Chem.* **2013**, No. 17, 3560–3566. https://doi.org/10.1002/ejoc.201300077.
33. Blondelle, S. E.; & Houghten', R. A.; Design of model amphipathic peptides having potent antimicrobial activities. *Biochemistry.* **1992**, 31:12688 – 12694. http://dx.doi.org/10.1021/bi00165a020.

34. Bolt, H. L.; Cobb, S. L. A Practical Method for the Synthesis of Peptoids Containing Both Lysine-Type and Arginine-Type Monomers. *Org. Biomol. Chem.* **2016**, *14* (4), 1211–1215. https://doi.org/10.1039/c5ob02279g.
35. Wender, P. A.; Mitchell, D. J.; Pattabiraman, K.; Pelkey, E. T.; Steinman, L.; Rothbard, J. B. The Design, Synthesis, and Evaluation of Molecules That Enable or Enhance Cellular Uptake: Peptoid Molecular Transporters. *Proc. Natl. Acad. Sci. U. S. A.* **2000**, *97* (24), 13003–13008. https://doi.org/10.1073/PNAS.97.24.13003.
36. Amirkhanov, N. V.; Bardasheva, A. V.; Tikunova, N. V.; Pyshnyi, D. V. Synthetic Antimicrobial Peptides: III—Effect of Cationic Groups of Lysine, Arginine, and Histidine on Antimicrobial Activity of Peptides with a Linear Type of Amphipathicity. *Russ. J. Bioorganic Chem.* **2021**, *47* (3), 681–690. https://doi.org/10.1134/S106816202103002X.
37. Kapoor, R.; Eimerman, P. R.; Hardy, J. W.; Cirillo, J. D.; Contag, C. H.; Barron, A. E. Efficacy of Antimicrobial Peptoids against Mycobacterium Tuberculosis. *Antimicrob. Agents Chemother.* **2011**, *55* (6), 3058–3062. https://doi.org/10.1128/AAC.01667-10.
38. Chongsiriwatana, N. P.; Patch, J. A.; Czyzewski, A. M.; Dohm, M. T.; Ivankin, A.; Gidalevitz, D.; Zuckermann, R. N.; Barron, A. E. Peptoids That Mimic the Structure, Function, and Mechanism of Helical Antimicrobial Peptides. *Proc. Natl. Acad. Sci. U. S. A.* **2008**, *105* (8), 2794–2799. https://doi.org/10.1073/pnas.0708254105.
39. Andreev, K.; Martynowycz, M. W.; Huang, M. L.; Kuzmenko, I.; Bu, W.; Kirshenbaum, K.; Gidalevitz, D. Hydrophobic Interactions Modulate Antimicrobial Peptoid Selectivity towards Anionic Lipid Membranes. *Biochim. Biophys. Acta - Biomembr.* **2018**, *1860* (6), 1414–1423. https://doi.org/10.1016/J.BBAMEM.2018.03.021.
40. Nielsen, S. L.; Frimodt-Møller, N.; Kragelund, B. B.; Hansen, P. R. Structure–Activity Study of the Antibacterial Peptide Fallaxin. *Protein Sci.* **2007**, *16* (9), 1969. https://doi.org/10.1110/PS.072966007.
41. Munk, J. K.; Ritz, C.; Fliedner, F. P.; Frimodt-Møller, N.; Hansen, P. R. Novel Method To Identify the Optimal Antimicrobial Peptide in a Combination Matrix, Using Anoplin as an Example. **2014**. https://doi.org/10.1128/AAC.02369-13.
42. Chen, Y.; Guarnieri, M. T.; Vasil, A. I.; Vasil, M. L.; Mant, C. T.; Hodges, R. S. Role of Peptide Hydrophobicity in the Mechanism of Action Of-Helical Antimicrobial Peptides.

Antimicrob. Agents Chemother. **2007**, *51* (4), 1398–1406. https://doi.org/10.1128/AAC.00925-06.

43. Maturana, P.; Martinez, M.; Noguera, M. E.; Santos, N. C.; Disalvo, E. A.; Semorile, L.; Maffia, P. C.; Hollmann, A. Lipid Selectivity in Novel Antimicrobial Peptides: Implication on Antimicrobial and Hemolytic Activity. *Colloids Surfaces B Biointerfaces* **2017**, *153*, 152–159. https://doi.org/10.1016/J.COLSURFB.2017.02.003.
44. Hollmann, A.; Martínez, M.; Noguera, M. E.; Augusto, M. T.; Disalvo, A.; Santos, N. C.; Semorile, L.; Maffía, P. C. Role of Amphipathicity and Hydrophobicity in the Balance between Hemolysis and Peptide-Membrane Interactions of Three Related Antimicrobial Peptides. *Colloids Surfaces B Biointerfaces* **2016**, *141*, 528–536. https://doi.org/10.1016/j.colsurfb.2016.02.003.
45. Ivankin, A.; Apellániz, B.; Gidalevitz, D.; Nieva, J. L. Mechanism of Membrane Perturbation by the HIV-1 Gp41 Membrane-Proximal External Region and Its Modulation by Cholesterol. *Biochim. Biophys. Acta - Biomembr.* **2012**, *1818* (11), 2521–2528. https://doi.org/10.1016/j.bbamem.2012.06.002.
46. Ivankin, A.; Kuzmenko, I.; Gidalevitz, D. Cholesterol Mediates Membrane Curvature during Fusion Events. *Phys. Rev. Lett.* **2012**, *108* (23), 238103. https://doi.org/10.1103/PHYSREVLETT.108.238103.
47. McPhee, J.; Scott, M.; Hancock, R. Design of Host Defence Peptides for Antimicrobial and Immunity Enhancing Activities. *Comb. Chem. High Throughput Screen.* **2005**, *8* (3), 257–272. https://doi.org/10.2174/1386207053764558. .
48. Zelezetsky, I.; Tossi, A. Alpha-Helical Antimicrobial Peptides—Using a Sequence Template to Guide Structure–Activity Relationship Studies. *Biochim. Biophys. Acta - Biomembr.* **2006**, *1758* (9), 1436–1449. https://doi.org/10.1016/J.BBAMEM.2006.03.021.
49. Chen, Y.; Guarnieri, M. T.; Vasil, A. I.; Vasil, M. L.; Mant, C. T.; Hodges, R. S. Role of Peptide Hydrophobicity in the Mechanism of Action of α-Helical Antimicrobial Peptides. *Antimicrob. Agents Chemother.* **2007**, *51* (4), 1398–1406. https://doi.org/10.1128/AAC.00925-06.
50. Tyagi, A.; Kapoor, P.; Kumar, R.; Chaudhary, K.; Gautam, A.; Raghava, G. P. S. In Silico Models for Designing and Discovering Novel Anticancer Peptides. *Sci. Rep.* **2013**, *3*. https://doi.org/10.1038/SREP02984.

51. Chen, Y.; Guarnieri, M. T.; Vasil, A. I.; Vasil, M. L.; Mant, C. T.; Hodges, R. S. Role of Peptide Hydrophobicity in the Mechanism of Action of α-Helical Antimicrobial Peptides. *Antimicrob. Agents Chemother.* **2007**, *51* (4), 1398–1406. https://doi.org/10.1128/AAC.00925-06.
52. Andreev, K.; Martynowycz, M. W.; Ivankin, A.; Huang, M. L.; Kuzmenko, I.; Meron, M.; Lin, B.; Kirshenbaum, K.; Gidalevitz, D. Cyclization Improves Membrane Permeation by Antimicrobial Peptoids. *Langmuir* **2016**, *32* (48), 12905–12913. https://doi.org/10.1021/acs.langmuir.6b03477
53. Shah, N. H.; Butterfoss, G. L.; Nguyen, K.; Yoo, B.; Bonneau, R.; Rabenstein, D. L.; Kirshenbaum, K. Oligo(N-Aryl Glycines): A New Twist on Structured Peptoids. *J. Am. Chem. Soc.* **2008**, *130* (49), 16622–16632. https://doi.org/10.1021/ja804580n
54. Makovitzki, A.; Avrahami, D.; Shai, Y. Ultrashort Antibacterial and Antifungal Lipopeptides. *Proc. Natl. Acad. Sci. U. S. A.* **2006**, *103* (43), 15997. https://doi.org/10.1073/PNAS.0606129103.
55. Kapoor, R.; Wadman, M. W.; Dohm, M. T.; Czyzewski, A. M.; Spormann, A. M.; Barron, A. E. Antimicrobial Peptoids Are Effective against Pseudomonas Aeruginosa Biofilms. *Antimicrob. Agents Chemother.* **2011**, *55* (6), 3054–3057. https://doi.org/10.1128/AAC.01516-10.https://doi.org/10.1128/AAC.01516-10
56. Avrahami, D.; Shai, Y. Bestowing Antifungal and Antibacterial Activities by Lipophilic Acid Conjugation to D,L-Amino Acid-Containing Antimicrobial Peptides: A Plausible Mode of Action †. **2003**. https://doi.org/10.1021/bi035142v. .
57. Lockwood, N. A.; Haseman, J. R.; Tirrell, M. V.; Mayo, K. H. Acylation of SC4 Dodecapeptide Increases Bactericidal Potency against Gram-Positive Bacteria, Including Drug-Resistant Strains. *Biochem. J.* **2004**, *378* (Pt 1), 93. https://doi.org/10.1042/BJ20031393.

CHAPTER 2: The design and synthesis of Lariatin A derivatives

2.1 Introduction

Potent anti-tuberculosis agents with a novel mode of action have not been developed in more than 30 years. Only cell wall synthesis and DNA metabolism inhibiting anti-tuberculosis drugs remain available to be administered clinically. The discovery of Lariatin A has drawn considerable attention as a new anti-TB agent due to its unique cyclic structure and bactericidal mechanism toward *Mtb.*[1] In this chapter, we explain the design of Lariatin A derivatives and their synthetic method. The solid phase peptide synthesis (SPPS) strategy principles will be discussed, including the various steps involved, such as coupling reactions for peptide bond formation, deprotection of protective groups, and cleavage. The Fmoc chemistry strategy selected for synthesizing the Lariatin A peptidomimetics will also be discussed.

2.2 Design of Lariatin A derivatives

2.2.1 Structure activity relationship (SAR) of Lariatin A

SAR studies are a good tool in drug discovery, allowing for the selection and optimization of ideal drug candidates. SAR for Lariatin A was carried out utilizing mutational analysis and demonstrated that four amino acid residues, namely Gly1, Arg7, Glu8, and Trp9, are important for the maturation and production in the biosynthetic machinery.[1] Additionally, this study demonstrated that the residues at positions 15 (Val), 16 (Ile), and 18 (Pro) in lariatin A are crucial for enhancing the biological activity and that Tyr6, Gly11, and Asn14 are responsible for the anti-mycobacterial action.[1,2] Furthermore, on the macrolactam ring, the aromatic amino acid residue at the residue at position 6 (Tyr6) was found to be favourable for anti-mycobacterial activity. The study also showed that the positively charged amino acid residue was favourable at position 17.[1,2]

2.2.2 Replacing lactone bond with disulfide bond

The cyclic lactone bond that gives Lariatin A its lasso structure can be difficult to form during synthesis because it involves several steps and is time-consuming and costly. Modifying the cyclic bond by a disulfide bond minimizes the number of steps and saves time and costs. The disulfide bridges are natural structural elements in proteins that bring about conformational constraints to a polypeptide backbone, enhancing their thermodynamic stability. They give an essential structural network that affects the protein's tertiary structure. The improved stability brought by cyclization gives the peptide a better resistance to environmental extremes like elevated temperatures, pH that is extremely basic or acidic and, organic solvent concentrations that are too high, or to increase the protein therapeutics' half-live.[3]

Lariatin A was derivatized by adding two cysteine (Cys) amino acid residues to the sequence for cyclization of the peptide through a disulfide bond formation between their sulfur groups (Figure 28). The Cysteine residues are placed in position 1 and in the 10th position.

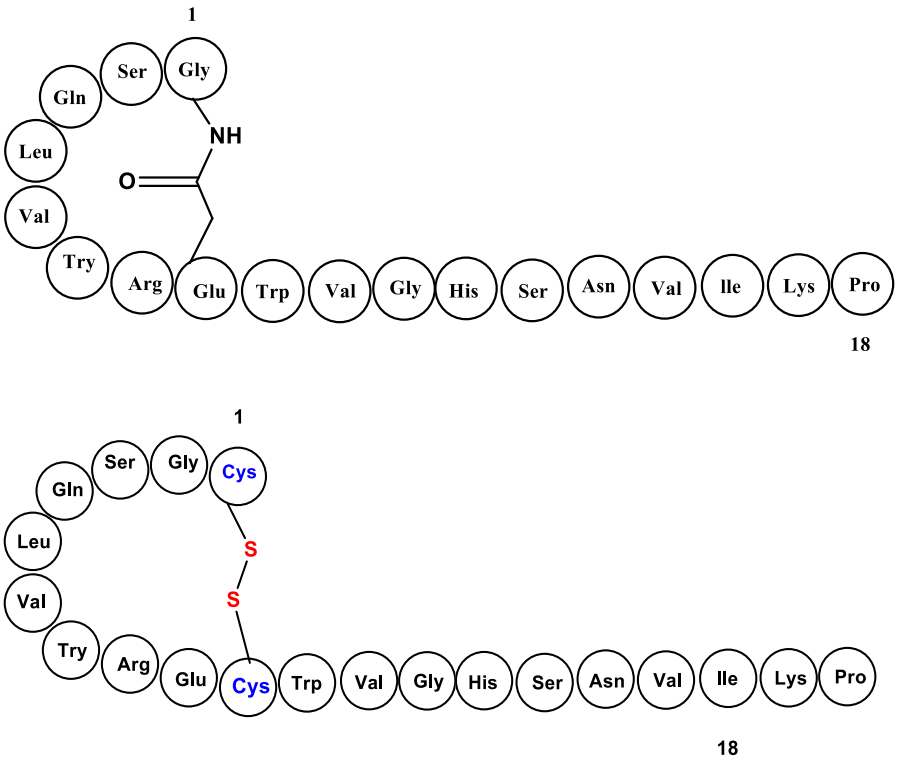


Figure 28: The structure of Lariatin A with a (top) lactone bond and (bottom) with a disulfide bond.

2.2.3 Short derivatives

Peptide drugs that are difficult to synthesize can only serve a limited number of patients because of their high prices and high production costs. This is evidently seen in the most expensive Anti-retroviral (ARV) drug, Enfuvirtide commercial known as fuzeon, which is a 36 amino acid long drug that costs about US$25000 annually for treatment.[4] To further simplify the synthetic procedure of the highly potent Lariatin A derivative, shorter derivatives of Lariatin A were designed. The synthesis of shorter derivatives is more cost-effective and easier to scale up than longer derivatives because fewer synthetic steps and highly pure peptides can be separated with fewer impurities accumulated.

The starting point in designing a shorter derivative was the linear tail region and the cyclic portions of Lariatin A (figure 29). As stated in the SAR studies Tyr6, Gly11, and Asn14 are responsible for the antimycobacterial activity, and the residues at positions 15, 16 and 18 in lariatin A are critical for enhancing the activity. These amino acid residues are found in the linear and cyclic regions, mostly in the linear region. Synthesizing these derivatives will help us determine which region of the peptide is most significant in enhancing the antimicrobial activity of Lariatin A. As a result, shorter Lariatin A peptidomimetics can be synthesised.

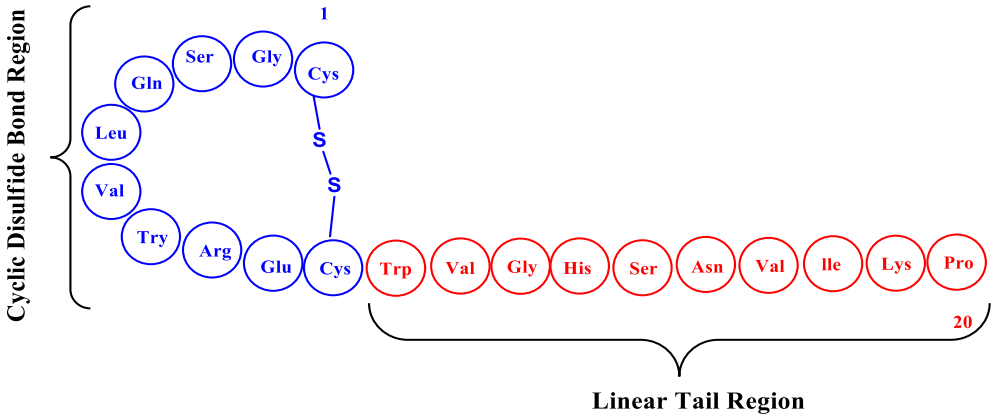


Figure 29: The structure of Lariatin A highligng the (red) linear tail region and (blue) cyclic region.

2.2.4 Incorporation of lipid moiety onto a peptide

Most pharmaceutical drugs such as antibodies and other small molecules, cannot interact with 75% of their potential drug targets.[5,6] Drugs that are antibody-based cannot access intracellular targets because of their heavier molecular weight. This means that numerous drug molecules on the market have trouble targeting an intracellular protein-protein

interaction (PPI) interface, and they account for a large portion of potential drug targets.[5] The delivery of peptide drugs to the site of action is often challenging, mostly due to membrane permeability. Chemical techniques have been utilized to structurally and functionally change native peptides to improve their affinity and enzymatic stability and make them more efficient than the parent peptide.[5]

One approach or strategy that can be considered to improve peptide pharmacokinetics and pharmacodynamic profiles of peptide-based drugs is to conjugate the peptide to lipids. A peptide called liraglutide is one example of many marketed peptides showing the success of peptide lipidation. This strategy increases the druggable potential of bioactive peptides by dramatically increasing their enzymatic stability, receptor selectivity, potency, bioavailability, and drug delivery potential (membrane permeability). A polycyclic cage molecule known as the adamantane moiety (figure 30) is frequently added to the structures of existing active compounds to boost their lipophilicity and enhance their pharmacological effects. Adamantane-based molecules benefit from the adamantyl scaffolds' well-defined three-dimensional structure, hydrophobicity, and lipophilicity for their transport through biological membranes.[7] Adamantane can function as a membrane anchor for mannose structures and therefore be exposed on liposome surfaces and, as such, be utilized in targeted drug delivery. The rigid cage moiety protects functional groups that are closeby from metabolic cleavage, enhancing the drug's stability and distribution in blood plasma. For these reasons, introducing this bulky and lipophilic molecule can make the peptide more membrane permeable.[7]

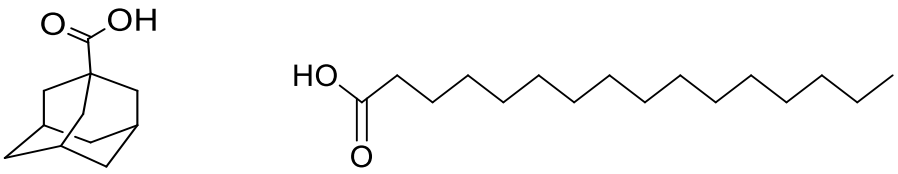


Figure 30: Structures of (left) 1-Adamantanecarboxylic acid and (right) palmitic acid.

Fatty acids with different chain lengths (such as C8-caprylic, C12-lauric, C10-capric acid, C14-myristic, and C16-palmitic (figure 30)) are often used as lipid motifs that are covalently connected to a peptide inhibitor via ester, ether, amide, or carbamate bonds. There are several methods for fatty acid conjugation. The fatty acids may be conjugated to either the N-terminus or the side chain of a lysine. Additionally, fatty acids can be used to modify the cysteine amino acid residues in peptides, producing corresponding thioester derivatives. [8]

The short peptide analogues will be derivatized by attaching palmitic acid to the Cys-10 amine group in the cyclic disulfide region. The adamantane will be attached to the end of the tail region derivative to improve its membrane permeability.

2.2.5 Lassomycine-Lariatin A hybrid

As mentioned in chapter 1, lassomycin and lariatin A share structural similarities. To further explore ways of improving the biological activity of lariatin A, the cyclic region of lariatin A will be replaced with that of lassomycin to make the lassomycin-lariatin A hybrid. The linear tail region of lariatin A was chosen because it consists of most of the important residues for enhancing the anti-TB activity. The ester C-terminal ending of naturally occurring lassomycin (Figure 7**B** in Chapter1) was replaced with an amide to encourage the stabilization of the peptide's secondary structure and to allow for a more profound interaction with the phospholipid cell membranes of bacteria and mammals. The C-terminal amidation is also reported to increase resistance towards the attack and degradation by exopeptidases that target and cleave peptides from the endings.[9,10,11] This peptide is also cyclized by forming a disulfide bond incorporating cysteine residues, as shown in figure 29.

Table 3: The designed lariatin A derivatives and their corresponding amino acid sequences.

Peptides	**Sequence**
1. Lariatin A (Pep_PNL1)	Pro-Lys-Ile-Val-Asn-Ser-His-Gly-Val-Trp-Cys-Glu-Arg-Tyr-Val-Leu-Gln-Ser-Gly-Cys
2.Lasso-Lariatin A (Pep_PNL2)	Ile-Asn-Arg-Arg-Gly-Val-Leu-Gln-Cys-Arg-tyr-Val-Leu-Gln-Ser-Gly-Cys
3. Tail alone (Pep_TA)	Pro-Lys-ile-Val-Asn-Ser-His-Gly-Val-Trp
4. Tail+adamantine (Pep_TAA)	Pro-Lys-ile-Val-Asn-Ser-His-Gly-Val-Trp-Adamantane
5.Head alone (Pep_HA)	Cys-Glu-Arg-Tyr-Val-Leu-Gln-Ser-Gly-Cys
6.Head + palmitic acid (Pep_HAP)	Cys-Glu-Arg-Tyr-Val-Leu-Gln-Ser-Gly-Cys-Palmitic acid

2.3 Peptide synthesis

A peptide bond is formed via a condensation reaction between a carboxylic acid and an amine of two amino acids. The amino end of one amino acid is protected, while the other is

protected at the carboxylic end.[12] Several methods to synthesize peptides can be used, such as; liquid phase, solid phase, microwave, and recombinant technology. Each method has its own advantages and disadvantages. The synthesis can be a combination of the synthetic strategies mentioned above depending on the nature of the peptide. The two major chemical techniques for producing peptides are SPPS and solution phase synthesis (SPS). [13]

R. Bruse Merrifield developed the SPPS method in 1963, and in this method, the peptide is attached to an insoluble solid support on which it is elongated.[14] Because synthesizing peptides requires several repetitive steps, using a solid support is advantageous because excess reagents at elevated concentrations can drive the coupling reactions to completion. In contrast to the SPS method, SPPS is a straightforward strategy that produces peptides fast and efficiently with good yields and high purity. For that reason, the SPPS is selected to improve yields. SPPS is currently the preferred strategy for synthesizing peptides in the laboratory and industry.[15] All the proposed derivatives (table 3) were synthesized *via* Fluorenylmethyloxycarbonyl (Fmoc-) SPPS strategy.

2.3.1 Principles of the SPPS method

Peptide synthesis in SPPS occurs in a succession of chemical reactions in a heterogenous reaction mixture utilizing insoluble polymer support, protected amino acids that are soluble, and a solvent.[14,15] The carboxylic end of the peptide is anchored to the solid support with its amino end protected, and the peptide synthesis occurs from the carboxyl-terminus towards the amino-terminus. The initially bound amino acid stays covalently anchored to the linker with its C-terminus during the synthesis to prevent possible side reactions from taking place on the C-terminus. The peptide is covalently "immobilized" to the solid support until all the amino acids are assembled.[4] Filtration and washings can separate the growing, insoluble peptide from the excess reagents and side products dissolved in the solvent. All the synthesis steps in SPPS can be performed in the same vessel without any material transfer.[5] By repeatedly deprotecting the N-terminus protecting group and connecting the subsequent amino acid derivative, the process of peptide elongation is carried out until the desired peptide is obtained (Figure 31).[12,15]

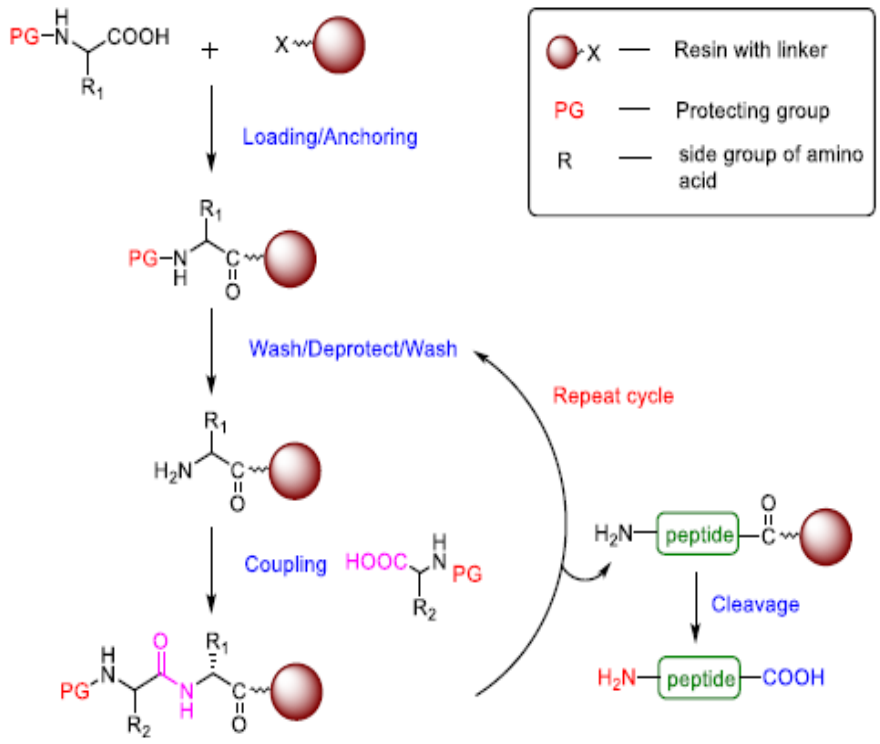


Figure 31: The general SPPS method.[12]

The final crude peptide is cleaved from the resin partially or completely deprotected using the proper cleavage solution, i.e., Trifluoroacetic acid (TFA) and scavengers which capture the highly reactive carbocations that are generated throughout the cleavage process and are responsible for the formation of undesirable by-products. Several carboxyl-terminus alterations are possible, depending on the linker.

2.3.1.1 Solid supports (Resin and linkers)

The selection of resins and linkers is vital to ensure the success of SPPS. The resin is made up of small, millimeter-scale solid beads treated with short organic moieties called linkers. The solid support is required to swell to permit the reagents easy access to the active site and provide stability during agitation in various solvents and temperatures.[12,15] A series of resins and linkers that enable a broad range of applications have been developed in the past. The choice of the polymer support and the linker directly influences the selection of coupling reagents, protecting groups and cleavage conditions.[12]

2.3.1.1.1 Resins

Polystyrene (PS) was the first polymer support to be utilized by Merrifield. Resins that are based on polystyrene with polyethylene glycol (PEG) chains (PS-PEG) in them and resins

composed of PEG chains carrying specific crosslinkers were developed (pure crosslinked PEG resins). The PS resins are made by suspension polymerisation of styrene in the presence of divinylbenzene. The styrene is cross-linked with 1% of divinylbenzene (DVB) (Figure 32) to make them insoluble in hydrophobic solvents and to avoid precipitation in aprotic organic solvents.[12,15,16]

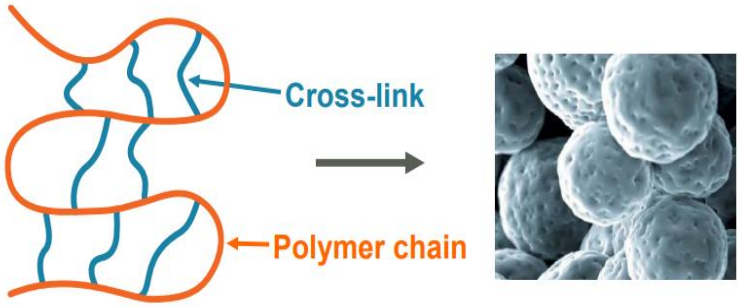


Figure 32: polystyrene (PS) cross-linked with 1% divinylbenzene (DVB).[7]

The PS polymer support is incompatible with polar solvents but swells properly in non-polar solvents like DCM or toluene. It is also compatible with solvents such as DMF, dioxane, or N-methyl-2-pyrrolidone (NMP).[15] PS resins are chemically and mechanically stable and have a wide spectrum of loading levels. PS resins are mainly chosen for synthesizing short- to medium-length peptides. PEG-based resins are often chosen for synthesizing medium- to long peptides in length or those considered to have "difficult sequences" although relatively expensive.[5] PEG-PS is amphiphilic and allows solvation by polar and non-polar solvents, including water. The hydrophilic PEG-based resins contain small amounts of PS or no amounts at all and swell well in the water allowing for the evaluation of peptide-proteins interactions when the protein is up to 3570 kDa.[4] Majority of the polymer supports mentioned above are retailed with various linkers, such as peptide amide linker (PAL), Fmoc-Rink linker, 4-Hydroxymethyl benzoic acid (HMBA) linker, etc.[7]

2.3.1.1.1 Linkers

The polymer support is permanently attached to a chemical entity known as the linker/spacer, temporarily linking the growing peptide onto the support.[3] The linkers act as a protecting group for the C-terminus carboxyl group and protect the peptide against aggregation as it grows. The linker also influences the C-terminus peptide modification and governs the best choice of the protecting groups, coupling reagents and the conditions under which the

peptide should be cleaved. Linkers are classified into high and low acid-labile linkers depending on the conditions under which they are cleaved.[4] Majority of linkers require acidic conditions for cleavage, usually, a TFA solution, which leads to a modified C-terminal end of a peptide, e.g., peptide acid, amide, hydrazine, or sulfonamides.[3] For instance, the 2-chlorotrityl (2- CTC) resin links peptides via an electrophilic substitution reaction. It is a high acid-sensitive resin that cleaves in 1% TFA.[3] Figure 33 shows more examples of resins and their cleavage conditions and the resulting modified C-terminal. Linkers are also categorized, based on their linkage with the solid support, as either integral or non-integral.[4]

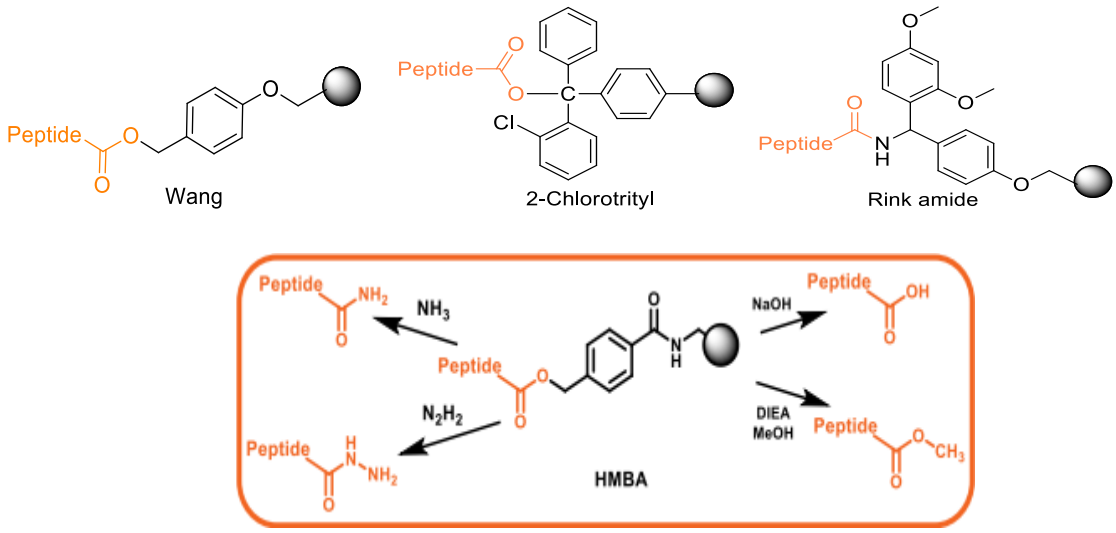


Figure 33: Wang resin results in Peptide Acids when cleaved, 2-Chlorotrityl resins results in Protected Peptide Acids under mildly acidic conditions, Rink Amides results in a Peptide Amides when cleaved, HMBA Resins (TFA stable) results in Peptide amides, hydrazide.[17]

Attaching the first amino acid to the 2-Chlorotrityl resins (C-terminal acid) has the following advantages: no epimerization during loading of the amino acid and has straight forward protocol. It is particularly advised for carboxyl-terminus of cystine, proline, and triptophan.[15]

2.3.1.2 Protecting groups

The functional groups of amino acids not taking part in the creation of the amide bond need to be protected if the intended peptide is to be obtained at the end of the synthesis. In SPPS, there are two basic categories of protection: temporary groups and permanent groups.[3] The Boc/Benzyl and Fmoc/tBu are the two protection methods related with SPPs. Boc and Fmoc groups are attached to the amino-terminus of amino acids. These groups function as short-term protecting groups, with the fmoc removed under basic conditions and boc group

removed under acidic conditions. The benzyl-type functionalities usually act as permanent protecting groups for the Boc/Benzyl strategy and are removed at the end of the synthesis when the peptide is cleaved off the resin. Strong acidic conditions like hydrofluoric acid (HF) with scavengers such as anisole are used to remove or inactivate the formed carbocations. Due to these harsh conditions, this strategy requires special instrumentation, and the peptide chain at the end of the synthesis can be damaged. The design of the Fmoc group by Carpino *et al.* was a considerable breakthrough in the synthesis of linear peptides. The Fmoc/t-Bu strategy is a more moderate method that employs an orthogonal protection system. This system demonstrates that multiple protecting groups can exist in a molecule and can be selectively deprotected. Figure 34 explains the orthogonality of Fmoc/t-Bu protection.[11]

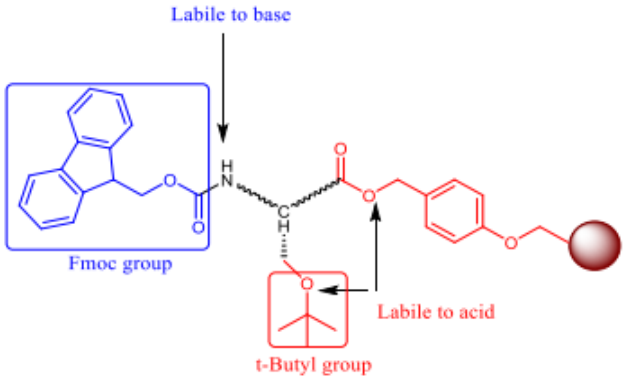


Figure 34: The Orthogonal protection system using Fmoc/t-Bu chemistry.[17]

2.3.1.3 Peptide cleavage

Following a series of cycles in amino acid coupling reactions, deprotection, and washings, protecting groups still attached to the peptide must be detached from the developed peptide.[3] These groups are cleaved by acidolysis, and the protection scheme that was used determines the chemical that will be used for cleavage. For Boc/Bzl protection, strong acids are used for cleavage, while a relatively milder acid such as TFA is used for the cleavage of the Fmoc/tBu groups (figure 35). Because free protecting groups will be generated during the cleavage process, it is important to include scavengers. The addition of scavengers should be optimized to ensure that there are no acid-catalyzed side reactions during the cleavage.

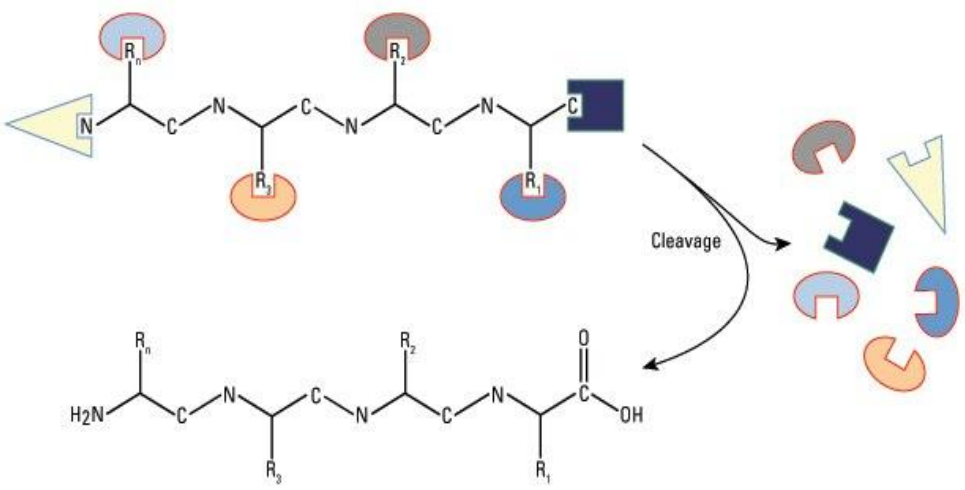


Figure 35: Cleavage of permanent and temporary protecting groups on peptide.[18]

2.3.1.4 Peptide purification

Even though the synthetic methods of peptides have been optimized and peptides produced in large quantities, the process is still imperfect. Occurrences like incomplete deprotection or side reactions with protecting groups during the synthesis can result in truncated or deletion sequences and other side products. The probability of such events occurring increases as the length of the peptide sequence increases. Therefore, there is an inverse correlation between the peptide yield and the peptide length.[11]

The peptide purification strategies normally combine separation techniques that use physiochemical peptides' traits, such as charge, hydrophobicity, and size. The separation techniques include size-exclusion chromatography, Ion exchange chromatography (IEC), partition chromatography, and high-performance liquid chromatography (HPLC). Reverse-phase chromatography (RPC) is the most extensively applied technique for the purification of peptides. Normally in HPLC, the stationary phase attracts polar, hydrophilic molecules eluted at different retention times by increasing the concentration of polar solvents in the mobile phase. In contrast, the stationary phase in RPC is a hydrophobic C4, C8, or C18 n-alkyl hydrocarbon ligand, which attracts hydrophobic molecules from aqueous solutions, and their retention time is a function of the hydrophobicity of the molecule and that of the mobile phase.

Purity is expressed as a ratio of the intended peptide to contaminants that absorb at the wavelength of the peptide bond (210-220nm). Depending on the application for which the peptides will be utilized, various levels of purity are commercially accessible:[18]

- >95% purity is acceptable for quantitative studies like NMR, receptor-ligand binding studies, and *in vivo* studies,
- >80% purity for High-throughput screening, non-quantitative enzyme-substrate studies, antibody affinity purification and plate coating for cell attachment, and
- >70% purity is acceptable for ELISA standards, ELISPOT assays and polyclonal antibody production.[18]

2.4 Synthetic method

The peptides were synthesized manually utilizing preferred glass peptide vessels over plastic vessels due to the corrosive nature of the solvents used in the peptidomimetic synthetic process. A peptide vessel with a porous glass frit minimizes subsequent transfer to another apparatus because the filtering and washing of the resin remove by-products and excess reagents done in the same vessel. Vessels come in various frit sizes, and it is important to use the frit with appropriate porosity for the mesh size of the resin bead to avoid the resin from getting trapped in the frit during washes. Nitrogen gas is funnelled through the peptide vessel to mix the heterogeneous mixture properly.

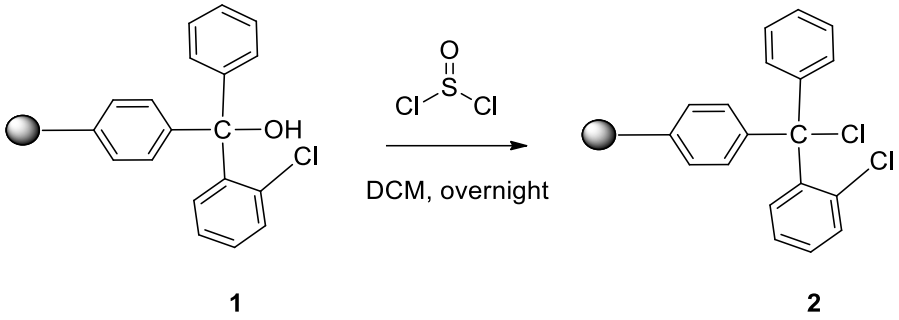
The Lariatin A peptidomimetics Pep_PNL1, Pep_TA, Pep_TAA, Pep_HA, and Pep_HAP were synthesized following the general SPPS synthetic route on a 2-chlorotrityl resin to afford a carboxylic end. The rink amide resin was used to synthesize the Pep_PNL2 to afford an amide C-terminal ending. The synthetic method that was developed during the synthesis of the Pep_PNL2 is discussed below.

Method 1

2.4.1 Activation and swelling of 2-chlorotrityl resin

The 2-chlorotrityl chloride resin is highly hygroscopic. It can react with atmospheric moisture and convert to the inactive 2-chlorotrityl alcohol resin. Since the resin must be stored and handled under inert conditions and at low temperatures, the beads must be allowed to acclimate to room temperature for 24 hours before reaction setup. This allows resin beads to

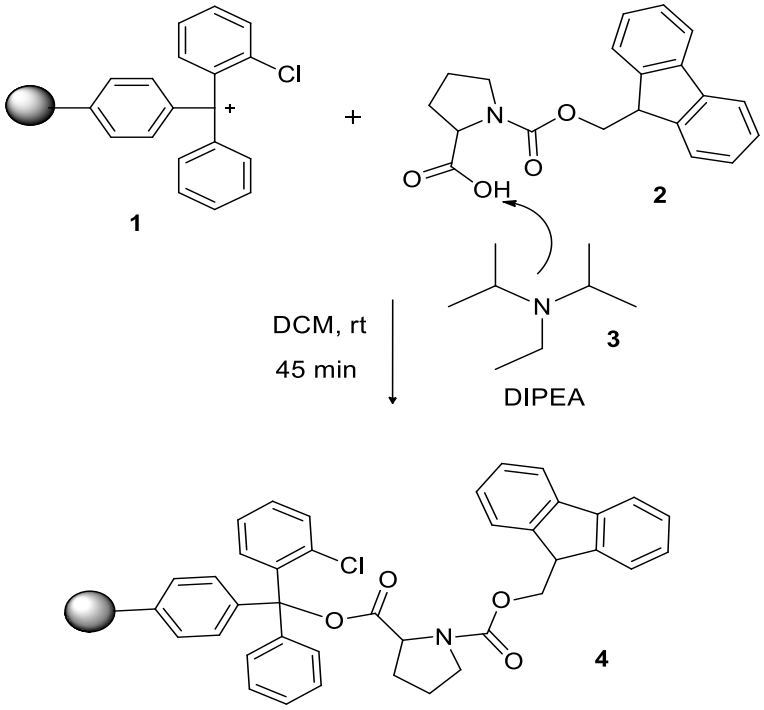
swell properly and expose the reaction sites. The glassware and reagents were carefully dried before use to avoid hydrolysis of the activated resin into the alcohol form. Activation was achieved by suspending the 2-chlorotrityl resin in dry DCM and 1.2 eq of thionyl chloride (Scheme 1). The resin's terminal hydroxyl group was restored to its chloride form, making it reusable for further synthesis. After 24 hours, the activated resin was decanted into the dry vessel, and the solvent was filtered off, followed by multiple washes with dry DCM while bubbling with inert nitrogen gas. The solution of the first amino acid was added immediately after washing.



Scheme 1: The activation mechanism of 2-chlorotrityl resin.

2.4.2 Activation of the first amino acid and its attachment to the resin

First, the amino acid (Fmoc-Pro-OH) was dissolved in dry DCM and DIPEA (1.0 equivalent) then the solution was added to the resin. The fmoc protecting group introduces a sterically hindered functionality to the amine, increasing the likelihood of preferential binding at the carboxyl end. The base (DIPEA) deprotonates the carboxylic proton on the proline to allow the nucleophilic oxygen to attach to the resin (Scheme 2). The reaction was gently mixed by bubbling nitrogen gas for 45 minutes. The coupling was repeated to ensure that all the reactive sites on the resin were occupied.



Scheme 2: The reaction of 2-chlorotrityl with fmoc-Pro-OH.

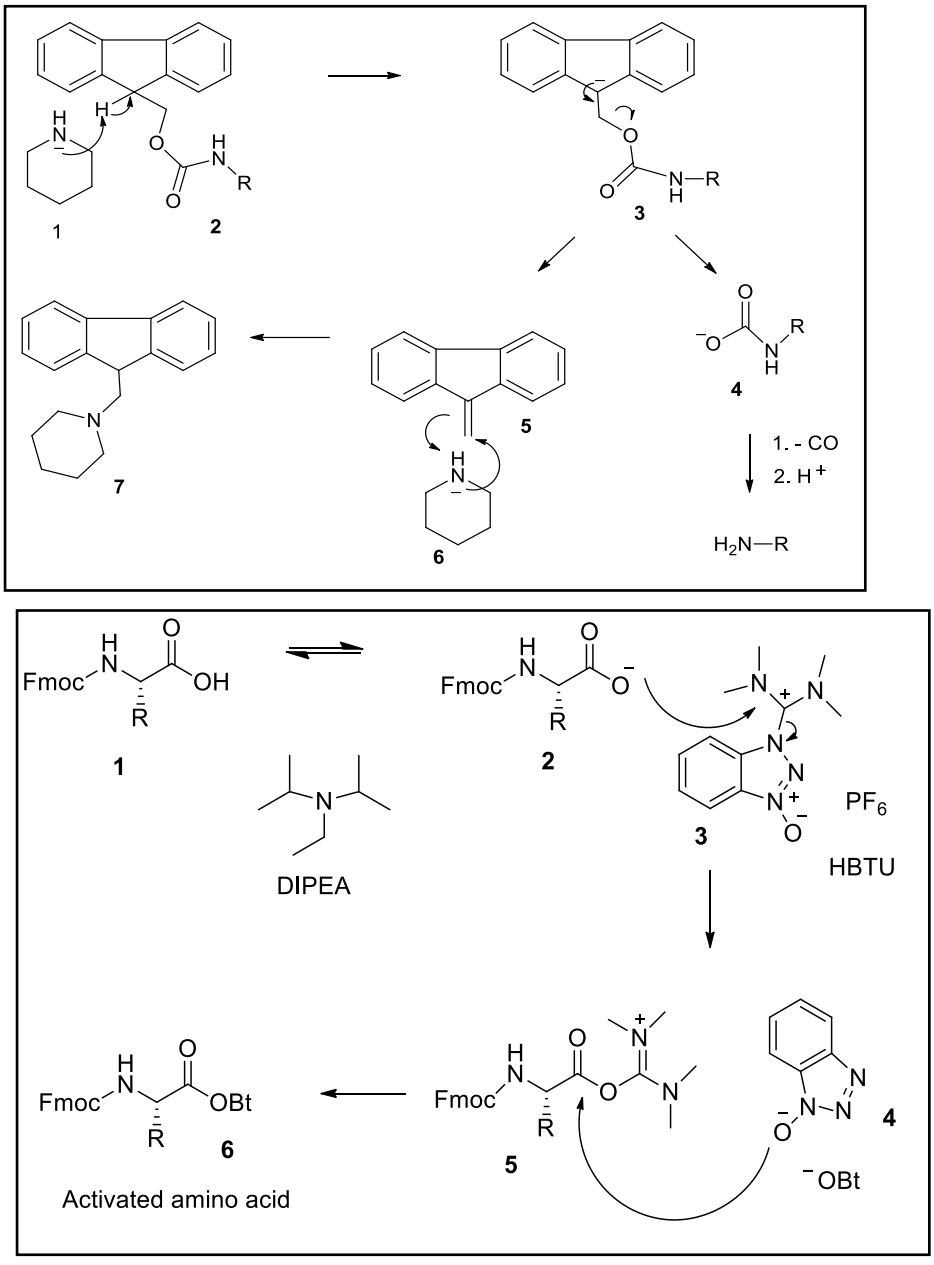
2.4.3 Determination of the loading capacity

Coupling of the first amino acid is crucial because its loading capacity is used to determine the mass of the subsequent amino acids required to ensure effective coupling. The mass of the first amino acid and the volumes of DIPEA and DCM were calculated based on the estimate that the loading capacity of the 2-chlorotrityl resin was 0.5 mmol/g. The loading capacity was determined after coupling the first amino acid by analyzing the piperidine-dibenzofulvene by-product using the UV spectrophotometer. The absorbances of two samples from this resin were measured in triplicate using a UV spectrophotometer (method described in more detail in section 7.3.3). The absorbances were averaged and used to calculate the number of moles that will be used to determine the mass of subsequent amino acids, coupling agent (HBTU), and the volume of n-methylmorpholine (NMM).

2.4.4 Peptide elongation

The fmoc on the resin attached proline was removed with 20% piperidine in DMF (scheme 3). The second amino acid (Fmoc-Lys-OH was weighed and mixed with HBTU. HBTU activates the carbonyl of this amino acid by reacting with the free carboxy group to generate a reactive species. The base (DIPEA) was added to deprotonate the NH_2 group to make it more nucleophilic (Scheme 3). The nucleophile attacks the highly electrophilic carbonyl to enable

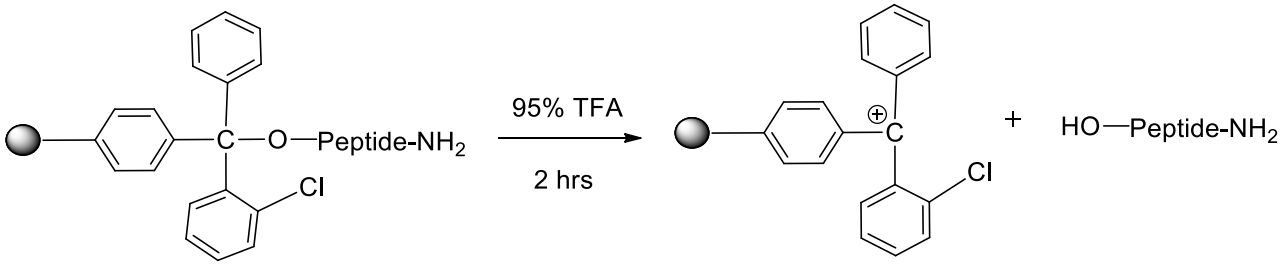
the formation of a new amide bond and the coupling of Fmoc-Lys-OH to the resin-attached amino acid. The fmoc group of the second amino acid was then deprotected to expose the amine group, which reacted with the upcoming activated third amino acid. The excess reagents and by-products in each step were filtered off the reaction. The resin was washed with DCM (5 ml x 2) and DMF (5 ml x 2) before coupling the next amino acid. Each coupling was conducted over 45 minutes, and double couplings were done for each amino acid to improve the peptide yield.



Scheme 3: (top) removal of fmoc protective group with piperidine and (bottom) activation of amino acid in presence of DIPEA and HBTU.

2.4.5 Cleaving the peptide

The fully assembled peptide was cleaved from the solid support, and the permanent protecting groups were removed by acidolysis using a 95% trifluoroacetic acid (TFA) cocktail with 2.5% triisopropylsilane (TIS), and 2.5% water (Scheme 4). TIS and water are used as free radical scavengers for the cleaved protecting groups because the highly reactive cationic species generated during cleavage can cause damage to the peptide structure by irreversibly attacking the backbone and alkylating it, causing impurities and low yield. Scavengers quench any reactive species that may be generated during exposure from this strong acid cleavage. The peptide cleavage time from the resin was 2 hours. The peptide was then precipitated using cold diethyl ether, and the solution was decanted after centrifuging. The washing process was repeated four times.



Scheme 4: Cleavage of the desired peptide from the 2-chlorotrityl resin.

2.4.6 Cyclization using iodine

The cleaved peptide was dissolved in an iodine solution in DMF:water (4:1). Iodine cleaves the cysteine triphenylmethyl (Trt) protecting group and oxidizes Cys to form a disulfide bridge simultaneously. The iodine also acts as a scavenger for the Trt carbocation. To prevent intermolecular disulfide bridges, which can be brought on by a concentrated solution, a dilute iodine solution was employed. Cyclization is achieved when an iodine-bound Cys reacts with another Cys upon Trt cleavage. Excess iodine is reduced and removed using ascorbic acid.

2.4.7 Peptide purification and characterization

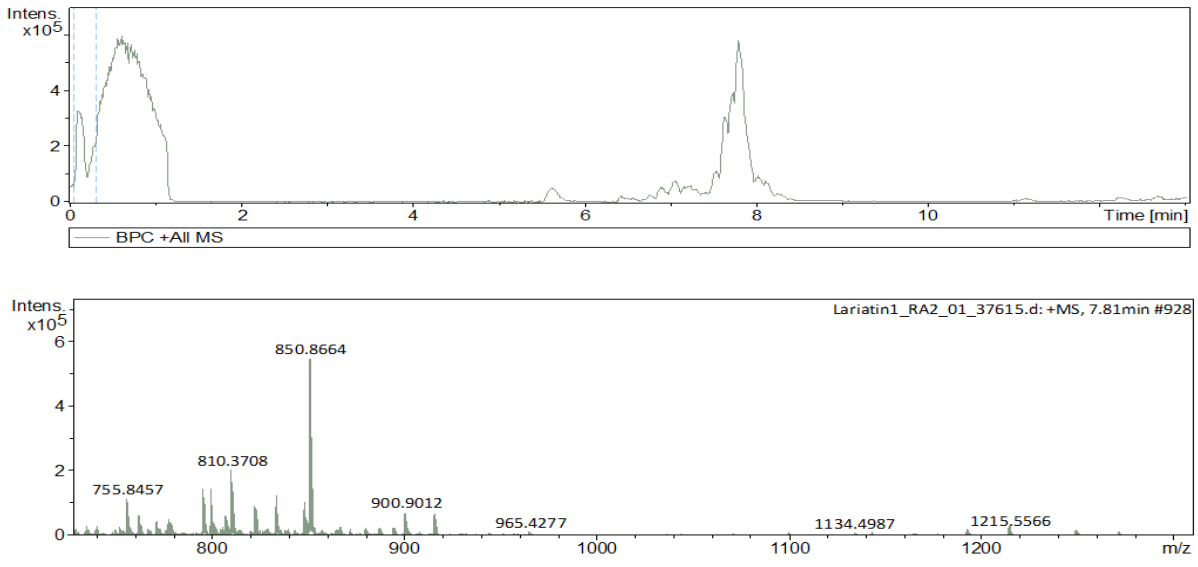
All synthesized derivatives were purified using a semi-preparative HPLC instrument via reversed-phase chromatography. The samples were eluted using a flow rate of 15 ml/min and collected using a fraction collector. An acetonitrile/water mobile phase solvent system was used. Each solvent had 0.1% formic acid (v/v) used as an ion pairing agent. The peptides were analyzed using Liquid Chromatography Mass Spectrometry (LC-MS) and eluted with a gradient

method from 5 – 95 % ACN in 10 min with a 0.3 ml/min flow rate. A two-buffer system was employed, Buffer A consisted of 0.1 % formic acid/H_2O (v/v), and Buffer B consisted of 0.1 % formic acid/acetonitrile (v/v). A Phenomenex Kinetex XB-C18 column (5 34 µm, 100 Å, 250 mm × 21.2 mm) was used to separate the compounds at a 16 ml/min flow rate.

2.5 Results and discussion

2.5.1 Synthesis of Pep_PNL1 (lariatin A)

Analysis from the LCMS confirmed the synthesis of the Pep_PNL1 derivative following the SPPS method described above. The expected masses of of 1249.6009 $[M + 2H]^{2+}$ and 833.4028 $[M+3H]^{3+}$ were observed however, the peaks intensities were very low compared to the impurities. Figure 36 shows the chromatogram for the full peptide; the desired molecular peak was found at a retention time of 7.8 minutes. The peak region on the spectra had to be zoomed in to observe the expected mass due to the very low-intensity peaks. This was attributed to poor ionization or many impurities in the sample matrix that suppressed the ionization. Formic acid was added to the peptide to improve the ionization. Low levels (0.1%) of formic acid often facilitate ionization by ensuring the analyte is more basic than the solvent, even in small amounts. However, the intensity did not improve after adding a few drops of formic acid. The ionization could have been affected by incomplete deprotection of the Fmoc group, which hindered the NH_2 group at the N-terminal end from getting ionized.



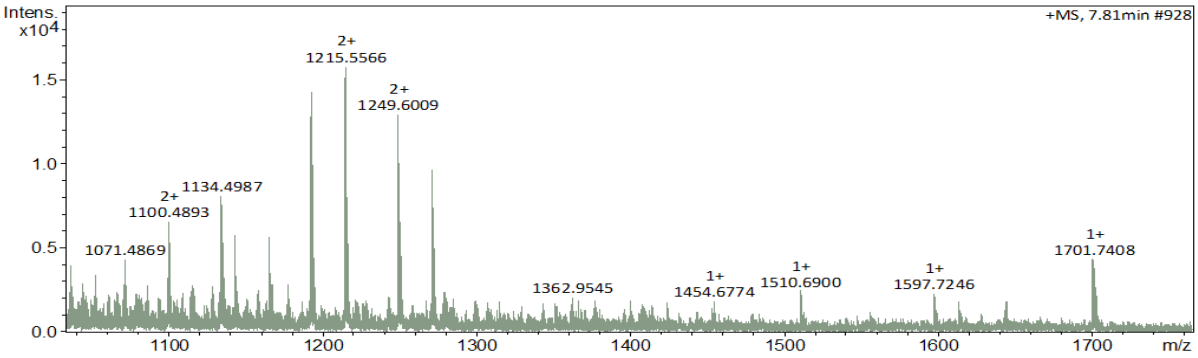


Figure 36: The chromatogram of the full peptide showing the desired molecular peaks 1249.6009 $[M + 2H]^{2+}$ and 833.4028 $[M+3H]^{3+}$

Attempts to cyclize this peptide using the iodine method described above led to more side reaction fragments that could not be assigned. Furthermore, the peptide was not cyclized (Figure 37).

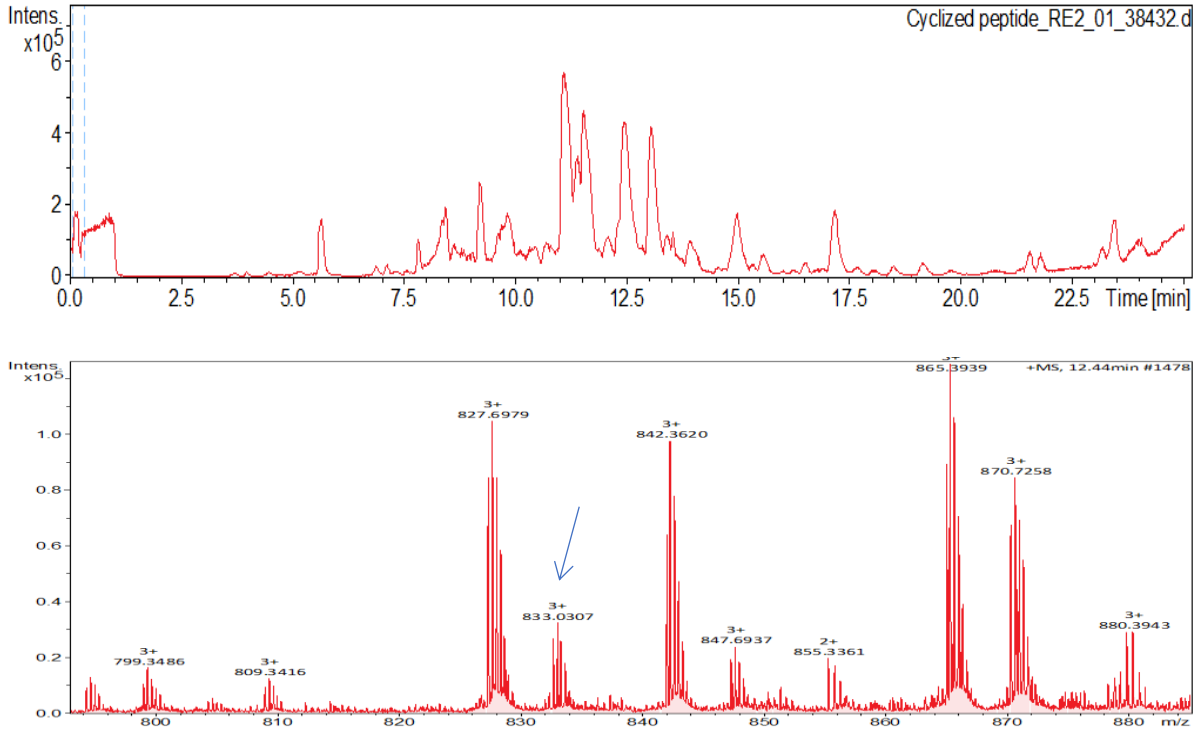


Figure 37: The chromatogram obtained after the cyclization of the peptide.

Although the developed synthetic procedure was successful in coupling the amino acids until the peptide was complete, more work was required to improve the large-scale synthetic procedure. Due to the low yield and impurities, this peptide was not considered for purification because separating the desired peptide would have been more difficult, time-

consuming, and costly. The conditions of the original procedure were varied to optimize the yield and purity of the Pep_PNL1 peptide. Problems with the method described above were identified.

2.5.2 Problem identification for Method 1

During the synthesis, the LCMS was used to monitor the coupling reactions. Small samples were periodically cleaved from the 2-CTC resin during the peptide elongation and analyzed via mass spectrometry to characterize intermediates. The decision to couple the same amino acid more than twice (adding the activated amino acid twice before removing Fmoc) was made from the results obtained during the monitoring process. Some amino acids do not couple easily due to factors such as steric hindrance and must be coupled multiple times for the reaction to complete.

The first problem identified in the synthesis was the incomplete reaction between the first amino acid (Proline) on the sequence and the second amino acid (lysine). Incomplete deprotection of proline was observed as the molecular peak for Fmoc-Pro-OH (338 m/z) was present even after double coupling lysine. Increasing the number of couplings would not drive the reaction to completion because the amine on the fmoc-pro is not accessible. The difficulty prediction software also predicted that coupling the two amino acids may be difficult (Figure 39).

A	B	C	D	E	F	G	H	I	J	K	L	M	N	O	P	Q	R	S	T
Sequence	**Predict Coupling Difficulty**																		
PKIVNSHGVWCRYVLQSGC	P 1,18	K 1,26	I 1,13	V 0,98	N 0,98	S 0,98	H 1,06	G 1,03	V 1,09	W 1,09	C 1,13	R 1,07	Y 1,11	V 1,05	L 0,92	Q 0.88	S 0.88	G 0.88	C 0.88

Figure 38: The coupling difficulty prediction spreadsheet.

The most likely cause for this difficulty is that the reactive nitrogen in proline is a secondary amine and considerably less reactive than the reactive nitrogen in other amino acids. The pKa of the proline nitrogen, which is approximately 1 full log unit lower than all other amino acids (10.6 vs. average 9.5), with the exception of cysteine, serves as evidence for this. This means that the fmoc deprotection step needs to be improved by introducing a stronger base or increasing the deprotection reaction time. After ensuring complete deprotection, lysine was coupled more than once because of the less reactiveness of proline nitrogen and lysine's bulkiness which caused steric hindrance.

The second problem encountered was coupling glycine, which followed histidine on the sequence. Histidine coupled easily to serine with just a single coupling, however, incomplete coupling was observed after double coupling glycine for 45 minutes. Glycine is a small flexible residue without a side chain; therefore, it could not have encountered steric hindrance. Double coupling improved the coupling, however, just as with Pro-Lys coupling, the fmoc deprotection of histidine did not complete.

From Gly-8 amino acid onward, truncated peaks and molecular peaks were observed, which could not be explained. This meant side reactions were taking place and impurities growing as the peptide chain elongated. Peptide folding or aggregation during synthesis may be the root of this problem. The primary cause of this, particularly for hydrophobic sequences, is the creation of parallel sheets through folding during synthesis or intermolecular hydrogen bonding between polypeptide strands, which slowed down or prevented deprotection from occurring completely, as well as coupling from occurring completely.This aggregation was mostly observed from the 5^{th} or 6^{th} amino acid to the 12^{th} amino acid.[19]

Because of the suspected aggregation challenge, attempting to couple bulky amino acids while the chain is already 10 amino acids long can be difficult. Arginine is in the 13^{th} position, and it was challenging to couple it due to the bulky side chain protecting group, the 2,2,4,6,7-pentamethyldihydrobenzofuran-5-sulfonyl chloride (pbf). Coupling bulkier amino acids like tryptophan and tyrosine required longer reaction times and double coupling, which could give ample time for other undesired reactions. Sequence modifications made during cleavage, inadequate deprotection, deletion, and truncation are other issues that could arise during peptide synthesis. Although inevitable, these problems can be minimized by varying the reaction conditions.

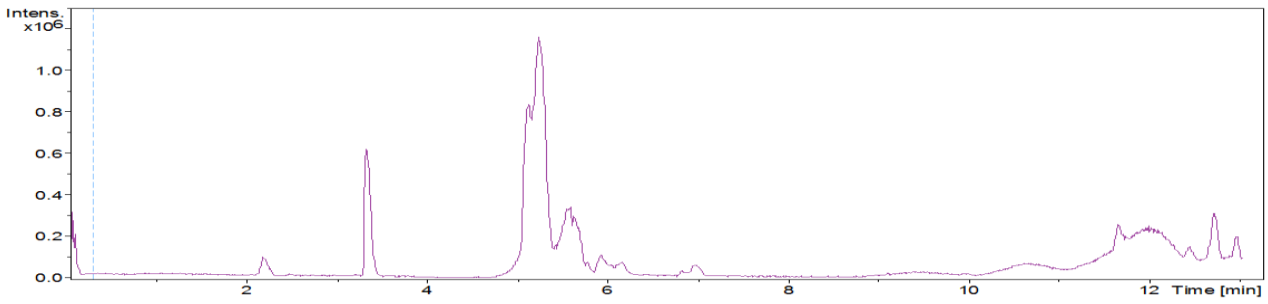
Method 2

On the second attempt, the removal of fmoc was carefully monitored on the LCMS. Analysis showed that the deprotection of the Fmoc group from Fmoc-Proline-1 using 5 ml of 20% piperidine for 5 minutes (x2) was not effective. In light of this, 5 % of a stronger base (1,8-Diazabicyclo[5.4.0]undec-7-ene) was added to the 20% piperidine and the deprotection was repeated twice for 10 minutes each time. Analysis by LCMS showed that the deprotection occurred completely for proline. The deprotection of fmoc for all amino acids improved when the time was increased from 5 minutes to 10 minutes and fewer truncated sequences were

observed. This method efficiently deprotected histidine-7 to completion, and the double coupling was done for the incoming amino acid after histidine and coupled arginine three times.

N,N-Diisopropylethylamine (DIPEA), a sterically hindered base, was changed to N-Methylmorpholine (NMM). Lysine-2 was coupled using NMM and HBTU as the coupling reagent (preferred because it is cheap and works efficiently with most peptide sequences) for 40 minutes. LCMS showed that there was still some unreacted resin attached proline without fmoc. Thus, lysine was coupled again, and the reaction time was then lowered to 30 minutes to minimize the side reactions that may occur if the reaction is prolonged. This was an effective method as no proline was present on LCMS. The bulky amino acids like tyrosine-14 and tryptophan-10 were coupled twice except for arginine-13, which was coupled three times.

The modifications were efficient in minimizing the impurities and improving the yield of the peptide. Removal of fmoc at the end of the synthesis was also carefully monitored, and deprotection of fmoc with 20% piperidine for 10 minutes repeated twice was effective. The chromatogram below shows the crude product before the peptide was cyclized. The most intense and broad peak, which eluted in the 4.5-5.5 minutes range, consisted of the desired peptide with minimum impurities compared to the first attempt. The second shoulder of this peak showed a molecular ion peak corresponding to an additional mass of 43.9 with a mass-to-charge ratio (m/z) of 774.0405 $[M+2H]^{2+}$ and 580 $[M+3H]^{3+,}$ and it eluted very closely to the peptide of interest (Figure 39 **(bottom)**). The plausible explanation for this molecular peak is the formic acid adduct attached to the peptide, thus increasing its mass by 44 and causing the split observed on the chromatogram.



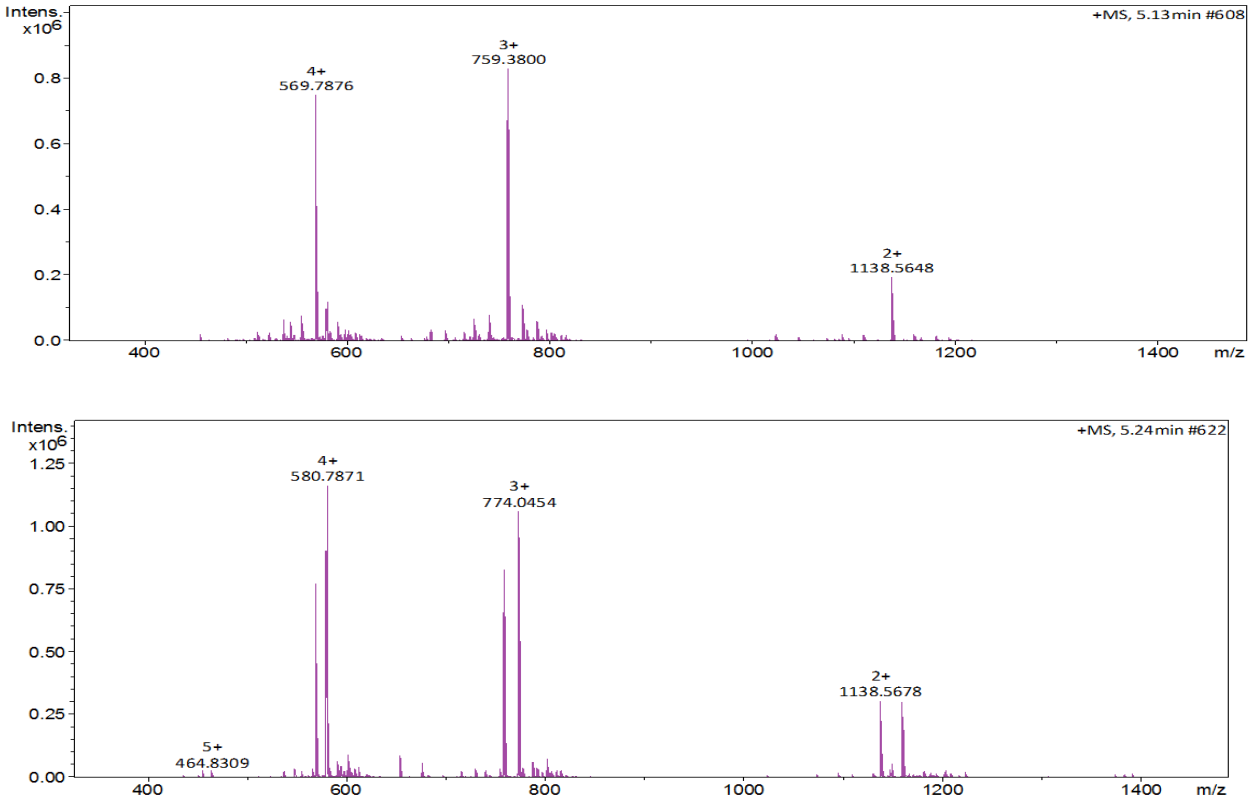


Figure 39: top; The chromatogram of the full lariatin A peptide, (middle) the spectrum showing the mass of the peptide, and (bottom) the spectrum showing the impurity that elutes closely to the peaks of interest.

The peptide was cleaved off from the resin by suspending the resin in a cocktail of 94 % TFA: 2.5 % H_2O: 2.5 % EDT: 1 % TIS and leaving it to shake for 3 hours. The solution was filtered off and cold diethyl ether was added to precipitate out the peptide from the cleavage solution and soluble by-products.

Cyclization using the proposed iodine method resulted in more chromatogram impurities and a mixture of cyclized and uncyclized products. A different approach was considered to cyclize the peptide. The cleaved crude product was dissolved in a solution of 20% DMSO in millipore water. The peptide was left to cyclize at room temperature overnight. Analysis using LCMS confirmed that a bond had formed between the thiol groups on Cys residues, as the peptide mass is now missing two protons. Figure 40 shows the expected mass of 1137.5565 $[M+2H]^{2+}$, 758.7092 $[M+3H]^{3+}$, and 569.2855$[M+4H]^{4+}$. Hence the Lariatin A derivative was successfully cyclized (Figure 40).

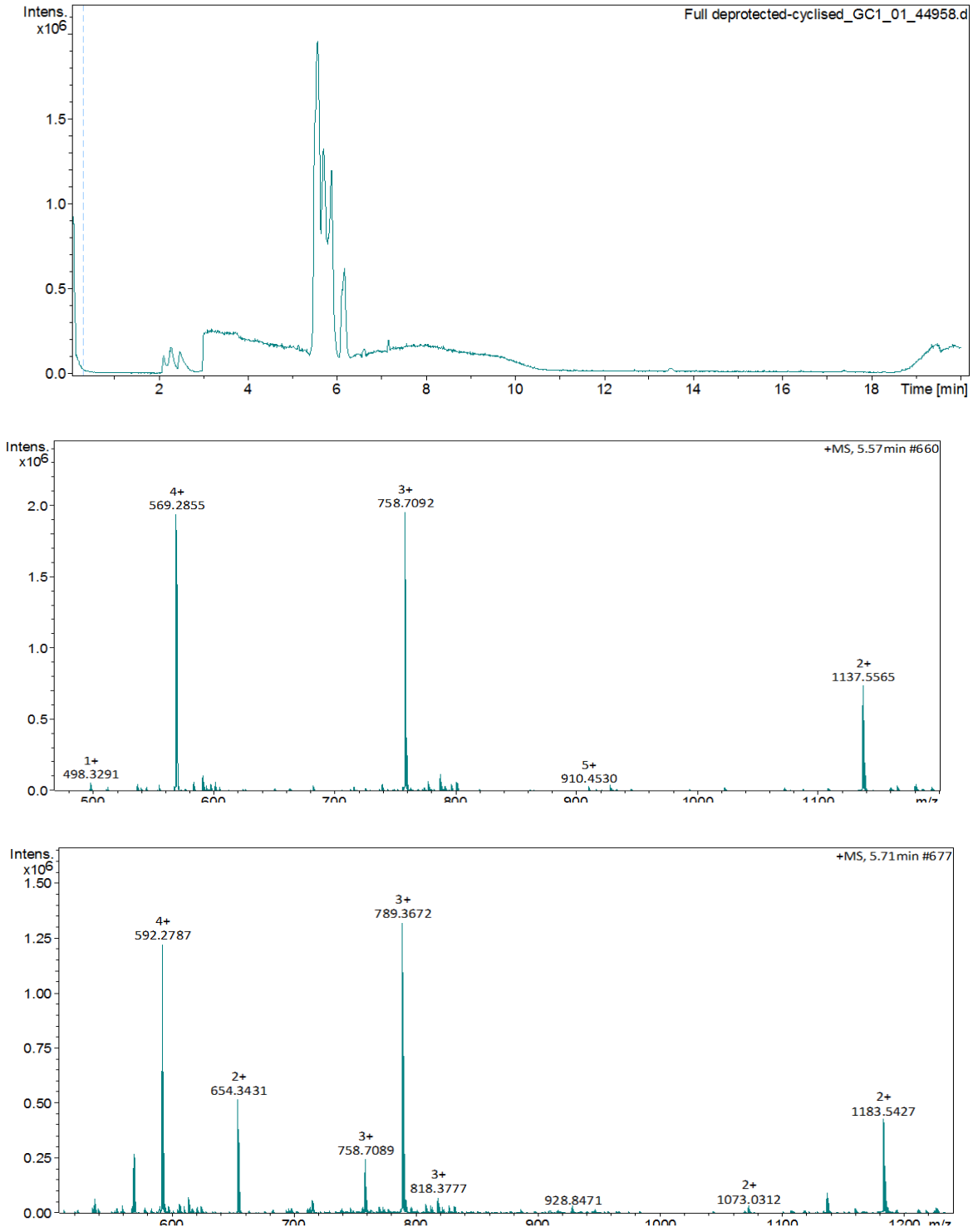


Figure 40: The chromatogram of the full lariatin A peptide after cyclization.

This peptide was then purified using a solvent gradient method of 5 – 95 % acetonitrile in 10 minutes, it was observed that desired peak started eluting when acetonitrile was at 35 %, but the separation from other impurities was not good (**Method 2-1)**. On the second attempt, the acetonitrile percentage increased from 5-20% in 5 minutes, allowing all the DMSO and polar

by-products to elute from the column. Then the percentage was increased from 20-30% in 1 minute followed by a 30-40% ACN increase in 3 minutes (**Method 2-2)**. Since the peptide was eluting at 30-40% acetonitrile, the time taken for this increase was prolonged and the percentage was adjusted to 34-37% to separate the lariatin A peak which eluted out close to 35% ACN but the peaks would not separate (**Method 2-3)**.

The peptide fractions were then collected, re-concentrated, and purified again. Although the peptide purity improved, the impurities were still eluting with the peptide. To check if there is any possibility for these impurities to separate, the collected fractions peptide was separated on the LCMS using an isocratic method. This did not yield positive results as the impurity coeluted with the peptide, even when the acetonitrile was replaced with methanol. Figure 41 shows the poor separation of the desired peak from an impurity.

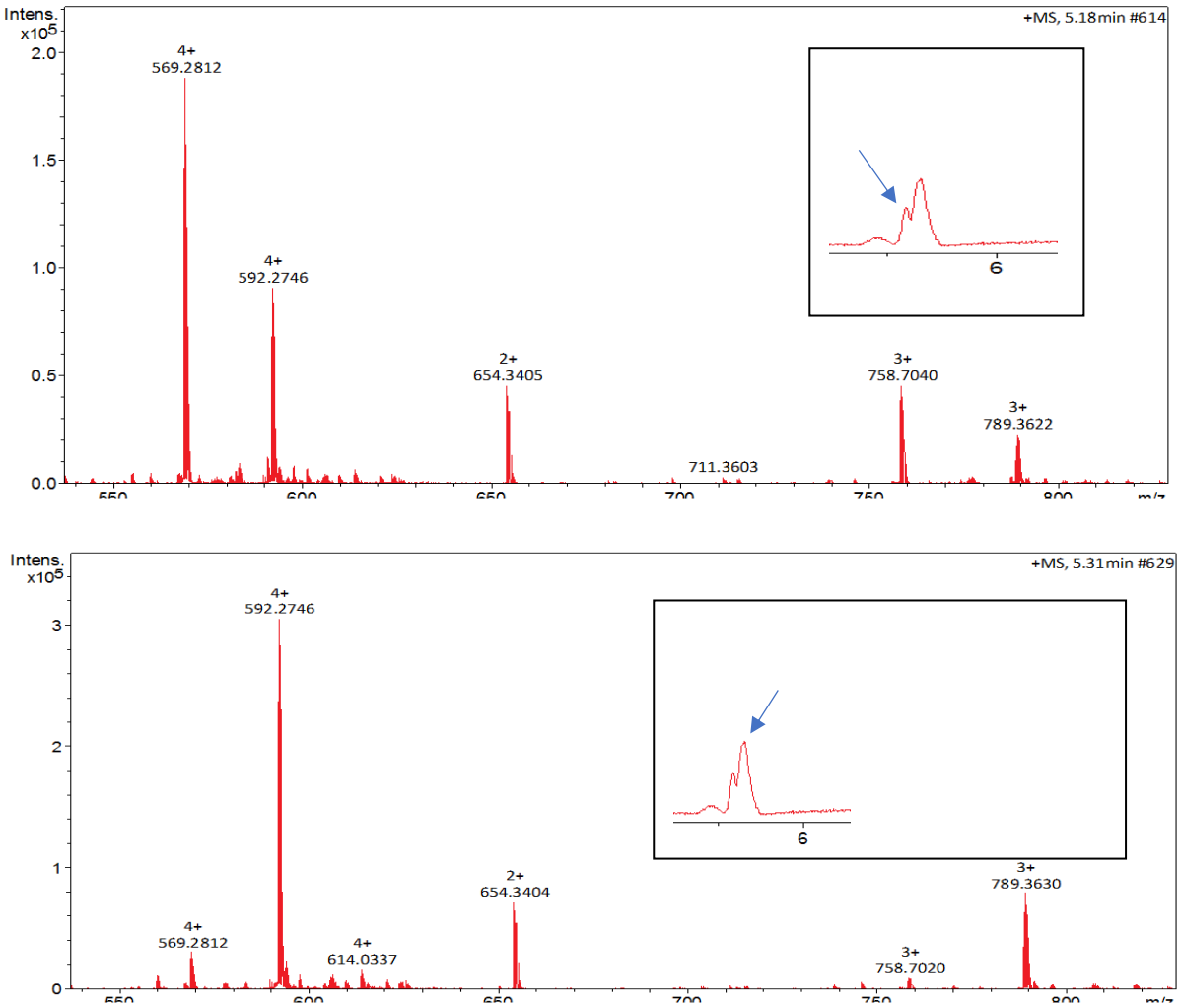
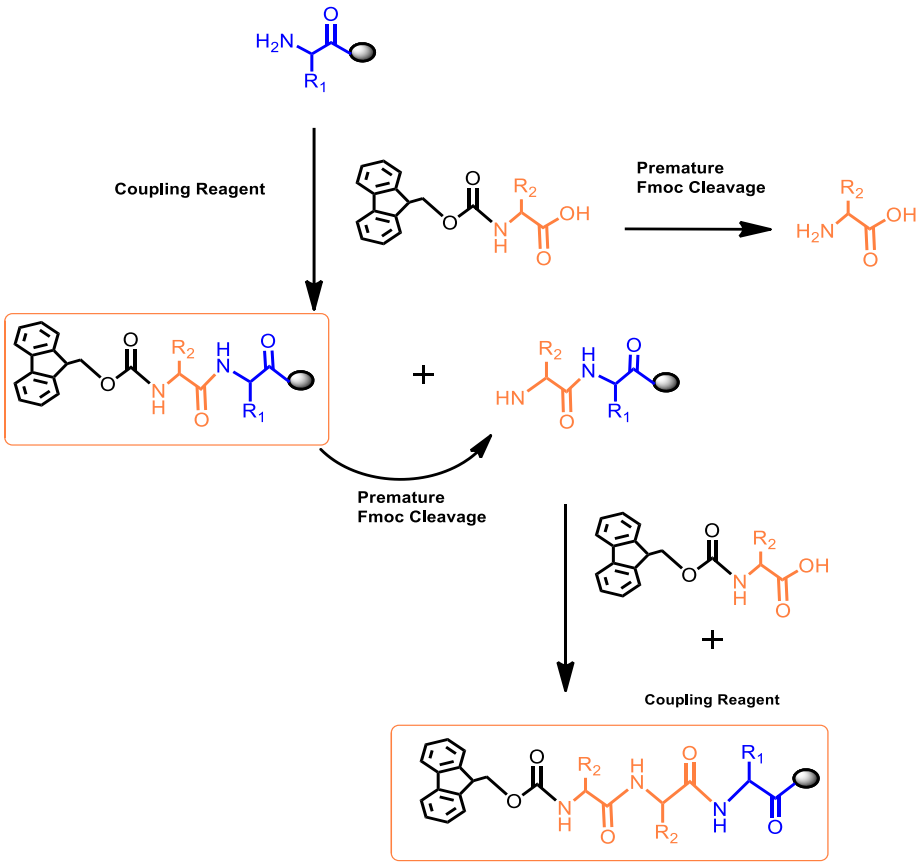


Figure 41: The spectra of Pep_PNL1 showing the co-eluting impurity peak.

2.5.3 Problem Identification

The peak with a retention time of 5.57 minutes from the cyclized peptide has an additional mass of 87 m/z to the desired peptide mass. This peak posed a problem during purification because it was coeluting with the desired peak. Initially, the additional mass of 87 m/z was suspected to be caused by EDT, which could have incorporated itself in between the disulfide bond of the peptide. This was supported by literature, and the peptide structure mass drawn in ChemDraw with EDT between the disulfide bond had the same mass as the impurity observed in the spectra. Another plausible reason is an amino acid insertion/addition, which could be serine. The plausible amino acid that could have coupled twice is serine on position 18. This is also supported by the molecular weight of the peptide with two serines matching the impurity mass observed. Amino acid addition can be due to premature Fmoc-deprotection of the Fmoc-AA-OH. The insertion (Scheme 5) is even more possible since double coupling was done for the amino acids to improve the yield of the desired peptide. Residual piperidine from insufficient washings could be another cause for this.



Scheme 5: Amino acid insertion/addition mechanism.

Method 3

The coupling reaction time was reduced to 30 minutes. The longer reaction times may have resulted in side reactions and poor yields.

The amino acids were coupled only once except for those difficult to couple, such as arginine and lysine, which required long coupling times. HATU was used as the coupling agent for these amino acids to avoid long reaction times. HATU and HBTU use the same mechanism to activate amino acids; however, the presence of the pyridine ring in HATU made it more reactive. HATU increased reaction rates and reduced epimerization, thus resulting in a low contamination risk and an increased aminoacylation efficiency. HBTU/NMM was used for the rest of the amino acids. The results improved significantly, and the purity of the peptides increased. Including EDT in the TFA cocktail was to prevent cysteine from cyclizing during the cleavage. However, since the peptide needed to be cyclized, it was excluded from the cocktail. The peptide was cyclized using the DMSO method, and Figure 42 shows the spectra of the final peptide with fewer impurities.

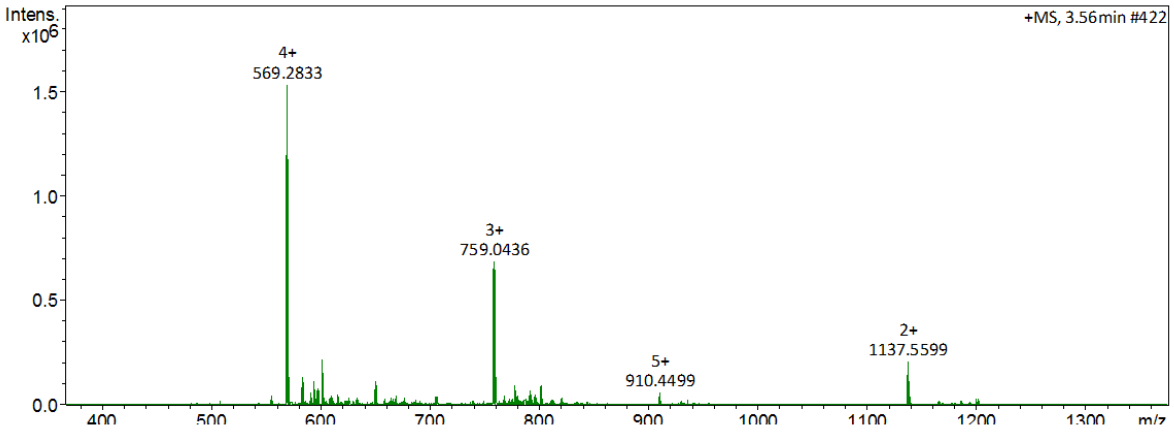


Figure 42: The spectra for lariatin A peptidomimetic after cyclization.

2.5.4 Purification of Pep_PNL1

The peptide was purified following **method 2-3** and an improvement in the purity was observed (Figure 43). The purity of the peptide was found to be 98%. The water and acetonitrile were removed, resulting in a final mass of 24 mg and a yield of 15.7%

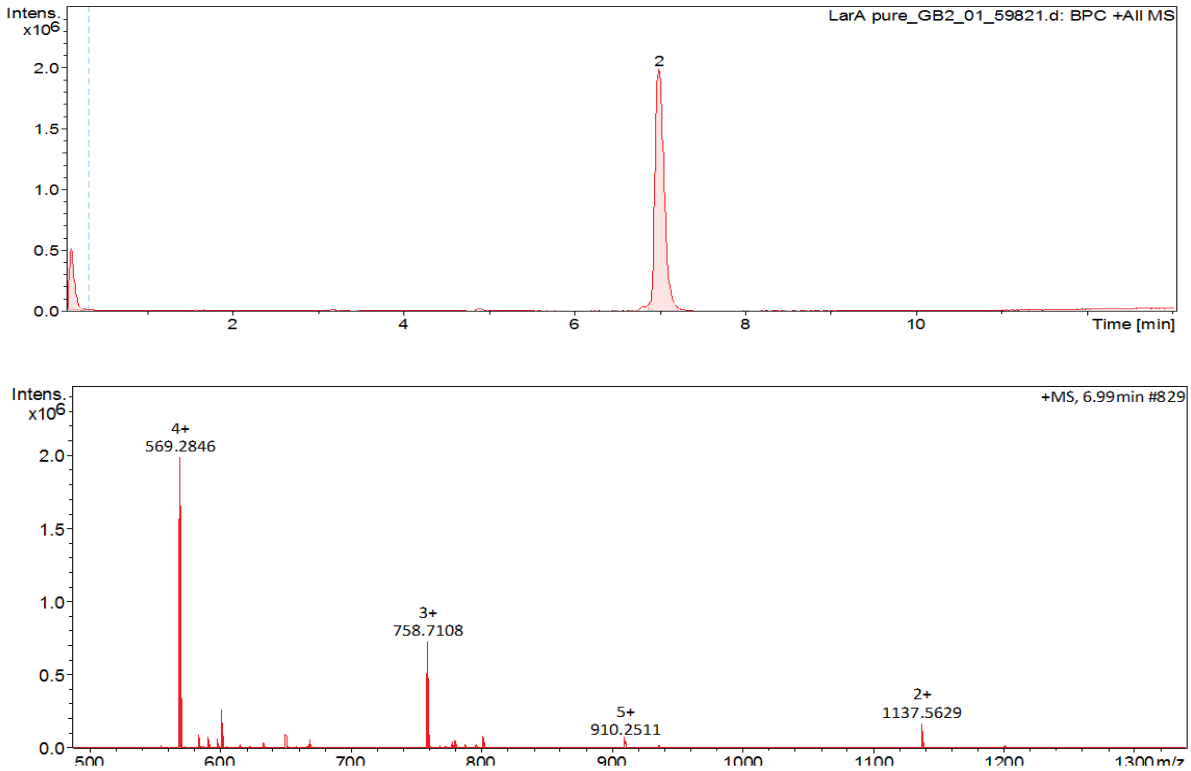
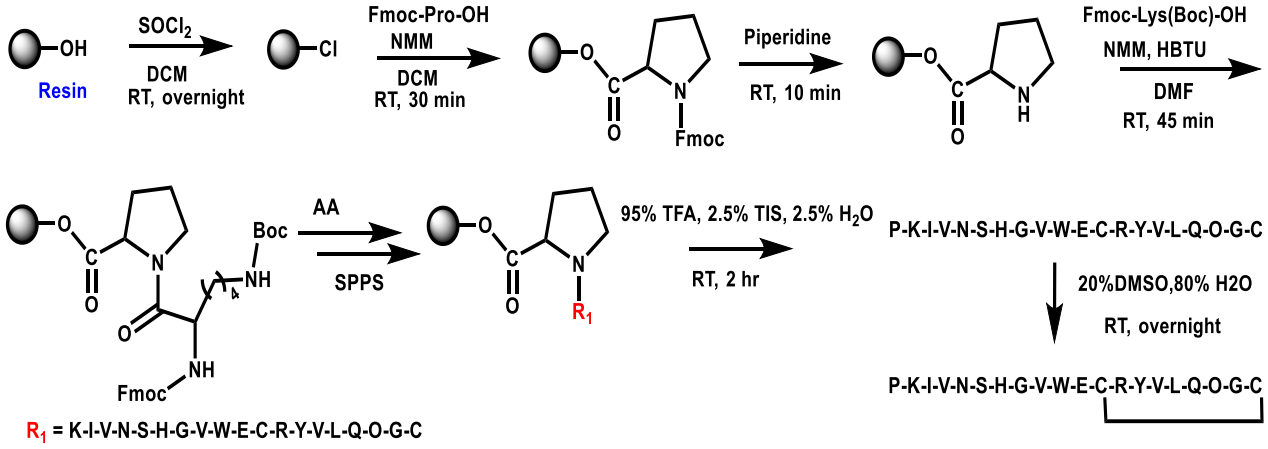


Figure 43: The spectra of pure Pep_PNL1

Method 3 was thus used as a general method to synthesize other derivatives. Scheme 6 shows the summarized synthetic method.



Scheme 6: The general SPPS method used to synthesize Lariatin A peptidomimetics.

2.5.5 Synthesis of shorter Lariatin A peptidomimetics

Pep_TA and Pep_HA were successfully synthesised following **Method 3** described above. Pep_HA was cyclized in 20% DMSO in millipore water overnight at room temperature.

2.5.6 Purification of Pep_TA

After cleavage using the TFA cocktail and precipitation of the peptide in cold diethyl ether, the crude product was dissolved in 80:20 (H_2O: DMSO). The peptide could dissolve in 100% water; however, large volumes of water were needed to dissolve the whole product. Large volumes were impractical when separating the peptide using prep-HPLC because more injections would be required, and more solvents would be used. Hence DMSO was added to ensure a small volume was used to dissolve the peptide for purification. The optimum ratio was 80:20 (H_2O: DMSO) as a solvent.

Some modifications were made to **methods 2 & 3** for the purification of Pep_TA. It was observed that desired peak started eluting when acetonitrile was at 50%. The acetonitrile percentage was allowed to increase from 5-30% in 5 minutes allowing all the DMSO and polar by-products to elute from the column. Then the percentage was increased from 30-40% in 1 minute, followed by a 40-50% ACN increase in 3 minutes. Since the peptide was eluting at 50-54% acetonitrile, the time taken for this increase was prolonged, and the percentage was adjusted to 50-54%, giving a better separation of the peptide.

The analyte fractions were collected and run on prep-HPLC again to check the purity. The chromatograph showed two rabbit ears peak, as shown below. The fractions collected from these two peaks had the same masses. Peptides are very flexible and can exist as an ensemble of conformations in solution, especially linear peptides. The conformers could be caused by the proline presence.

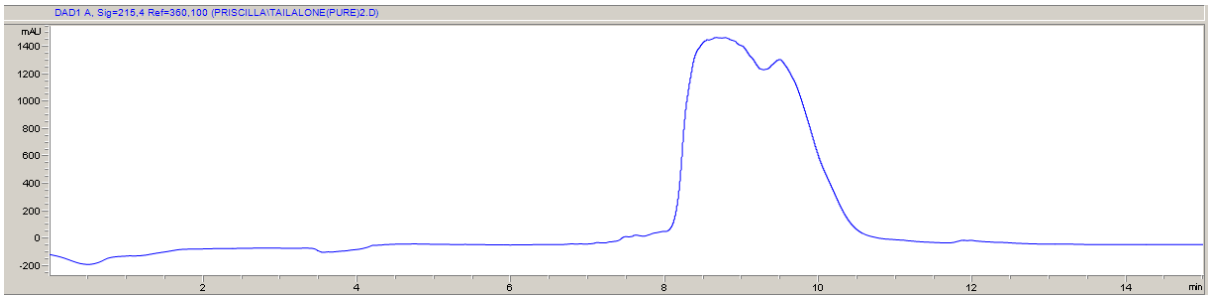


Figure 44: The chromatogram of Pep_TA from prep-HPLC showing the two peaks with similar mass.

Demonstrated in Figure 45 is the UHPLC-MS showing the retention time at 4.95 minutes for the peptide. The calculated mass for Pep_TA was 1135 m/*z* and the mass found was

1136.6872 $[M+H]^+$ m/*z*. The purity was also evaluated using the UHPLC-MS which was found to be 99%. The solvent was evaporated using the rotary-evaporator and the resulting powder had a mass of 153.3 mg and a yield of 35%.

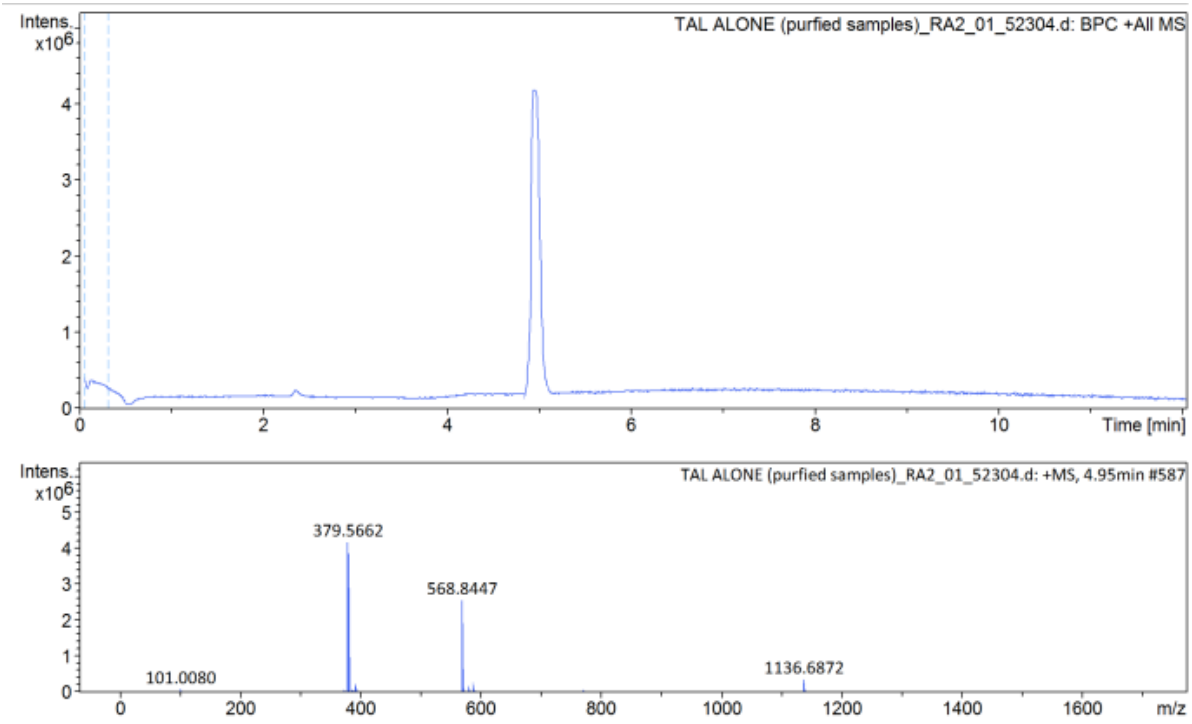


Figure 45: The LCMS spectrum of the pure Pep_TA peptide.

2.5.7 Purification of Pep_HA

After cleavage, the peptide was cyclized following **method 2-1**. Some modifications were made to the **method 2-3** for the purification of Pep_TA. It was observed that desired peak started eluting when acetonitrile was at 30%. The acetonitrile percentage was allowed to increase from 5-20% in 6 minutes to allow all the DMSO and polar by-products to elute from the column. Then the percentage was increased from 20-30% in 1 minute followed by 30-40% ACN increase in 5 minutes which gave a better separation of the peptide.

Figure 46 shows the UHPLC-MS showing the retention time at 5.39 minutes for the peptide. The calculated mass for Pep_HA was 1155.30 m/*z* and the mass found was $[M+H]^+$ 1155.30 m/*z*. Interestingly, the at 5.28 min consist of double the mass of the desired peptide ($[M+2H]^{2+}$ 1155.30). The plausible explanation for this could be the formation of intermolecular disulphide bond between two peptides. The purity was also evaluated using the UHPLC-MS

which was found to be 97%. The solvent was evaporated and the resulting powder had a mass of 20 mg and a yield of 12.04%.

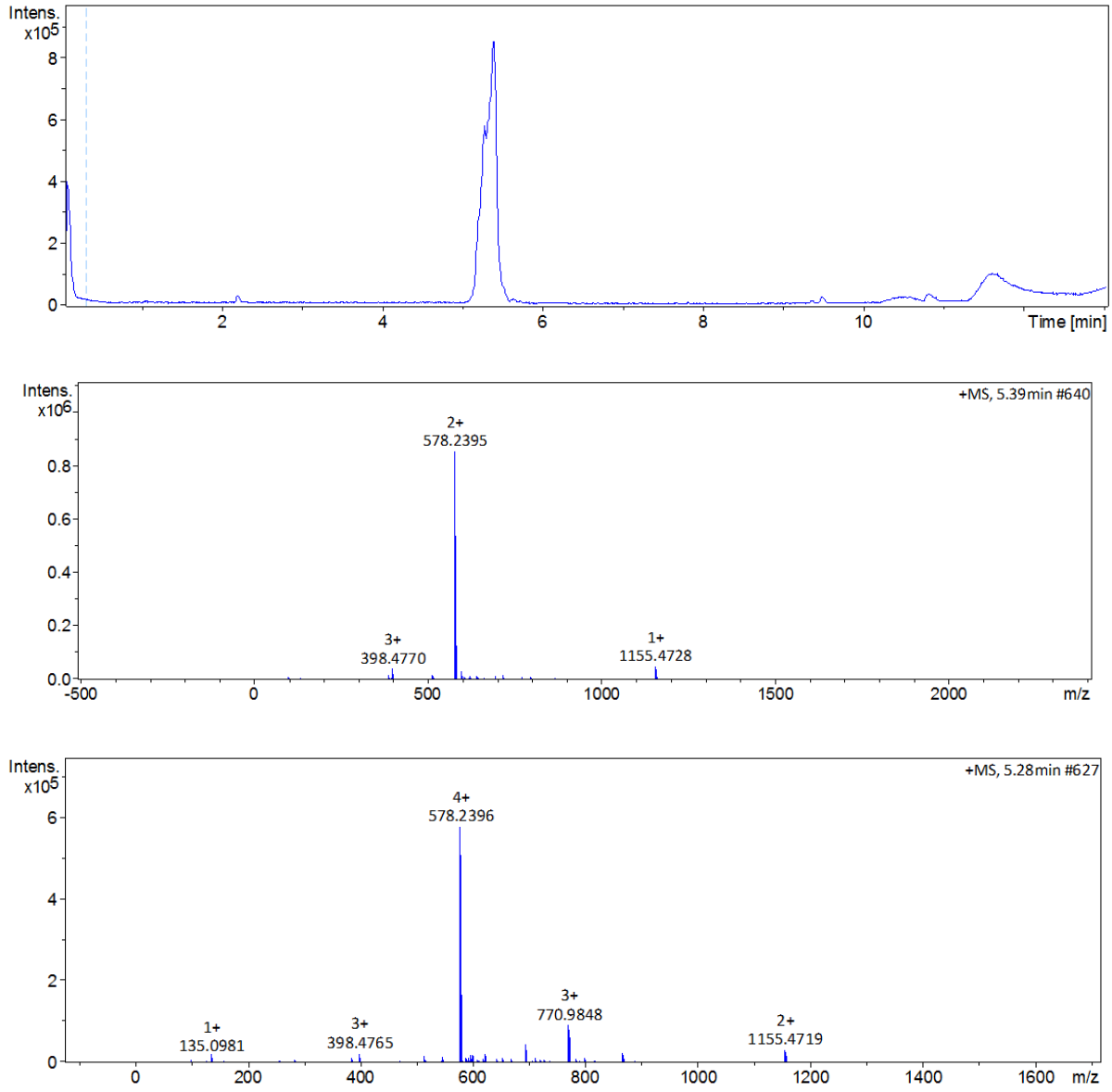


Figure 46: The LCMS spectrum of Pep_HA after purification.

2.5.8 Incorporate a lipid moiety onto a peptide

2.5.8.1 Synthesis of Pep_TAA

Pep_TAA was synthesized following the method described above (**Method 3**). After removing Fmoc at the end of the linear tail region peptide, adamantane was coupled. The lipid moiety was weighed, and the coupling reagent, HBTU, was added. The powders were dissolved in DMF, and NMM was added to the resin and left to react for 30 minutes. The resin was washed and dried before cleaving the peptide with the TFA cocktail. The peptide was crashed out

using cold diethyl ether, and the crude product was dissolved in 20% DMSO and millipore water.

2.5.8.2 Purification of Pep_TAA

Some modifications were made to **methods 2 & 3** for the purification of Pep_TA. It was observed that desired peak started eluting when acetonitrile was at 47%. The acetonitrile percentage was allowed to increase from 5-40% in 5 minutes, allowing all the DMSO and polar by-products to elute from the column. Then the percentage was increased from 40-50% in 5 minutes, giving the peptide a better separation.

Demonstrated in Figure 47 is the UHPLC-MS showing the retention time at 9.89 minutes for the peptide. The calculated mass for Pep_TA was 1297.798 m/*z* and the mass found was $[M+H]^+$ 1298.6663 m/*z*. The purity was also evaluated using the UHPLC-MS which was found to be 98%. The solvent was evaporated using the rotary-evaporator and the resulting powder had a mass of 15.7 mg and a yield of 23.5%.

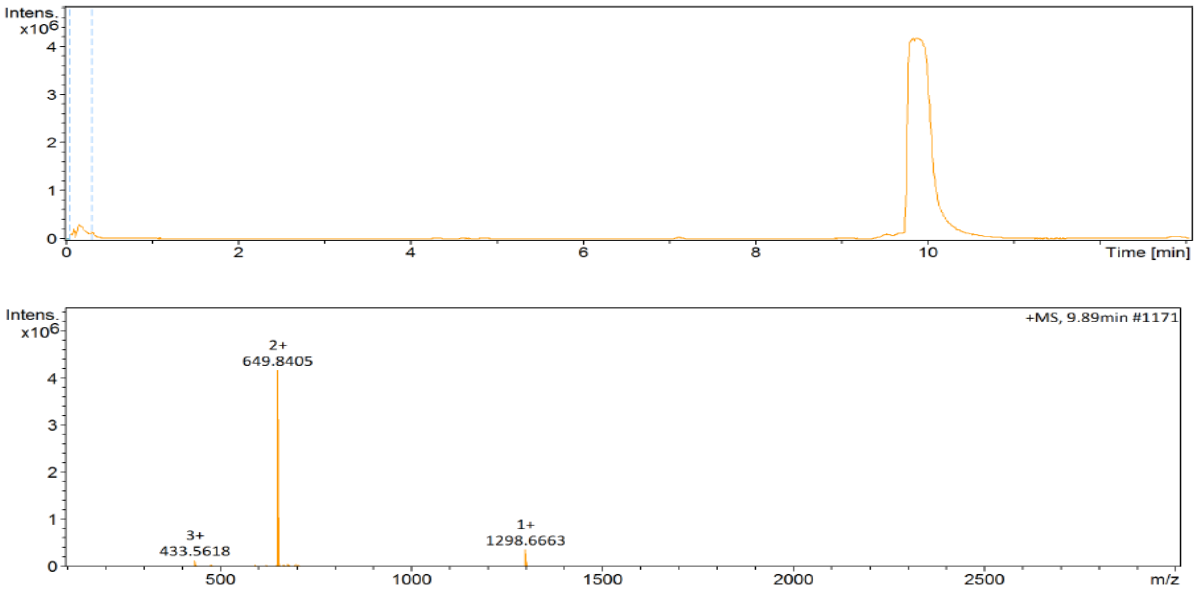


Figure 47: The LCMS spectrum of the pure Pep_TAA peptide.

There was an obvious change in the polarity of Pep_TA with the addition of the adamantane moiety. A 13-minute gradient elution method (5-95% Acetonitrile) was used with the following solvent system: Solvent A: H_2O with 0.1% and Solvent B: Acetonitrile with 0.1% formic acid on UHPLC-MS. Pep_TA had a retention time of 4.95 minutes, while Pep_TAA had a retention time of 9.89 min. The cage moiety, adamantane, increased the retention times

and caused the linear tail derivative to be more non-polar. Thus the peptide can potentially diffuse through the lipid bilayer cell membrane more effectively.

2.5.8.3 Synthesis of Pep_HAP

Pep_HAP was synthesized following the method described above (**Method 3**). After removing Fmoc- the palmitic acid with HBTU was dissolved in the powders in DMF and NMM and then added to the resin. The reaction was left to react for 30 minutes. Due to the foam produced during the reaction, a spatula was often used to gently push down the resin from the vessel walls into the solution. The resin was washed and dried before the peptide was cleaved with a TFA cocktail. The peptide was precipitated out using cold diethyl ether. Dissolving the crude product was a challenge. The solution of 80:20 (H_2O: DMSO), also used for the cyclization, did not dissolve the peptide completely. This mixture was left to shake at room temperature overnight, then about 0.4 ml of this solution was dissolved in 1.6 ml of ACN and then analyzed using the UHPLC-MS. The cyclization was confirmed.

For the rest of the peptide solution, the solvent was removed by freeze drying then several solvent combinations were tried. The peptide dissolved completely in DMSO, but due to its highly non-polar nature, the addition of water or acetonitrile, or methanol caused it to precipitate out of the solution. The peptide's inability to dissolve in bioassay-friendly solvents but only in 100% DMSO will pose problems in the future potential clinical trial. Purifying this peptide using the semi-preparative HPLC instrument was complicated because the solvents compatible with the prep-HPLC columns caused the sample to precipitate out immediately when introduced as the mobile phase. It was challenging to purify it while dissolved in 100% DMSO because the peptide coeluted with the broad DMSO peak, making it difficult to isolate the pure peak from the other impurities. Furthermore, the precipitation of the peptide during the run can result in blocked capillaries and columns and potentially cause subsequent damage to the instrument. Another option was to inject the peptide dissolved in 100% DMSO into the instrument in small volumes. This would have wasted solvent and taken much time. The peptide had another drawback of aggregating when it was left in a DMSO solution over a long period of time. Efforts to dissolve it again in DMSO were fruitless as the jelly peptide could not dissolve even when formic acid was added or when the solution was heated to 50 degrees Celsius. This is a common problem with peptide drugs.[85] This further prompted

alternative modifications that could be done to improve the solubility properties of the analogues without compromising the activity.

A different method was used where solvents with different polarities were used to separate the non-polar peptide from the other polar and slightly non-polar impurities. In addition to acetonitrile in the solution of peptide in DMSO, a precipitate was centrifuged, and the solvent was then separated and analyzed on the LCMS. The chromatograph showed the expected mass of the peptide with minor impurities (Figure 48). This method was repeated until a gel-like precipitate remained in the centrifuge tube. In the end, although the peptide was cleaner and dissolved in acetonitrile, the yield was very low. When the solvent extraction was performed with water, the peptide was not observed in the spectra.

The peptide extracted with acetonitrile was reconcentrated, dissolved in 2 ml of acetonitrile, and then injected into the prep-HPLC for further purification. The purity obtained was 90%, with a yield of 5.6%. One of the reasons behind the low yield was the difficulty in dissolving and purifying the peptide. More product was also lost during the process of solvent extraction.

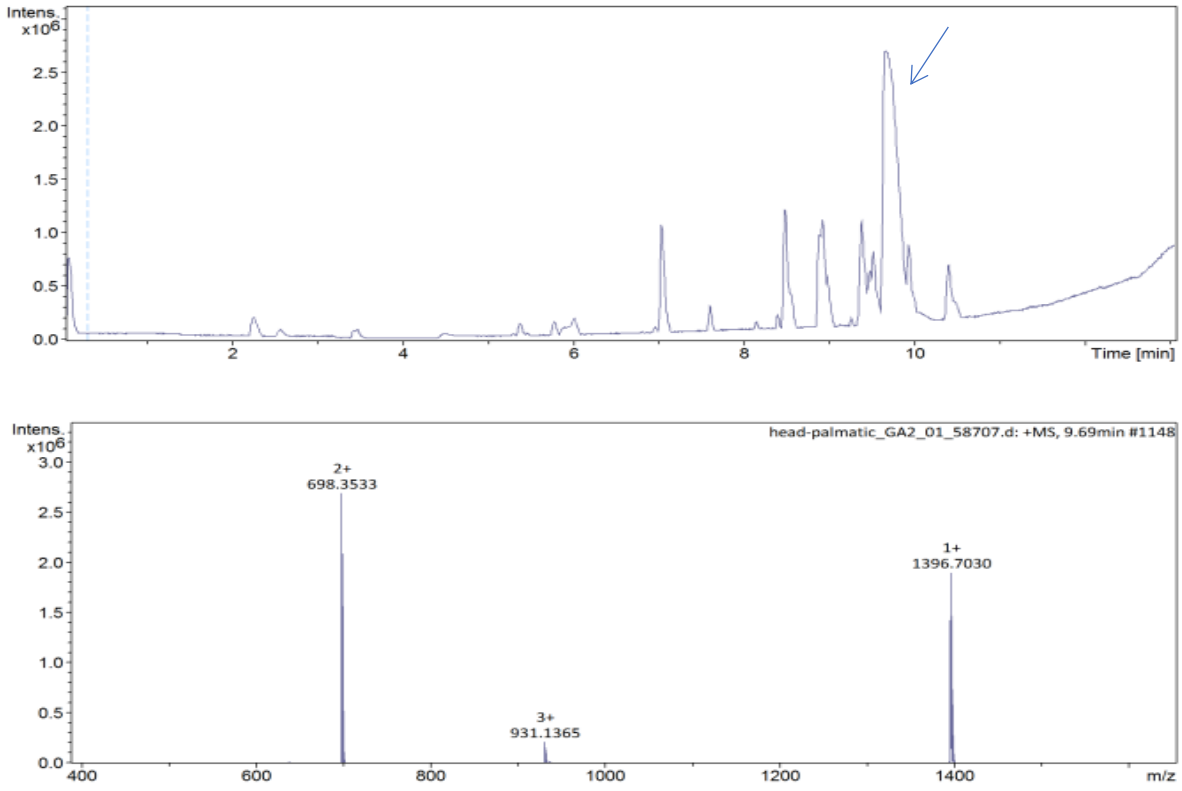


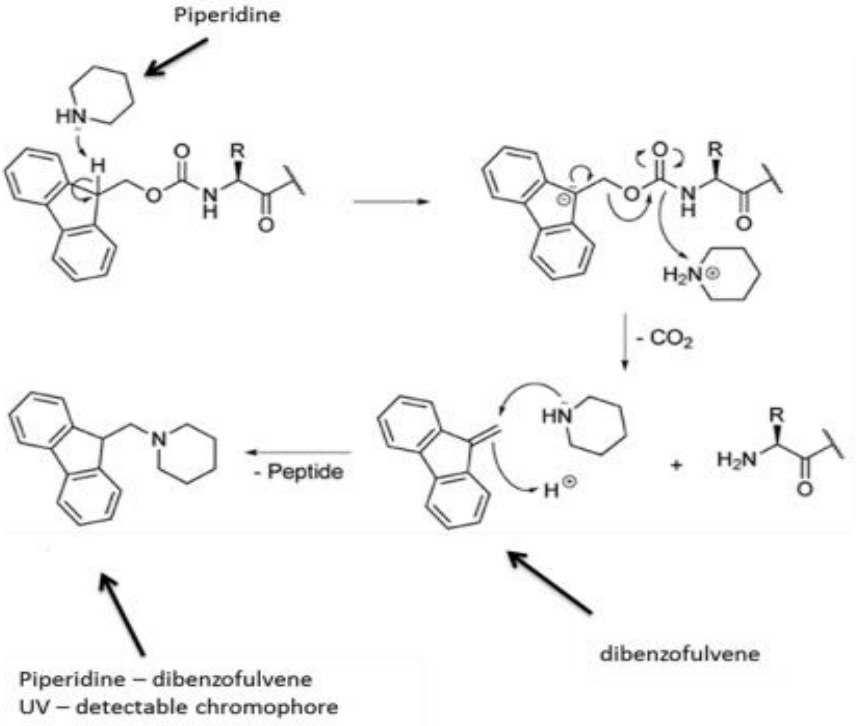
Figure 48: The LCMS spectrum of the pure Pep_HAP peptide.

2.5.9 Synthesis of Pep_PNL2

The rink amide resin was used to synthesize Pep_PNL2 to afford an amide ending at the C-terminal of the derivative.

2.5.10 Swelling of rink amide resin and Fmoc removal

The Fmoc- protected Rink Amide MBHA resin was swelled in dimethylformamide (DMF) to expose the active sites because the synthesis occurs inside the beads. The piperidine solution was used to irreversibly cleave the base-labile Fmoc- group and expose the free amino group (NH_2) and this mechanism is shown in Scheme 7. Washing with DMF was done to remove contaminants.



Scheme 7: The deprotection of the Fmoc group.

After the activation and Fmoc deprotection of the rink amide resin, the peptide was then synthesized following **method 3.**

2.5.11 Purification of Pep_PNL2

Just as with the purification of Pep_PNL1, the purification method was developed by applying a gradient elution method of 5-95% acetonitrile over 12 minutes at a 16 mL/min flow. The collected fractions indicated that the peak of interest was collected in the 25-30% ACN. Thus,

the gradient method was developed using this information. The acetonitrile percentage was allowed to increase from 5-17% in 5 minutes to allow all the DMSO and polar by-products to elute from the column. Then the percentage was increased from 17-25% in 3 minutes, followed by a 25-30% ACN increase in 3 minutes. Figure 34 shows the achieved purity of 95%. The mass was found to be 10.51 mg and a yield of 8.7%.

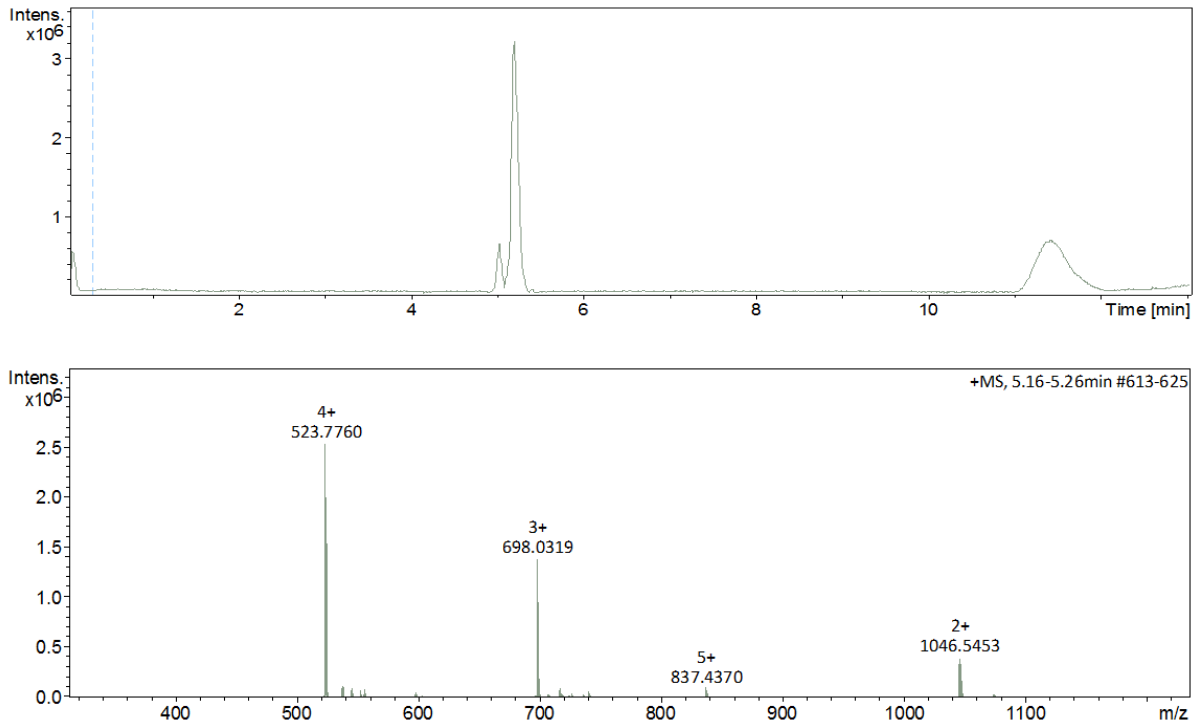


Figure 49: The LCMS spectrum of the pure Pep_PNL2 peptide.

The results of the synthesized peptides are summarized in table 4 below.

Table 4: The purity and yield obtained for the synthesized Lariati A peptidomimetics.

Peptides	Purity	Mass (mg)
Pep_PNL1	98%	24
Pep_PNL2	95%	10.5
Pep_TA	99%	153.3
Pep_TAA	98%	15.7
Pep_HA	98%	20
Pep_HAP	<95%	9.3

Concluding remarks

The lariatin A peptidomimetics were designed considering the SAR studies done on naturally occurring Lariatin A. Several changes were made by swapping the lactone link for a disulfide bond and adding a lipid moiety into a peptide to improve their biological activity and synthesis process. The created **Method 3** produced peptides in higher yields compared to methods 1 and 2. Successful cyclization of Pep PNL1, Pep HA, Pep HAP, and Pep PNL2 in 20% DMSO in water was achieved. Fatty acid additions boosted the peptides' non-polarity; however, palmitic acid was not the best choice because it made the final peptide less soluble in HPLC-compatible solvents.

References

(1) Iwatsuki, M.; Tomoda, H.; Uchida, R.; Gouda, H.; Hirono, S.; Omura, S. Lariatins, Antimycobacterial Peptides Produced by Rhodococcus Sp. K01-B0171, Have a Lasso Structure. *J. Am. Chem. Soc.* **2006**, *128* (23), 7486–7491. https://doi.org/10.1021/ja056780z.

(2) Iwatsuki, M.; Uchida, R.; Takakusagi, Y.; Matsumoto, A.; Jiang, C. L.; Takahashi, Y.; Arai, M.; Kobayashi, S.; Matsumoto, M.; Inokoshi, J.; Tomoda, H.; Omura, S. Lariatins, Novel Anti-Mycobacterial Peptides with a Lasso Structure, Produced by Rhodococcus Jostii K01-B0171. *J. Antibiot. (Tokyo).* **2007**, *60* (6), 357–363. https://doi.org/10.1038/ja.2007.48.

(3) Li, P.; Roller, P. Cyclization Strategies in Peptide Derived Drug Design. *Curr. Top. Med. Chem.* **2005**, *2* (3), 325–341. https://doi.org/10.2174/1568026023394209.

(4) Gochin, M.; Zhou, G. Amphipathic Properties of HIV-1 Gp41 Fusion Inhibitors. *Curr. Top. Med. Chem.* **2011**, *11* (24), 3022–3032. https://doi.org/10.2174/156802611798808488.

(5) Sugita, M.; Sugiyama, S.; Fujie, T.; Yoshikawa, Y.; Yanagisawa, K.; Ohue, M.; Akiyama, Y. Large-Scale Membrane Permeability Prediction of Cyclic Peptides Crossing a Lipid

Bilayer Based on Enhanced Sampling Molecular Dynamics Simulations. *J. Chem. Inf. Model.* **2021**, *61* (7), 3681–3695. https://doi.org/10.1021/acs.jcim.1c00380.

(6) Verdine, G. L.; Walensky, L. D. The Challenge of Drugging Undruggable Targets in Cancer: Lessons Learned from Targeting BCL-2 Family Members. *Clin. Cancer Res.* **2007**, *13* (24), 7264–7270. https://doi.org/10.1158/1078-0432.CCR-07-2184.

(7) Grillaud, M.; Bianco, A. Multifunctional Adamantane Derivatives as New Scaffolds for the Multipresentation of Bioactive Peptides. *J. Pept. Sci.* **2015**, *21* (5), 330–345. https://doi.org/10.1002/psc.2719.

(8) *Fatty acid conjugation*. https://www.pepscan.com/custom-peptide-synthesis/peptide-modifications/fatty-acid-conjugation/ (accessed 2023-03-18).

(9) Da Silva, A. V. R.; De Souza, B. M.; Dos Santos Cabrera, M. P.; Dias, N. B.; Gomes, P. C.; Neto, J. R.; Stabeli, R. G.; Palma, M. S. The Effects of the C-Terminal Amidation of Mastoparans on Their Biological Actions and Interactions with Membrane-Mimetic Systems. *Biochim. Biophys. Acta - Biomembr.* **2014**, *1838* (10), 2357–2368. https://doi.org/10.1016/j.bbamem.2014.06.012.

(10) Vijayadas, K. N.; Nair, R. V.; Gawade, R. L.; Kotmale, A. S.; Prabhakaran, P.; Gonnade, R. G.; Puranik, V. G.; Rajamohanan, P. R.; Sanjayan, G. J. Ester vs. Amide on Folding: A Case Study with a 2-Residue Synthetic Peptide. *Org. Biomol. Chem.* **2013**, *11* (48), 8348–8356. https://doi.org/10.1039/c3ob41967c.

(11) N. Jisha, V.; B. Smitha, R.; Pradeep, S.; Sreedevi, S.; N. Unni, K.; Sajith, S.; Priji, P.; Sarath Josh, M.; Benjamin, S. Versatility of Microbial Proteases. *Adv. Enzym. Res.* **2013**, *01* (03), 39–51. https://doi.org/10.4236/aer.2013.13005.

(12) Ramkisson, S. Solid Phase Peptide Synthesis : New Resin and New Protecting Group. **2018**.

(13) Chandrudu, S.; Simerska, P.; Toth, I. Chemical Methods for Peptide and Protein Production. *Molecules* **2013**, *18* (4), 4373–4388. https://doi.org/10.3390/molecules18044373.

(14) Mitchell, A. R. Bruce Merrifield and Solid-Phase Peptide Synthesis: A Historical Assessment. *Biopolym. - Pept. Sci. Sect.* **2008**, *90* (3), 175–184. https://doi.org/10.1002/bip.20925.

(15) Petrou, C.; Sarigiannis, Y. *Peptide Synthesis: Methods, Trends, and Challenges*; Elsevier Ltd, 2017. https://doi.org/10.1016/B978-0-08-100736-5.00001-6.

(16) Mäde, V.; Els-Heindl, S.; Beck-Sickinger, A. G. Automated Solid-Phase Peptide Synthesis to Obtain Therapeutic Peptides. *Beilstein J. Org. Chem.* **2014**, *10* (Scheme 1), 1197–1212. https://doi.org/10.3762/bjoc.10.118.

(17) Góngora-Benítez, M.; Tulla-Puche, J.; Albericio, F. Handles for Fmoc Solid-Phase Synthesis of Protected Peptides. *ACS Comb. Sci.* **2013**, *15* (5), 217–228. https://doi.org/10.1021/co300153c.

(18) Peptide Synthesis. https://www.thermofisher.com/za/en/home/life-science/protein-biology/protein-biology-learning-center/protein-biology-resource-library/pierce-protein-methods/peptide-synthesis.html

(19) Zapadka, K. L.; Becher, F. J.; Gomes dos Santos, A. L.; Jackson, S. E. Factors Affecting the Physical Stability (Aggregation) of Peptide Therapeutics. *Interface Focus* **2017**, *7* (6). https://doi.org/10.1098/rsfs.2017.0030.

CHAPTER 3: Design and synthesis of Lariatin A peptoids

3.1 Introduction

AMPs are potential antimicrobial agents; however they have limitations relative to their drug likeness character. Antimicrobial peptoids and peptide–peptoid hybrids are promising alternatives to AMPs which exhibit unique pharmacokinetic properties due to their greater protease resistance and membrane permeability due to the lack of protons on the amide bond on their structure.[1] Further information about peptoids is provided in a review article presented in Chapter 1.1. In this chapter, we show the design of Lariatin A peptoid derivatives and the fundamentals of the sub-monomeric synthetic procedure.

3.2 Design of lariatin A peptoid derivatives

Peptoids have their side chain on the nitrogen atom instead of the chiral α-carbon as seen on the peptide. Peptoids that consist of different side chains can be produced due to the abundance of monosubstituted amines that are structurally diverse.[2] The peptoid monomer has a nomenclature abbreviation, which is still not confirmed. A four-letter code NXaa is used for N-substituted glycine residue monomers that mimic a proteinogenic (protein-creating) amino acid. For instance, NLeu was used as a monomer that mimics the amino acid Leucine and NLys for Lysine. A four or five-letter abbreviation is utilized for proteinogenic amino acid homologs, for example, homoserine— Nhse or Nhser. The four-letter abbreviation is preferred over five letters. The name of the amine building block that is utilized to make peptoid monomer may also serve as a basis for the abbreviation (e.g., Nspe = (S)- N-(1-phenylethyl)- glycine; Naeg = N-aminoethylglycine). Because of the existence of ambiguity in the nomenclature of abbreviations of peptoid monomers clear definitions are needed for clarification in each peptoid study.[1]

The short derivatives from chapter 2, Pep_TA and Pep_HA, were derivatized by substituting certain amino acids with amine residues to afford peptide-peptoid hybrids. The amino acids replaced with amines within the sequence were selected based on the availability of the corresponding amines. On the Pep_TA derivative, Lys, Ile, Val, and Asn were replaced with

amines, and the rest of the amino acids were incorporated as natural amino acids. Below are the designed peptide-peptoid hybrids.

Pep_TA amino acid sequence: Pro-Lys-ile-Val-Asn-Ser-His-Gly-Val-Trp

Pep_HA amino acid sequence: Cys-Gln-Arg-Tyr-Val-Leu-Gln-Ser-Gly-Cys

Table 5: The sequence of peptide-peptoid hybrids.

Peptide-Peptoid hybrid	Sequence
Pep_PTA	Pro-*N*Lys-*N*ile-*N*Val-*N*Asn-Ser-His-Gly-Val-Trp
Pep_PHA	Cys-*N*Glu-Arg-*N*Tyr-*N*Val-*N*Leu-Gln-Ser-Gly-Cys

3.3 Synthesis of peptoids

There are currently various methods that can be used to synthesize peptoids. In general, there are two strategies: monomeric and sub-monomeric methods. In the monomeric approach, the N-substituted glycine is protected. When it is the first residue on the sequence, it is coupled to the resin or the amino group of a former peptoid residue. The coupling is then followed by removing the temporary N-protecting (Fmoc) group then the peptoid chain is grown (Figure 50). However, the drawback of the monomeric approach is the need to prepare suitable quantities of a diverse set of protected N-substituted glycine monomers. The sub-monomeric method incorporates each monomeric unit in two steps. The first step is acylation using a chloro- or bromoacetic acid and N, N'diisopropylcarbodiimide (DIC) then the second step involves a nucleophilic substitution reaction of this acid with the appropriate monosubstituted amine (Figure 50). The most common route involves solid phase "submonomer" synthesis, which is compatible with standard SPPS and involves the Fmoc/ tBu chemistry. In this method, primary amines are used as a source for the different amino side-chain substituents. These side-chain moieties are introduced upon displacement of bromide by primary amine "sub-mono-mer" synthons. Simon and co-workers were the first group to report the schematic solid phase synthesis of peptoids based on the monomeric approach in 1992. Zuckermann and coworkers later published the sub-monomeric approach, which simplified the solid-phase peptoid and peptide–peptoid hybrid synthesis.

Since the classical SPPS occurs from the C to the N terminus, it is possible to synthesize the peptide-peptoid hybrid polymers by combining the solid-phase peptoid and peptide synthesis. That approach may be applied when converting biologically active peptide ligands to highly potent peptide–peptoid peptidomimetics with enhanced properties. Such hybrids were referred to as “peptomers” by Ostergaard and Holm. In the past, Robey and colleagues have also used this phrase to refer to peptides that had been intentionally cross-linked in a head to tail.

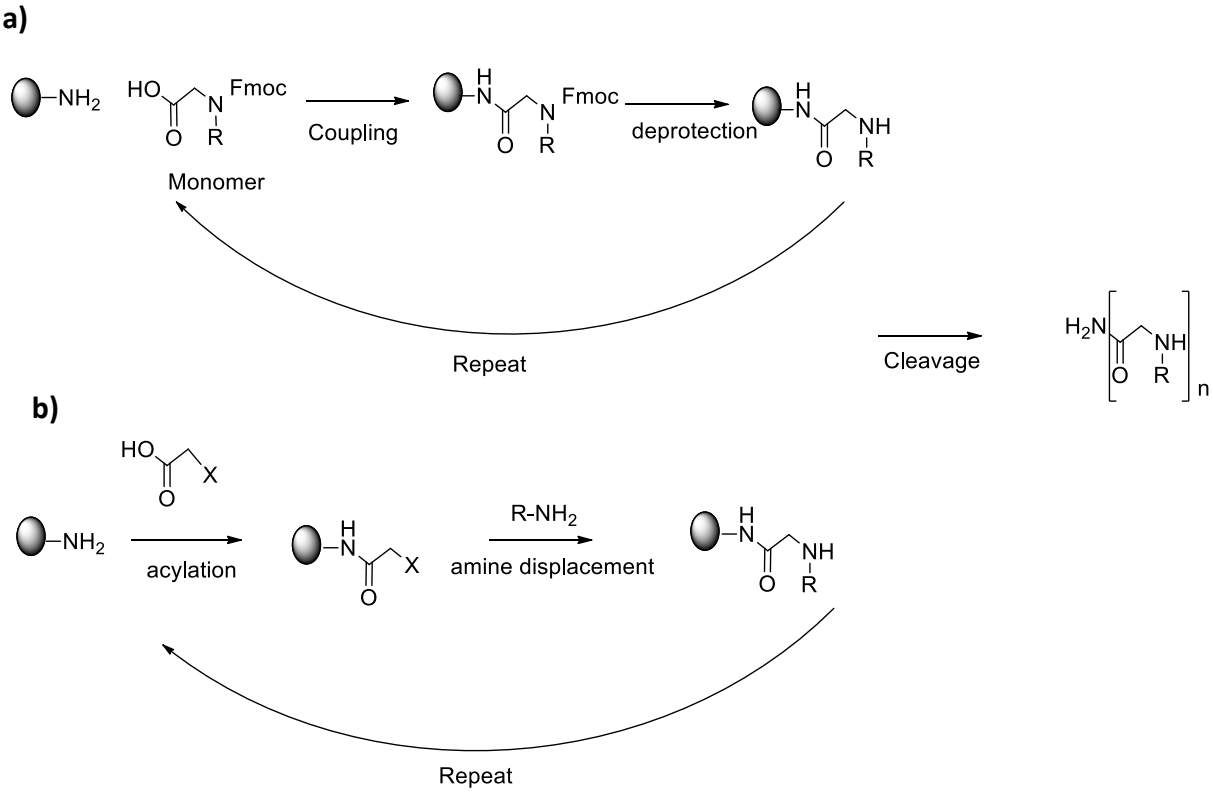
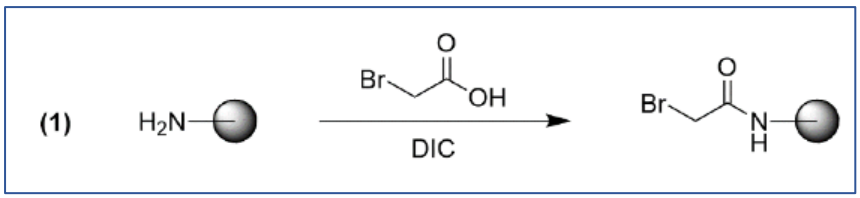


Figure 50: General methods for solid-phase peptoid synthesis. a) is the monomer approach and b) is the sub-monomeric approach.

3.3 1 The Acylation Step

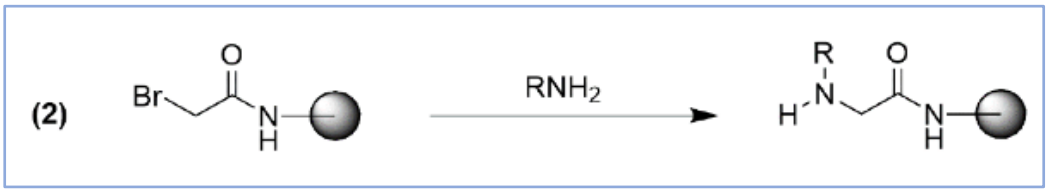
In this process, bromoacetic acid is coupled utilizing coupling agent such DIC in DMF as a solvent (Scheme 8).



Scheme 8: The acylation step of the sub-monomeric synthetic procedure.

3.3.2 The Amine Substitution Step

In the second step, the amine is incorporated to create the side chain of the peptoid residue (Scheme 9). The functional groups on the side chains should be protected appropriately regardless of the synthetic method used, to prevent undesired reactions from taking place.



Scheme 9: The amine substitution step of the sub-monomeric synthetic procedure.

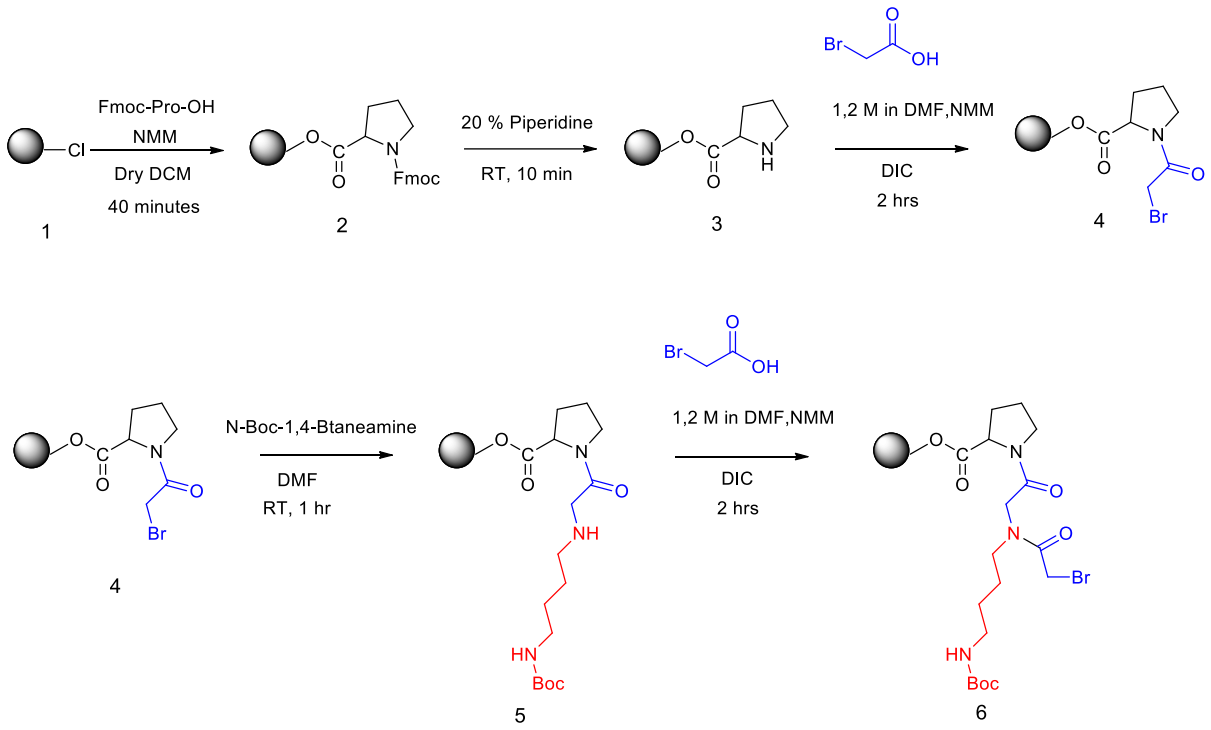
3.3.3 Cleavage and deprotection

Once the synthesis is complete, the peptoid and/or peptide–peptoid hybrid is cleaved from the solid support using “cleavage cocktails” like the ones used in classical Fmoc peptide chemistry. A wide range of TFA-based cleavage cocktails are successfully applied with a typical composition of TFA/TIS/H_2O (95:2.5:2.5, v/v). Other scavengers may also be used, such as thioanisole, anisole, or triethylsilane. Cleavage is performed at room temperature and for 2 h to ensure that side-chain protecting groups are also removed.

3.4 Synthetic method

2-Chlorotrityl was activated, and the first amino acid (Fmoc-Pro-OH for Pep_TA and Fmoc-Cys(trt)-OH for Pep_HA) was coupled following the method described in chapter 2. The Fmoc protecting group was removed from the proline using 20% piperidine in DMF (Scheme 10). After washing and filtration, acylation was performed by adding a mixture of Bromoacetic acid (1.25 g) in DMF (final concentration is 1.2 M), NMM (1 mL), and DIC (1.5 mL) into the reaction vessel and the mixture was gently mixed under a stream of nitrogen gas bubbles for 2 hours. The solvents were filtered out, and the resin was washed with DCM (3 x 10 mL) and

DMF (3 x 10 mL). Nucleophilic displacement was performed with monosubstituted amine dissolved in DMF. For Pep_TA, the amine was N-boc-1,4-butanediamine (1 M) in DMF, while for Pep_HA, the amine was beta-alanine. The solution of the amine was added to the reaction vessel and bubbled under nitrogen for 60 minutes. After removing the solvent by filtration, the resin was washed with DCM (3 x 10 mL) and DMF (3 x 10 mL). The peptoid was elongated by repeated sequential coupling steps of bromoacetic acid and amines. Once the elongation was completed, cleavage was performed using a cocktail of TFA/H_2O/TIS for 2.5 hours. Following cleavage, the peptide was precipitated in Et_2O and dissolved in water and acetonitrile (50:50). .



Scheme 10: The general synthetic procedure for the synthesis of peptide-peptoid derivatives.

3.5 Results and discussion

3.5.1 Synthesis of Tail alone peptoid synthesis (Pep_PTA)

The designed synthetic sequence for Pep_PTA is as follows (Figure 51):

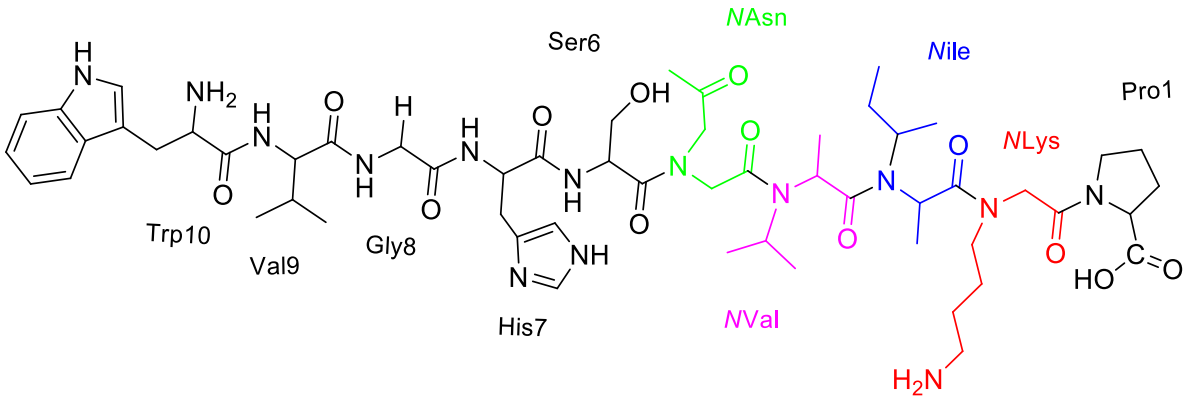


Figure 51: The structure of Pep_PTA

Certain modification of the synthesis described above was required, involving dissolving the corresponding amine for asparagine, glycinamide hydrochloride, which did not dissolve completely in DMF alone. Glycinamide hydrochloride dissolves completely in water; however, the addition of DMF, a salt-like precipitate was observed. In order to dissolve the salt, a base was required to quench the hydrochloride salt. Adding approximately 1 ml of DIPEA in 6 ml of DMF was inadequate to dissolve the salt. We then checked the literature and found that the glycinamide hydrochloride was dissolved in DMF (50%), DIPEA (30%), and water (20%).[3] This method effectively dissolved the amine, which was then added to the reaction vessel, and the mixture was bubbled under nitrogen for an hour. The resin was washed with DCM (3 x 10 ml) and DMF (3 x 10 ml). A small portion of the resin was cleaved using a cocktail of TFA (95%): TIS (2.5%): H_2O (2.5%) for 20 minutes. Analysis using LCMS showed that the amine was successfully coupled to the resin, as the expected mass of 571 was observed on the spectrum. The addition of the next three amino acids (Ser, His, Gly) was also successful. The complete peptoid was then cleaved off the resin using the same TFA cocktail for 2 hours and precipitated in cold diethyl ether.

3.5.2 Purification of Pep_PTA

The crude product was dissolved in 20% DMSO and 80% water. The purification method used for Pep_TA above (Chapter 2) effectively purified Pep_PTA. The solvents were removed after purification using the rotary evaporator resulting in a mass of 10 mg and a yield of 17.0%. The overall purity was determined by LCMS and found to be 98%. The retention times of analysed peaks were between 4.96-5.28 minutes (Figure 52).

(LCMS gradient method 5-95% acetonitrile in 10 minutes fully described in the experimental Chapter 7)

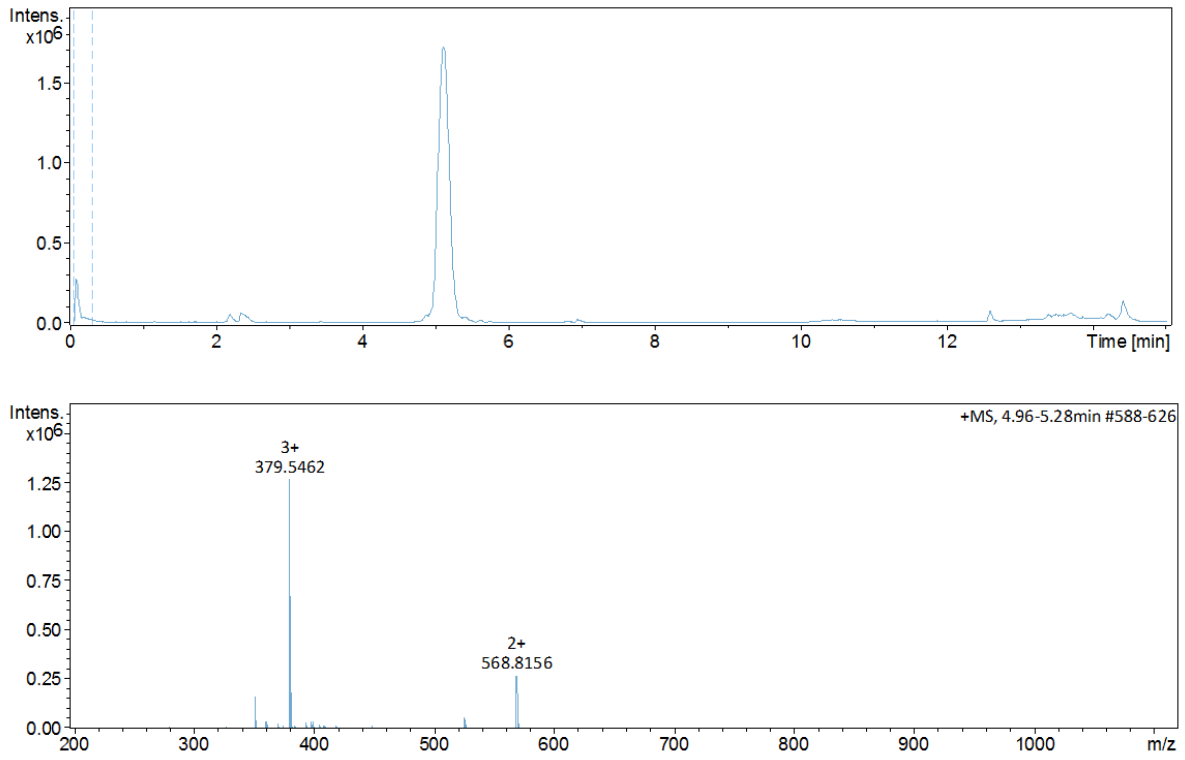


Figure 52: The Mass spectrum of Pep_PTA after purification.

3.5.3 Synthesis of Head alone peptoid synthesis (Pep_PHA)

Method 1

Initially, the designed synthetic sequence for Pep_PHA was as follows:

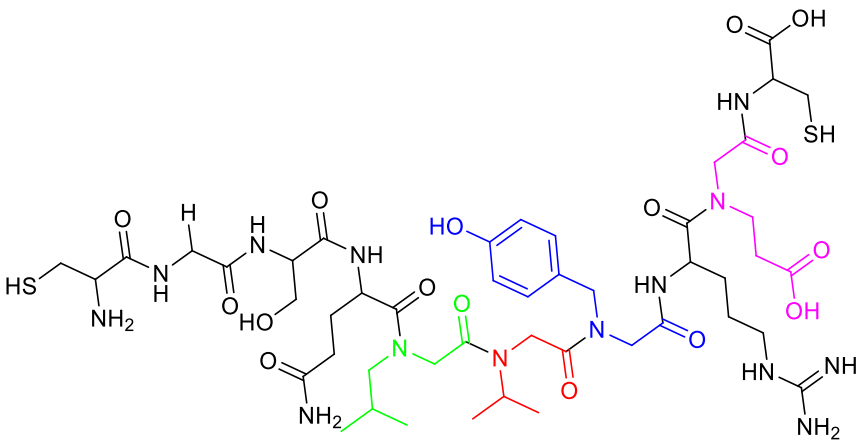
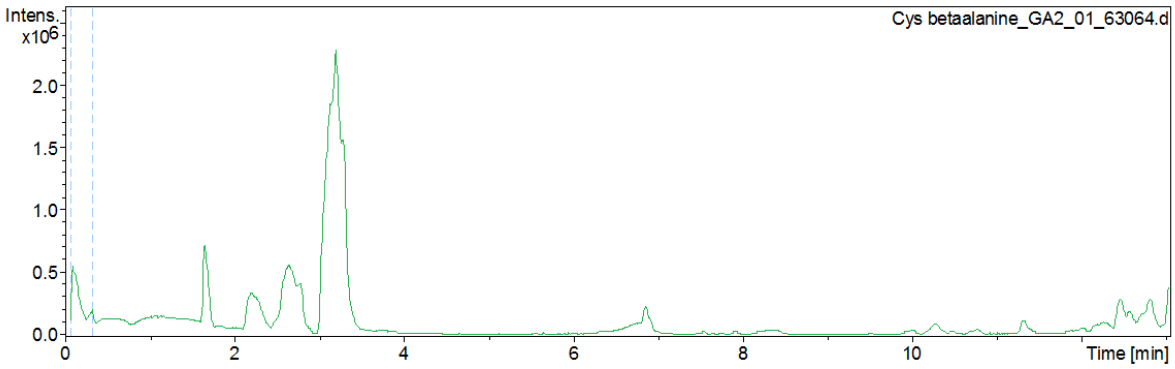


Figure 53: The structure of Pep_PHA.

Attaching the Bromoacetic acid (BAA) to the cysteine was complicated, and very low-intensity peaks were observed on the mass spectrum. Furthermore, the corresponding amine for glutamic acid, beta-alanine, only dissolves completely in water, and it was not easy to dissolve in DMF and DMSO. According to the study carried out by Panpan *et al.* on the solubility of beta-alanine, they found that the dissolving capacity of β-Alanine in the binary solvent mixtures could be ranked as methanol + water > ethanol + water > DMF + water at given temperatures. Furthermore, it is not strictly following the order of polarity of solvents. The method used to dissolve glycinamide hydrochloride for Pep_PTA was then applied (DMF (50%), DIPEA (30%), and water (20%)). The beta-alanine salt was partially dissolved using this method, and the resin was then added to this mixture in a centrifuge tube and left to shake for 90 minutes. Upon filtration, the resin was washed with DCM (3 x 10 ml) and then DMF (3 x 10 ml). After washing and filtration, powdery white residues from the beta-alanine remained in the reaction vessel with the resin. About 5 ml of water was added to the reaction vessel, and the mixture was bubbled for 1 minute, followed by washing with DMF (10 mL) three times and DCM (10 mL) two times. The water successfully dissolved the white powder then a small dry portion of the resin was cleaved using a cocktail of TFA (95%): TIS (2.5%): water (2.5%) for 30 minutes. The expected mass was observed on the LCMS chromatograph. However, the intensity was very low (figure 54).



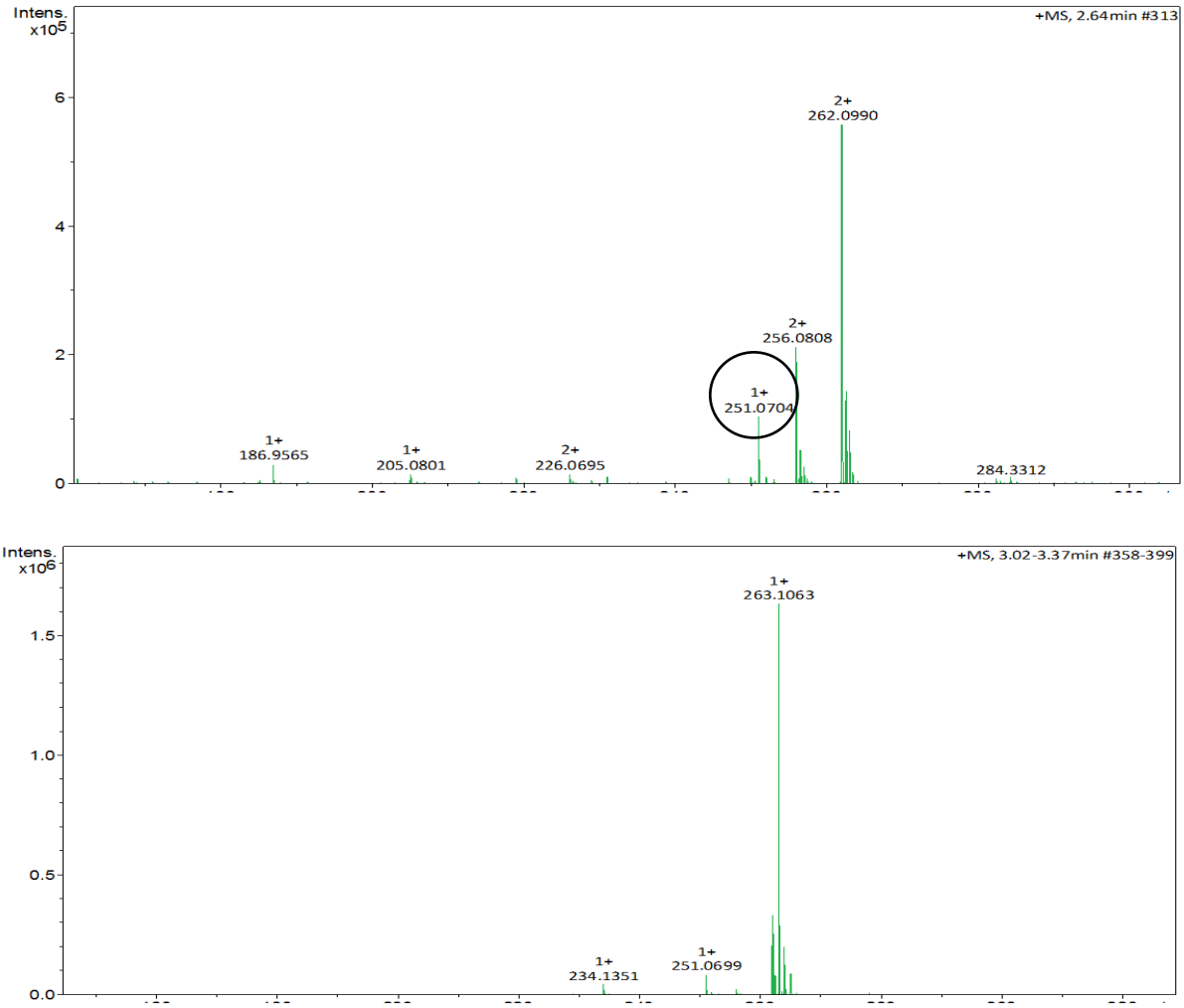


Figure 54: The chromatogram for the Cys-BAA-Beta-alanine reaction.

The following amino acid on the sequence, arginine, was coupled by dissolving the amino acid and HBTU coupling reagent in 5 ml DMF and adding 1 ml of NMM. This solution was added to the resin and bubbled under nitrogen for 45 minutes. The expected mass of 628.23 was observed on the HRMS, but the intensity was low (Figure 55). Furthermore, the coupling of BAA to arginine did not occur, despite double coupling. The plausible explanation for this could be that washing the resin with water could have affected the efficiency of the resin. As stated in Chapter 2, the PS polymer support is incompatible with polar solvents but swells properly in the presence of non-polar solvents like DCM or toluene. It is also compatible with solvents such as DMF. Additionally, poor coupling was observed from the beginning of the synthesis when BAA was coupled to Cys. [4]

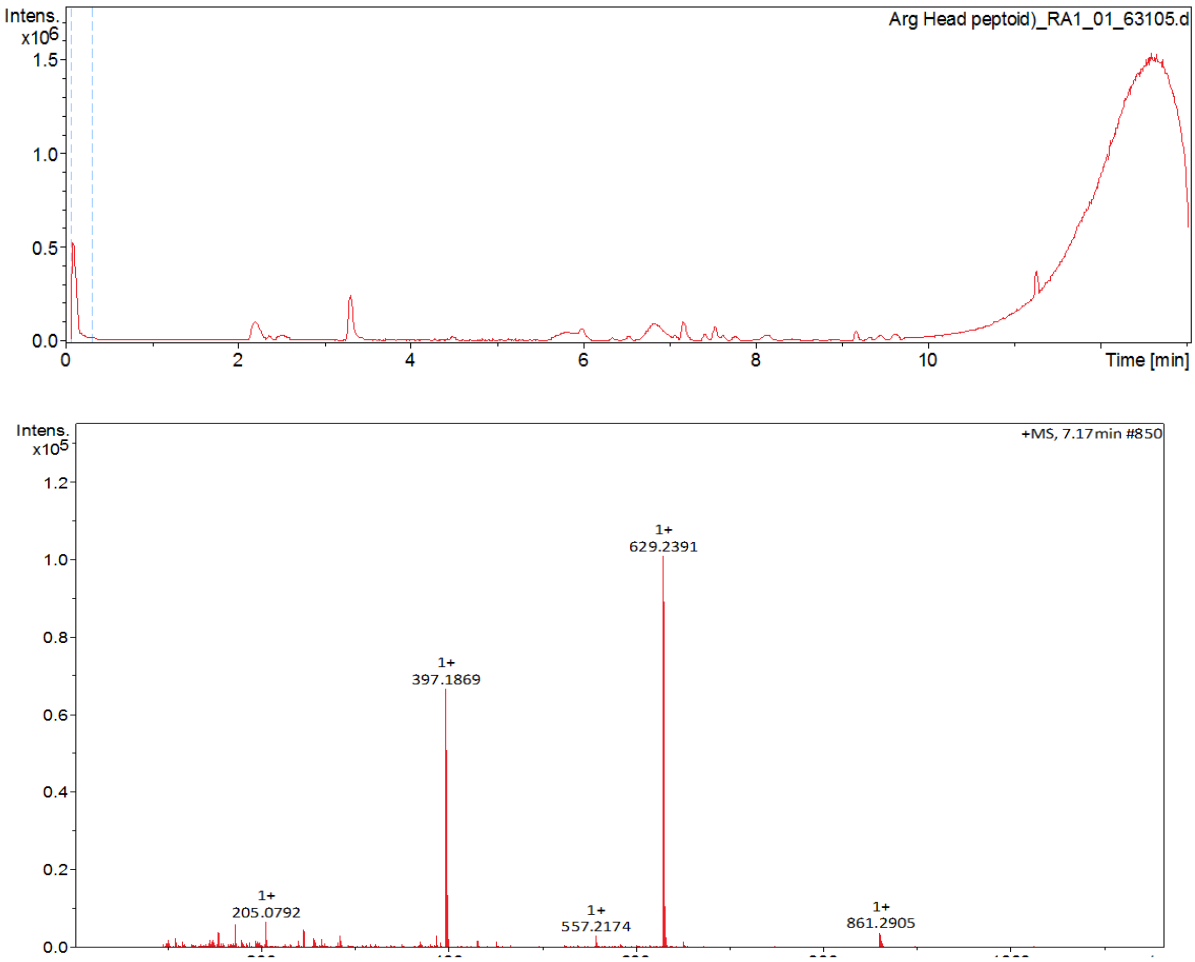


Figure 55: The Mass Spectrum of the Cys-BAA-Beta-alanine-Arg-fmoc reaction.

Method 2

Due to the need to wash the white residue left in the reaction vessel and the lack of a better method to dissolve beta-alanine with the solvents compatible with the resin during this synthesis, beta-alanine was replaced with the normal amino acid. This was done to avoid using water and side reactions that could occur within the growing chain. The resulting design of the sequence is shown in figure 56.

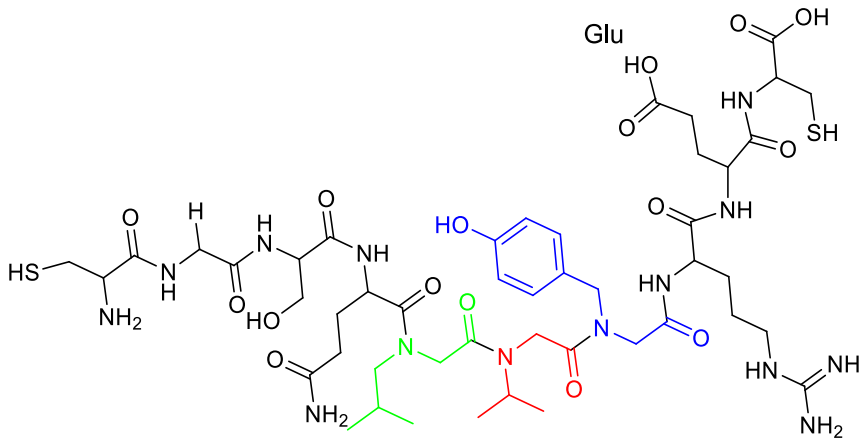


Figure 56: The design of Pep_PHA

Shown in Figure 57 is the chromatogram obtained for the sequence Cys-Glu-Arg-fmoc during the synthesis.

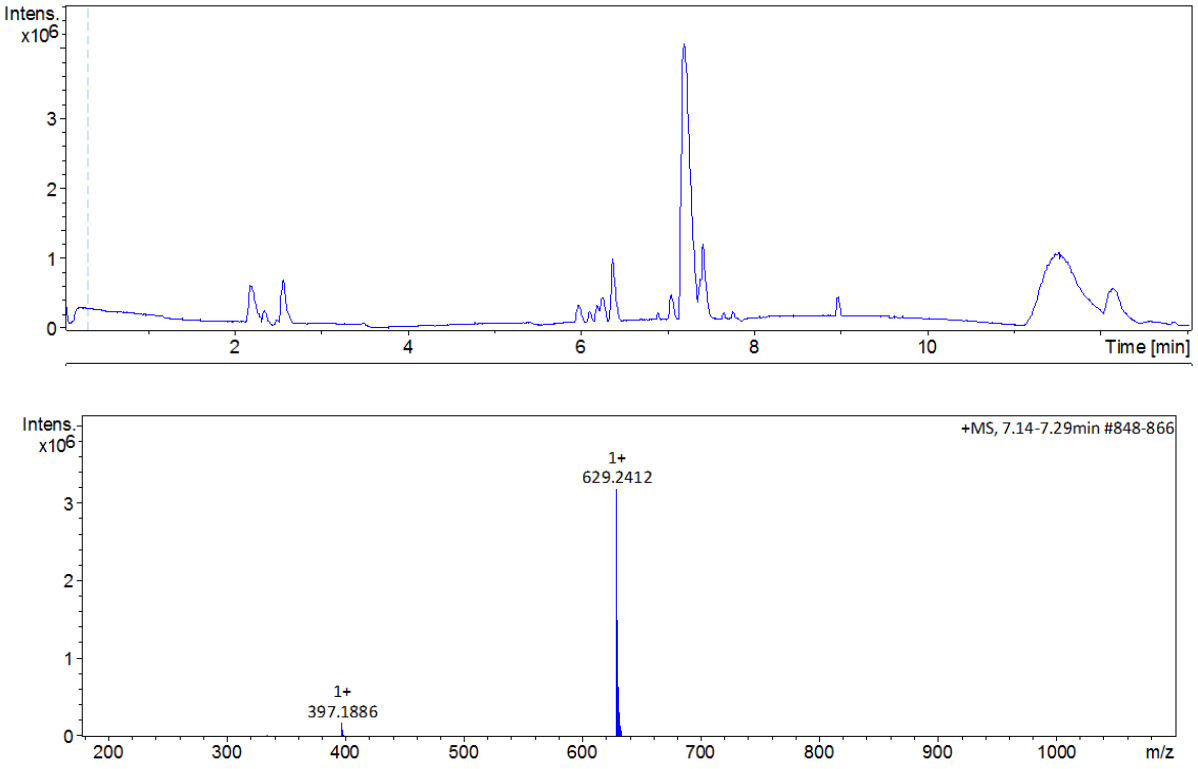


Figure 57: The chromatogram of Cys-Gln-Arg-Fmoc reaction.

The peptide-peptoid hybrid was elongated until the last amino acid. At the end of the synthesis, the expected mass of 578 $[M+H]^{2+}$ was observed on the chromatogram (Figure 58), and just as observed in the mass spectrum of Pep_HA, the retention time of Pep_PHA was around 5 minutes. However, the yield of the desired peptoid was very low (Figure 58).

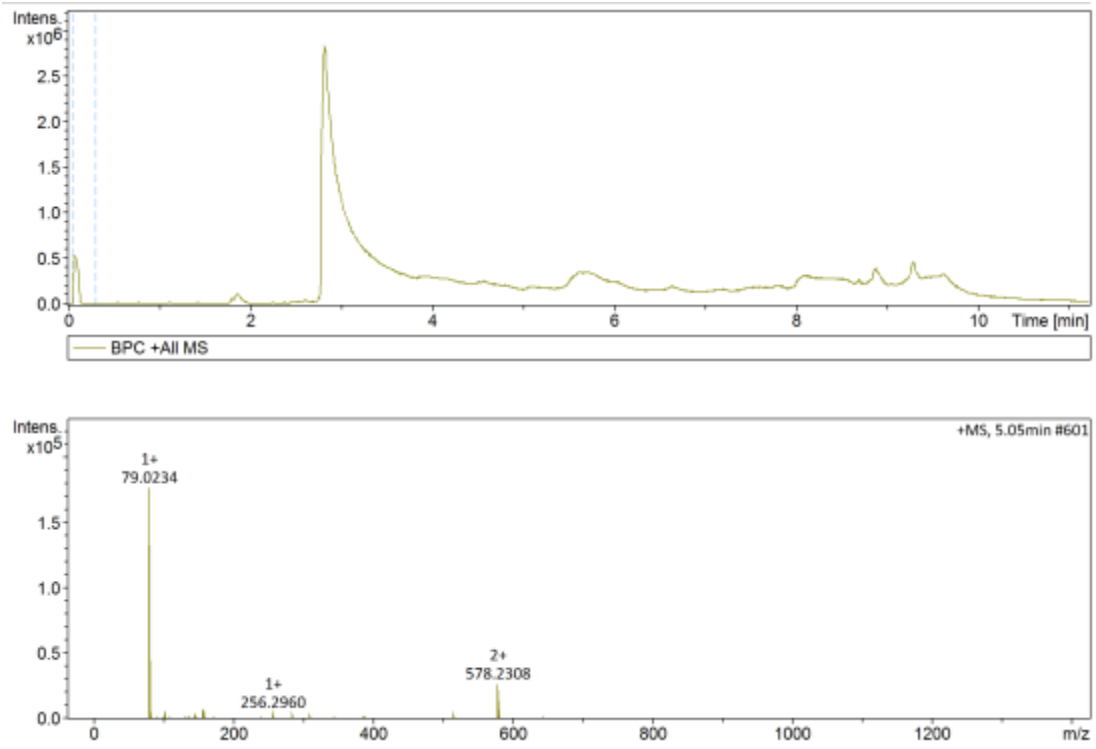


Figure 58: The mass spectrum of Pep_PHA before purification.

These low yields further complicated the semi-preparative HPLC purification process of this peptoid. Several gradient methods were tried, including the one used to purify Pep_HA, but the analyte was coming out as a broad peak. Fractions were collected from this broad peak and when analysed on the HRMS, the peak of interest was suppressed by the solvent peaks and other impurities co-eluting with the peptoid. Because this peptoid was synthesised on a small scale (starting with 300 mg resin), much of the final cleaved product was lost during the synthetic method development while monitoring the couplings, the purification method development, and the attempts to achieve better ionization of the analyte on the HRMS. As a result of the low yield, we did not attempt further purification.

Unlike Pep_PTA, the coupling of BAA to the Pep_PHA was not as efficient. This was observed after the coupling of BAA to Cys (**Method 1**) and BAA to Arg (**Method 2**). On both occasions, the intensity of the desired peak on HRMS decreased significantly. More work needs to be done to improve the yield of the Pep_PHA.

2.6 Concluding remarks

Pep_PTA was easier to synthesize using the developed sub-monomeric method than Pep_PHA. This method was designed for the peptide-peptoid derivatives. While Pep_PTA had a good purity of 98%, Pep_PHA's low yields made purification difficult. For Pep_PHA, method optimization is necessary.

References

1. Stawikowski, M. J. Peptoids and Peptide-Peptoid Hybrid Biopolymers as Peptidomimetics. *Methods Mol. Biol.* **2013**, *1081*, 47–60. https://doi.org/10.1007/978-1-62703-652-8_4.
2. Culf, A. S.; Ouellette, R. J. Solid-Phase Synthesis of N-Substituted Glycine Oligomers (α-Peptoids) and Derivatives. *Molecules* **2010**, *15* (8), 5282–5335. https://doi.org/10.3390/molecules15085282.
3. de Heuvel, E.; Singh, A. K.; Edink, E.; van der Meer, T.; van der Woude, M.; Sadek, P.; Krell-Jørgensen, M. P.; van den Bergh, T.; Veerman, J.; Caljon, G.; Kalejaiye, T. D.; Wijtmans, M.; Maes, L.; de Koning, H. P.; Jan Sterk, G.; Siderius, M.; de Esch, I. J. P.; Brown, D. G.; Leurs, R. Alkynamide Phthalazinones as a New Class of TbrPDEB1 Inhibitors. *Bioorg. Med. Chem.* **2019**, *27* (18), 3998–4012. https://doi.org/10.1016/j.bmc.2019.06.027.

Chapter 4: Biological testing

A caseinolytic protease (ClpP) assay was conducted to screen for anti-tubercular activity of the peptides Pep_TA and Pep_TAA presented in Chapter 2 (Figure 59).

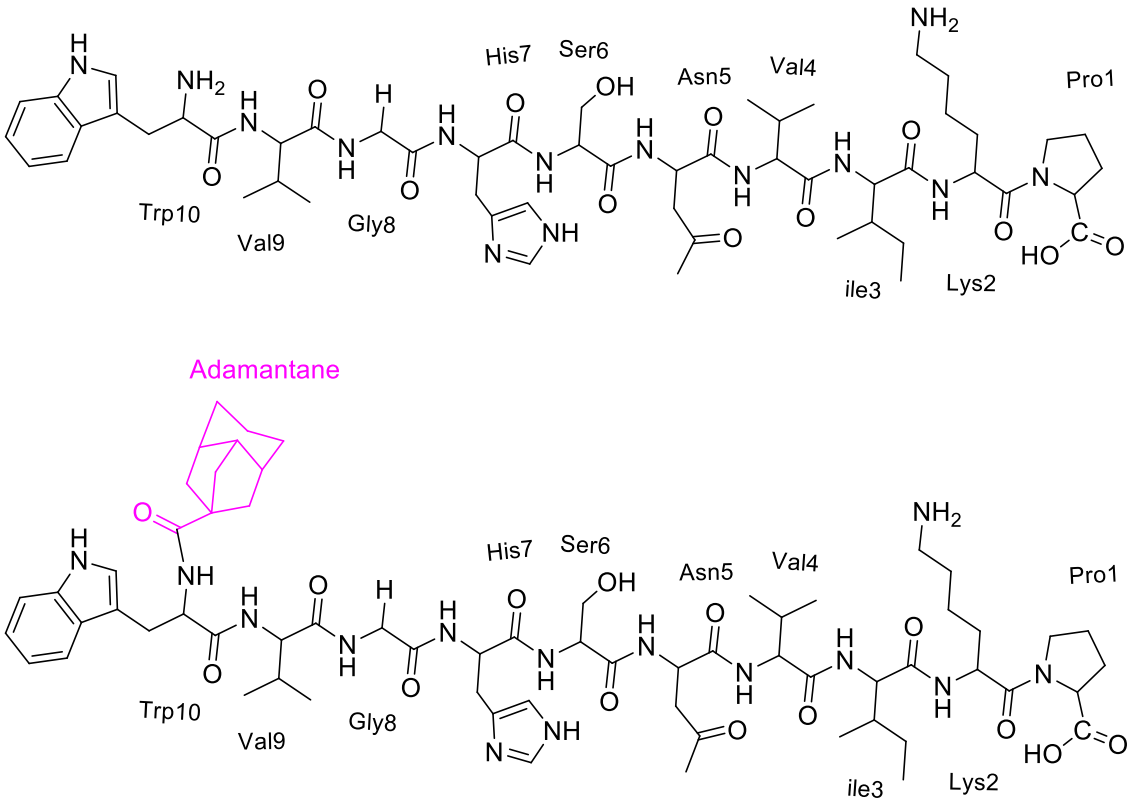


Figure 59: The structures of (top) Pep_TA and (bottom) Pep_TAA peptides.

This assay utilized the ClpP1P2 enzyme to cleave the ZPKM-AMC short peptide into two parts of the ZPKM moiety and AMC fluorophore. The 7-amino-4-methylcoumarin (AMC) is a highly fluorescing compound that generates fluorescence with a peak at 441 nm ±100 and excitation at 341 nm ±100 while the ZPKM-AMC conjugate has a low fluorescent coefficient. The peptidase activity of ClpP1P2 is determined by the presence of free AMC which was measured by fluorescence spectrophotometer. The emission was read at a range of 415-445 nm and excitation at 365 nm.

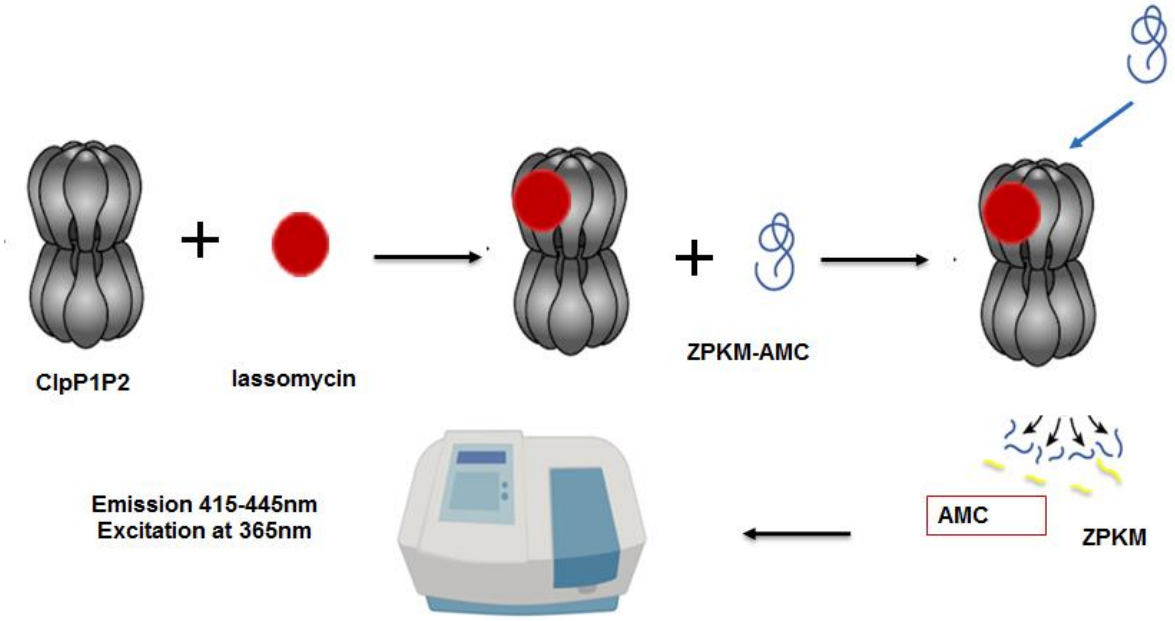


Figure 60: The procedure followed for the biological testing of Pep_TA and Pep_TAA against the ClpP.

A plot of fluorescence results against reaction time for ClpP activity was generated on excel which represented the influence of the synthesized peptide analogues on the ClpP activity while using DMSO as a control. ClpP activity increased with time as it was observed with the control reaction (Figure 38). Pep_TA and Pep_TAA inhibited the activity of the ClpP. Pep_TA showed a greater ClpP inhibition than Pep_TAA. The Pep_TA showed 70% inhibition while Pep-TAA had 49% inhibition factor.

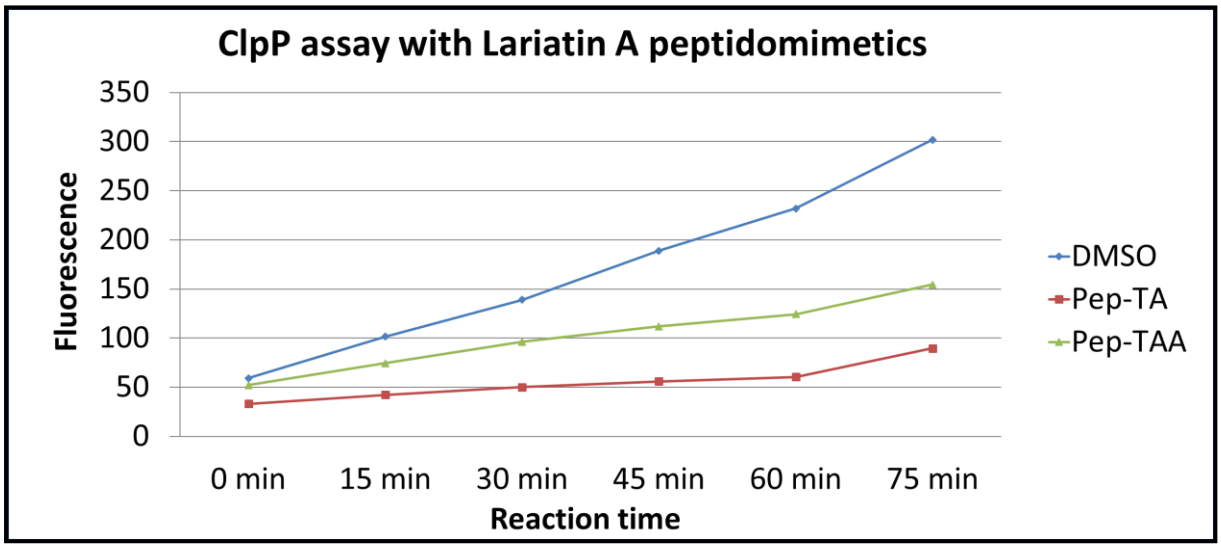


Figure 61: The ClpP essay of Pep_TA and Pep_TAA.

Concluding remarks

The SAR investigations for Lariatin A and Pep TA's demonstrated potency against the *Mtb*s caseinolytic protease are consistent. According to reports, the Gly and Asn residues on the tail are among those responsible for lariatin A's anti-mycobacterial activity. Additionally, the residues at positions 15, 16, and 18 in the structure of natural lariatin A, which correspond to Val4, ile3, and Pro1 in Figure 36, are said to be essential for enhancing lariatin A's biological activity.[1] The biological activity of Pep_TAA was reduced as a result of the addition of adamantine.

References

(1) Iwatsuki, M.; Tomoda, H.; Uchida, R.; Gouda, H.; Hirono, S.; Omura, S. Lariatins, Antimycobacterial Peptides Produced by Rhodococcus Sp. K01-B0171, Have a Lasso Structure. *J. Am. Chem. Soc.* **2006**, *128* (23), 7486–7491. https://doi.org/10.1021/ja056780z.

CHAPTER 5: Structural Elucidation of peptides

5.1 Introduction

The tertiary structure of a peptide plays an important role in its function; thus, knowing the 3-dimensional structure of therapeutic peptides can assist in the design of derivatives with improved activity. Several experimental approaches are typically used, such as nuclear magnetic resolution (NMR), X-ray crystallography, Fourier transform infrared (FT-IR) spectroscopy, and circular dichroism (CD), to identify the three-dimensional structure of peptides. In this chapter, we describe the structural analysis of peptides using NMR and CD to determine the conformations of the synthesized peptides. As X-ray crystallography requires the peptide to be crystallized, NMR has been the most extensively used method in this field of research.[1] Moreover, the relatively short synthesized peptides derived from the tail sequence are less complex than the whole sequence of Lariatin A and can be analysed by NMR spectroscopy. CD was utilized to probe the secondary structure in aqueous and organic solutions.

5.2 Secondary structures

The hydrogen bonds between the partially positive nitrogen atom and the partially negative oxygen atom of the polypeptide backbone give the secondary structure its form.[2] Most proteins' form is influenced by polypeptide chain segments that are either coiled or folded in specific ways. Several of these coils and folds are classified according to their corresponding names based on amino acid sequence arrangement since they repeat so frequently.[2]

The secondary structures include (a) helices (alpha - α, 3_{10}, and pi -π), which occur when the hydrogen bonds are within a short continuous stretch of amino acids; (b) beta strands (sheets), whereby the hydrogen bonds are between backbone atoms (again, amide H's and carbonyl Os) on non-continuous stretches of the protein; and (c) reverse turns, which occur within a very small continuous stretch of amino acids (Figure 62).[3]

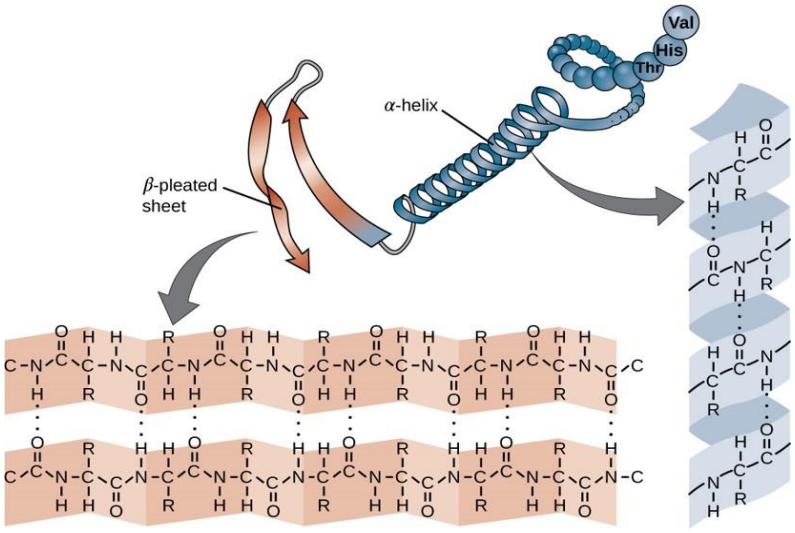


Figure 62: Secondary structural components of protein structure. Most proteins contain the right-handed alpha helix and the beta-pleated sheet, which are frequent structural motifs. The amine and the carbonyl oxygen in the backbone of the amino acid form a hydrogen bond, which holds them together.[4]

5.2.1 Alpha helix

There are two alpha helical structures: right-handed and left-handed, with the former being more prevalent than the latter. This is because the left-handed α-helical structure requires the Phi (Φ) and Psi (ψ) torsion angles. Before the protein could assume the proper orientation for the left-handed helix, it would have to fold and twist through many times to form undesirable angles. As a result, they are uncommon in nature. Every helical turn in the right-handed α-helix contains 3.6 amino acid residues (Figure 63). The R groups of the polypeptide, sometimes referred to as its variation groups, stick out from the α-helix chain. The polypeptide backbone's repetitive helical structure is maintained by carbonyl oxygen and amine hydrogen bonds. Different amino acids have varying propensities to produce helices. In proteins, methionine, alanine, leucine, glutamate, and lysine prefer to assume helical conformations. Proline and glycine rarely combine to generate helices.[4]

Similar to the original description of the α-helix, the 3_{10} helix has 10 atoms in the main chain (counting Cα-N-C-Cα atoms) and 3 amino acids in each turn.[3]

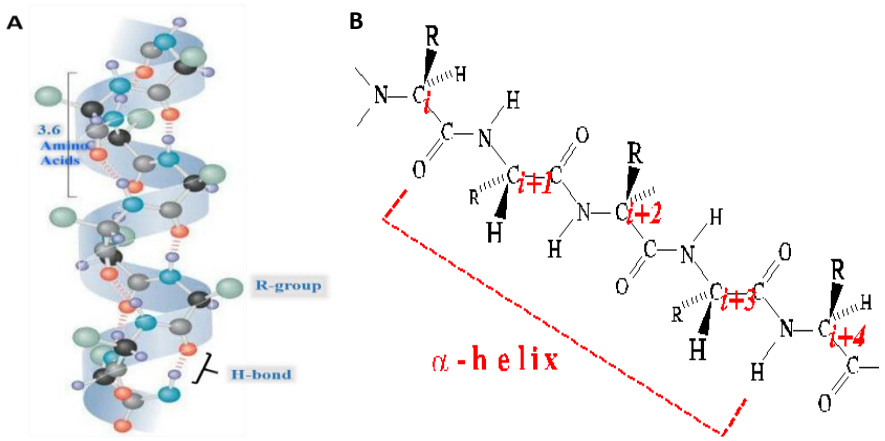


Figure 63: Right-handed α-Helix Structure. A) Ball and Stick Model Side View. A total of 3.6 amino acids are required to form one turn of an α-helix. Hydrogen bonding between the carbonyl oxygen and the nitrogen of the 4th amino acid stabilizes the helical structure.[4] **B**) The Carbonyl of residue I in α-helices is hydrogen-bonded to the NH of residue i+4.[5]

5.2.2 Beta sheet

The β-pleated sheet has pleats because of the hydrogen bonds between the atoms on the polypeptide chain's backbone. In the trans conformation connected to the carbons, the R groups extend above and below the pleat's folds. The partially positive nitrogen atom in the amino group and the partially negative oxygen atom in the carbonyl group of the peptide backbone form hydrogen bonds as the pleated segments line up parallel or antiparallel to one another (Figure 64).[4]

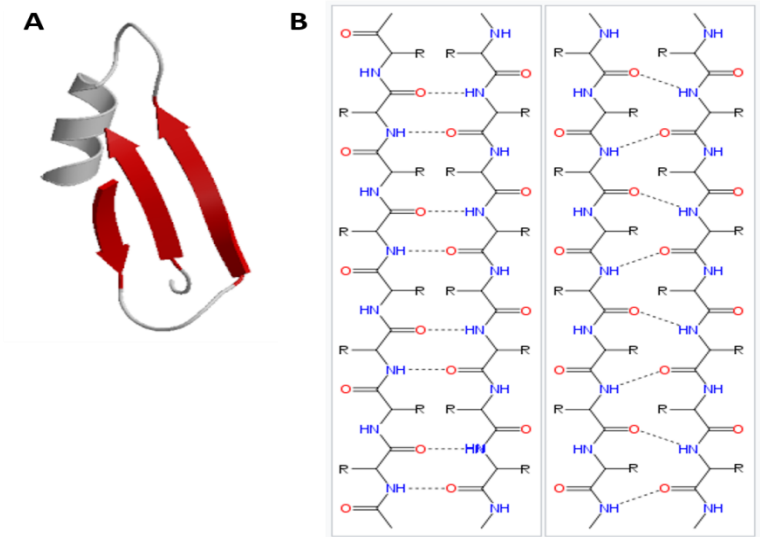


Figure 64: Structure of pleated sheets. The parallel or antiparallel orientation of the -pleated sheet is depicted in (A) above, with the pleated sheet being represented by the red ribbon

arrows. The direction of the arrow indicates the protein's orientation, which is pointing from N to C. The parallel and antiparallel pleated sheet structures (B right and B left, respectively) are both stabilized by hydrogen bonding between the backbone carbonyl and the backbone amine functional groups.[4]

5.3 Solution-state NMR studies

5.3.1 How does it work?

The magnetic moment (spin) of a nucleus aligns with the magnetic field when it is positioned in a magnetic field. A radio frequency (RF) energy pulse deflects the nuclei. Upon eliminating this energy, the nucleus subsequently relaxes to its previous state and emits an electromagnetic pulse. A coil within the NMR picks up the RF pulse, and a computer converts the signal into a spectrum. In accordance with the chemical structure, every nucleus situated in a distinct chemical environment corresponds to a peak in the NMR spectrum. Scientists can learn more about each nucleus's environment by looking at the peak's position (the chemical shift value on the x-axis) and multiplicity. Because of the relationship between the peak's area and the signal's number of generating nuclei, quantitative analysis is possible.[6]

For total confidence in complex chemical structures elucidation, combining 1-D and 2-D NMR investigations is typically necessary. The following experiments often determine structures:

- It is possible to verify the number of hydrogen and carbon atoms in a molecule using 1-D ^{1}H-NMR and ^{13}C-NMR, respectively.
- The ^{1}H-^{1}H Correlation spectroscopy (COSY), which shows how adjacent carbons' hydrogen atoms are correlated.
- ^{1}H-^{13}C Heteronuclear single quantum coherence spectroscopy (HSQC) for the identification of which hydrogen is attached to which carbon atom
- ^{1}H-^{13}C Heteronuclear multiple bond correlation spectroscopy (HMBC) displays the correlations between protons and carbons atoms distanced by two or three bonds.[6]

5.3.2 NMR for peptides

The preferred technique for elucidating biomolecular structures in solution under nearly physiological conditions is two-dimensional (2D) NMR spectroscopy. An antimicrobial peptide's high-resolution three-dimensional (3D) structure impacts how it works because the

conformation of the peptide sheds light on the intermolecular interactions that control how it binds to its biological target.[7,8] A normal ten amino acid peptide has about 50 different protons, some of which may be detected by NMR spectroscopy. Depending on the local chemical environment, each proton on the peptide can either absorb or emit RF radiation at a particular frequency when subjected to a magnetic field. In units of "chemical shift," the frequency of the RF energy emitted by each proton on the peptide is reported. Actually, "chemical shift" is proportional to Hz (a more widely accepted unit of frequency), and the proportionality constant differs according to the magnetic field strength of the particular NMR device utilized during the experiment.

The determination process for the structure consists of two steps. First, the "assignment problem" needs to be solved. The assignment problem can be solved by determining the distinct NMR resonance frequency (or chemical shift) of each chemically distinct proton on the peptide. The term "total correlated spectroscopy" refers to the 2-D TOCSY. The chemical shifts of proton pairs inside the same amino acid are identified using the 2-D TOCSY spectrum. When J coupling correlation methods like COSY and TOCSY are combined with cross-relaxation measures like NOESY and ROESY, medium-sized proteins and nucleic acid fragments with molecular weights up to roughly 15,000 can have their three-dimensional structures determined.[9]

5.4 CD measurements

CD spectroscopy is often utilized in experiments to determine the secondary structure of peptoids because it enables quick analysis instead of characterization by NMR or X-ray crystallography. Although CD spectroscopy studies provide relevant information on the secondary structure, NMR and X-ray crystallography findings provide more information. CD spectroscopy is a form of light absorption spectroscopy that, instead of measuring the absorbance of isotropic light as is typically done, it measures the difference in the absorbance of right- and left-circularly polarized light by a substance. Right- and left-circularly polarized light interact differently with chromophores that are naturally asymmetric (uncommon) or symmetric chromophores in asymmetric surroundings, leading to two related concepts.[10] Due to the varying indices of refraction for right- and left-circularly polarized light, known as optical rotation or circular birefringence, circularly polarized light rays will move through an

optically active medium at various speeds. Dichroism is the term for the differential absorption of radiation that is polarized in two directions as a function of frequency. This is known as linear dichroism when applied to plane polarized light and circular dichroism when used to circularly polarized light.[10,11]

In peptides (such as proteins), CD for conformational analyses can be broadly divided into two categories: 1. monitoring modifications, such as monomer-oligomer, substrate binding, denaturation, etc., and 2. Prediction of the secondary structural content (for example, this peptide is 25% helical under these environments). As indicated, the CD is especially suitable for identifying structural alterations in proteins and peptides. Absolute structural content, however, presents greater challenges and is open to over-interpretation. One possible exception is the length-dependencies of the CD spectra of "pure" secondary structures. Assuming a spectrum is a linear combination of CD spectra of each contributing secondary structure type—for instance, "pure" beta strand, "pure" alpha helix, etc.—weighted by its quantity in the polypeptide conformation—is the simplest way to use CD data to determine secondary structure information. This method's primary flaw is the absence of standardized reference CD spectra for "pure" secondary structures.

It has been shown that CD spectra within 260 and around 180 nm can be used to discern the secondary structural types of alpha helix, parallel and antiparallel beta sheet, turn, and other molecules (Figure 65).[12]

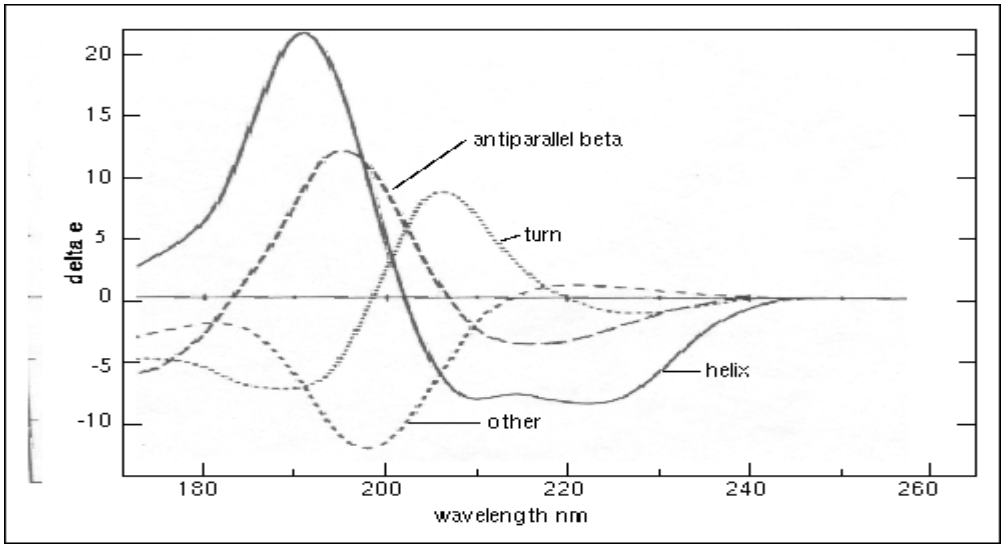


Figure 65: "Pure" secondary structure circular dichroism spectra. From Brahms & Brahms, 1980, redrawn.[12]

It is reported in literature that a peptide β-sheet structure, usually shows a minimum absorption between the wavelengths of 210 and 220 nm and a relatively strong maximum absorption of around 195 nm. The α-Helical structures exhibit two pronounced minima bands at 208 and 222 nm and a maximum at 198 nm, whereas the random coil has a minimum at 198 and a small positive band at 217 nm.[12]

5.5 Results and discussion

5.5.1 Determination of the secondary structure using CD

The procedure used for the CD experiments is explained in detail in Chapter 7. The data obtained from the CD measurements were analysed using the BeSTSEL software (https://bestsel.elte.hu/index.php). The result are presented in table 6 below, which shows the presence of Helices, beta Sheets and Coils in Pep_PNL1, Pep_PNL2, Pep_HA, Pep_TA and Pep_PTA. The CD spectra for each analogue are shown in the appendix (Figures 77 - 81) The software is able to categorise the data into the following conformations:

- α-Helices, which are divided into two components, regular (the regular or middle part of α-helices (helix1)) and distorted (the distorted ends (helix2)),
- β-sheets that are parallel as opposed to antiparallel. Considering the antiparallel β-sheets' twist, three categories were further created: relaxed (slightly right-hand twisted), right-hand twisted, and left-hand twisted.
- The turn and the "others" are the final two elements (BeStSel sorts 3_{10} helix to “others” as well as the pi-helix, beta-bridge, bend, loop/irregular and invisible regions of the structure).[13]

Pep_PHA and Pep_HAP were not considered because of low yield and purity while Pep_TAA was completely utilized during biological studies.

Table 6: The percentage composition of presence of Helices, beta Sheets and Coils in Pep_PNL1, Pep_PNL2, Pep_HA, Pep_TA and Pep_PTA.

Sequence*	**Helix (%)**	**Anti-parallel (%)**	**Parallel (%)**	**Turns (%)**	**Other (%)**
P-K-I-V-N-S-H-G-V-W-C-E-R-Y-V-L-Q-S-G-C (**Pep_PNL1**)	62.9	27.2	0.0	0.0	9.9
P-K-I-V-N-S-H-G-V-W (**Pep_TA**)	46.9	26.7	0.0	0.0	26.4
C-E-R-Y-V-L-Q-S-G-C (**Pep_HA**)	55.6	10.7	5.4	0.0	28.3
I-N-RR-G-V-L-G-C-R-Y-V-L-Q-S-G-C (**Pep_PNL2**)	34.1	17.5	0.0	0.0	48.4
P-*N*Lys-*N*ile-*N*val-*N*Asn-S-H-G-V-W (**Pep_PTA**)	26.6	34.0	0.0	0.0	39.4

* The peptides were dissolved in millipore water for the measurements, except Pep_HA which was dissolved in ACN: water (50:50)

The main peptide (Pep_PNL1) has a helical conformation that can be attributed to the tail region and an antiparallel beta-sheet conformation which may be used to explain the relationship of the amino acids within the ring. The peptide exhibits two stable conformations and is more structured than the other derivatives. Lasso peptides tend to be more structured as the tail sequence is fixed inside the ring, and other possible conformations are limited. When the head (Pep_HA) and Tail (Pep_TA) are separated, the amount of other conformations increases, further supporting the assumption about the threaded conformations providing stability. Furthermore, the presence of different conformations for Pep_TA agrees with the presence of conformers observed during its purification (**Chapter 2**). Combining the Lariatin A head region with the Lassomycin tail to form the Pep_PNL2 sequence increased random conformation; therefore, the lasso structure might not have formed.

As stated in Chapter 3, Pep_PTA is the peptide-peptoid hybrid of Pep_TA. An expected decrease in helicity is observed for Pep_PTA. Peptoids cannot form hydrogen-bonds and alpha-helices are stabilized by i to i + 4 backbone hydrogen bonds. The proportion and positioning of the charged residues may also contribute to the moderation of peptoid helicity. Lysine is known as a helix-promoting residue. [14,15] In Pep_PTA, the NLys might have contributed to the observed helical conformation. The length of the charged side chains and their positioning within the sequence affected helix formation in peptides. The antiparallel beta sheets can be attributed to the peptide region of the peptide-peptoid hybrid.

5.5.2 NMR structure elucidation of Pep_TA

Pep_TA was selected for the NMR structural elucidation because of its observed activity against the *mycobacterium tuberculosis* caseinolytic protease, its short sequence and good purity. As stated in Chapter 2, Pep_TA consist of 10 amino acids (Figure 66) with the following sequence: Pro-Lys-ile-Val-Asn-Ser-His-Gly-Val-Trp. The peptide (75 mg) was dissolved in 0,5 ml of deuterated DMSO and two-dimensional NMR spectra, including TOCSY, ROESY, COSY, and HSQC experiments, recorded at 300 K on a 500 MHz NMR spectrometer. The detailed conditions used for the aforementioned experiments are specified in Chapter 7.

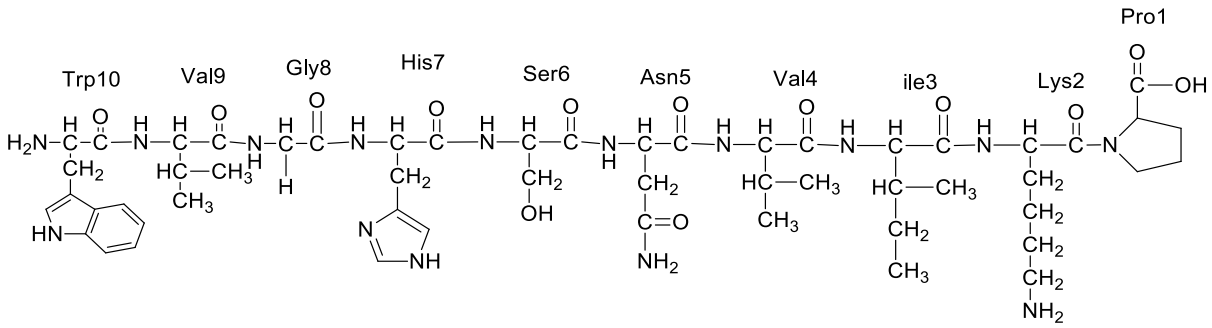


Figure 66: The structure of Pep_TA.

Even smaller peptides are impossible to assign from a 1D spectrum because of the high proton density per residue and the resonance overlap that result. However, using two- or three-dimensional correlation spectra is necessary. The following figure 67 indicates the positions of the protons in the 1D spectrum:

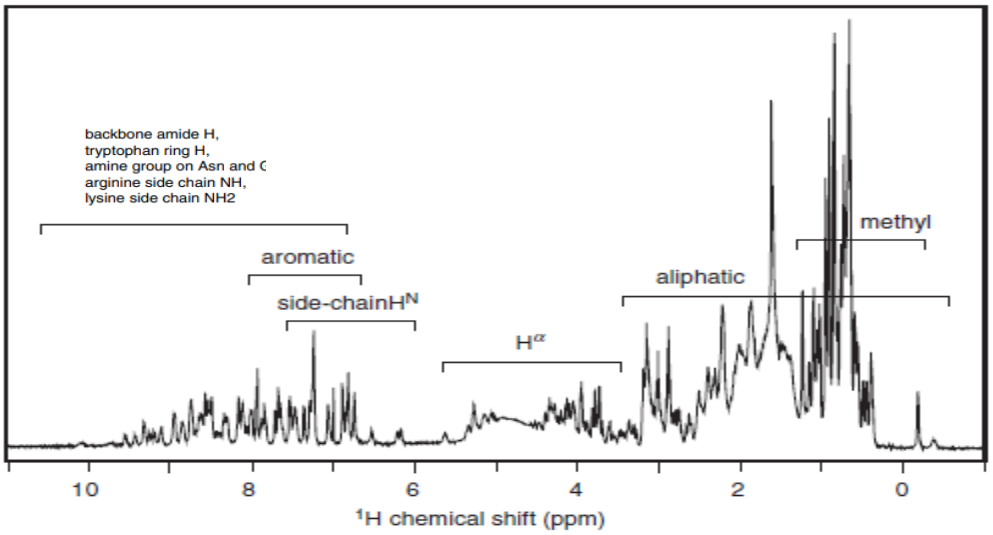


Figure 67: The usual positions of the protons in a 1D spectrum.[16]

5.5.2.1 Spin system and Sequential spin specific assignment of amino acid residues for Pep_TA

The COSY and TOCSY spectra were used to assign the various spin systems. This method depends on variations on the side chains of amino acids, which produce distinct spectra patterns in the amide fingerprint area of the spectrum. Each specific residue possesses a unique pattern connecting an amide (NH) to its backbone Cα proton and the remaining side chain protons. Identifying each side chain's spin system helps identify the specific amino acid residues present.

Protons produce all cross-peaks in a TOCSY experiment with the same spin system because the amide bond has no scalar coupling; thus, protons from various amino acids are always in separate spin systems. The spin system lines up vertically in the amide fingerprint region, and the position of peaks is unique for each amino acid (Figure 68).

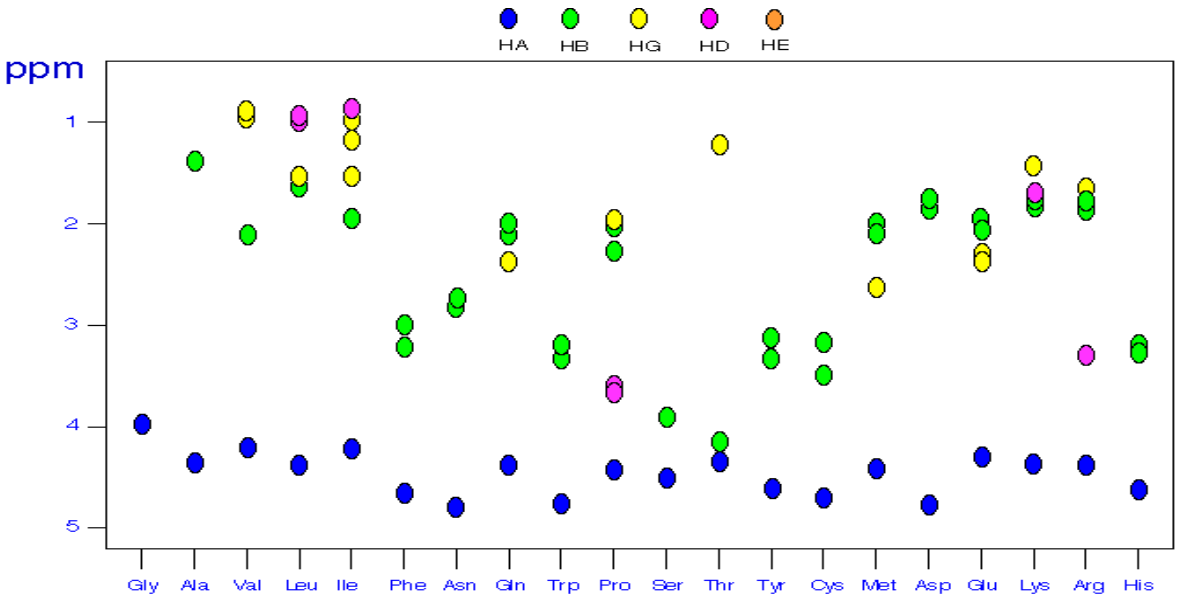
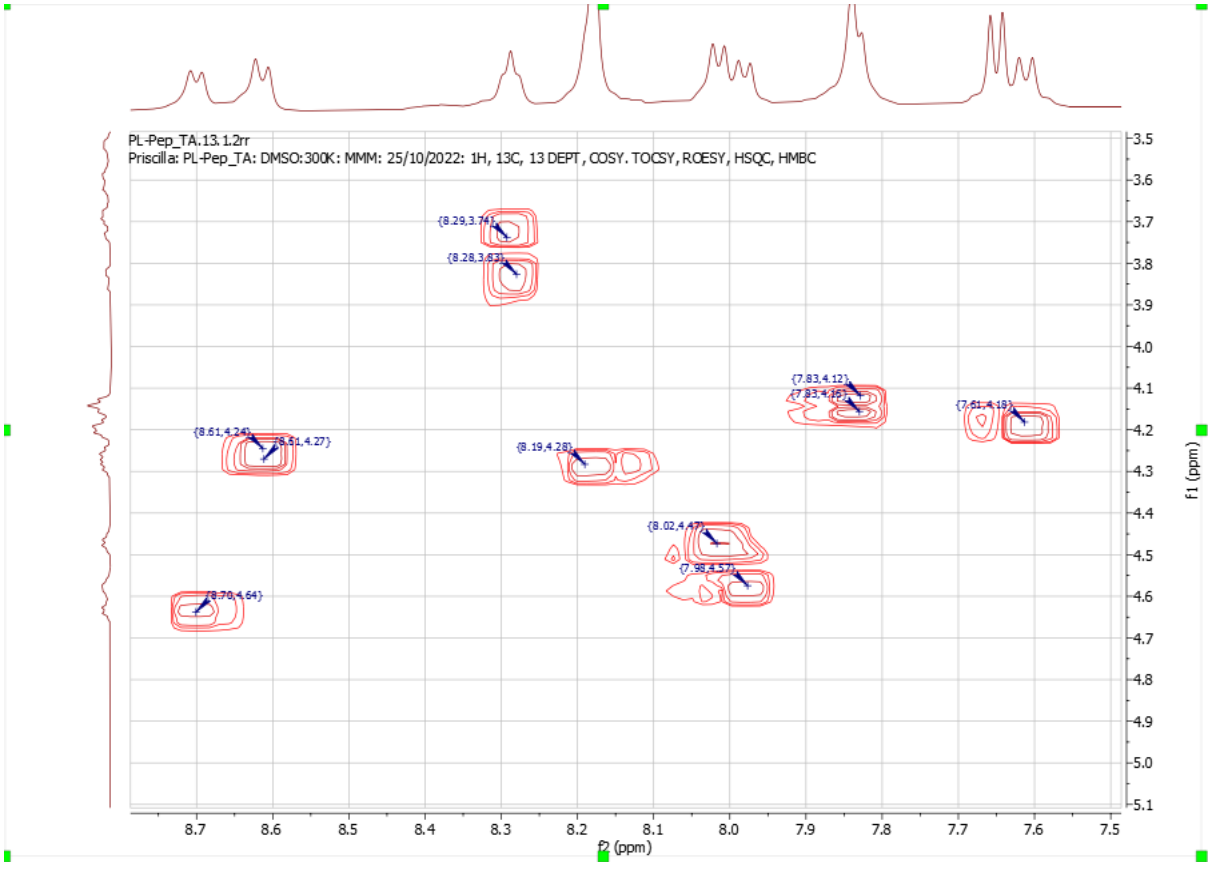


Figure 68: The fingerprint region for different amino acids. HA = alpha protons, HB = beta protons, HG = gamma protons, HD = delta protons, HE = epsilon protons.[17]

The COSY and TOCSY spectrum of Pep_TA showing the fingerprint region of amide protons-f2 (7.2-8.5 ppm) and alpha-aliphatic region-f1 (0-5 ppm) are shown in Figure 69.



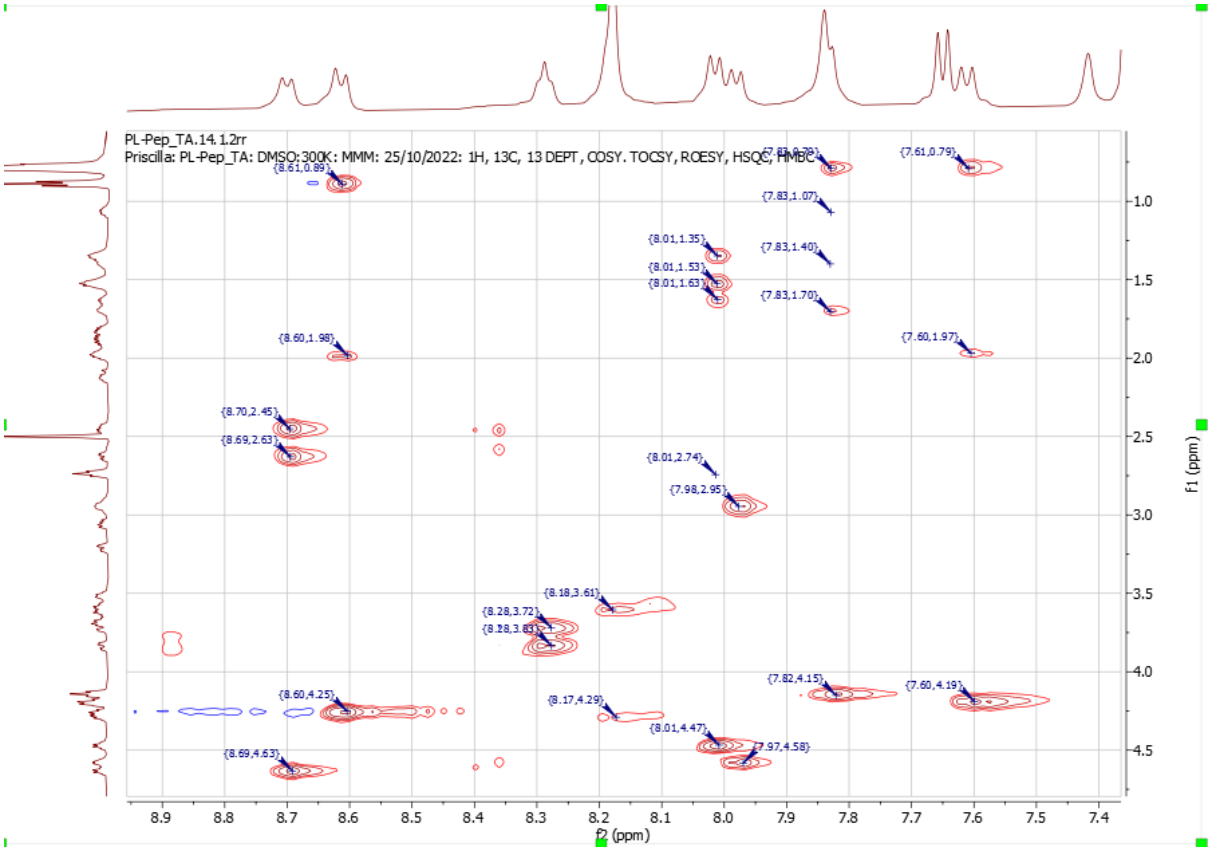


Figure 69: The TOCSY and COSY spectrums showing the fingerprint region.

Glycine was not difficult to identify because it is the only amino acid with 2 α-protons (Hα1 and Hα2) whose chemical shift appears around 3.5-4 ppm. On the same amide H line in the COSY or TOCSY spectra, the HN-Hα coupling is frequently seen for both α-protons. Usually, the Hα1 to Hα2 coupling can be seen in the COSY or TOCSY spectra appearing quite strongly. The Hα1 to Hα2 linkage may not always be seen because the two alpha protons occasionally exhibit chemical shifts that are equal or nearly equivalent. The Gly amide proton is the only one that shows up as a triplet due to its coupling to two α-protons. In this case Hα1 and Hα2 were observed at the following chemical shifts δ = 3.72 ppm and δ = 3.83 ppm respectively and the NH (δ = 8.29 ppm) peak appears as a triplet.

Val and Ile are methyl-group-containing amino acids and can be distinguished from each other based on their COSY connectivity. The CH_3 group with a resonance peak at 0.89 ppm has a COSY correlation with a CH peak (1.97, 30.50 ppm) while the CH_3 group at 0.79 has a cosy correlation with a CH_2 (1.07, 24.2 ppm) hence the methyl at 0.89 was assigned to a Val and the one at 0.79 to Ile. A spin system with an NH amide proton with a chemical shift of 7.60 ppm showed a correlation to a methyl resonance peak at 0.78 ppm and a CH_2 with a chemical

shift of δ = H-1.97, C-30.4, this spin was assigned to the second valine. The ile NH (7.83 ppm) showed a ROESY correlation to the valine's alpha proton (δ = 4.18 ppm); therefore, this valine was assigned to the 4th position in the sequence.

The long spin systems like Lys and Pro (which do not have an amide proton) all contain two γ protons, coupled to the β−protons. Lys; which consists of γ and δ protons in its side chain, was identified from the TOCSY spectra. The side chain amine of Lys is often not observed or is often a broad peak. The NH with a chemical shift of 8.01 ppm was assigned to lysine which is the longest spin. The alpha proton of Lys (δ = 4.47ppm) correlates to two resonances at 3.68 and 3.58 ppm which were assigned to proline beta protons since they also show a TOSCY correlation to a CH_2 peak at 2.13 and 1.88 ppm.

The short spin systems (only NH, α- and β-protons) for Ser, Asn, and His, were challenging to assign using either COSY or TOCSY spectra. This is because the backbone of these amino acid residues contains one α-protons and two β-protons with similar spin patterns. Ser, Trp, Asn and His were then assigned using the ROESY. On the ROESY, the NH proton with a chemical shift of 7.98 ppm correlates with the alpha protons of Gly-8 (δ = 3.72 and 3.83 ppm), this NH was therefore assigned to His-7. Again, the already assigned NH (δ = 8.29 ppm) of Gly-8 has a ROESY correlation with a resonance at 4.26 ppm an alpha proton of valine, therefore this confirms the position of Val- 9 in the sequence. The NH resonance peak at 8.61 ppm of Val-9 correlates to a peak with a chemical shift of δ = 4.14 ppm which belongs to a spin with an amide proton at δ =7.65 ppm which did not appear in the TOSCY. This spin was assigned to Trp-10 and it also has β protons belonging to a CH_2 group

Val-4 NH resonance peak at 7.60 correlates to an alpha proton with a chemical shift of 4.63 ppm which was assigned to the spin of Asn-5 with a resonance amide proton at 8.70 ppm. The alpha proton of His (4.58 ppm) showed a ROESY correlation to the NH resonance at 8.18 ppm which was then assigned to Ser-6.

The 2D ^{1}H-13C HSQC (Heteronuclear single quantum coherence) spectrum (aliphatic region) was also used to assign Cα of the corresponding spin systems. On the ^{13}C NMR, the alpha carbon for Hα1 to Hα2 were coupled to the same alpha carbon.

Table 7: NMR chemical shifts (ppm) of identified spin and assignment for Pep_TA using TOCSY and ROESY spectrum (Appendix II, Figure 86).

Residue	H-NH	δ^1Hα	δ^{13}Cα	δ^1Hβ	δ^1Hγ	δ^1Hδ	COSY δ^1H	ROESY δ^1H
Pro1	-	4.20	24.38	3.68; 3.51	1.88; 2.13			
Lys2	8.01	4.47	30.18	1.63	1.53	1.35	2.74	(8.01;4.14)
Ile3	7.83	4.10	36.14	1.70		0.79		(7.83; 4.19)
Val4	7.60	4.19	30.50	1.97	0.79			(7.60;4.63)
Asn5	8.70	4.63	36.46	2.45; 2.63				(8.70;3.60)
Ser6	8.18	4.29	61.43	3.60				(8.18;4.58)
His7	7.98	4.58	52.41	2.94				(7.98; 3.73) (7.98;3.84)
Gly8	8.29	3.72; 3.83	41.78					(8.29-4.26)
Val9	8.61	4.26	57.89	1.98	0.89			(8.81; 4.14)
Trp10	7.65	4.14	52.52	3.06; 3.21				

5.5.2.2 Determination of the secondary structural elements of Pep_TA

The secondary structure or backbone interactions that stabilize the peptide can be characterized by long-range correlations using the ROESY ^{1}H NMR spectra. The NOEs interaction observed between the δ^1Hα (NH 4.20 ppm) of Pro-1 and the δ^1Hβ (3.61 ppm) of Ser-6 suggests the presence of a non-linear conformation since amino acids that are separated by 4 amino acids have a ROESY interaction. The long-range correlation between Trp-10 and Ile-3 and Pro-1 and Ile-3 further suggests that the peptide might have a helical conformation observed from the CD experiment in section 5.4.1. The long-range correlations are highlighted in Table 8. In the future, hydrogen bond surrogate-derived alpha helix mimics will be synthesized to investigate the importance of the helical conformation on biological activity.

Table 8: The long-range correlations observed on ROESY NMR.

Residue	Long range Correlation	H-NH	δ^1Hα	δ^{13}C	δ^1Hβ	δ^1Hγ	δ^1Hδ	ROESY δ^1H
Pro1	**Pro1-Ile3** **Pro1-Ser6**	-	4.20	24.38	3.68; 3.51	1.88; 2.13		(**3.68;0.79**) **(4.20;3.61)**
Ile3	**Ile3-Trp10**	7.83	4.10	36.14	1.70	1.07;1.40	0.79	**(1.40;4.14)** **(1.07;4.14)**

5.6 Concluding remarks

CD experiments confirmed the formation of stable conformations for Pep_PNL1 and indicated a loss of conformity for the separate tail (Pep_TA) and cyclic (Pep_HA) region derivatives Pep_PNL1. This suggests that the head and tail are crucial to each other and stabilize each other to form an active molecule. The CD results also suggested a loss of conformational rigidity and stability for Pep_PNL2. This suggests that the head and tail regions from different lasso peptides might not be structurally compatible with stabilizing each other. Pep_PTA exhibited both peptide and peptoid properties, as seen from its formation of beta sheets. Pep_TA was found to exist in a helical conformation by both NMR and CD experiments. In the future, all the observed structural behaviour will be related to the biological activity, and a structure-activity relationship will be used to guide further design.

References

(1) Singh, B. R. Basic Aspects of the Technique and Applications of Infrared Spectroscopy of Peptides and Proteins. *ACS Symp. Ser.* **2000**, *750*, 2–37. https://doi.org/10.1021/bk-2000-0750.ch001.

(2) Rehman I, Farooq M, B. S. *Biochemistry, Secondary Protein Structure*; StatPearls, 2021.

(3) Flatt, H. J. and P. *4.2: Secondary Structure and Loops*; LibreTexts Biology, 2023.

(4) Chapter 2: Protein Structure. In *CH450 AND CH451: BIOCHEMISTRY - DEFINING LIFE AT THE*

MOLECULAR LEVEL.

(5) Landry, D. *Biochemistry 601*. http://www2.tulane.edu/~biochem/med/second.htm?cv=1 (accessed 2023-03-21).

(6) *Reveal details of your chemical's molecular structure in solids and liquids*. Triclinic Labs. https://www.tricliniclabs.com/page-directory/materials-analysis-services/nuclear-magnetic-resonnance-NMR-spectroscopy-services-from-triclinic-labs.html?cv=1 (accessed 2023-03-21).

(7) Haney, E. F.; Hunter, H. N.; Matsuzaki, K.; Vogel, H. J. Solution NMR Studies of Amphibian Antimicrobial Peptides: Linking Structure to Function? *Biochim. Biophys. Acta - Biomembr.* **2009**, *1788* (8), 1639–1655. https://doi.org/10.1016/j.bbamem.2009.01.002.

(8) Singh, H.; Singh, S.; Raghava, G. P. S. Peptide Secondary Structure Prediction Using Evolutionary Information. *bioRxiv* **2019**, 558791.

(9) Griesinger, C.; Sorensen, O. W.; Ernst, R. R. Novel Three-Dimensional NMR Techniques for Studies of Peptides and Biological Macromolecules. *J. Am. Chem. Soc.* **1987**, *109* (23), 7227–7228. https://doi.org/10.1021/ja00257a074.

(10) Chakraborty, J.; Das, S. Application of Spectroscopic Techniques for Monitoring Microbial Diversity and Bioremediation. *Appl. Spectrosc. Rev.* **2017**, *52* (1), 1–38. https://doi.org/10.1080/05704928.2016.1199028.

(11) Miles, A. J.; Wallace, B. A. *Biopharmaceutical Applications of Protein Characterisation by Circular Dichroism Spectroscopy*; Elsevier B.V., 2019. https://doi.org/10.1016/B978-0-444-64173-1.00006-8.

(12) Berndt, K. D. *4.2.1 Circular dichroism spectroscopy*. https://www.cryst.bbk.ac.uk/PPS2/course/section8/ss-960531_21.html#:~:text=The application of CD for,%25 helical under these conditions).

(13) Micsonai, A.; Wien, F.; Kernya, L.; Lee, Y. H.; Goto, Y.; Réfrégiers, M.; Kardos, J. Accurate Secondary Structure Prediction and Fold Recognition for Circular Dichroism Spectroscopy. *Proc. Natl. Acad. Sci. U. S. A.* **2015**, *112* (24), E3095–E3103. https://doi.org/10.1073/pnas.1500851112.

(14) Huyghues-Despointes, B. M. P.; Scholtz, J. M.; Baldwin, R. L. Effect of a Single Aspartate on Helix Stability at Different Positions in a Neutral Alanine-based Peptide. *Protein Sci.* **1993**, *2* (10), 1604–1611. https://doi.org/10.1002/pro.5560021006.

(15) Yang, J.; Zhao, K.; Gong, Y.; Vologodskii, A.; Kallenbach, N. R. α-Helix Nucleation Constant in Copolypeptides of Alanine and Ornithine or Lysine. *J. Am. Chem. Soc.* **1998**, *120* (41), 10646–10652. https://doi.org/10.1021/ja982319d.

(16) John Cavanagh, Wayne J. Fairbrother, Arthur G. Palmer, III, N. J. S. *Protein NMR Spectroscopy*; 1995.

(17) Two-dimensional nuclear magnetic resonance spectroscopy. *Wikipedia*, *the free encyclopedia*. https://en.wikipedia.org/wiki/Two-dimensional_nuclear_magnetic_resonance_spectroscopy.

CHAPTER 6: Conclusion and recommendations

The discovery of drug agents capable of combating the rise of *Mtb*-resistant strains is of great interest. This work focused on designing and synthesizing the Lariatin A derivatives reported to show potency against the *Mtb.* The peptidomimetics reported herein were further screened to determine their activity against *Mtb* caseinolytic protease, essential for *mycobacterium* survival. The following chapter summarizes the results obtained from this study, the conclusion, and recommendations for future work.

6.1 Summary and Conclusion

6.1.1 Summary

8 Peptidomimetics of Lariatin A were designed, and their synthetic procedure was developed. Among several attempted SPPS procedures, **Method 3** resulted in improved yields, and it was used as the general method to synthesize other derivatives. The best coupling reaction time was 30 minutes for each amino acid to avoid the possible side reactions that could occur and lead to poor yields of the final peptide. The amino acids were coupled only once, except for the amino acids that were difficult to couple. HBTU/NMM was used to couple most of the amino acids, except for those that were difficult to couple, in which HATU was used to improve the coupling efficiency. For cyclic derivatives, cyclization was achieved by forming a disulfide bond between the incorporated cysteine residues. Thus, better results were achieved with this method involving dissolving the peptide to be cyclized in DMSO and water (20:80) and allowing for overnight cyclization. Incorporating fatty acid moieties to increase the cell permeability of the peptidomimetic, adamantane, and palmitic made the peptides more non-polar; however, the more non-polar palmitic resulted in difficulty dissolving the peptide, hence its purification was challenging. Adamantane was more favourable for the solubility of the peptide. Except for Pep_HAP, all the peptides were successfully purified, and low to moderate yields were achieved.

The peptide-peptoid hybrids were also designed based on the Tail (Pep_PTA) and cyclic Pep_HA) regions of Pep_PNL1. They were then successfully synthesized following the sub-monomer approach. Pep_PTA was successfully purified while the low yields achieved during the synthesis of Pep_PHA made its purification more challenging.

The short peptide derivative, Pep_TA and its analogue with adamantane, PepTAA, were screened for biological against the *Mtb*'s ClpP. Both peptides showed activity with a 70% inhibition for Pep_TA and 49% for Pep_TAA.

With the aid of CD, the possible conformations and secondary structural features of Pep_PNL1, Pep_PNL2, Pep_TA, Pep_HA, and Pep_PTA were successfully determined. Pep PNL1 was found to be more structured than the other derivatives, according to CD experiments. It has a structure with two stable conformations. This was explained by the threaded lasso structure it created. The observation of a loss in conformational stability for Pep_HA and Pep_TA adds evidence in favour of the hypothesis that threaded conformations provide stability. The CD data also suggested that the increased random conformation may not have formed Pep PNL2's lasso structure. Because peptoids cannot form hydrogen bonds, a decrease in helicity was observed, as anticipated for Pep_PTA. The 2D ^{1}H NMR (ROESY and TOCSY) results supported the helical shape discovered by the CD experiment and provided crucial complementary tools in elucidating the secondary structre of Pep_TA.

6.1.2 Conclusion

Lariatin A peptidomimetics were successfully designed, and solid phase peptide synthesis is a good technique resulting in moderate to good yields. The sub-monomeric synthesis of the peptide-peptoid hybrids proved to be a feasible technique, however, further improvements are necessary to achieve better yields for the Lariatin A hybrids. Except for Pep_HAP and Pep_PHA, the derivatives were purified successfully using the Prep-HPLC techniques, and purities ranging from 95-99% were achieved. The addition of cysteine enabled successful cyclization. Lariatin derivatives can bind to the protease; Pep_TA and Pep_TAA showed biological activity against *Mtb's* caseinolytic protease with 70 and 49% inhibition, respectively.

From all the mentioned results, it can be suggested that Lariatin A derivatives targeting the *Mycobacterium tuberculosis* caseinolytic protease can be synthesized using the solid phase peptide synthesis strategy.

6.2 Future scope of research

The synthesized peptides will be screened for biological activity against the ClpP. The structural conformations reported in this study will be related to the biological activity and a conclusion on the structure-activity relation will be used to guide further design.

The peptide-peptoid hybrid Pep_PTA's mode of action will be evaluated using computational chemistry. In the future hydrogen bond surrogate derived alpha helix mimics will be synthesized to investigate the importance of the helical conformation on biological activity.

CHAPTER 7: Experimental

7.1 Materials and reagents

N,N'−Dimethylformamide (DMF) and acetonitrile (ACN) were purchased at Pyramid Scientific. Dichloromethane (DCM) was purchased from Sigma Aldrich and dried upon distillation over calcium hydride. Fmoc protected amino acids, chlorotrityl resin, Rink amide MBHA, Diisopropylethylamine (DIPEA), N-methylmorphine (NMM), piperidine, N,N,N',N'-Tetramethyl-O-(1H-benzotriazol-1-yl)uronium hexafluorophosphate (HBTU), Triisopropylsilane (TIS), formic acid, trifluoroacetic acid (TFA), (N,N'-Diisopropylcarbodiimide) DIC, thionyl chloride were purchased from Dld Scientific. Dimethylformamide (DMF), methanol, acetonitrile, hexane, dimethyl sulfoxide and ether were purchased from Radchem.

7.2 Instrumentation used for peptides and amino acids and general techniques

7.2.1 Ultra High Pressure Liquid Chromatography (UHPLC)

A Thermo Scientific Dionex Ultimate 3000 Ultra High-Pressure Liquid Chromatography (UHPLC) coupled to a Bruker Compact Q-TOF mass spectrometer and a Diode Array Detector (215 nm and 254 nm) was used to analyze as well as determine the purity of the peptides and peptoids. A 0.30 ml/min flow rate on the Phenomenex C18 column (5 µm, 100 Å, 4.60 mm x 150 mm) was used to separate the compounds with a solvent system utilizing formic acid as the ion-pairing agent. Solvent A consisted of 0.1% formic acid/H_2O (v/v), and solvent B consisted of 0.1% formic acid/Acetonitrile (v/v). Mass spectrometry analysis was done using a positive mode electrospray ionization source (ESI).

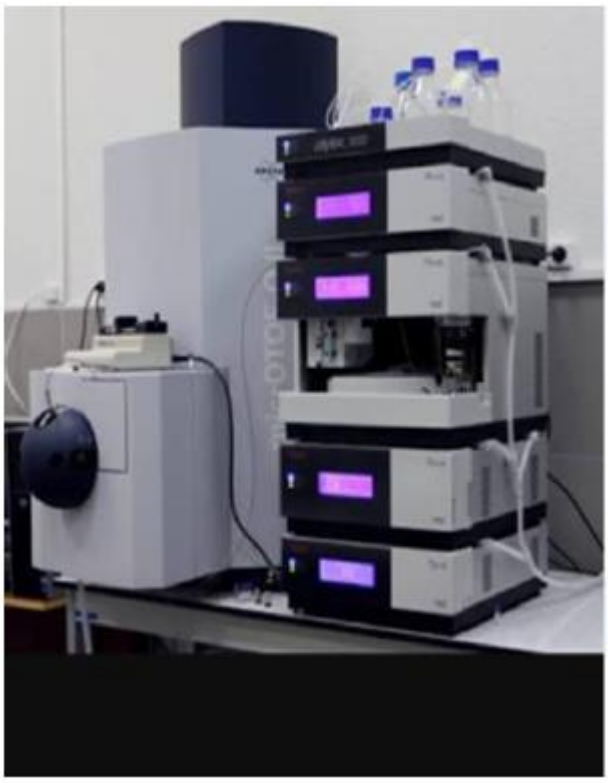


Figure 70: Ultra-High-Performance Liquid Chromatography (Thermo Scientific Ultimate 3000, RS diodearray detectors) with a Diode Array (190, 195, 215, 254, and 300 nm) coupled to a Bruker Compact QTOF high-resolution mass spectrometer.

7.2.2 Semi-Preparative High Pressure Liquid Chromatography (semi-PREP-HPLC)

Purification of the peptides was carried out on an Agilent 1260 Infinity semi-preparative instrument via reverse-phase chromatography. A Phenomenex Kinetex XB-C18 (5 µm, 100 Å 250 mm x 21.2 mm) column was used with a 15 ml/min flow rate. A UV/VIS detector was used to detect the compounds at 215 nm and 254 nm wavelengths and desired fractions were collected on an automated fraction collector. A two-buffer system was employed, utilizing formic acid as the ion-pairing agent. Two buffer system was used for the mobile phase, consisting of 0.1% formic acid/H_2O (v/v) as Buffer A and 0.1% formic acid/acetonitrile (v/v) as Buffer B.

7.2.3 Ultraviolet–visible spectroscopy

The absorption spectra were acquired using an Agilent Technologies Cary Series UV-Vis spectrophotometer. The theoretical yield of the peptides were obtained using the absorbance at 301 nm see section 7.3.3 below for full calculations.

7.2.4 Mass spectroscopic analysis

Analysis of amino acids and small portions of peptides was performed on the applied Advion expression-MS (ESI) mass spectrometer in positive mode.

The Thermo Scientific Ultimate 3000 UHPLC was used for sample analysis. It was coupled to a Bruker compact Qq TOF high-resolution mass spectrometer instrument. The autosampler was set at 5°C with an injection volume of 5 µL. The ionization technique used was electrospray ionization (ESI), and the ion source was kept at 220 °C in the positive ion mode.

7.2.5 Nuclear magnetic resonance spectroscopy (NMR)

1H-NMR spectra were recorded on a Bruker Avance 300 MHz, Bruker Avance 400 MHz and on Bruker III 500 MHz spectrometer. The chemical shift (δ) values are reported in parts per million (ppm) relative to deuterated chloroform ($CDCl_3$, 7.26 ppm) and dimethyl sulfoxide (DMSO-d6, 2.49 ppm) and referenced against the internal standard, tetramethylsilane (TMS, 0.00 ppm). The spectra were analyzed in the first order, and the coupling constant (J) values were reported as Hertz (Hz). Multiplicity of signals are expressed as: s=singlet, br s=broad singlet, d=doublet, dd=double doublet, t=triplet, q=quartet, m=multiplet. ^{13}C NMR spectra were recorded on Bruker Avance 300 MHz, Bruker Avance 400 MHz and on Bruker III 500 MHz spectrometer. The chemical shift values are reported in (ppm) relative to DMSO-d6, 39.52 ppm. 2D NMR spectra, including COSY, ^{13}C-HSQC, TOCSY, NOESY and ROESY experiments, were recorded at 300K on a 500 MHz NMR Bruker III spectrometer. The first ROESY experiments were recorded with mixing time of 200 ms; while TOCSY was recorded with mixing time of 70; each increment was the sum of 32 scans with a relaxation delay of 2.0 s; 2048 data points were collected per experiment.

7.2.6 CD

CD spectra were recorded on a JASCO J-18 spectropolarimeter between the range of 190 to 250 nm in the specified solvents (water and acetonitrile), with 10 scans at 20°C. The quartz cuvette used had a pathlength of 0.2 cm with a resolution of 0,2 mm, a bandwidth of 1.0 nm and a sensitivity of 10-20 mdeg. The peptides (0, 00061 mol L^{-1}) were prepared in water and a ACN. The value of absorption was measured as molar ellipticity per residue ($deg.cm^2 . dmol^{-1}$). The signals obtained were converted to mean residue ellipticity, [θ] using the equation below:

$[\theta] = (MRW \times \theta)\ 10 \times d \times c$ deg.cm^2 .dmol^{-1}

where MWR is the mean residue weight, θ the observed ellipticity in degrees, c is the peptide concentration in g/ml and d is the pathlength in cm.

7.3 General procedure for the solid phase synthesis of the peptides

7.3.1 General procedure for the swelling, activation and coupling of the first amino acid to 2-chlorotitryl resin

The resin was activated by weighing 2-chlorotrityl chloride (500 mg, 0.5 mmol/g) into a 15 ml centrifuge tube and adding thionyl chloride (2 ml) and dry DCM (10 ml). The mixture was left to shake overnight at room temperature on a shaker. The resin was then transferred into glass vessel fitted with a fritted filter and washed with dry DCM (5 x 15 mL). In order to avoid deactivation of the water sensitive resin, a mixture of the first amino acid Fmoc-Pro-OH (404,8 mg, 1,2 mmol) in dry DCM (10 mL) and DIPEA (2 ml) was immediately added to the resin. The reaction mixture was mixed by gently bubbling a steady stream of nitrogen gas at room temperature for 45 minutes. The reaction was filtered and the resin was washed with DMF (3 × 15 ml) followed by DCM (3 × 15 ml).

7.3.2 General procedure for the swelling, activation and coupling of the first amino acid to rink amide resin

The rink amide resin (300 mg, 0.160 mmol/g) was swollen in DMF (10.0 ml) for 3 hours in a 15 ml centrifuge tube. The resin was then dried in a reaction vessel fitted with a fritted filter using suction. A solution of 20% piperidine in DMF was added to the reaction vessel and bubbled in nitrogen gas (2 x 5 minute) to deprotect the resin. The solution was filtered, and the resin was washed with DMF (3 × 15 ml) and DCM (3 × 15 ml). A solution of the first amino acid Fmoc-Cys(trt) (0.2 M, 1.49 g) dissolved in DIPEA (1.0 M, 2.0 ml), HBTU (0.863 g, 0.19 M) were added to the reaction vessel. This mixture was reacted for 30 minutes and then dried under suction. Finally, the resin was washed with DMF (3 × 15.0 ml).

7.3.3 General procedure for analysing the substitution of the first amino acid on resin

A small amount of resin (5 to 10 mg), with the first amino acid attached, was weighed into two Eppendorf then 1 ml of 20% piperidine in DMF was added. The mixture was shaken for 15 minutes at 90 rpm to remove the Fmoc protecting group from the amino acid. The mixture was then centrifuged at 5000 rpm for 2 min, then 100 µl of the supernatant was drawn and

added to 10 ml of DMF. After thoroughly shaking the mixture, the solution (2.0 ml) was pipetted into one cuvette cell. DMF (2.0 ml) was added to another cuvette cell. Using 2 ml of DMF (blank), a UV-vis spectrophotometer was set to zero. A cuvette containing a sample solution was then placed in the sample cell and the absorbance was observed at the wavelength of 301 nm three times. This procedure was done in triplicate and the average loading capacity was then calculated to be 0.4 mmol/g.

The substitution of Fmoc-amino acid loaded was then used to calculate the loading capacity and the theoretical yield:

Loading capacity = 101(Absorbance)/7.8(mass of resin-Fmoc amino acid)

Example of the calculations:

Table 9: The mass and average absorbances of samples from the resin after attaching the first amino acid.

Sample no.	**Mass (mg)**	**Absorbance**	**Average Absorbance**
1.	**3.3**	**0.1398**	**0.1324**
		0.1189	
		0.1385	
2.	**5.5**	**0.1865**	**0.1844**
		0.1820	
		0.1847	

The loading capacity obtained for this derivative was found to be 0.4768 mmol/g.

Loading capacity = 101(Absorbance)/7.8(mass of resin-Fmoc amino acid)

= 101 (0.1584)/7.8(4.4)

= 15.9984/34.32

=0.4 mmol/g

7.3.4 General procedure for the synthesis of peptides

To the resin in the reaction vessel, 20% piperidine solution (10 ml) was added and allowed to bubble under nitrogen gas for 5 minutes in order to remove the protecting group. The resin was washed with DCM (5×10 ml) and DMF (5×10 ml) to remove excess reagents.

The next amino acid Fmoc-Lys-OH was coupled to the resin bound proline by adding Fmoc-Lys-OH (937.0 mg, 2 mmol), coupling agent HBTU (720. 56 mg, 1.9 mmol) and NMM (1.1 ml) into the vessel and allowing this solution to gently bubble under nitrogen gas for 45 min. Upon filtration the resin was washed with DMF (3 × 15 ml) and treated with 20% piperidine in DMF (10.0 ml) twice for 5 minutes and then the resin was then washed again with DMF (6 × 15.0 ml). This left the resin-peptide ready for another coupling cycle. The amino acids that follow according the desired sequence were coupled using the same procedure. The Fmoc group on the last amino acid was deprotected and the resin was washed with DMF (3 × 15 ml) followed by DCM (3 × 15 ml) and transferred into a cebtrifuge tube. A cocktail mixture of TFA (95%):water(2.5%): Triisopropylsiliane (2.5%) was prepared and about 30 ml of it was added to the resin. The mixture was left in the shaker for 3 hours. The solution was then filtered into centrifuge tubes (50 ml) and ice cold diethyl ether was added into the tube. The tubes were then shaken and placed in a -20 degrees fridge for 5 minutes. The tubes were centrifuged at 5000 rpm for 5 minutes and the ether/TFA solution was decanted. The resulting peptide precipitate was washed with cold ether three times.

7.4 General procedure for the synthesis of the peptoids.

In a sintered glass reaction vessel, activated 2-chlorotrityl chloride resin (1 g, 1.33 mmol) was swollen for 10 minutes in dry DCM. In the reaction vessel, bromoacetic acid (1.25 g) was mixed with DIPEA (2 mL), DCM (final concentration of 1.2 M), and nitrogen to bubble the mixture for two hours. Filtration was used to remove the solvent, and DCM (3 x 10 mL) and DMF (3 x 10 mL) were used to wash the resin. An amine (1 M) solution in DMF was added to the reaction vessel and bubbled for 1 hr using nitrogen. Filtration was used to remove the solvent, and DCM (3 x 10 mL) and DMF (3 x 10 mL) were used to wash the resin. Bromoacetic acid (1.25 g) in DMF (final concentration of 1.2 M) and DIC (2 mL) was added to the reaction vessel and bubbled for 2 hours using nitrogen. Until the necessary sequences were attained, these stages were repeated. The final cleavage of the peptoid from the resin was accomplished using methods similar to those mentioned above for peptides.

Appendices

Appendix I- Supplementary information for Chapter 2

Appendix II- Supplementary information for Chapter 5

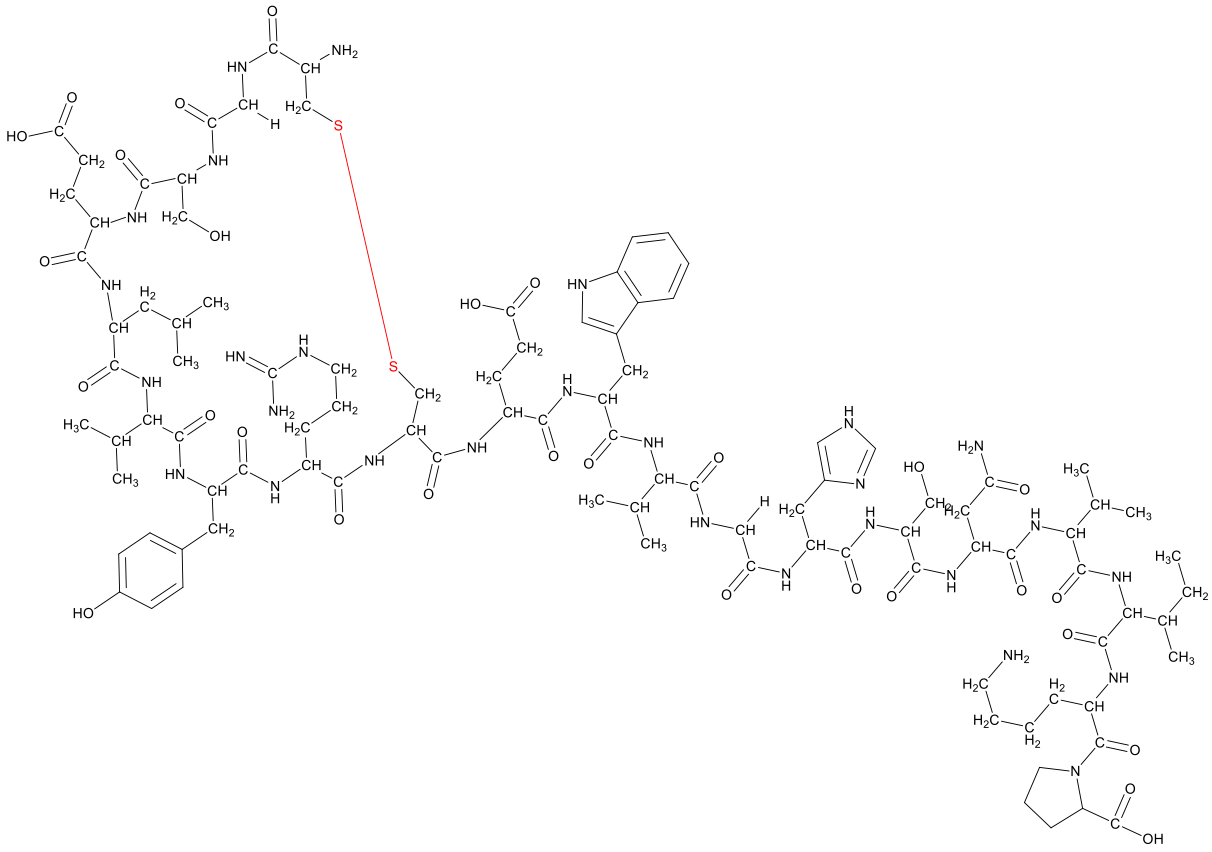


Figure 71: Structure of Pep_PNL1

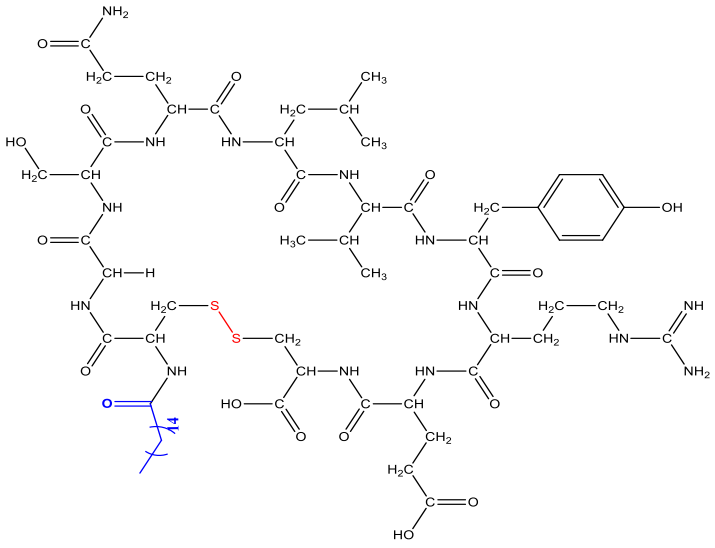


Figure 72: Structure of Pep_HAP.

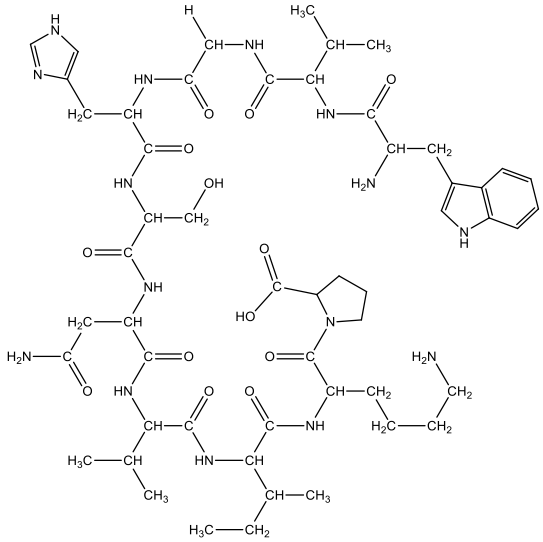


Figure 73: : Structure of Pep_TA

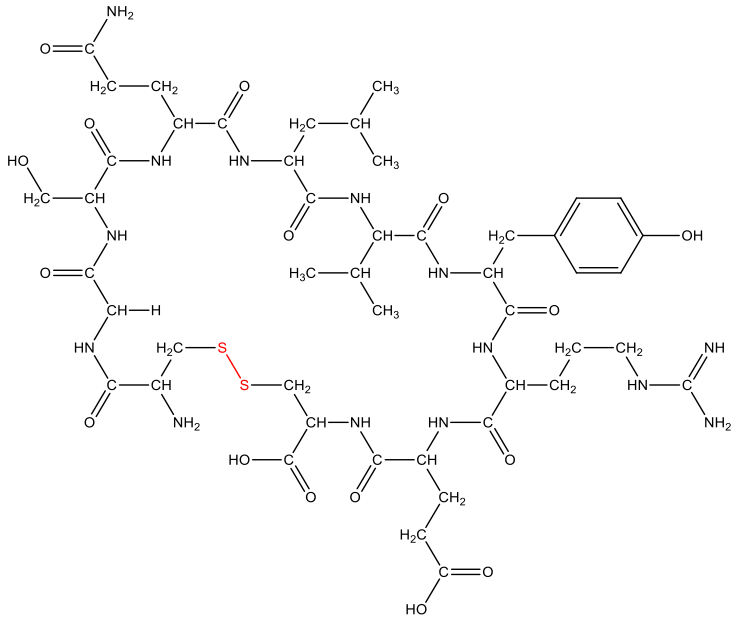


Figure 74: The structure of Pep_HA.

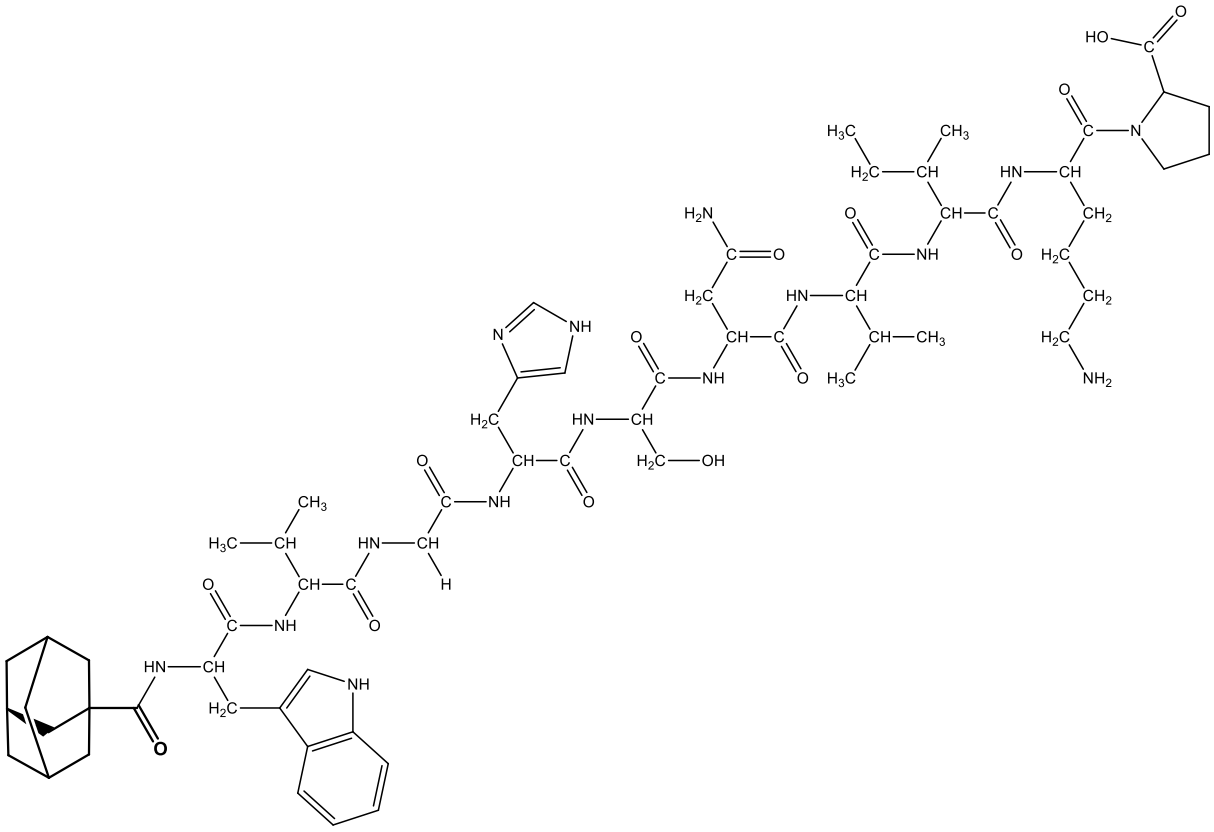


Figure 75: The structure of Pep_TAA

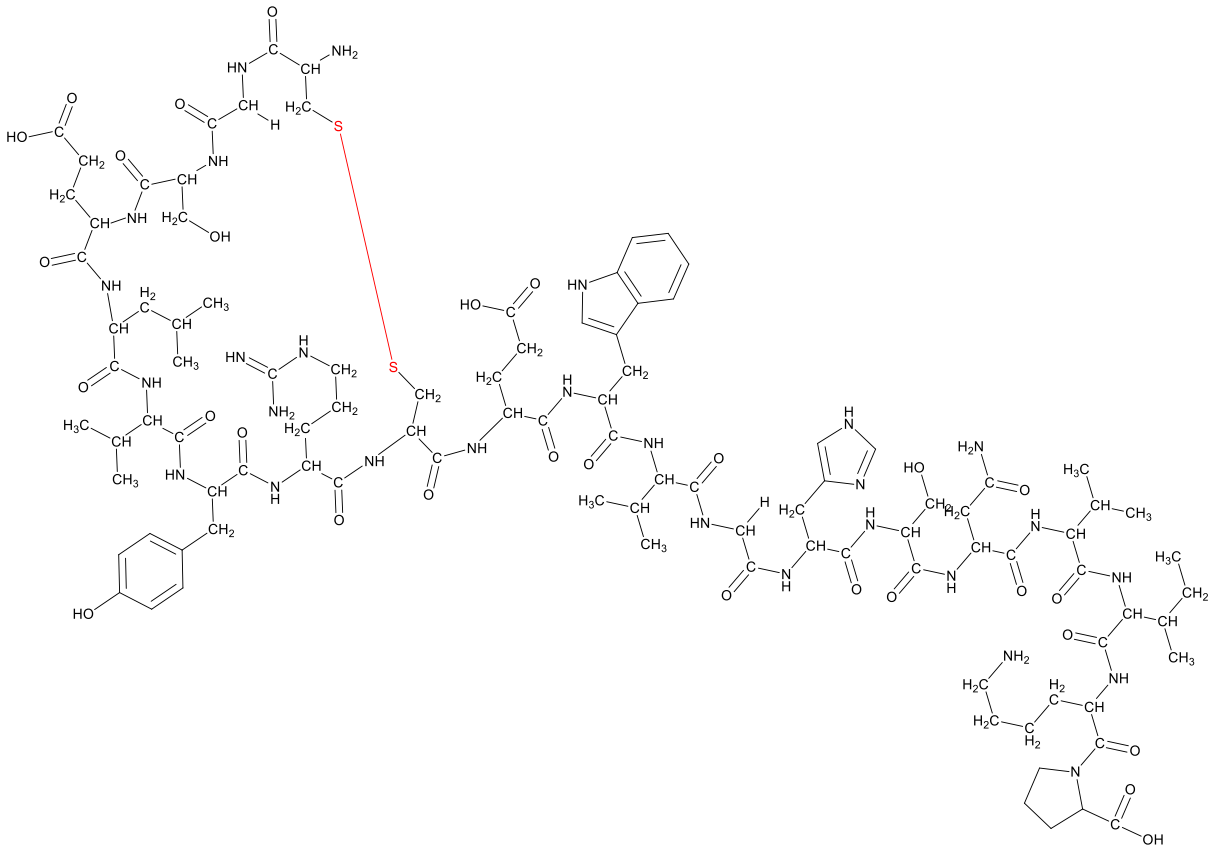


Figure 76: The structure of Pep_PNL2

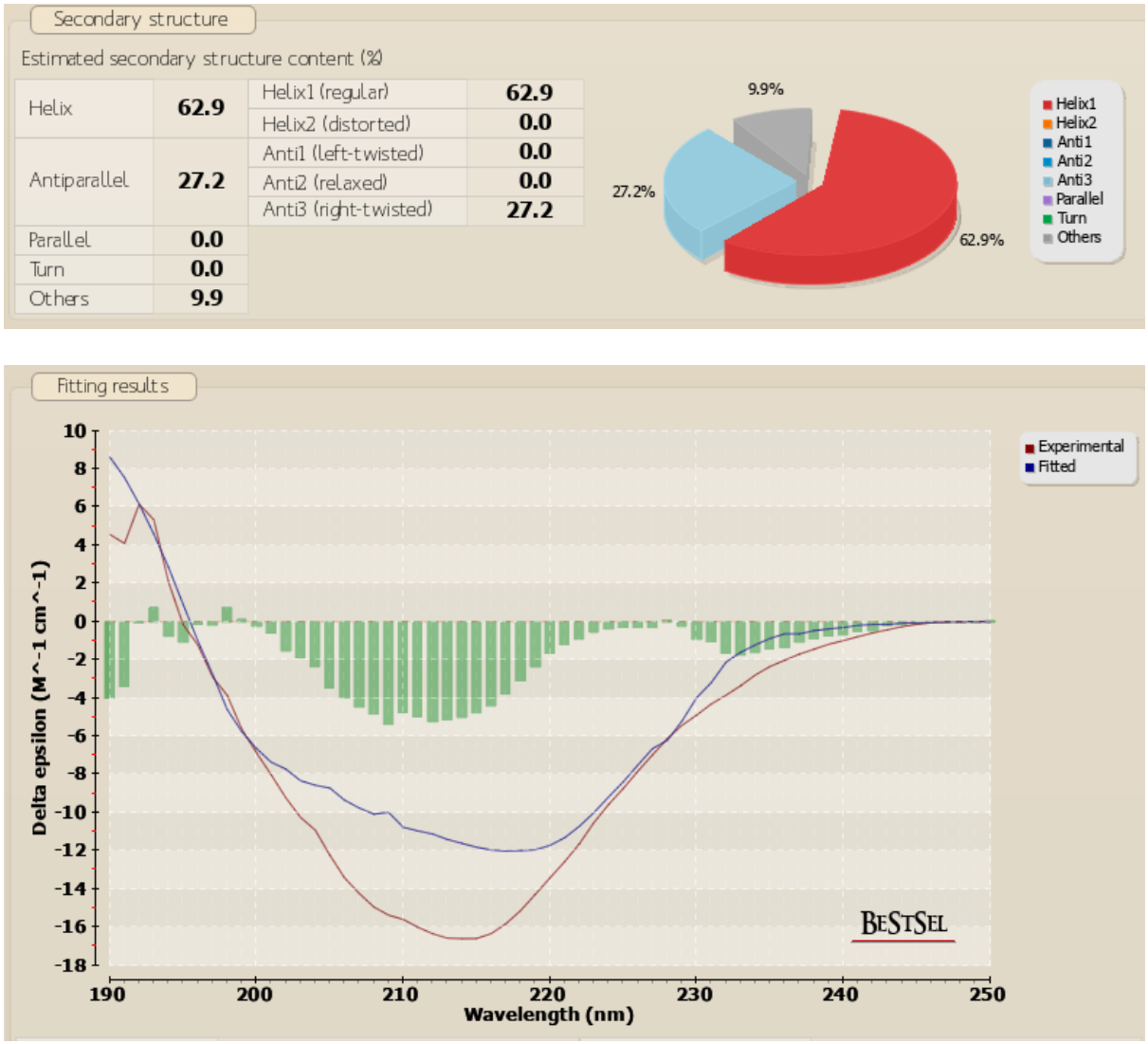


Figure 77: Plot and secondary structure data of Pep_PNL1 CD data using BeStSel software

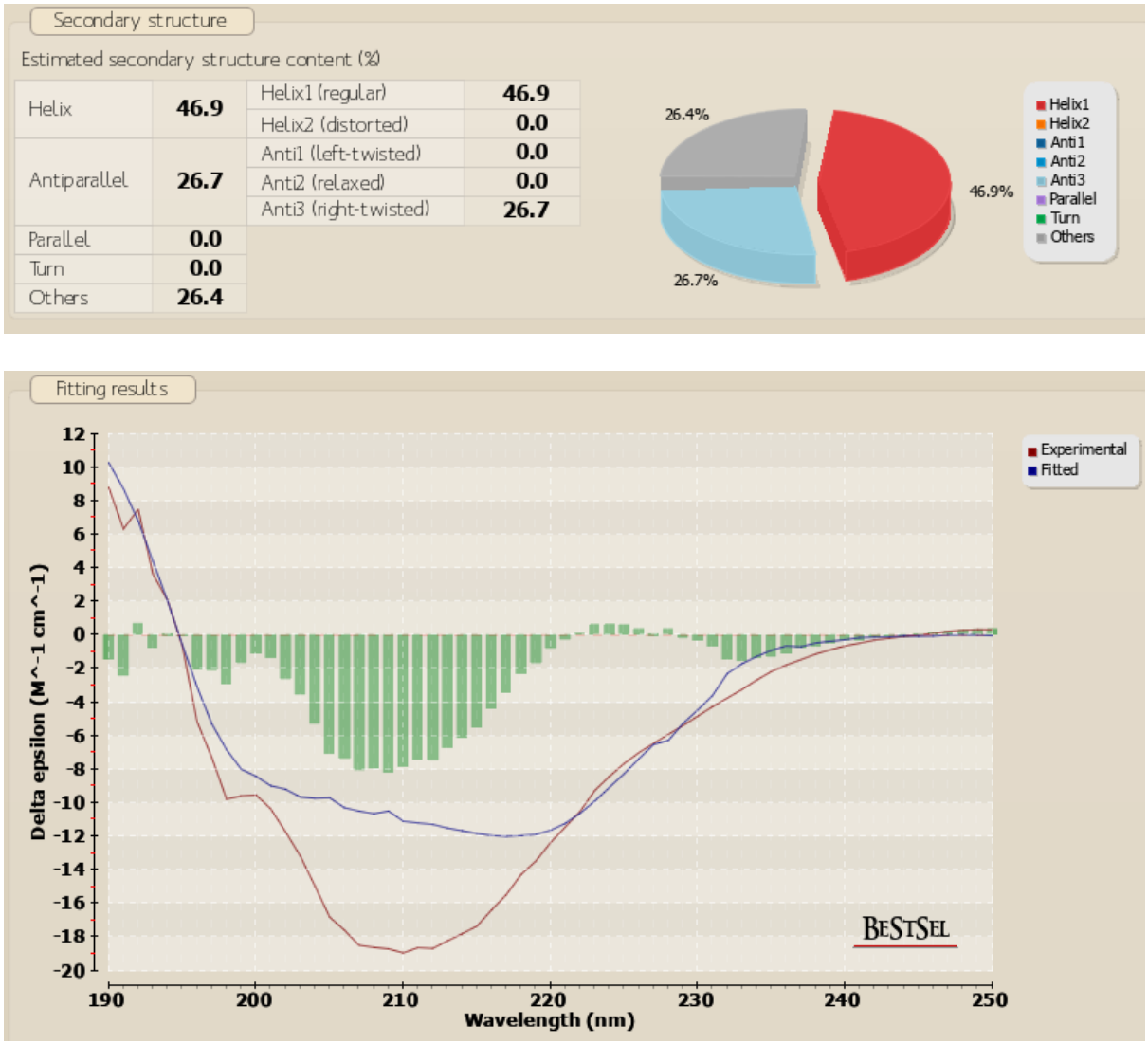


Figure 78: Plot and secondary structure data of Pep_TA CD data using BeStSel software.

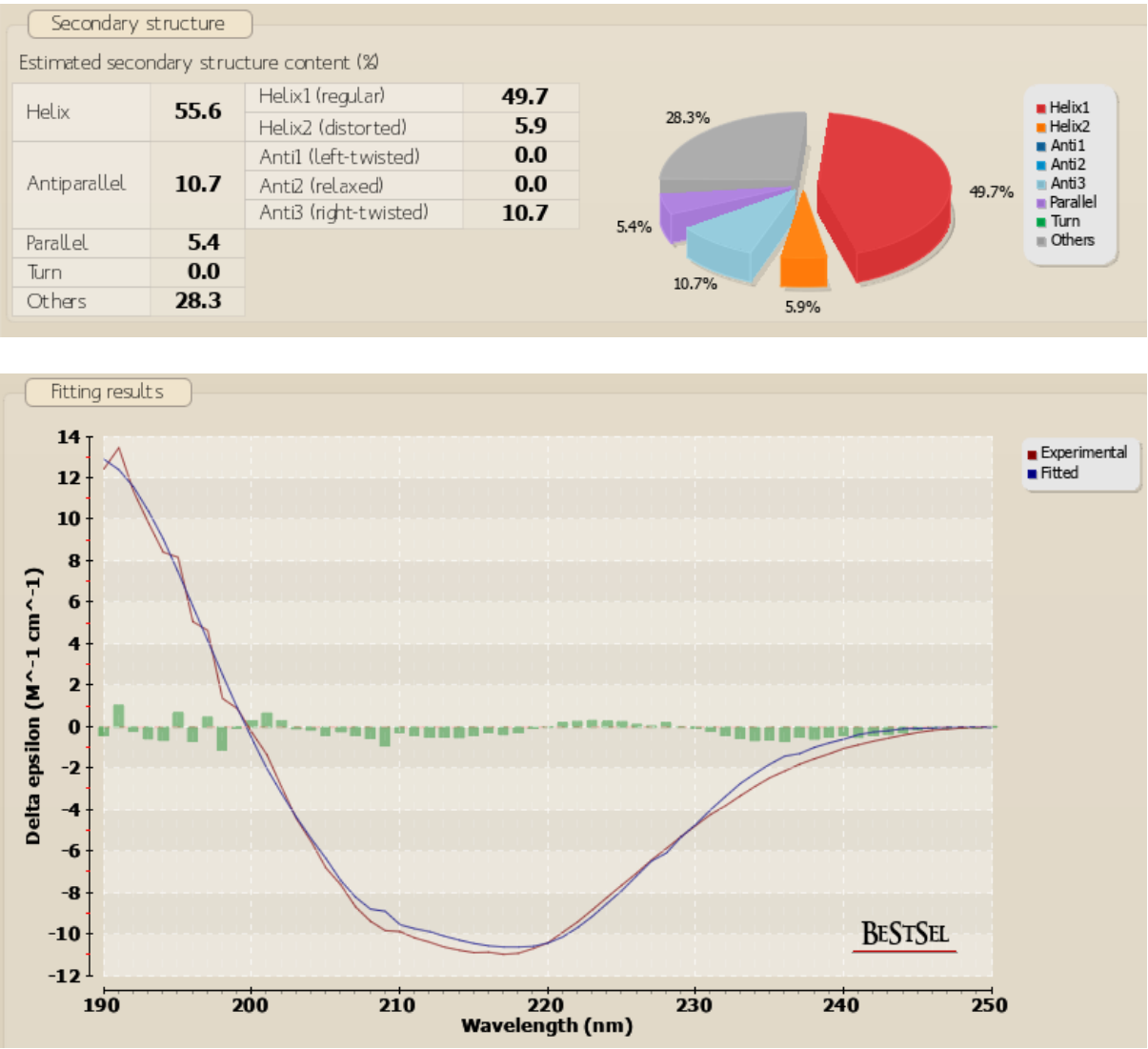


Figure 79: Plot and secondary structure data of Pep_HA CD data using BeStSel software.

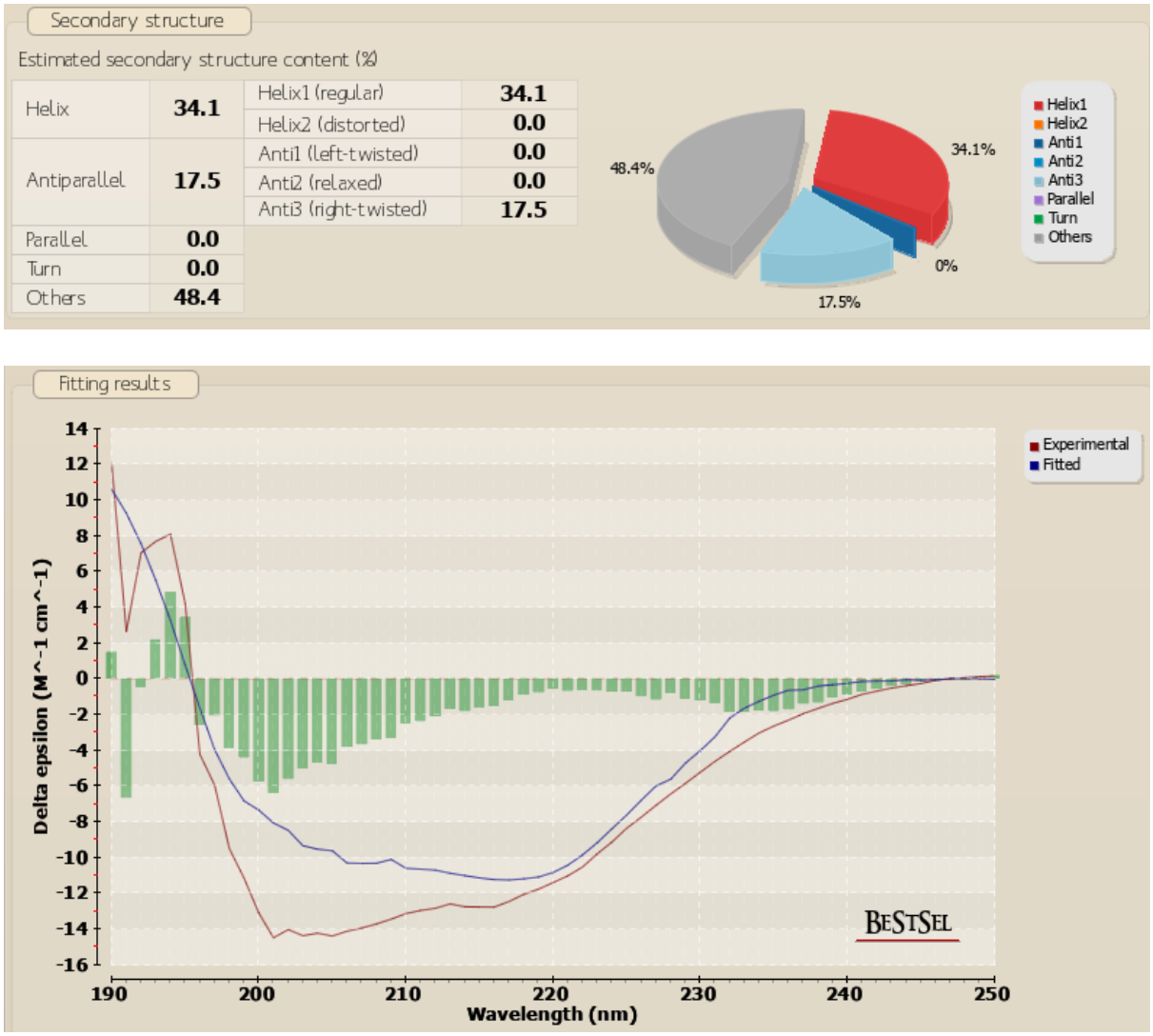


Figure 80: : Plot and secondary structure data of Pep_PNL2 CD data using BeStSel software.

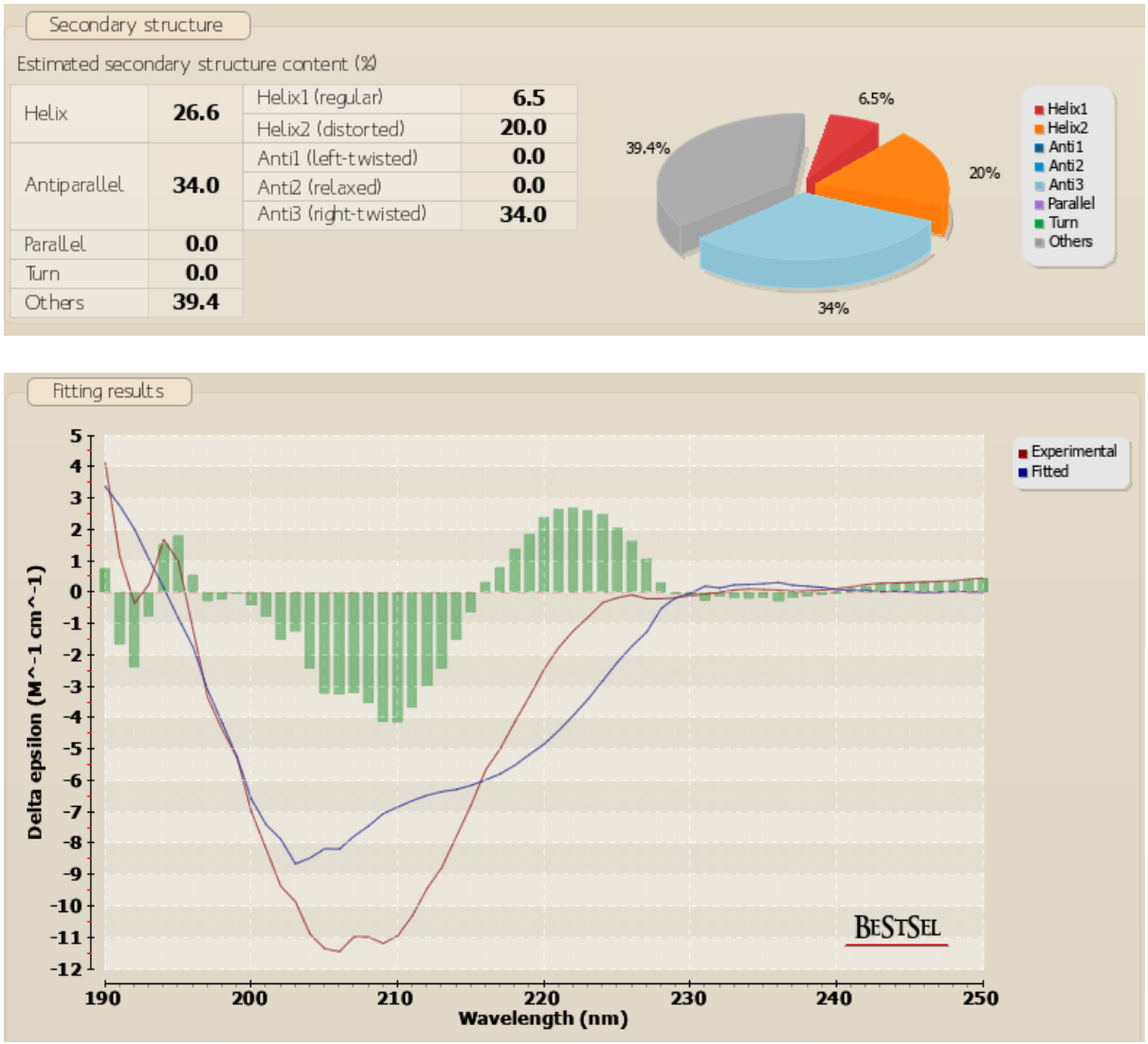


Figure 81: Plot and secondary structure data of Pep_PTA CD data using BeStSel software.

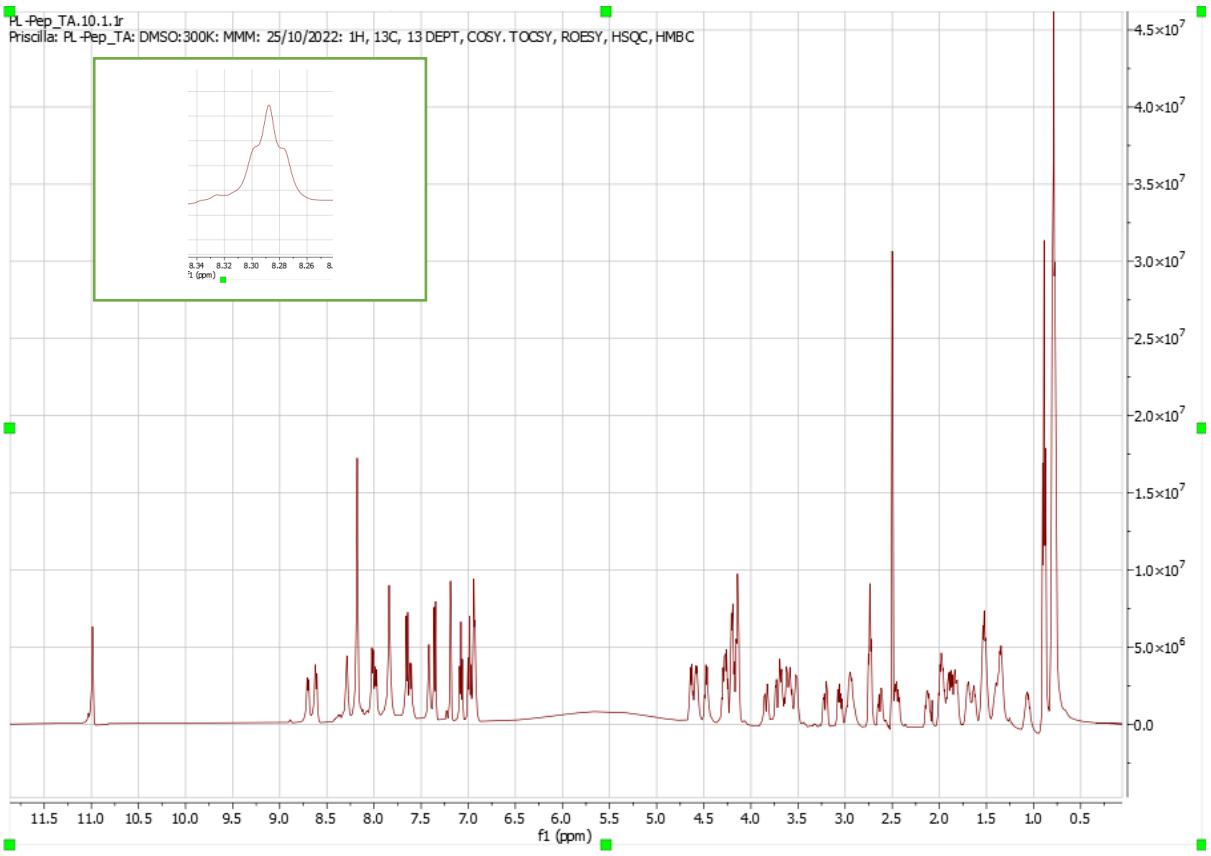


Figure 82: ^{1}H NMR of Pep_TA.

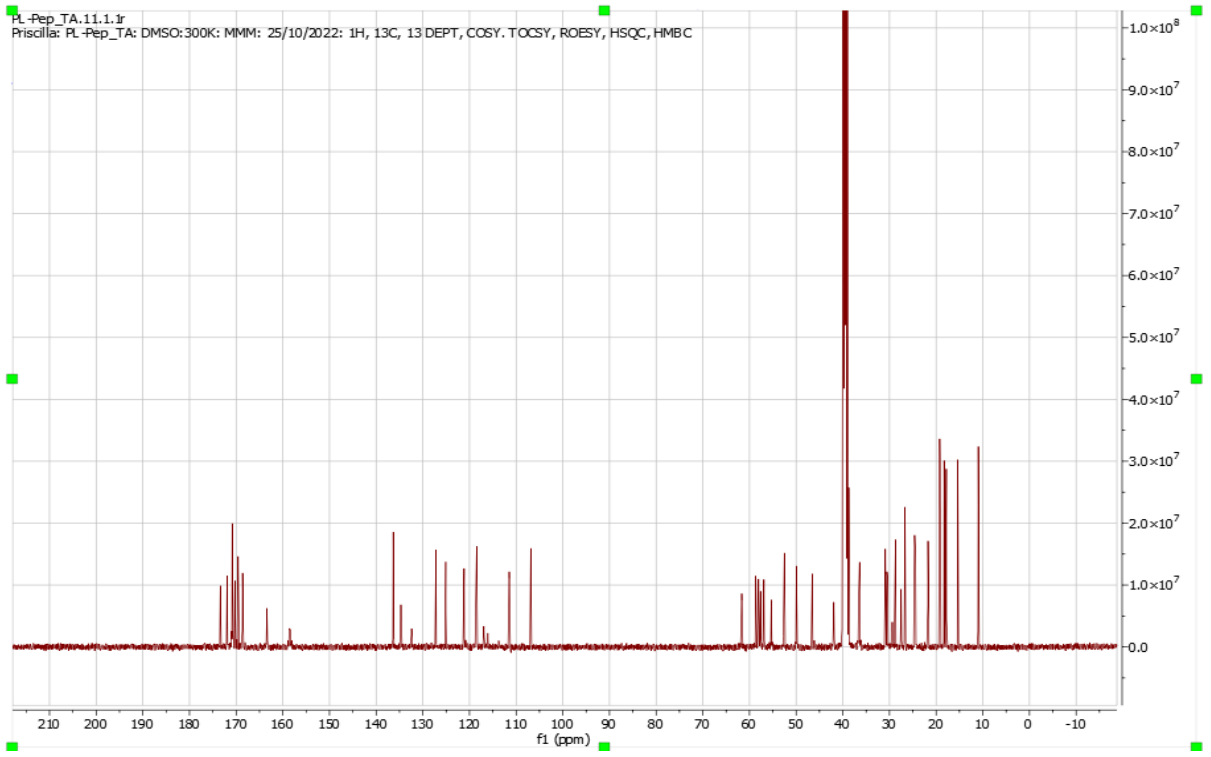


Figure 83: ^{13}C NMR of Pep_TA.

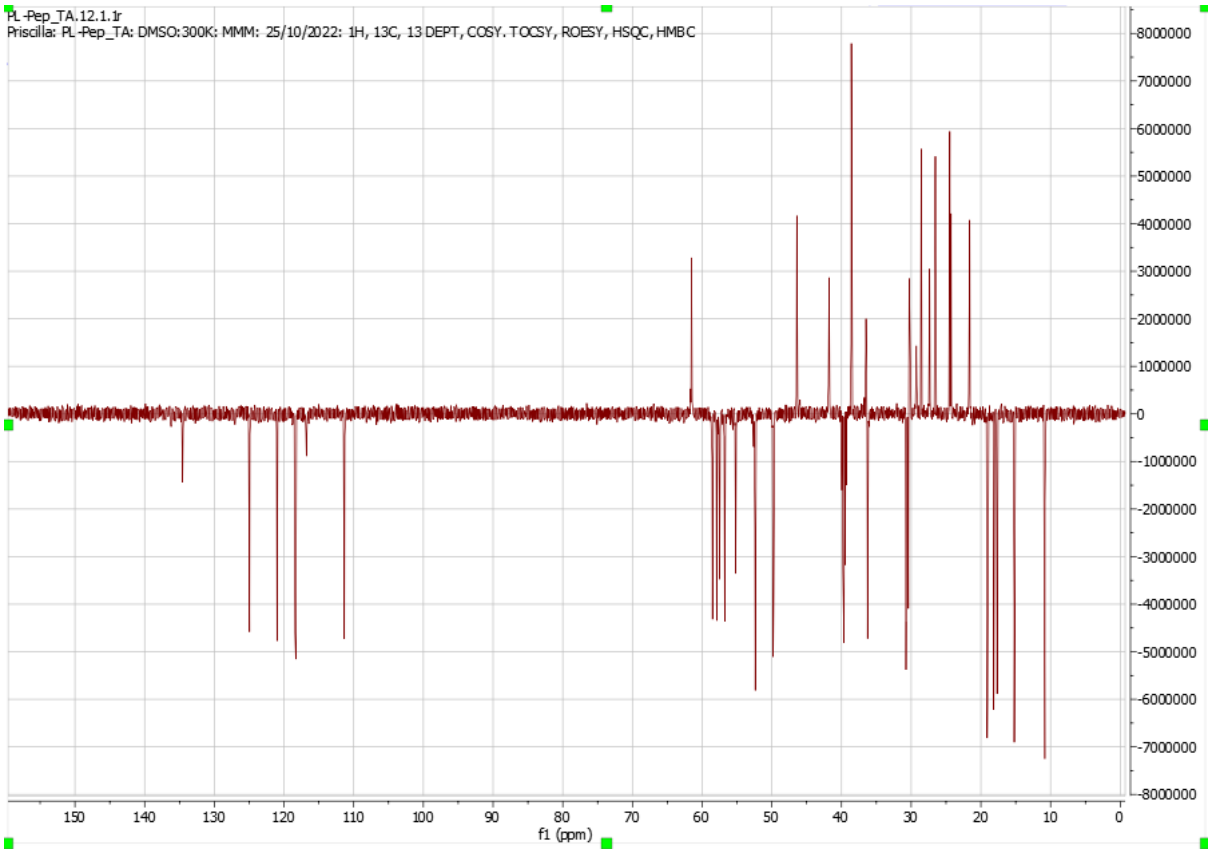


Figure 84: DEPT NMR of Pep_TA

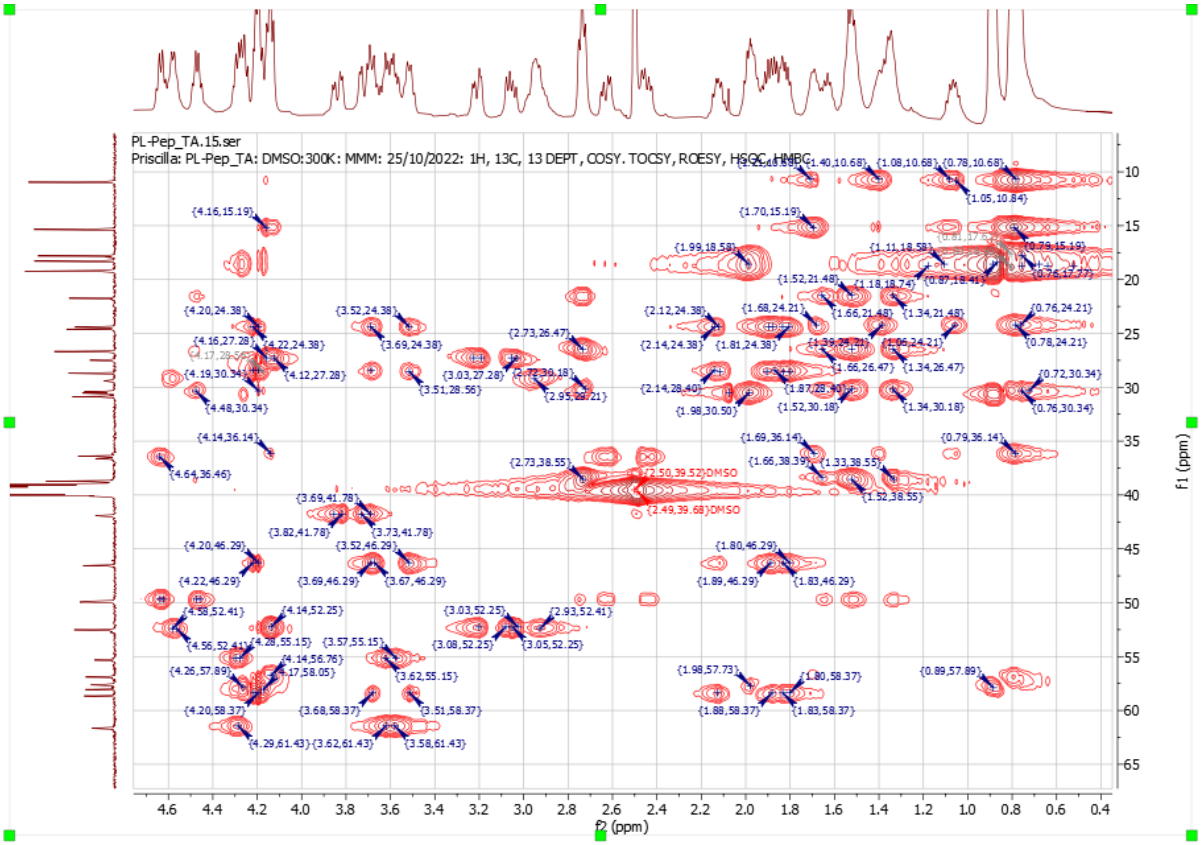


Figure 85: The HSQC of Pep_TA.

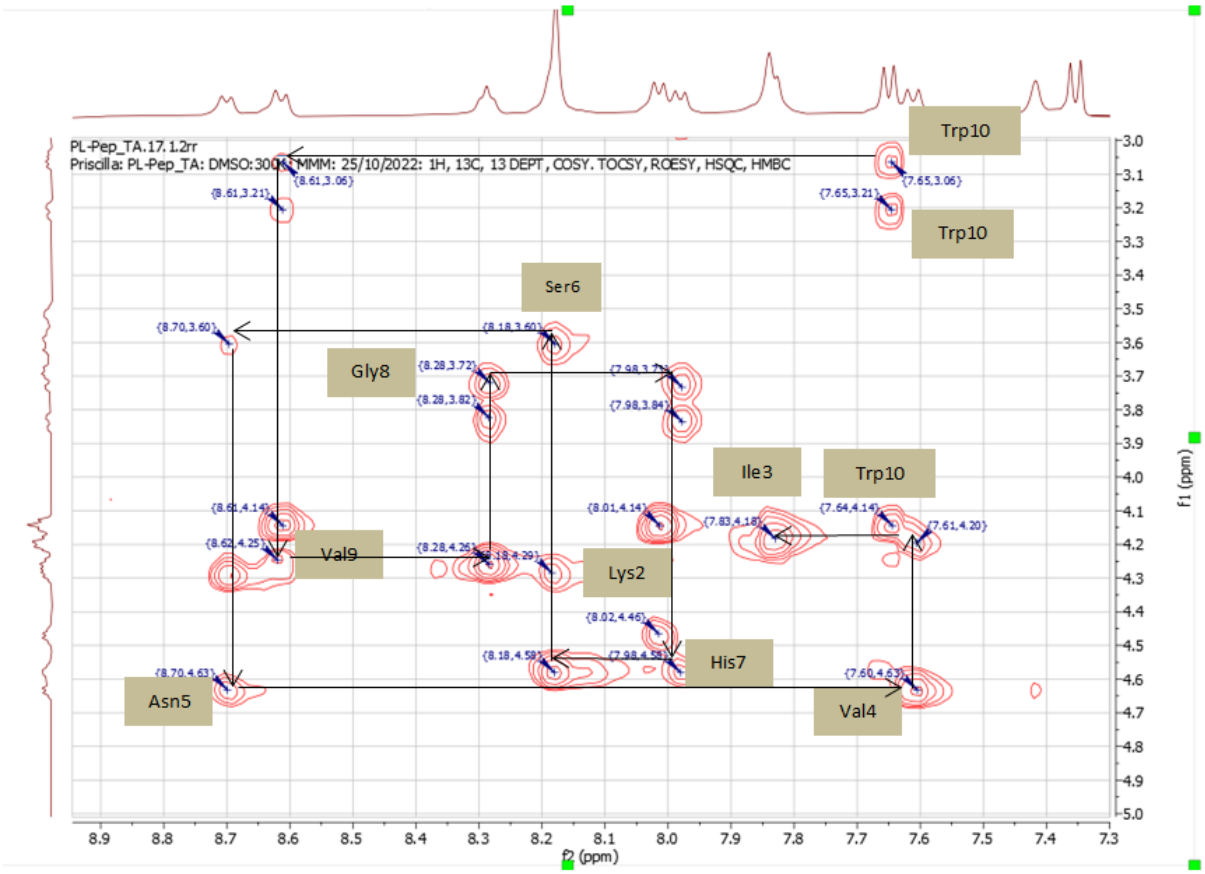


Figure 86: The ROESY of Pep_TA.

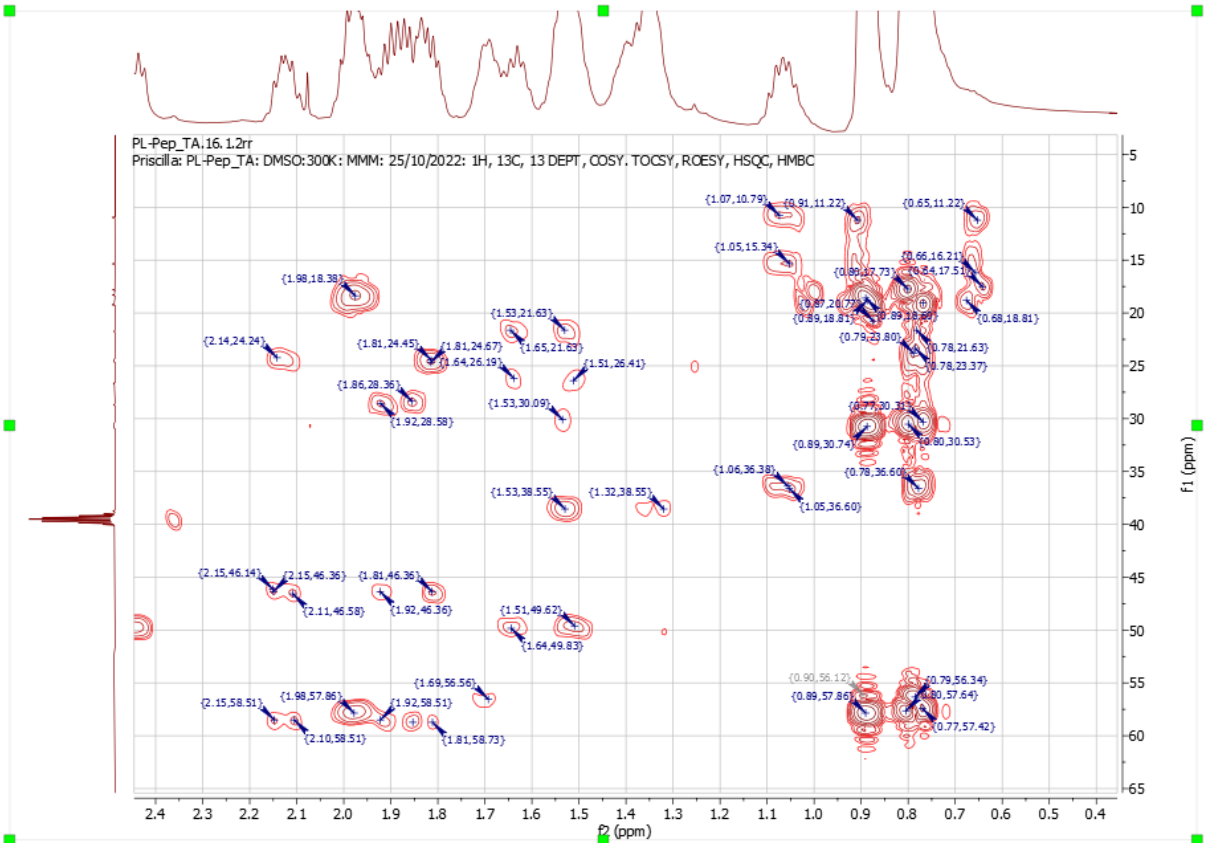


Figure 87: The HMBC of Pep_TA.